UNIVERSIDAD DE LA REPÚBLICA URUGUAY

FACULTAD DE CIENCIAS
UDELAR | fcien.edu.uy

Doctorado en Biotecnología

Del gen a la aplicación: exploración de enzimas modificadoras de lignina y su incorporación en preparados multienzimáticos para la industria

Lic. Mag. Célica Cagide Diflore

TESIS DE DOCTORADO EN BIOTECNOLOGÍA

Posgrado en Biotecnología – UdelaR

Del gen a la aplicación: exploración de enzimas modificadoras de lignina y su incorporación en preparados multienzimáticos para la industria

Estudiante: Lic. Mag. Célica Cagide Diflore

Tutora: Dra. Susana Castro- Sowinski

Co-tutor: Dr. Diego Vallés

Tribunal:

Dra. Cecilia Abreu

Dra. Paula González

Dra. Mariana Barraco

Sección Bioquímica

Facultad de Ciencias, UDELAR

Diciembre, 2025

AGRADECIMIENTOS

Esta tesis no habría sido posible sin el acompañamiento de muchas personas que, desde distintos lugares, supieron caminar conmigo este recorrido de forma cercana, generosa y profundamente humana.

Quiero agradecer especialmente a Susana, mi mentora, colega y amiga. Durante tantos estos años supo acompañarme con una enorme sensibilidad y sabiduría, alentándome siempre a construir mi propio camino, a animarme a volar sola, pero estando incondicionalmente presente cada vez que necesité una guía, una palabra justa o un gesto de contención. Su acompañamiento trascendió ampliamente lo profesional; fue y es una verdadera compañera de ruta, de esas que enseñan sin imponer y orientan sin limitar.

A Diego, por su permanente disposición para acompañar, enseñar y compartir. Su generosidad, apertura y compromiso hicieron de cada jornada de trabajo un espacio de aprendizaje genuino y de intercambio enriquecedor.

A mis compañeros de laboratorio, César, Juan, Santiago y Manuel, quienes hicieron que mi paso por el laboratorio fuera no solo productivo, sino también disfrutable. Gracias por el apoyo constante, la paciencia, las enseñanzas compartidas y por transformar largas horas de trabajo en días más livianos, eficientes y, por sobre todo, divertidos.

A mis socios y amigos, con quienes dimos forma a este proyecto inmenso que es hoy ANTARKA. Un verdadero desafío colectivo, una creación que creció mucho más de lo que alguna vez imaginamos. En ese camino no solo pude aplicar diariamente mi formación y experiencia profesional, sino que también aprendí cuán sorprendente puede ser la vida cuando uno se anima a tomar decisiones profundas y a construir algo propio junto a otros.

A mi familia, que es mi sostén permanente. A Ger, mi gran compañero de vida y de aventuras, por acompañarme en cada decisión, incluso en las más audaces, por tomarme de la mano cuando hace falta y ayudarme a enfrentar el mundo con valentía. A mis padres y a mis hermanas Yaqui y Ele, por creer en mí, por alentarme siempre y por elevarme cuando más lo necesité.

A todos y cada uno, gracias. Esta tesis también les pertenece**.**

CONTENIDO

ESTRUCTURA DE LA TESIS

La presente tesis se encuentra organizada de la siguiente manera:

Se inicia con un Resumen, seguido de una Introducción General que contextualiza al lector sobre los aspectos económicos y productivos vinculados a la revalorización del material lignocelulósico y al uso de enzimas modificadoras de lignina. Esta sección concluye con una revisión temática, publicada en una revista arbitrada, que abarca la clasificación, mecanismos de acción catalítica, aplicaciones y otros aspectos relevantes de estas enzimas.

Posteriormente, se presentan la hipótesis de trabajo, el objetivo general y los objetivos específicos.

Los resultados experimentales se presentan en tres capítulos. Cada capítulo comienza con un breve marco teórico que introduce el objetivo específico y la estrategia metodológica empleada. A continuación, se incluye el artículo correspondiente, publicado en una revista arbitrada. En el caso del segundo capítulo, además del artículo publicado, se incorporan resultados adicionales no publicados, que se presentan de forma sintética, destacando las distintas estrategias implementadas para alcanzar el objetivo propuesto.

Finalmente, la tesis cierra con una Discusión Globalizadora, que integra y amplía los análisis desarrollados en los capítulos, seguida de las Conclusiones y de una sección de Perspectivas que identifica oportunidades de exploración.

RESUMEN

La lignina es un polímero aromático complejo presente en la biomasa lignocelulósica, cuya estructura recalcitrante representa un desafío tanto para la valorización de residuos industriales como para la sostenibilidad de procesos como la producción de pulpa y papel. Las enzimas modificadoras de lignina (EML), entre ellas peroxidasas y laccasas, constituyen herramientas biotecnológicas con alto potencial para promover una transición hacia procesos industriales más limpios y eficientes.

En esta tesis se exploraron nuevas EML de origen bacteriano, con especial énfasis en enzimas provenientes de microorganismos antárticos, abordando su caracterización bioquímica y estructural, así como su aplicación en bioprocesos de modificación de lignina. Los objetivos incluyeron la producción recombinante y caracterización de una peroxidasa tipo DyP, la identificación genómica y expresión de una laccasa bacteriana, y la evaluación de la acción individual y combinada de ambas enzimas en preparados multienzimáticos.

Se caracterizó una peroxidasa tipo DyP proveniente de *Pseudomonas sp.* AU10, aislada de la Antártida. La enzima recombinante (rDyP-AU10) presentó actividad oxidativa a bajas temperaturas y capacidad para modificar lignina kraft, generando fenoles, aldehídos y cetonas. Estos resultados demuestran su potencial para aplicaciones en bioblanqueo, biotransformación de lignina y biorremediación.

Asimismo, se realizó el análisis genómico de *Sinorhizobium meliloti* CE52G, identificándose una laccasa periplásmica con dominios multicobre conservados. Si bien se implementaron distintas estrategias de expresión recombinante en *Escherichia coli*, no se logró obtener una forma catalíticamente activa de la enzima, lo que evidenció los desafíos asociados al plegamiento correcto y la incorporación de cobre en estas oxidasas bacterianas.

Finalmente, se evaluó la acción conjunta de rDyP-AU10 y una laccasa comercial sobre lignina kraft y pulpas celulósicas industriales, observándose efectos complementarios en la modificación química de la lignina. En conjunto, los resultados aportan conocimiento original sobre la diversidad y funcionalidad de EML bacterianas, destacando el potencial biotecnológico para generar procesos industriales sostenibles.

INTRODUCCIÓN GENERAL

La biomasa leñosa comercializada representa una de las principales fuentes renovables empleadas a nivel global en aplicaciones industriales, más allá de su tradicional uso energético. Este recurso está ampliamente valorizado en sectores como la industria de la pulpa y el papel, la fabricación de tableros de madera reconstituida y más recientemente, en el desarrollo de bioproductos y materiales lignocelulósicos de alto valor agregado. Según datos de la FAO [1], actualmente se producen cada año alrededor de 1,92 mil millones de m^3 de madera industrial, y la industria papelera se posiciona como uno de los principales destinos no energéticos de este recurso. En 2023, la producción mundial de pulpa de madera alcanzó 193 millones de toneladas, con un comercio internacional récord de 71 millones de toneladas. Este flujo sustancial de biomasa leñosa hacia la fabricación de pulpa, papel y cartón, impulsado por países como Brasil, Canadá, Estados Unidos y China, refleja la importancia estratégica de este sector en el uso industrial de los recursos forestales, así como su creciente adopción de tecnologías más eficientes y sostenibles [2].

Esta industria se basa en el procesamiento de madera primaria (material leñoso), especialmente de especies de rápido crecimiento como eucalipto y pino, así como de subproductos forestales. A través de procesos mecánicos, químicos o combinados, se obtiene pulpa celulósica, que constituye el insumo base para la fabricación de papel y cartón. Paralelamente, los residuos generados, como lignina, hemicelulosa y licor negro, se reutilizan comúnmente como fuente interna de energía térmica y eléctrica, cerrando parcialmente el ciclo de aprovechamiento de la biomasa (https://www.upmpulp.com/pulp-production/how-is-pulp-made/).

Industrias como la alimentaria y la farmacéutica llevan varias décadas utilizando herramientas biotecnológicas en sus procesos productivos, pero otras industrias han tardado más en adoptar estas herramientas. Desde principios de la década del 2000, se ha observado una adopción más amplia de los procesos biológicos en sectores tradicionalmente dominados por procesos químicos, como la industria papelera (Tabla 1). En este caso, la incorporación de tecnologías basadas en enfoques biológicos ha representado una estrategia clave para optimizar procesos, reducir el impacto ambiental y avanzar hacia prácticas más sostenibles. Esta transición ha sido impulsada tanto por los avances tecnológicos como por la creciente presión ambiental y regulatoria que enfrenta el sector. En particular, la industria papelera ha explorado el uso de enzimas como xilanasas y laccasas (UPM en su planta de Alemania, por ejemplo), con el propósito de reducir el empleo de agentes químicos agresivos en etapas críticas como el blanqueo o preblanqueo, una estrategia respaldada por numerosos reportes científicos [3–5]. Esto no solo mejora la eficiencia del proceso, sino que disminuye la carga

contaminante de los efluentes generados [6, 7]. A pesar de que las investigaciones en este campo llevan más de dos décadas, su implementación a escala industrial continúa siendo difícil, ya que enfrenta tanto desafíos técnicos como económicos. Entre ellos, se destacan la limitada estabilidad de algunas enzimas en condiciones industriales, la variabilidad en la estructura química del sustrato lignocelulósico, la necesidad de adaptar los procesos ya existentes y el costo de la producción de biocatalizadores a gran escala. A esto se suma que los métodos químicos tradicionales están fuertemente consolidados y siguen siendo más económicos, lo que reduce el incentivo para el cambio tecnológico en ausencia de políticas de estímulo o marcos regulatorios más exigentes, como fue corroborado en intercambios con profesionales de la multinacional UPM (comunicación personal).

Paralelo al interés por aplicar herramientas biológicas durante el proceso de producción de pulpa y papel, hay un gran interés en el desarrollo de estrategias biotecnológicas orientadas al tratamiento de los residuos lignocelulósicos generados por la propia industria forestal y sectores afines. Se generan cantidades significativas de residuos lignocelulósicos, cuya gestión representa un desafío clave para las industrias. Entre las principales fuentes se encuentran: 1) la industria de la celulosa y el papel, que produce entre 150 y 200 m^3 de efluentes líquidos por tonelada de pulpa, y entre 160 y 450 kg de sólidos residuales por tonelada procesada; pero también otras industrias generan cantidades de residuo significativas, como 2) las destilerías a base de melaza de caña de azúcar, que generan aproximadamente 15 litros de efluente por cada litro de alcohol producido, alcanzando un volumen estimado de 7,5 millones de toneladas anuales; 3) los residuos agrícolas, con un volumen global superior a 200 mil millones de toneladas por año; y 4) la industria alimentaria, responsable de cerca de 1.300 millones de toneladas de residuos anuales [8, 9]. El empleo de enzimas modificadoras de la biomasa lignocelulósica, como estrategia biológica, no solo persigue reducir la carga ambiental asociada a efluentes líquidos y residuos sólidos, sino también convertir estos subproductos en insumos de valor agregado, como azúcares fermentables, biopolímeros o fuentes de bioenergía [10–12].

Tabla 1. Uso de enzimas en industrias basadas en biomasa lignocelulósica

Empresa	País	Tratamiento enzimático	Industria	Referencia
UPM	Alemania	Hidrólisis enzimática de celulosa y hemicelulosa	Bioquímica / Biorefinería	UPM Biochemicals (2024). https://www.upmbiochemicals.com/products-and-markets/biorefinery-leuna/
Raízen	Brasil	Enzimas celulolíticas para producción de azúcares fermentables	Biocombustibles (etanol 2G)	Raízen (n.d.). https://www.raizen.com.br/
GranBio	Brasil	Pretratamiento físico-químico + cócteles enzimáticos	Bioenergía (etanol celulósico)	GranBio (n.d.). https://www.granbio.com.br/
Clariant	Suiza (planta en Rumania)	Proceso sunliquid®: hidrólisis enzimática + fermentación	Biocombustibles (etanol 2G)	Clariant (2023). https://www.clariant.com/en/Innovation/Sunliquid
Biochemtex / Beta Renewables	Italia	PROESA®: pretratamiento + enzimas lignocelulósicas	Bioenergía / Química verde	Beta Renewables (n.d.). https://www.beta-renewables.com/
Borregaard	Noruega	Enzimas para fraccionamiento de lignocelulosa	Química fina / Lignina técnica	Borregaard (n.d.). https://www.borregaard.com/
Enviral	Eslovaquia	Hidrólisis enzimática para producción de etanol	Biocombustibles / Etanol industrial	Enviral (n.d.). https://www.envirochemie.com/
Sekab	Suecia	Tecnología CelluAPP® con hidrólisis enzimática	Bioquímicos / Etanol 2G	Sekab (n.d.). https://www.sekab.com/celluapp-technology/
Novozymes	Dinamarca	Desarrollo de enzimas (xilanasas, laccasas, celulasas)	Proveedora para múltiples industrias	Novozymes (n.d.). https://www.novozymes.com/en/advance-your-business/bioenergy

AIMPLAS (ENZPLAST)	España	Enzimas en síntesis y degradación de biopolímeros	Plásticos biodegradables / materiales	AIMPLAS (n.d.). https://enzplast.com/
AB Enzymes	Alemania	Celulasas y hemicelulasas	Textil (algodón, lino)	AB Enzymes (n.d.). https://abenzymes.com/
DuPont (IFF)	EE.UU.	Celulasas industriales	Textil (celulosa)	DuPont (IFF) (n.d.). https://www.iff.com/segments/health-biotech/industrial-biosciences
Amano Enzyme	Japón	Diversas enzimas textiles	Textil (acabado vegetal)	Amano Enzyme (n.d.). https://www.amano-enzyme.com/
CHT Group	Alemania	Formulaciones enzimáticas para fibras vegetales	Textil / sostenible	CHT Group (n.d.). https://www.cht.com/

Ejemplos representativos de empresas que aplican tecnologías enzimáticas para modificar biomasa lignocelulósica, en diversos sectores industriales. La tabla incluye el país de origen u operación de cada empresa, el tipo de biotecnología aplicada y el sector industrial correspondiente.

Composición y estructura del material lignocelulósico

Para comprender el potencial de las herramientas biológicas en el tratamiento de la madera, es necesario primero conocer la biomasa lignocelulósica desde una perspectiva química. Esta se compone principalmente por celulosa (40–50%), hemicelulosa (25–30%) y lignina (15–20%), organizadas en una red estructural altamente resistente (Figura 1). La celulosa es un polisacárido lineal de D-glucosas unidas por enlaces β-1,4-O-glicosídico, donde varias hebras se agrupan entre sí por intermedio de múltiples puentes de hidrógeno, y forman microfibrillas que aportan rigidez mecánica a la pared vegetal. La hemicelulosa es un heteropolisacárido formado por una cadena principal constituida básicamente por glucosas, galactosas y fructosas unidas por enlaces β-1,4-O-glicosídico, y ramificaciones; entre estos se encuentran los xilanos y mananos, que actúan como una matriz que conecta las microfibrillas de celulosa. Por su parte, cuando el material vegetal es lignocelulósico, la pared también contiene lignina, quien aporta rigidez, hidrofobicidad, impermeabilidad y resistencia frente a la degradación química y biológica. La lignina es un polímero aromático complejo, compuesto por unidades de guayacilo, siringilo y p-hidroxifenilo, derivadas de los alcoholes coniferílico, sinapílico

y p-cumarílico, respectivamente, unidas mediante enlaces éter y éster altamente estables. Esta configuración estructural hace que la biomasa lignocelulósica sea extremadamente recalcitrante, lo que dificulta su degradación, pero también ofrece oportunidades para su valorización biotecnológica como fuente renovable [13, 14].

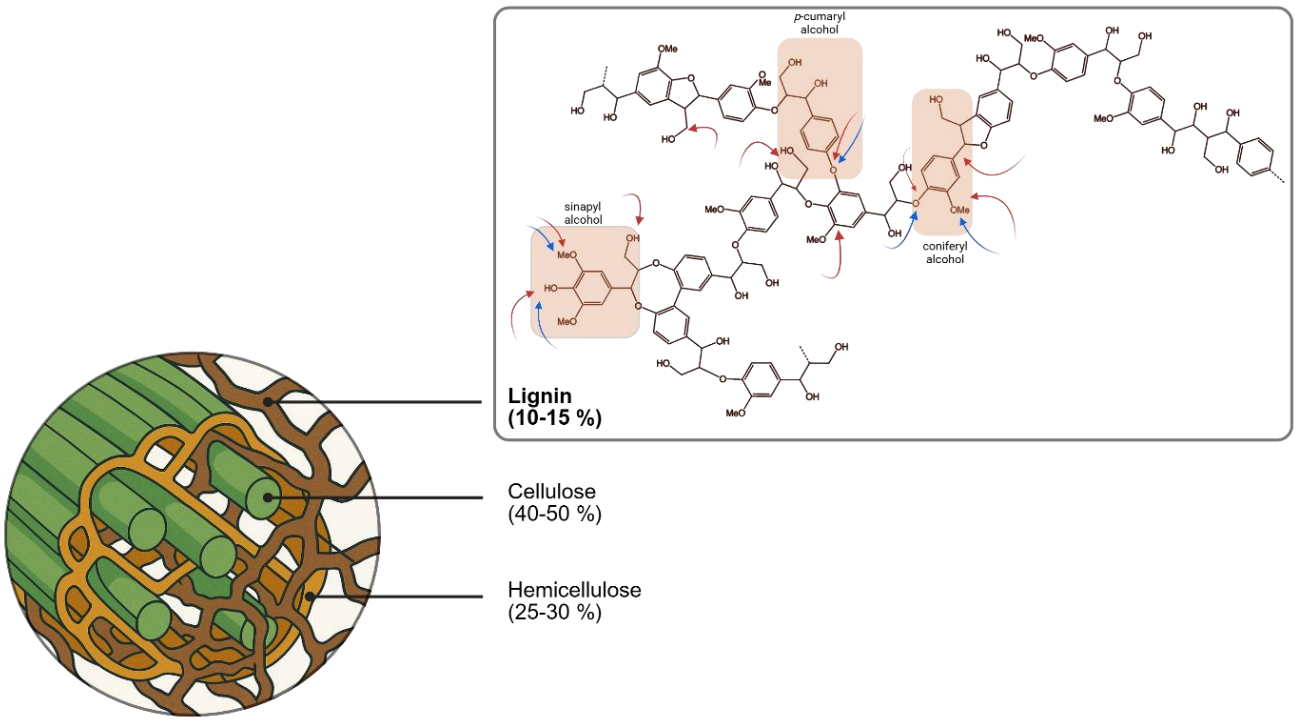

Figura 1. Representación esquemática de la biomasa lignocelulósica, destacando sus tres componentes principales: celulosa, hemicelulosa y lignina. A la derecha se muestra la estructura química de la lignina, compuesta por unidades derivadas del alcohol p-cumarílico, alcohol coniferílico y alcohol sinapílico. Las flechas azules indican los sitios de oxidación dirigidos por las lacasas, mientras que las flechas rojas indican aquellos dirigidos por peroxidasas del tipo DyP. Creado en https://BioRender.com.

Por otra parte, la lignina, debido a su estructura compleja, y rica en grupos funcionales como fenoles, carboxilos e hidroxilos, tiene una notable capacidad para interactuar con moléculas catiónicas presentes en el ambiente acuoso. Esta afinidad facilita la formación de complejos estables que contribuyen a la persistencia de contaminantes en los ecosistemas acuáticos. Por ejemplo, Singh et al.

(2021) [15] destacan que la lignina puede formar complejos con metales pesados, dificultando su eliminación y aumentando su toxicidad en el medio ambiente. Kumar y Chandra (2020) [16], también señalan que la lignina puede unirse a compuestos catiónicos, formando estructuras recalcitrantes que son resistentes a la biodegradación. Estas interacciones no solo complican los procesos de remediación natural, sino que también potencian la acumulación de contaminantes persistentes, representando un desafío significativo para el tratamiento de efluentes industriales ricos en residuos lignocelulósicos. La gestión inadecuada de estos residuos puede generar lixiviados ácidos ricos en compuestos fenólicos, que son tóxicos para los organismos acuáticos y pueden alterar la calidad del agua [17]. Estos lixiviados, al filtrarse, pueden provocar eutrofización y afectar negativamente a la biodiversidad acuática.

Bioprocesos modificadores de lignina

Tanto en el proceso de blanqueo de la pulpa de celulosa (etapa necesaria durante la producción de pulpa para eliminar el color marrón originado por la lignina remanente) como en el tratamiento de efluentes, el empleo de herramientas biológicas orientadas a la modificación o eliminación de lignina representa una alternativa prometedora para reducir la carga química contaminante y mejorar la sostenibilidad del proceso.

El conjunto de enzimas capaces de despolimerizar o modificar la estructura de la lignina a través de mecanismos oxidativos se denomina actualmente enzimas modificadoras de lignina (EML). En la literatura más antigua se las mencionaba como enzimas ligninolíticas, un término hoy considerado impreciso, ya que el proceso no es de naturaleza lítica, sino oxidativa. Dentro de las EML se incluyen las lignina peroxidasas (LiP), peroxidasas de manganeso (MnP), peroxidasas versátiles (VP), peroxidasas tipo DyP (dye-decolorizing peroxidases, o decolorantes de tinte) y laccasas, todas ellas responsables de atacar de manera directa el entramado aromático de la lignina [18]. Por otro lado, existen otras enzimas modificadoras de lignina, denominadas enzimas auxiliares. Estas no alteran la lignina directamente; en cambio, participan realizando modificaciones químicas que alteran su estructura polimérica, facilitando así su posterior despolimerización. Las enzimas auxiliares actúan de manera secuencial y cooperativa, generando transformaciones como la introducción o remoción de grupos funcionales, el reordenamiento de enlaces o la modificación del grado de ramificación y entrecruzamiento de la macromolécula [19].

En este contexto, la aplicabilidad de las EML y/o enzimas auxiliares sobre la biomasa lignocelulósica ha despertado interés no solo en el ámbito ambiental y de sostenibilidad, sino también económico y comercial, por tener potenciales aplicaciones en una variedad de sectores, incluidos la producción de pulpa de celulosa y papel, alimentos, textiles, detergentes, biosensores, química sintética, biorremediación y biodegradación, así como la eliminación de disruptores endocrinos, la industria farmacéutica, y cosmética [16].

Desde una perspectiva comercial, los datos reflejan la inmensa oportunidad de mercado que existe alrededor de esta problemática. El mercado global de enzimas industriales está experimentando un crecimiento notable. Según el informe de análisis de tendencias publicado por Strait Research (https://straitsresearch.com/report/enzymes-market), el mercado mundial de enzimas se valoró en USD 14.30 mil millones en 2024 y se espera que crezca a USD 15.36 mil millones en 2025, y a USD 27.55 mil millones para 2033, creciendo a una CAGR del 5.7% durante el período pronosticado (2025-2033). El índice CAGR expresa la tasa de crecimiento anual compuesta, y muestra el crecimiento en el promedio anual de un indicador durante un período, asumiendo que ese crecimiento fue constante para cada año.

Particularmente, el mercado global de enzimas en la industria de pulpa y papel se valoró en USD 135,70 millones en 2022 y se prevé que alcance un valor de USD 211,63 millones para 2030, expandiéndose a un CAGR de 5,8% en el período 2023-2030 (https://www.congruencemarketinsights.com/report/enzyme-for-pulp-and-paper-market?utm_source=chatgpt.com). Según este informe, la creciente adopción de tecnologías enzimáticas en el sector responde a múltiples objetivos estratégicos por parte de las empresas: incorporar alternativas sostenibles en sus procesos, implementar soluciones rentables y de alta eficiencia, mejorar la calidad del papel producido y fomentar el desarrollo de nuevas tecnologías que les permitan aumentar su competitividad y reducir su impacto ambiental.

Nuestro enfoque, basado en el uso de EML, se enmarca en este creciente interés global por este tipo de biocatalizadores, reflejado también en su proyección de mercado. Se estima que el mercado específicamente de EML alcanzará los USD 2,5 mil millones en 2025, con una tasa de crecimiento anual del 7% hasta 2033 (https://www.archivemarketresearch.com/reports/lignocellulolytic-enzyme-62497?utm_source).

Este escenario refleja una gran oportunidad de implementación de procesos enzimáticos, por ejemplo, en el pretratamiento de la pulpa kraft (compuesta por fibras de celulosa casi puras). Las xilanasas han sido identificadas como las enzimas más utilizadas para esta función, ya que su acción hidrolítica sobre

la hemicelulosa abre la matriz lignocelulósica y facilita la extracción de la lignina [20, 21]. Además, se han empleado otras enzimas para reducir el tiempo de batido de las pulpas vírgenes, mejorar la fibrilación (desprendimiento de las microfibrillas en la superficie de las fibras de celulosa) y aumentar la retención de agua. También se emplean para blanquear y mejorar la capacidad de refinación de las fibras recicladas [22–25]. La etapa de blanqueo de la pulpa de celulosa, orientada a eliminar la lignina remanente en la pulpa, resulta esencial tanto para optimizar las propiedades del papel como para mejorar su aspecto visual, al reducir la tonalidad marrón característica de este polímero. Tradicionalmente, este proceso ha requerido grandes volúmenes de cloro y sus derivados, los cuales generan compuestos orgánicos clorados. Estos compuestos son frecuentemente tóxicos, mutagénicos, persistentes y bioacumulables, y pueden producir alteraciones perjudiciales en sistemas biológicos [15, 26, 27].

También, las enzimas ofrecen una alternativa ecológica y posiblemente más económica para reducir el uso de productos químicos agresivos como el cloro. Además, permiten aumentar el nivel de blancura del papel sin comprometer la integridad de las fibras. Hasta el momento, se han investigado principalmente dos estrategias enzimáticas de pretratamiento o blanqueo alternativas: una basada en hemicelulasas, y otra en EML, dependiendo del tipo de pulpa y del objetivo del tratamiento[3, 15, 27].

En el marco de esta tesis doctoral, desarrollamos y publicamos tres artículos científicos y una revisión bibliográfica, que aportan de manera complementaria al conocimiento y la aplicación biotecnológica de las EML. En primer lugar, llevamos a cabo una revisión exhaustiva sobre las características bioquímicas y tecnológicas de las enzimas modificadoras de lignina, resaltando su potencial en diversas industrias, publicada bajo el título *"Technological and biochemical features of lignin-degrading enzymes: a brief review"*, Cagide y Castro-Sowinski, 2020 [28]. Dicha revisión se incluye como parte del marco introductorio general de esta tesis, la cual proporciona una visión actualizada sobre la temática y establece las bases conceptuales que sustentan el desarrollo del trabajo.

Posteriormente, se caracterizó bioquímica y estructuralmente una peroxidasa tipo DyP proveniente de un organismo psicrófilo antártico, destacando sus propiedades de actividad a baja temperatura y su capacidad de modificación de lignina, trabajo titulado *"A bacterial cold-active dye-decolorizing peroxidase from an Antarctic Pseudomonas strain",* por Cagide et al., 2023a [29]. A su vez, reportamos la caracterización genómica de una bacteria productora de laccasa, incluyendo el análisis del borrador de su genoma y la identificación de genes de interés biotecnológico en el trabajo titulado *"Descriptive analysis of the draft genome from the melanin-producing bacterium Sinorhizobium (Ensifer) meliloti CE52G*", por Cagide et al., 2023b [30]. La laccasa producida por CE52G se produjo en forma recombinante, usando diferentes estrategias, pero no se logró obtener la proteína de forma activa, por

Environmental Sustainability
https://doi.org/10.1007/s42398-020-00140-y

REVIEW

Technological and biochemical features of lignin-degrading enzymes: a brief review

Célica Cagide[1] · **Susana Castro-Sowinski**[1,2]

Received: 8 July 2020 / Revised: 21 September 2020 / Accepted: 15 October 2020

Abstract
For many industries, the committed step during the treatment of lignocellulosic materials is the elimination of lignin. This recalcitrant material is commonly removed by many physical/chemical procedures that produce hazardous effluents that poison the environment, and usually the treatment of these effluents are cost-expensive. An eco-friendly alternative to the use of traditional treatments is the degradation of lignocellulosic materials using microorganisms or enzymes, mainly by the use of lignin-degrading enzymes. They are classified as lignin-modifying enzymes (ligninolytic enzymes that catalyze an oxidative cleavage of lignin) and lignin-degrading auxiliary enzymes. The lignin-modifying enzymes include phenol oxidases (such as laccases) and heme-peroxidases (lignin-peroxidases, manganese-peroxidases, versatile-peroxidases and, dye-decolorizing peroxidases), both classes of enzymes are members of the oxidase super-family. These enzymes have biochemical features that point them as excellent tools for being used in several industrial processes. They show a great versatility and can oxidize a wide range of organic and inorganic substrates, such as vanillyl alcohol, catechol, acetosyringone, syringic acid, and guaiacol, several dyes, phenolic and non-phenolic lignin model compounds. Their prospective applications include pulp and paper making, bio-refinery (biofuel), bioremediation and, textile, pharmaceutical and dermatological industries, among others. In this review, we summarize some of their biochemical features and potential industrial applications.

✉ Susana Castro-Sowinski
s.castro.sow@gmail.com; scs@fcien.edu.uy

[1] Biochemistry and Molecular Biology, Faculty of Sciences, Universidad de la República, Iguá 4225, Montevideo, Uruguay

[2] Laboratory of Hydrolytic Enzymes, Faculty of Sciences, Universidad de la República, Iguá 4225, Montevideo, Uruguay

Published online: 10 November 2020

Graphic abstract

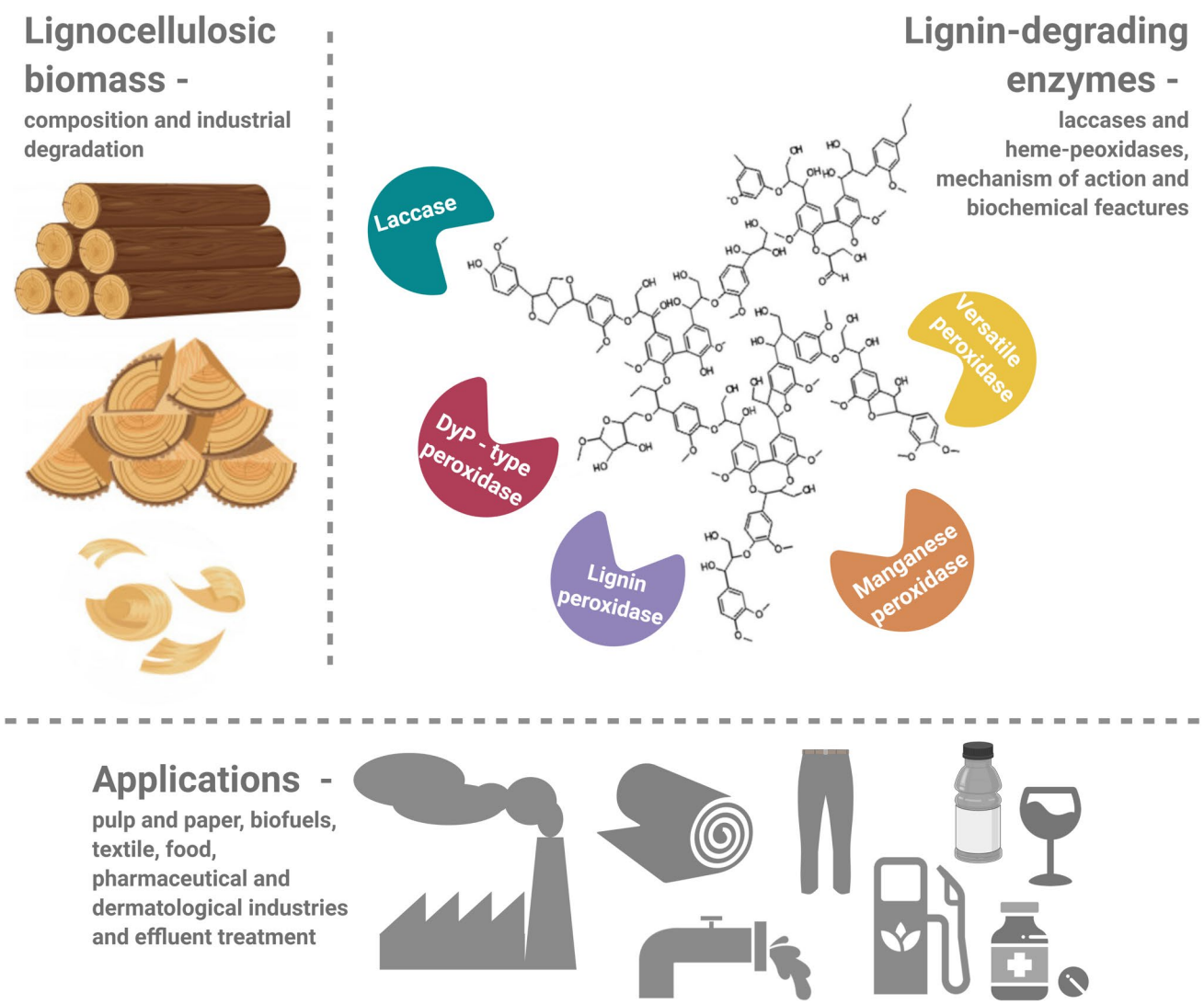

Keywords Lignocellulose · Lignin-degrading enzymes · Phenol oxidase · Peroxidase

Introduction

The lignocellulosic biomass is the most abundant raw material on the Earth. It is mainly composed of complex higher-order structure molecules such as cellulose, hemicellulose and lignin, and constitutes the main components of plant cell walls. From a chemical viewpoint, these complex structures are as follows: (a) cellulose, a linear chain polysaccharide with hundreds or thousands of β(1 → 4) linked D-glucose units; (b) hemicellulose, a polymer with a random and amorphous structure, that includes sugars with five-carbons (mainly xylose and arabinose) and six-carbons (glucose, mannose and galactose, and the deoxy sugar rhamnose) and; (c) lignin, an amorphous polyphenolic molecule. Lignin contains three building blocks: (i) sinapyl alcohol (syringyl alcohol or 3,5-dimethoxy 4-hydroxycinnamic), (ii) *p*-hydroxyphenyl propanol or 4-hydroxycinnamoyl and, (iii) coniferyl alcohol (guaiacyl propanol or 3-methoxy 4-hydroxycinnamyl) units, connected with carbon atoms from phenylpropanoil monomers (Hatakeyama and Hatakeyama 2010; Ponnusamy et al. 2019).

This lignocellulosic biomass is an underused feedstock at the industrial level. The cellulosic material is used in the biofuel (bioethanol), pulp (paper) and polyurethane production industries, but for its further use the lignin has to be removed from the lignocellulosic biomass. On the other hand, lignin is the largest source of aromatic building blocks worldwide and serves as starting material

for the production of bio-based products. Lignin is classified as native (lignin in the lignocellulose, without any modification) and technical lignin (the lignin extracted from biomass, a raw material or by-product from industrial origin). Among technical lignin, Kraft lignin is the major one, but according to their source and obtaining method we find other kind of technical lignins such as hydrolysis lignin, organosolv lignin, pyrolytic lignin, etc.

The hydroxyl groups found in lignin are the target for chemical modifications (Chio et al. 2019). Heating is the most common treatment for breaking chemical bonds; however, other physical/chemical treatments are also used (pyrolysis, hydrogenolysis, hydrolysis, etc.), including microwave assisted depolymerization of lignin.

An inconvenience during the depolymerization of lignin is the repolymerization, with formation of new polymers by the esterification of hydroxyl groups. Oxidative methods, even in mild conditions, may add functionalities to the complex lignin-derived aromatic compounds, by increasing the formation of reactive isomers; in addition, the use of methods that involves the production of chemical radicals increases the problem of repolymerization. The addition of a few compounds such as formaldehyde during the organosolv process may avoid the repolymerization (Sun et al. 2018).

A few examples of lignin-derivative chemicals are: vanillin (produced by the alkali-nitrobenzene method), oils with relatively low oxygen contents (produced by both batch-wise and continuous hydropyrolysis, at high concentrations of Ni/Mo hydro-treating catalyst), syringols, guaiacols and catechols (produced by hydrolysis and dealkylation in supercritical water), methane (formed by methanation and dealkylation), sorbents, activated carbons or carbon fibers with very high surface areas and pore volumes (Brebu and Vasile 2010).

Physical/chemical treatments of lignocellulosic materials are efficient and well-characterized, but usually, they produce many environmental contaminants. More than 250 chemicals have been found in effluents from papermaking (Ali and Sreekrishnan 2001), suggesting that the research in technological innovations to reduce toxic compounds has to be encouraged. An eco-friendly alternative to the use of physical/chemical treatment is the biological treatment of lignocellulosic materials. The limited-step during the degradation of lignocellulosic material is the elimination of lignin. Once the recalcitrant lignin is destroyed, the remaining cellulosic/hemicellulosic matter can be used in several industries (e.g. biofuel and paper pulp). Herein we review information regarding the lignin-degrading enzymes and their potential use in different industries.

Lignin-degrading enzymes: general aspects

Lignin-degrading enzymes catalyze the breakdown of lignin, acting by an oxidative mechanism (not by a hydrolytic mechanism). They have been divided into two main groups: lignin-modifying enzymes and lignin-degrading auxiliary enzymes. The lignin modifying enzymes (ligninolytic oxidative enzymes that catalyze an oxidative cleavage) have been divided into phenol oxidases and heme-peroxidases. Peroxidases and phenol oxidases are both members of the oxidase super-family (Fig. 1).

Phenol oxidases belong to the multi-copper oxidase (MCO) superfamily and, their information has been collected in the "Laccase and Multicopper Oxidase Engineering Database" (LccED; https://lcced.biocatnet.de/; part of the BioCatNet database). MCOs contain at least one out of three different copper sites (type 1, 2 and the binuclear type 3) and are found in the genome of organisms from the three domains of life. These enzymes catalyze the four-electron transfer and reduction of O_2 to two molecules of water (Kosman 2010). Among phenol oxidases are the following enzymes: laccases (EC 1.10.3.2), ascorbate oxidase (EC 1.10.3.3), ferroxidase (EC 1.16.3.1), nitrite reductase (EC 1.7.2.1) and ceruloplasmin (EC 1.16.3.1) (Giardina et al. 2010).

Peroxidases (including heme-peroxidases) and other oxido-reductases catalyze the reduction of hydrogen peroxide (to water) and oxidize various substrates. Their information has been comprehensively collected in the RedoxiBase (http://peroxibase.toulouse.inra.fr/). According to the PeroxiBase, heme-peroxidases are mainly classified into two super-families (non-animal and animal peroxidases), or in one of four smaller protein families (catalases, Dyp-type peroxidases, haloperoxidases and di-heme cytochrome C peroxidases). Non-animal peroxidases include four families: class I (intracellular; APx, CcP, CP, APx-CcP), class II (fungal or bacterial peroxidases; LiP, MnP, VP, CII), class III (Prx) and other non-animal peroxidases (NAnPrx) (Koua et al. 2009; Falade et al. 2017; Janusz et al. 2017) (Fig. 1). Some of the heme-peroxidases are secreted to the milieu and they have lignin-degrading activity, such as the manganese peroxidase (MnP), lignin peroxidase (LiP) and versatile peroxidase (VP), which are typically produced by fungi (Pollegioni et al. 2015).

The Dye-decolorizing peroxidase (DyP) family (EC 1.11.1.19) constitutes a new group of heme-containing lignin-degrading peroxidases, which are phylogenetically unrelated to the classical family II peroxidase catalase enzymes (Zámocký et al. 2015). The first reported DyP peroxidase was isolated from fungi (Kim and Shoda 1999). They have also been found in archaea (Sugano 2009) and

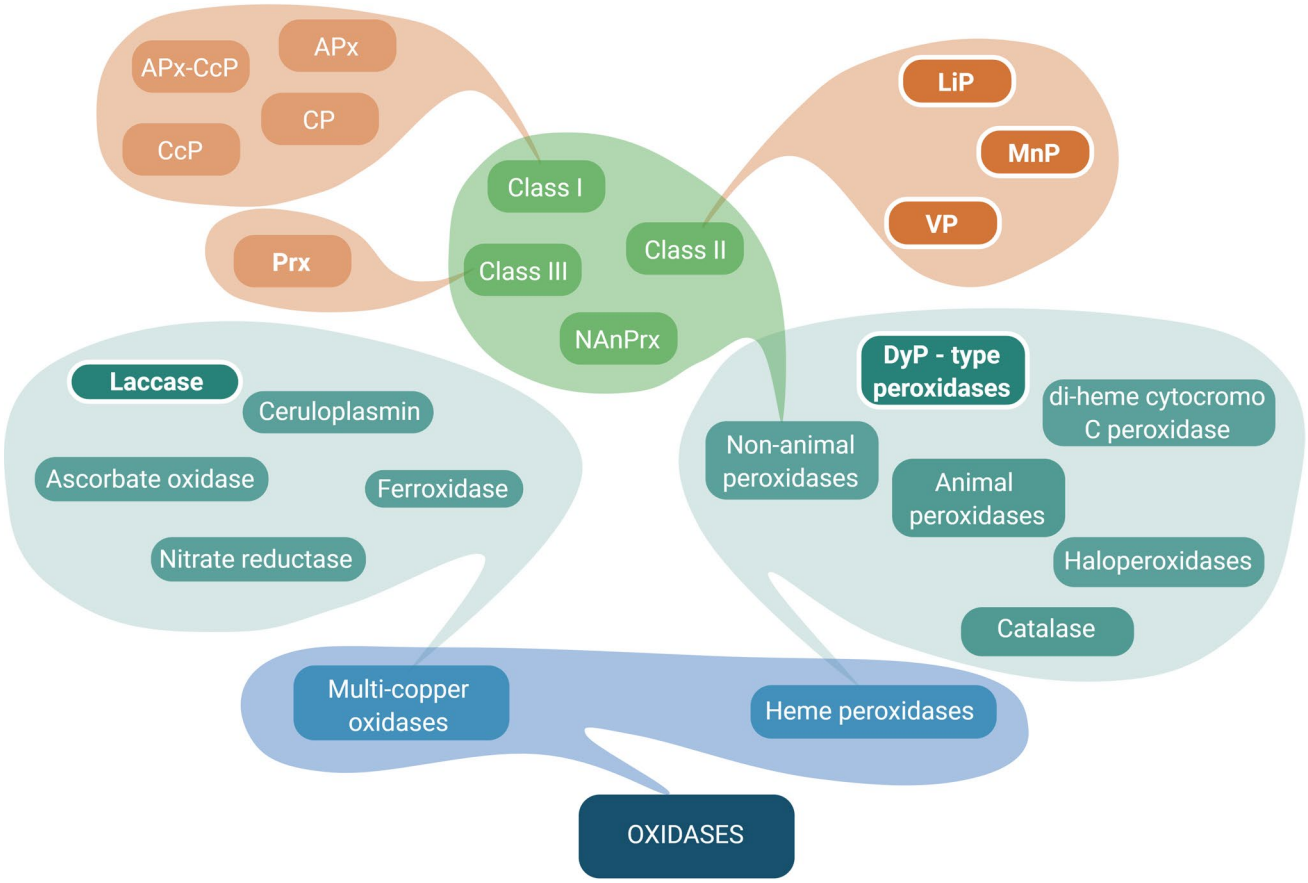

Fig. 1 Diagram showing the enzymes belonging to the oxidase super-family

are common in bacteria (Brown et al. 2011; Chen et al. 2015a, b; Rahmanpour and Bugg 2015).

Lignin-degrading auxiliary enzymes are supplementary enzymes that complete the degradation process of lignin. These include the following enzymes: glyoxal oxidase, heme-thiolate haloperoxidases, aryl alcohol oxidase, pyranose 2-oxidase, cellobiose dehydrogenase and glucose oxidase (Janusz et al. 2017).

Biochemical features and distribution of lignin-degrading enzymes

Laccases

Laccases are oxido-reductase enzymes that belong to the superfamily of multicopper oxidases; they oxidize a wide variety of organic and inorganic substrates, including mono-, di-, and poly-phenols, amino-phenols, methoxy-phenols, aromatic amines, ascorbate, as well as phenolic and non-phenolic lignin compounds. As described above, they use molecular oxygen as an electron acceptor producing water (Reiss et al. 2013; Janusz et al. 2017). Based on the redox-potential (affinity of a chemical species to acquire electrons) of the reaction that laccases catalyze, they are divided into low and high redox-potential enzymes. Low redox-potential enzymes are produced by bacteria, plants, and insects, whereas high redox-potential enzymes are produced by fungi (Munk et al. 2015).

Laccases contain four copper atoms in their catalytic sites and three cupredoxin domains (a conserved typical rigid Greek-key arrangement, consisting of an eight-stranded β-sandwich); however, some bacterial and fungal laccases contain two cupredoxin domains (Hakulinen and Rouvinen 2015).

The four catalytic copper ions are coordinated to conserved histidine residues as follows: (i) one Cu is in a type 1 Cu (T1) that shows a strong absorption around 600 nm, responsible for the characteristic blue color of laccases, and; (ii) the remaining three Cu atoms are coordinated by a highly conserved motif of four histidine residues, called as trinuclear cluster (TNC). The TNC contains a type 2 Cu (mononuclear, T2) and two type 3 Cu (binuclear, T3), both types are electronically and spectrally different to T1. The TNC is the binding site of O_2, where the four-electron reduction happens, with the release of two molecules of water (Giardina

et al. 2010; Kosman, 2010). Briefly, as shown in Fig. 2, the organic substrate (a phenolic compound) is oxidized in the catalytic site by one electron transfer. In this reaction, the substrate undergoes the mono-electronic oxidation of the Cα, catalyzed by the T1-Cu, followed by the Cα-Cβ and aryl–alkyl cleavage. Then four electrons acquired by the T1-Cu are transferred to the TNC through an intramolecular electron transfer pathway. In the TNC the O_2 is reduced and, two molecules of H_2O are released. This mechanism also involved the production of intermediates: the enzyme

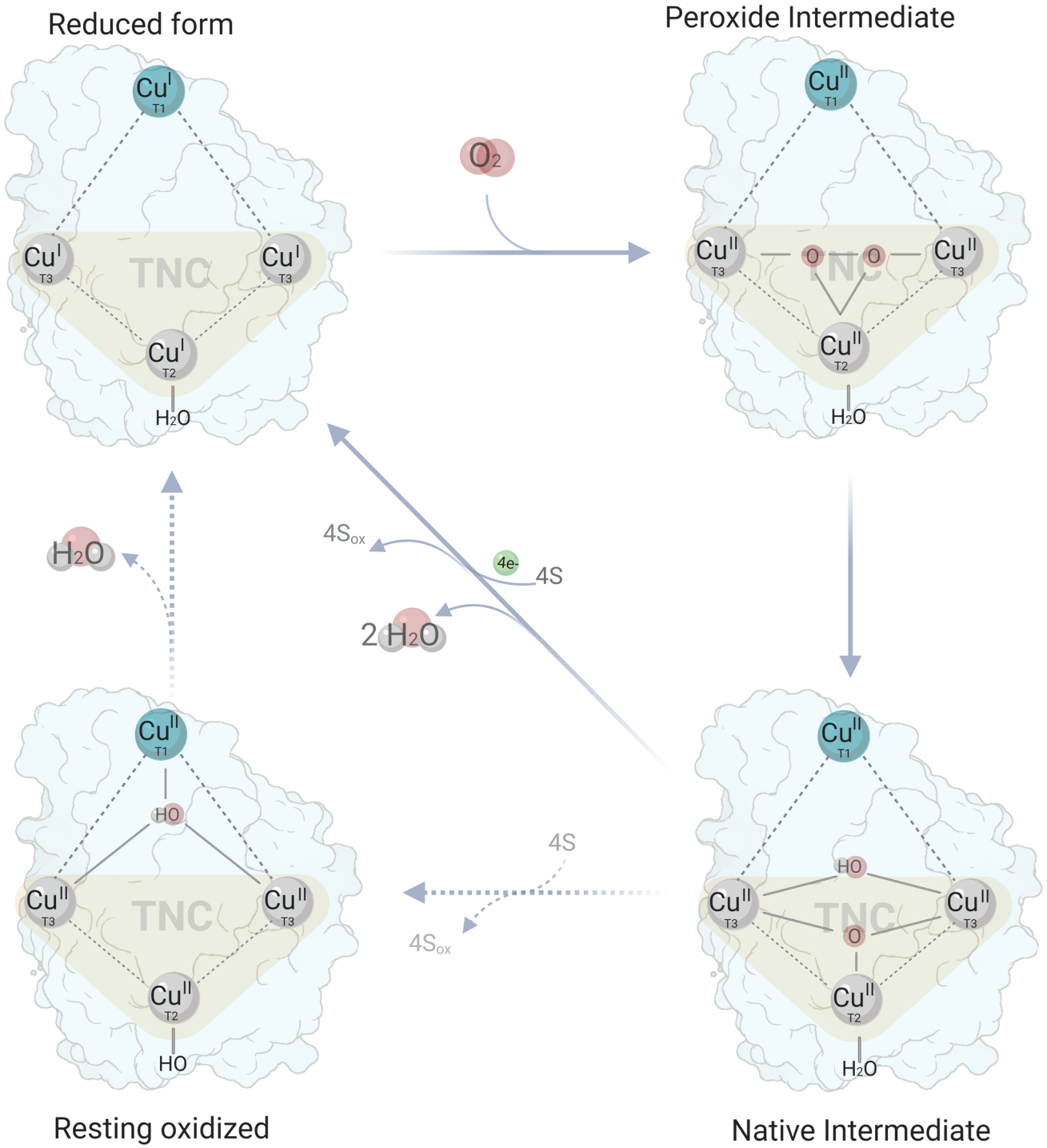

Fig. 2 Simplified catalytic cycle of laccases, showing the mechanism of oxide-reduction of the enzyme and substrate. Dot arrows indicate the steps that are not part of the catalytic cycle

accepts the four electrons (reduced form) and a molecule of O_2, with the production of a reaction radical (peroxide intermediate, PI), that may react non-enzymatically forming a native intermediate (NI). The release of the molecule of water undergoes the transformation of the NI, with the recycling of the resting enzyme (Solomon et al. 2008).

These enzymes are found in a wide variety of organisms such as plants (Dean and Eriksson 1994; Shiba et al. 2000), insects (Arakane et al. 2005; Coy et al. 2010), fungi (Leonowicz et al. 1999; Morozova et al. 2007; Millati et al. 2011) and bacteria (Alexandre and Zhulin 2000) as shown in Table 1.

Laccases are extracellular enzymes, but a few reports suggest that some laccases have a periplasmic or cytoplasmic localization. Structurally, they can be found as monomeric, dimeric or trimeric glycoproteins. Fungal and bacterial laccases usually show a low degree of glycosylation as compared with plant laccases, being the addition of mannose, glucose, hexoamines, galactose, fucose and/or arabinose the main glycosylation moiety already found. These glycosylations are involved in the secretion, proteolytic susceptibility, activity, copper holding capacity, and thermal stability of laccases (Nunes and Kunamneni 2018). They have a molecular size around 50–90 kDa (Chandra and Chowdhary 2015; Janusz et al. 2017), with a broad range of

Table 1 Lignin-degrading enzymes from Fungi and Bacteria

Organism		Enzymes produced	References
Fungi	*Auricularia auricular-judae*	DyP	Liers et al. (2010)
	Bjerkandera adusta	MnP; VP	Heinfling et al. (1998)
	Bjerkandera fumosa	VP	Nowak et al. (2006)
	Ceriporiopsis subvermispora	Laccase, MnP	Lobos et al. (1994), Baldrian (2006)
	Dichomitus squalens	MnP	Périé et al. (1996)
	Irpex lacteus	DyP	Salvachúa et al. (2013)
	Phanerochaete chrysosporium	LiP, MnP	Glenn et al. (1983), Glenn and Gold (1985)
	Phanerochaete eryngii	Laccase, MnP; VP	Heinfling et al. (1998), Ruiz-Dueñas et al. (1999), Baldrian (2006)
	Phanerochaete sordida	LiP, MnP	Sugiura et al. (2009)
	Phlebia radiata	Laccase,LiP; MnP	Lundell et al. (1993), Moilanen et al. (1996), Baldrian (2006)
	Phlebia tremellosa	VP	Vares et al. (1994)
	Pleurotus ostreatus	VP	Ruiz-Dueñas et al. (2001)
	Thanatephorus cucumeris	DyP	Kim et al. (1995)
	Tramates hirsuta	Laccase	Baldrian (2006)
	Tramates ochracea	Laccase	Baldrian (2006)
	Tramates versicolor	Laccase, LiP, MnP	Welinder et al. (1992), Johansson et al. (1993), Paice et al. (1993), Baldrian (2006)
Bacteria	*Amycolatopsis sp.*	DyP	Brown et al. (2011), Brown et al. (2012)
	Bacillus subtilis	Laccase, DyP	Martins et al. (2002), Min et al. (2015)
	Bacillus atrophaeus	Laccase	de Gonzalo et al. (2016)
	Bacillus licheniformis	Laccase	Koschorreck et al. (2008)
	Bacillus pumilus	Laccase	de Gonzalo et al. (2016)
	Escherichia coli	DyP	de Gonzalo et al. (2016)
	Pseudomonas fluorescens	DyP	Rahmanpour and Bugg (2015)
	Rhodococcus jostii	DyP	Ahmad et al. (2011)
	Streptomyces griseus	Laccase	Suzuki et al. (2003)
	Streptomyces ipomoea	Laccase	Margot et al. (2013)
	Streptomyces lavendulae	Laccase	Claus (2004)
	Streptomyces cyaneus	Laccase	Arias et al. (2003)
	Steptomyces viridosporus	DyP	de Gonzalo et al. (2016)
	Steptomyces coelicolor	Laccase, DyP	Machczynski et al. (2004), de Gonzalo et al. (2016)
	Thermus thermophilus	Laccase	Miyazaki (2005)
	Thermobifida fusca	DyP	Adav et al. (2010)
	Thermomonospora curvata	DyP	Chen et al. (2015a, b)

pH (3–7 and 4–8 for fungal and bacterial laccases, respectively) and an acid or slightly acid optimal pH (3.6–6.8) (Bollag and Leonowicz 1984; Rosconi et al. 2005; Chauhan et al. 2017). Usually laccases are pH- and thermo-stable proteins, which are important features for their potential biotechnological applications (Castro-Sowinski et al. 2002; Hildén et al. 2009).

Laccases have many physiological functions. They are involved in both anabolic (morphogenesis of plants) and catabolic (degradation of lignin) pathways (Janusz et al. 2020). Laccases that oxidize lignin with a low redox potential can improve their activity by the addition of mediator compounds, which act as an intermediate substrate. These enzymes can also oxidize non-phenolic lignin compounds with high redox potentials, by an indirect mechanism (Bourbonnais and Paice 1990). The mediators are small size molecules that diffuse into the complex lignin structure, thus easily reaching the target substrate. Many compounds have been reported as mediators, such as 2,20-azinobis-(3-ethylbenzothiazoline-6-sulphonic acid) (ABTS), 2,2,6,6-tetra-methyl-1-piperidinyloxy (TEMPO), 1-hydroxybenztriazole (HBT), violuric acid (VA), promazine (PZ) and 1-nitroso-naphthol-3,6-disulfonic acid (NNDS); and natural mediators as acetosyringone (AS), syringaldehyde, sinapic acid, vanillin, acetovanillone, *p*-coumaric acid, ferulic acid, and sinapic acid (Kunamneni et al. 2008).

Laccases do not depolymerize lignin in its native state, but they do affect its surface. Thus, most biochemical studies about laccases have been conducted using lignin model compounds as substrates (Munk et al. 2015). These compounds usually are cleavage between the C1 and C2 (Cα–Cβ cleavage), and between Cα and the aryl group (alkyl–aryl cleavage), and do need mediators for activity. Instead, for the cleavage of non-phenolic compounds, laccases do need mediators (Janusz et al. 2020). For examples of laccase-catalyzed oxidation reactions using model lignin-related compounds, please see Fig. 3.

Lignin-degrading heme-peroxidases

Lignin-degrading heme-peroxidases (MnP, LiP, VP and DyP) (Ruiz-Dueñas and Martínez 2009; Lambertz et al. 2016) catalyze the H_2O_2-dependent oxidative degradation of specific components of the lignin structure, including phenolic as well as non-phenolic ones, using a pong–pong mechanism (Falade et al. 2017). These enzymes have an internal cavity containing the heme-group, and this cavity is connected to the protein surface by two channels. The largest one guides the hydrogen peroxide toward the heme-group (place for the exchange of electrons; oxidation of Fe^{3+} to Fe^{4+} and release of water). The second channel goes to the heme-propionate side chain and, in specialized ligninolytic peroxidases, is the place for the oxidation of the mediator molecules (such as Mn^{2+} to Mn^{3+}). Heme-peroxidases have a peroxidase catalytic cycle similar to that from horseradish peroxidases. The catalytic cycle involves three steps: (i) oxidation of the native enzyme by H_2O_2 (formation of the compound I; oxo-feryl intermediate); (ii) chemical reduction of compound I (formation of compound II) by the donation of one electron from the substrate (substrate oxidation); (iii) full oxidation of the substrate (donation of another electron) to compound II (the enzyme goes back at native resting state) (Wong 2009) (Fig. 4).

Lignin peroxidases

Lignin peroxidases (LiPs) are oxido-reductases that oxidize a wide range of aromatic compounds, including lignin and its derivatives. Based on the information found in the Protein Data Bank (PDB), LiPs are glycosylated monomeric hemeproteins, with a molecular weight in the range of 38–48 kDa, a isoelectric point that ranges from 3.2 to 4.7 and an acid optimum pH (pH 3, using veratryl alcohol as substrate) as compared to other peroxidases (Pollegioni et al. 2015; Falade et al. 2017). LiPs are globular proteins formed by eight α-helices arranged in two domains, structure stabilized by a disulfide bridge. The crystal structure of LiPs (e.g. the LiP from *Phanerochaete chrysosporium*; PDB-ID: 1LLP) shows a conserved tryptophan residue, probably essential for their catalytic activity (Choinowski et al. 1999; Sigoillot et al. 2012). These enzymes are commonly produced in different isoforms (with different degree of glycosylation, and therefore different isoelectric points), and the production of these isoforms is mainly determined by the chemical composition of the growth medium where they are produced (Janusz et al. 2017). These enzymes are found mainly in fungi as shown in Table 1.

LiPs oxidize various high redox potential aromatic and non-phenolic aromatic compounds, with or without a mediator; however, the activity increases when a redox mediator such as veratryl alcohol (VA) is used (Wong 2009; Houtman et al. 2018). In a reaction that proceeds without a mediator, the first (or immediate) oxidation product is an aryl cationic radical; this one is then spontaneously cleavage at the C1 and C2 at the propyl side chain as part of the lignin depolymerization process (Houtman et al. 2018) (see Fig. 5a, b). A few examples of other phenolic compounds chemically oxidized by LiPs are: vanillyl alcohol, catechol, acetosyringone, syringic acid, and guaiacol, etc. (Wong 2009).

Manganese peroxidases

Manganese peroxidases (MnPs) are lignin-degrading enzymes commonly secreted by white and brown rot

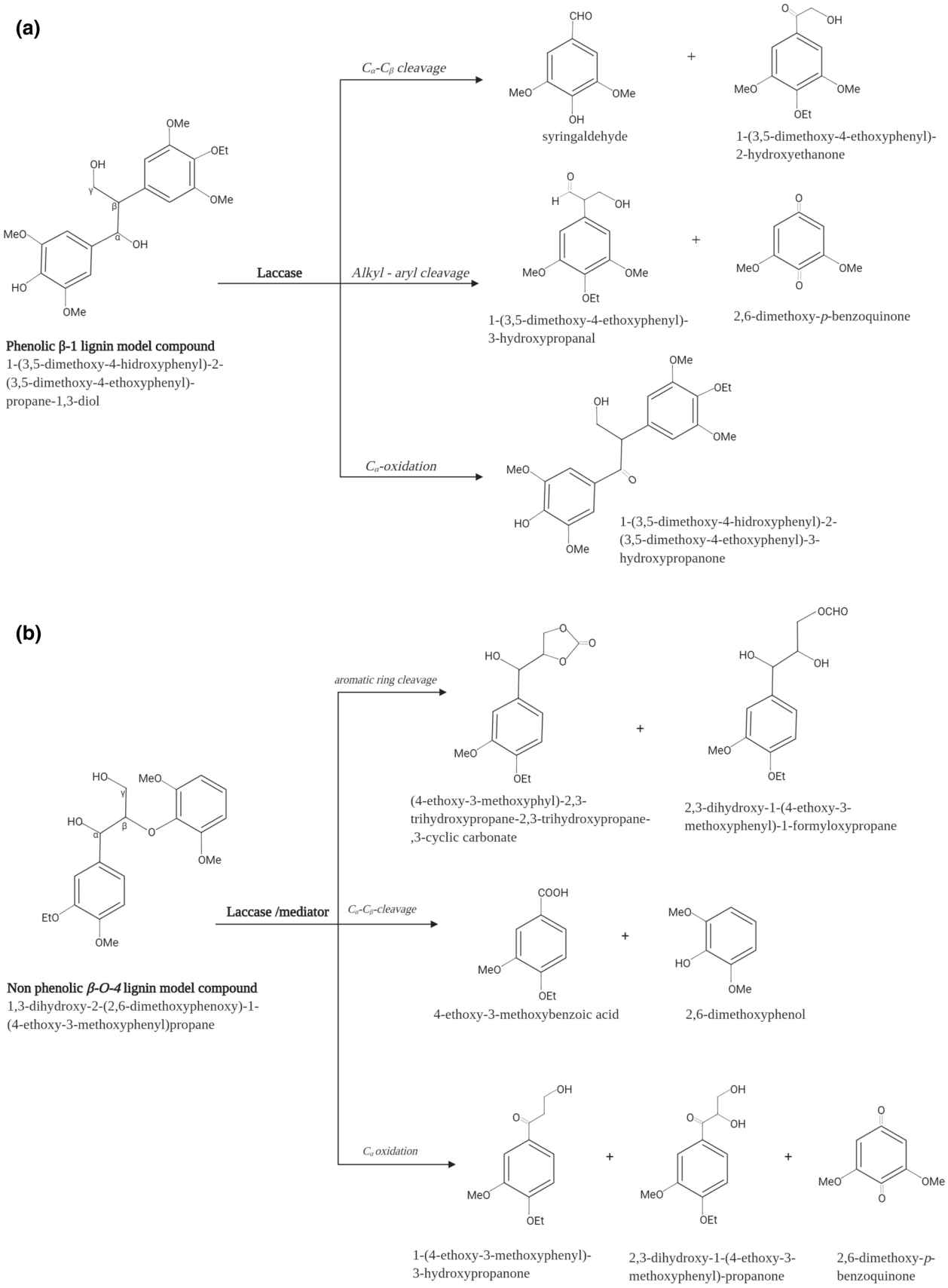
(a)
Laccase
C_α-C_β cleavage
Alkyl - aryl cleavage
C_α-oxidation
syringaldehyde
1-(3,5-dimethoxy-4-ethoxyphenyl)-2-hydroxyethanone
1-(3,5-dimethoxy-4-ethoxyphenyl)-3-hydroxypropanal
2,6-dimethoxy-p-benzoquinone
1-(3,5-dimethoxy-4-hidroxyphenyl)-2-(3,5-dimethoxy-4-ethoxyphenyl)-3-hydroxypropanone
Phenolic β-1 lignin model compound
1-(3,5-dimethoxy-4-hidroxyphenyl)-2-(3,5-dimethoxy-4-ethoxyphenyl)-propane-1,3-diol
(b)
Laccase /mediator
aromatic ring cleavage
C_α-C_β-cleavage
C_α oxidation
(4-ethoxy-3-methoxyphyl)-2,3-trihydroxypropane-2,3-trihydroxypropane-,3-cyclic carbonate
2,3-dihydroxy-1-(4-ethoxy-3-methoxyphenyl)-1-formyloxypropane
4-ethoxy-3-methoxybenzoic acid
2,6-dimethoxyphenol
1-(4-ethoxy-3-methoxyphenyl)-3-hydroxypropanone
2,3-dihydroxy-1-(4-ethoxy-3-methoxyphenyl)-propanone
2,6-dimethoxy-p-benzoquinone
Non phenolic β-O-4 lignin model compound
1,3-dihydroxy-2-(2,6-dimethoxyphenoxy)-1-(4-ethoxy-3-methoxyphenyl)propane

◂**Fig. 3** Different pathways of oxidation of lignin model compounds by laccase. **a** Three different pathways of oxidation of phenolic β-*1* lignin model compound. **b** Three different pathways of oxidation of non-phenolic β-*O*-4 lignin model compounds in the presence of a mediator. Adapted from Wong, (2009)

basidiomycetes (see Table 1), that play an important role as waste decomposers (Singh and Singh 2016). MnPs are mainly produced by fungi and; despite their slower rate of degradation, bacteria and algae also produce these enzymes (de Oliveira et al. 2009; Ng et al. 2015). MnPs are monomeric heme-glycosylated proteins organized in two domains, with the heme-group located in between domains. They are globular proteins formed by 11–12 α-helices stabilized by five disulfide bonds (one involved in the coordination of Mn) and two Ca^{2+} binding sites (Bugg et al. 2011; Chowdhary et al. 2018). MnPs are found in multiple isoforms with different isoelectric points and, they have a molecular weight size that ranges from 32 to 75 kDa, at least in fungus (Hofrichter 2002; Wong 2009).

MnPs use a manganese ion as mediator. They catalyze the oxidation of Mn^{2+} to Mn^{3+}, which in turn oxidizes a wide range of phenolic substrates including lignin phenolic compounds and some organic pollutant (Chandra and Madakka 2019) (see Fig. 5c for reactions). The mechanism of reaction is initiated by the transfer of two electrons from the heme-group (Fe^{3+}) to H_2O_2 (production of an oxidized intermediate called compound I or oxo-porphyrin radical complex MnP-Fe^{4+}, and H_2O); then, the compound I binds a chelated Mn^{2+} ion with a further donation of an electron from Mn^{2+} to the radical (formation of the compound II or Fe^{4+} oxo-porphyrin complex and, Mn^{3+}); compound II oxidizes another Mn^{2+} to Mn^{3+} and the Fe^{4+} present in the heme-group is reduced to Fe^{3+}, accompanied by the release of a second molecule of water. The Mn^{3+} (chelated to carboxylic acids, such as oxalate and malate) works as an oxidant of phenolic compounds, producing a phenoxy radical intermediate that yields various degradation products (Chandra and Madakka 2019). The Mn^{3+} is a small size and very reactive compound, with high redox potential, that diffuses easily in the lignified cell wall and oxidize phenolic compounds (Pollegioni et al. 2015; Chowdhary et al. 2018).

Versatile peroxidases

Versatile peroxidases (VPs) are also glycosylated monomeric proteins with molecular weight sizes that range from 40 to 50 kDa and, an isoelectric point between 3.4 and 3.9 (Janusz et al. 2017). These enzymes have polyvalent catalytic sites (for the oxidation of manganese and low- and high-redox potential compounds), and features that resembled LiPs, MnPs and other microbial peroxidases; therefore, they have been called as versatile enzymes. According to the crystal structure of the VP from *Pleurotus eryngii* (PBD ID: 2BOQ), they have 11 or 12 α-helices, four disulfide bridges, two structural Ca^{2+} binding sites and, a Mn^{2+} binding site (a triad of Glu/Glu/Asp residues), as found in MnPs. The structure of VPs shows an exposed tryptophan (like found in LiPs) involved in a long-range electron transfer towards the heme-group (Pérez-Boada et al. 2005; Sigoillot et al. 2012).

Their catalytic cycle is similar to the cycles described above, including the formation of compounds I and II, but due to the widest range of potential substrates, the cycle for VPs is more complex. The molecular mechanism is as follows. The heme-group of the resting enzyme (Fe^{3+}) binds the hydrogen peroxide, leading to the formation of compound I (Fe^{4+} oxo-porphyrin radical complex with an activated heme) and the release of water. Compound I then reacts with either an aromatic compound (AH) or a Mn^{2+}, producing compound II and Mn^{3+}; then the compound II goes to the resting enzyme form thanks to the oxidation of a second molecule of Mn^{2+} (and release of water). The radical products that are formed are unstable and undergo non-enzymatic reactions (breakdown of different linkages, yielding simple breakdown products) (Sigoillot et al. 2012; Ravichandran and Sridhar 2017). For the occurrence of VPs see Table 1.

Dye-decolorizing peroxidases

Dye-decolorizing peroxidases (DyPs) constitute a family of heme-peroxidases which have received high attention due to their novel substrate specificity and reactivity. These characteristics encouraged many investigators to study their potential applications as ligninolytic, decolorizing and bioremediation enzymes.

DyP proteins have been subdivided into four types (A, B, C and D) based on their primary sequences (Sugano 2009). DyP type A enzymes have mainly been reported in bacteria, and contain a TAT-dependent translocation signal sequence, suggesting that these enzymes have a extracellular function. Class B and C are cytoplasmic enzymes, and their localization suggest that they are involved in the intracellular metabolism of phenolic compounds, in both bacteria and fungi (Koua et al. 2009; Colpa et al. 2014). Class D DyPs are less studied and are mainly from fungal sources. Examples of DyP enzymes from fungi and bacteria are summarized in Table 1.

DyPs have a highly conserved 3D structure that contains a non-covalently bound heme-group. These enzymes show a molecular size that ranges between 40 and 60 kDa and can adopt a quaternary structure (from monomeric to hexameric structure). The C-terminal domain contains the heme-binding motif with a highly conserved histidine residue, and

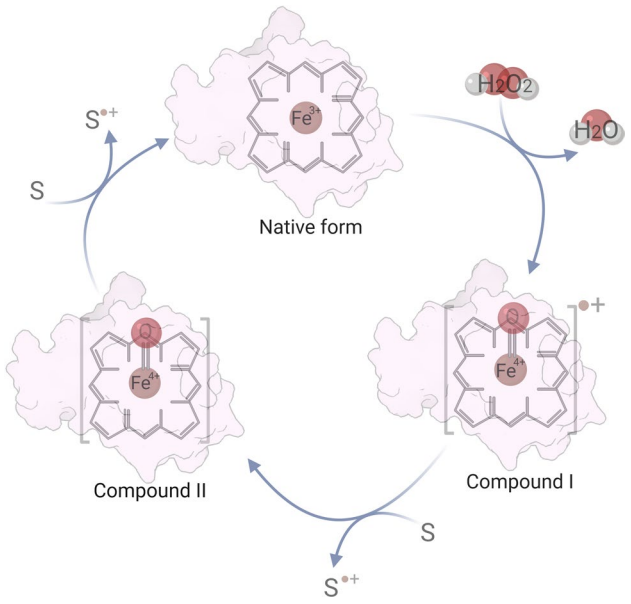

Fig. 4 Catalytic cycle of lignin-degrading heme-peroxidases. Compounds I and II are intermediates with different oxidation state of the heme-group

a characteristic GXXDG motif. Some reports suggest that in fungal DyPs, the conserved aspartate (D) of this motif is responsible for the interaction with a molecule of H_2O_2, thereby allowing the formation of compound I (Colpa et al. 2014). Based on phylogenetic studies, DyP enzymes may be ancient peroxidases as compared with general peroxidases; and they have bifunctional activity (hydrolase and peroxidase) (Sugano 2009).

The DyP catalytic mechanism is similar to those found in other peroxidases (Fig. 4). These enzymes can oxidize substrates that are too large to fit in the active site (Yoshida et al. 2011; Singh et al. 2012) as described below. Long-range electron transfer (LRET) studies allowed to decipher how the electron transfer-flow goes from the heme cofactor to a surface-exposed oxidation site (facilitated by Tyr and Leu residues), explaining how DyPs react with bulky substrates, such as lignin (Colpa et al. 2014). These enzymes decolorized diverse xenobiotic dyes as anthraquinone (including Reactive Blue 5), azo dyes, phenolic compounds such as 2,6-dimethoxy-phenol, guaiacol, veratryl alcohol (Sugano 2009), as well as also oxidize β-*O*-4 non-phenolic and phenolic lignin model compounds (Lambertz et al. 2016). For an example of a DyP-catalyzed oxidation reaction using a model lignin-related compound, please see Fig. 5d.

Industrial applications

Based on the market analysis report from Grand View Research (https://www.grandviewresearch.com/industry-analysis/lignin-market) the global market for lignin in 2019 was predicted at USD 954.5 million and the estimation predicts an increase of 2.0% for 2027. According to the BBC Research (https://www.bccresearch.com/partners/verified-market-research/global-industrial-enzymes-market.html), the global market for enzymes with industrial applications was valued at USD 4.58 billion in 2016, and projected a growth of 5.6% (USD 7.48 billion) by 2025. This huge market has been accompanied with a high number of published patents. In Table 2 are summarized the most relevant patents registered during the last decade (according to the World Intellectual Property Organization, https://www.wipo.int, and the European Patent Office, https://www.epo.org) and their potential industrial applications. In this scenario (worldwide market and patents), lignin-degrading enzymes have showed a great industrial interest and have revealed a wide variety of biotechnological applications. Some of these applications are described below.

Pulp and paper industry

The physical/chemical elimination of lignin from lignocellulosic biomass, during the pulp and paper production, is costly and a very polluting procedure. Usually, the cellulosic pulp is produced from wood by chemical delignification, mechanical separation of the fibers, or a combination of both methods. The production of cellulosic pulp has several stages: (1) the mechanical production of wood chips; (2) its entry into the digester, where with high pressure and temperature the chemical bonds between lignin and cellulose are broken (the Kraft process), followed by filtering and washing of the brown cellulose residue; (3) the bleaching of the cellulosic pulp (that still has 1–2% lignin), generally by the Elemental Chlorine Free (ECF) method; and (4) the drying of the cellulosic pulp, that still contains a water content of 10%.

Lignin-degrading enzymes can be used after the step 2), allowing the removal of the lignin residue that was not removed by the physical/chemical methods. The biological alternatives for the degradation of this material have been studied thoroughly (Barreca et al. 2003). LiP, MnP, VP, DyP and laccases can be used in the delignification and biobleaching of wood pulp, replacing the traditional non-environmentally friendly delignification treatment. Among lignin-degrading enzymes, laccases are the most studied enzymes due to their: (i) high production rate and activity by fungi, which are considered among the main decomposers of wood, (ii) great capacity for lignin degradation, (iii)

use of oxygen (as an electron donor) as co-substrate and, (iv) production of an eco-friendly end-product, water (Abdel-Hamid et al. 2013).

The main impact of using laccases in the degradation of lignin is that the industrial end-product (paper pulp) shows a better quality (increase in bleaching, brightness and resistance) as compared with other bleaching methods. However, the lignin degradation by laccases is limited by their instability when working under industrial conditions and by their low redox potential. The use of mediators overcome these difficulties and enhances the degrading capacity of laccases (Munk et al. 2015). Currently, more than 100 mediator compounds are known (natural or synthetic mediators involved in the oxidation of lignin and lignin model compounds). Laccases are versatile biocatalysts, that may also remove lipophilic wood extractive constituents (e.g. resins), which cause important problems at industrial level. Laccases alone or along with peroxidases can also act on the toxic compounds released in paper industry effluents (e.g. black liquors that contain chlorolignins, chlorophenols, and chloroaliphatics), transforming them in nontoxic compounds (Singh 2017).

Unfortunately, the enzyme-catalyzed depolymerization of lignin also depends on the balance between depolymerization and repolymerization reactions, which produce either polymeric or aromatic products (Zeng et al. 2017). The factors that control the balance between depolymerization and polymerization are still not clearly understood. During the delignification treatment many organic acids are released (decrease of the pH to 2–4). In this condition, carbonium ions are produced from the lignin and they polymerize with the aromatic rings of the lignin, forming complex structures. In order to avoid repolymerization, the addition of highly nucleophilic compounds has been effective. Lai et al. (2018) showed that the addition of the nucleophilic compound 2-naphthol-7-sulfonate improves the enzymatic hydrolysis. This is probably due to the production of high negative surface charges, a lower enzyme non-productive binding, and the increase in the accessibility of the enzyme to the cellulose of pretreated substrates. In agreement with this report, Galliano et al. (1991) reported that the combined use of laccases and peroxidases minimize the repolymerization compared with physical–chemical treatments. As well, the addition of the flavin-dependent dehydrolipoamide dehydrogenase from *Thermobifida fusca* (prevents the dimerization of lignin model compounds) could be used as accessory enzyme for lignin degradation (Rahmanpour et al. 2016).

Another potential use of lignin-degrading enzymes is the degradation and/or deinking of waste newspapers, laser printed papers and written papers. The combined use of cellulotytic, hemicellulotytic and lignin-degrading enzymes is usually preferred compared with the conventional chemical deinking processes. The biological process has attracted attention because of its high efficacy and minimum environmental impact. The chemical process requires a large amount of chemicals that are unfriendly for the environment; thus, it is non-recommended (Saxena and Chauhan 2016). The deinking of paper waste was achieved by the use of a laccase-violuric acid mediator system in combination with cellulases and hemicellulases. The delignification process can also be done by using laccases and xylanases, without a mediator system, suggesting again that the use of a combination of enzymes that acts synergistically is a good alternative for the recycling of waste inked paper (Xu et al. 2009; Singh 2017). Among other examples, the laccase from *Myceliophthora thermophile* was used in combination with a natural mediator (methyl syringate) and showed good results in the decolorization rate for red papers (Valls et al. 2019). However, the cost–benefit analysis of using a laccase-mediator system has still to be considered. Interestingly, natural mediators are ecological and cost-effective alternative to synthetic mediators (Morozova et al. 2007; Virk et al. 2012), and the search for this kind of molecules are in progress.

Biofuel industry

Production of ethanol as fuel using lignocellulosic substrates is an alternative to the use of fossil fuel. A wide variety of natural products can be used as a source of sugars for the production of bioethanol: sugar beets, sugar cane, starch (wheat, corn, etc.), lignin (wood, straw), etc. Currently, the production of second generation biofuels (unlike those of the first generation that use raw materials that could be used for food production) not only uses lignocellulosic materials as a starting material, but also uses various by-products or wastes from other industries. The bioconversion of these materials in ethanol involves four general processes: pretreatment (delignification), hydrolysis (saccharification by cellulases), fermentation, and distillation of bioethanol (Alvira et al. 2010; Dogaris et al. 2013). The use of lignin-degrading enzymes in the pretreatment of lignocellulosic biomass provides an alternative to the thermal and chemical pretreatment, but the enzymatic pretreatment is less effective than the traditional one.

Laccases are mainly used in the bleaching and delignification in the paper industry, but they are also used for the delignification of some biofuel feedstock materials, e.g. cotton gin trash, corn stover, wheat straw, elephant grass and eucalypt wood. Unfortunately, the use of specific mediator compounds for improving the delignification of these feedstock materials has not been fully investigated (Plácido and Capareda 2015). The combination of synergic enzymes such as LiP, MnP and laccase, isolated from *Pleurotus ostreatus,* has shown good performance in the delignification of sugarcane bagasse as compared to the traditional treatments

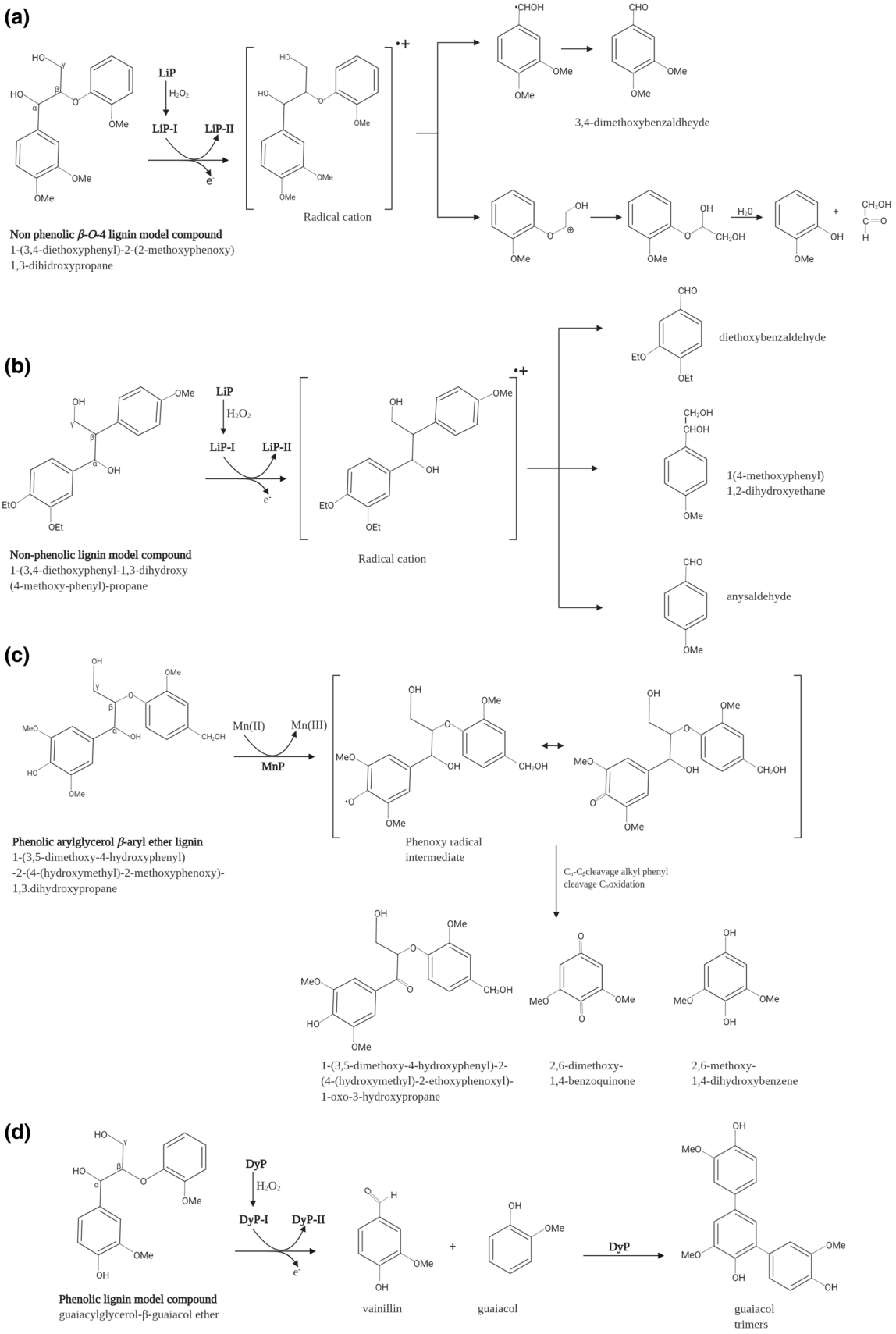
(a)
LiP
H_2O_2
LiP-I
LiP-II
e⁻
Radical cation
3,4-dimethoxybenzaldheyde
Non phenolic β-O-4 lignin model compound
1-(3,4-diethoxyphenyl)-2-(2-methoxyphenoxy)
1,3-dihidroxypropane
(b)
LiP
H_2O_2
LiP-I
LiP-II
e⁻
Radical cation
diethoxybenzaldehyde
1(4-methoxyphenyl)
1,2-dihydroxyethane
anysaldehyde
Non-phenolic lignin model compound
1-(3,4-diethoxyphenyl-1,3-dihydroxy
(4-methoxy-phenyl)-propane
(c)
Mn(II)
Mn(III)
MnP
Phenoxy radical
intermediate
C_α-$C_\beta$cleavage alkyl phenyl
cleavage $C_\alpha$oxidation
1-(3,5-dimethoxy-4-hydroxyphenyl)-2-
(4-(hydroxymethyl)-2-ethoxyphenoxyl)-
1-oxo-3-hydroxypropane
2,6-dimethoxy-
1,4-benzoquinone
2,6-methoxy-
1,4-dihydroxybenzene
Phenolic arylglycerol β-aryl ether lignin
1-(3,5-dimethoxy-4-hydroxyphenyl)
-2-(4-(hydroxymethyl)-2-methoxyphenoxy)-
1,3.dihydroxypropane
(d)
DyP
H_2O_2
DyP-I
DyP-II
e⁻
vainillin
guaiacol
DyP
guaiacol
trimers
Phenolic lignin model compound
guaiacylglycerol-β-guaiacol ether

◂**Fig. 5** Different pathways of oxidation of lignin model compounds by heme peroxidases. **a** LiP-catalyzed oxidation of non-phenolic β-*O*-4 lignin model compound. **b** LiP-catalyzed oxidation of non-phenolic diarylpropane lignin compound. **c** MnP-catalyzed oxidation of phenolic β-*aryl* lignin compound. **d** DyP-catalyzed oxidation of phenolic guaicylglycerol-β-guaiacol lignin compound. Adapted from Wong (2009) (**a**–**c**) and de Gonzalo et al. (2016) (**d**)

(Asgher et al. 2013). These treatments can be done using the enzymes or the enzyme-producing microbes. In this regard, the enzymatic treatments (with commercial or native enzymes) shows better delignification results as compared with the microbial pre-treatment, but the main challenge faced is the reduction of the cost of the process (Plácido and Capareda 2015).

Among recent reports, we can mention the high lignin depolymerization potential of laccase produced by the white-rot basidiomycete *Marasmiellus palmivorus*. This enzyme successfully degraded the lignin from *Eucalyptus globulus* wood without any mediator. Besides, the authors reported a 10% increase in the glucose yield after saccharification (Schneider et al. 2019).

The traditional pretreatment of the lignocellulosic material releases several enzyme inhibiting compounds; these compounds may influence the efficiency of the saccharification process (inhibition of cellulases and hemicellulases), with a subsequent reduction in the production of ethanol by fermentation. These inhibiting compounds are furans (hydroxymethyl furfural, furfural), organic acids (acetic, formic, levulinic) and phenolic compounds (with the highest inhibitory potential) (Kim et al. 2011). Phenolic compounds can inhibit up to 50% of cellulase activity (Ximenes et al. 2010). Polyphenols form adducts with proteins, which causes their precipitation and the inhibition of enzymes (cellulases and amylases, among others). After lignin, tannins (mainly tannic acid) are the most abundant polyphenols in plants. Tannin content can be reduced by treatment with laccases, as demonstrated in cocoa powder (Mensah et al. 2012). Pretreatment of apple peels with laccases proved to be very efficient in degrading phenolic compounds and increasing the degree of released fermentable sugars. In this case, the use of laccases, cellulases and pectinases increased the yield of bioethanol production, as demonstrated by Parmar and Rupasinghe (2013), who reported 19 g of ethanol per 100 g of dry pomace. Thus, lignin-degrading enzymes can also be used for the detoxification of phenolic compounds that act as inhibition-enzyme molecules.

Textile industry

Based on the Market Analysis Report (https://www.grandviewresearch.com/industry-analysis/textile-market) the global textile market was valued at USD 961.5 billion in

Table 2 Industrial applications and patents of lignin-degrading enzymes published in the last decade

Enzyme	Applications	Patent numbers
Laccase	Paper and pulp, food, textile, biofuels, nanotechnology, synthetic chemistry, cosmetics, distillery industry and bioremediation	WO2020002187; IN201831034933; KR102076120B1; CN109234266A; KR102052132B1; CN108103036A; CN108192878A; CN107956177A; CN108570855A; CN106965289A; CN105543250A; CN105417725A; CN105639717A; CN105255842A; CN105441412A; CN105274067A; CN105420204A; CN105671011A; KR101806223B1 CN104478068A; CN104831573A; CN104726520A; JP2014042511A; CN104047062A; CN103556517A; CN103571801A; WO2014009849A2; CN100497551C; CN102899195A; CN102583769A WO2012054485A1; CN102310451A; CN102174484A; CN102234948A
LiP	Paper and pulp, food, textile, biofuels, cosmetic industry and bioremediation	EP3626310; CN109499040A; CN109136003A; CN108841800A; CN108977433A; KR20170000740A; US2016101034A1; CN103964567A; CN102719483A; WO2012153336A2; CN102154810A; CN101857859A
MnP	Paper and pulp, food, textile, biofuels pharmaceutical industry and bioremediation	CN109504666; JP2012175911A; WO2012025650A1
VP	Industrial biocatalyst, biofuels and bioremediation	ES2342701A1; WO2012025650A1
DyP	Paper and pulp, food, textile, effluent treatments, biofuels, cosmetics industry and bioremediation	CN108676783A; CN110016468A; CN111073867A; CN109777789A; CN109943544A; CN107460176A; CN106754803A

Data were obtained from the EPO (https://www.epo.org) and WIPO (https://www.wipo.int) database or the review of the literature regarding the major industrial applications of the enzymes described in the text. The patent number indicated here corresponds to that reported in EPO

APx ascorbate peroxidase, *CcP* cytochrome c peroxidase, *CP* catalase-peroxidases, *APx-CcP* hybrid A peroxidases, *LiP* lignin peroxidase, *MnP* manganese peroxidase, *VP* versatile peroxidase, *Prx* other peroxidases

2019. The report also estimated an increase of 4.3% from 2020 to 2027. This industry improves the appearance of fabrics using many chemicals for finishing and dyeing. Dyes are commonly used in textile, tannery, cosmetic and food industries, and they are found in environmental samples. They are hazardous micropollutants that threat the animal and human health (Tkaczyk et al. 2020). The textile industry is among the major environmental pollution industries worldwide. It releases large volumes of wastewaters or dye effluents, and different national environmental legislations have to control the way different industries process their effluents (Yaseen and Scholz 2019).

Among potential bioremediation strategies for dyes degradation, laccase and peroxidase (LiP, MnP and DyP) enzymes have been studied. In addition, these enzymes also degrade recalcitrant aromatic pollutants (Falade et al. 2017). DyP peroxidases are especially useful because of their ability to degrade anthraquinones that are widely used as textile dye (Abdel-Hamid et al. 2013). The purified laccases from *Trametes hirsuta* and *Sclerotium rolfdii*, used in combination with redox mediators, were successful for the degradation of indigo dye, both in fabrics and in effluents (Campos et al. 2001). Also Pazarlioğlu et al. (2005) reported the effective use of the laccase from *Tremetes versicolor* during the discoloring of fabrics.

In the last decade, the use of bleaching laccases has increased. Denim washing with enzymes is one of the most widely used techniques in the textile industry. The laccase/mediator system is capable of bleaching indigo dye in denim, producing fabrics with various bleached appearances. Currently, laccases have replaced the use of hypochlorite (that gives yellowness to the fabrics), which if not neutralized properly, attacks cotton and reduces its strength (Rodriguez-Couto 2012; Chowdhary et al. 2018). In denim garment processing, laccases are used for desizing and abrasion look, causing minimal fiber damage. In addition, laccases assist in effluent discoloring and if it is immobilized, the enzyme can be reused (Muthu 2017). On the other hand, the use of laccases to bleach cotton (Basto et al. 2007), to synthesize new dyes (Mostafa and Samarkandy 2005) and for the wool anti-shrink treatment (Lantto et al. 2004) has been reported. Although enzymatic denim bleaching is done mainly using laccases, other lignin-degrading enzymes have showed jean bleaching ability. For example, Zhang et al. (2018) characterized a fungal MnP and demonstrated that it was a valuable enzyme with superior performance in dye decolorization and denim bleaching, with a potential use in the textile industry. Currently there are some commercial products designed based on these enzymes for textile industry applications (Rodriguez-Couto and Toca-herrera 2006; Chowdhary et al. 2018), and some of the products that have been protected (patented) are shown in Table 2.

Effluent treatment

Chemical dyes and other toxic compounds are extensively used in various industries such as the textile, paper, cosmetic, pharmaceutical, and leather. It was estimated that 20–50% of these dyes are turned over or get lost into mill effluent; most of these dyes are persistent environmental pollutants that compromise the health of the environments (Kuhad et al. 2004). There are several mechanical and chemical methods for treating these effluents; however, the current focus of the industries is the reduction or elimination of contaminants via biological tools, such as the use of enzymes or microbes.

The pulp or paper industry generates important volumes of highly toxic wastes, as black liquors, chlorolignins, chlorophenols, chloroaliphatics, chloromethane, chloroform, among others (Ali and Sreekrishnan 2001; Pokhrel and Viraraghavan 2004). Paper mill effluents treated with the laccase and MnP from *T. versicolor*, produced the discoloration and a significant decrease in the level of chlorinated compounds (Singh 2017).

The textile industry also produces toxic effluents (toxic dyes, bleaching agents, salt acids, and alkalis) involved in the pollution of fertile soils and water bodies (Kuhad et al. 2004; Singh and Singh 2016). The decolorization and detoxification of these dye-containing effluents (azo compounds, triphenylmethane, anthraquinone, heterocyclic, polymeric, and metal-complexes, among others) by laccases (from *Pyricularia oryzae*, *Pycnoporous sanguineus*, *T. hirsuta*, and *Sclerotium rolfsii*; (Singh, 2017), LiP and other oxidative enzymes from bacteria and fungi have shown successful results (Falade et al. 2017); thus, suggesting the potential use of these enzymes in the decontamination of effluents containing toxic dyes. This cleaning procedure of decontamination using biological materials (enzymes or enzyme-producing microorganisms) is known as bioremediation. The bioremediation of dye-containing effluents using laccases and peroxidases has been recently reviewed by Theerachat et al. (2019) and Ali et al. (2019), respectively.

Laccases and peroxidases decolorize and decontaminate effluents containing dyes, but a question remains: is this process achievable at an industrial scale? The best chance is the stabilization and immobilization of enzymes (allowing the reuse of the enzymes) as was reported by Bilal et al. (2017), who worked with LiP, MnP and laccases. The immobilization of peroxidases in Fe_3O_4 magnetic nanoparticles improved the enzyme stability, efficiency and recyclability of the enzymes; the authors successfully employed these nanoparticles in the decolonization of dyes of different chemical natures in a lab-scale bioreactor (Darwesh et al. 2019). So this bioremediation technology seems to be very promising.

Food industry

Lignin-degrading enzymes have numerous applications in the food industry, including the combined used of laccases and xylanses in the bakery [improving the strength of gluten structures, crumb structure, among other properties (Selinheimo et al. 2006)].

Among oxido-reductases, laccases are among the most used enzymes, and are usually used to improve or modify foods and beverages parameters (as color, texture and flavor) by removing unwanted phenolic compounds, but also other lignin-degrading enzymes can be used (Chowdhary et al. 2018). Laccase are used in the beverage (wine, fruit juice and beer) processing. The aroma, color, taste, and texture of juices and spirits are in part determined by their content of polyphenolic compounds (e.g. some polyphenols affect the maderization process of wines). For example, the quality of wines can efficiently be improved reducing the content of specific polyphenols, without damaging its organoleptic properties. In addition, a good wine can be damaged by the use of a bad quality cork stopper (containing undesirable fungal strains or by the presence of naturally occurring phenols). This problem can be solved using cork stoppers treated with laccases (Chowdhary et al. 2018). Laccases are also used in biosensors for the detection and/determination of oxygen, aromatic amines and phenolic compound (Minussi et al. 2002; Bilir et al. 2016; Sekretaryova et al. 2016; Yashas et al. 2018). Amperometric laccase-based biosensors are also used for monitoring of chloro-substituted phenols, catecholamines, lignin, tea tannins, and also ascorbic acid in different beverages. These biosensors indirectly measure the oxidation of a solution by determining the amount of oxygen (Morozova et al. 2007; Osma et al. 2010; Rodríguez-Delgado et al. 2015).

Pharmaceutical and dermatological industry

The capacity of lignin-degrading enzymes seems promising for the pharmaceutical and cosmetic industries. For example, the combined use of a laccase and peroxidase (DyP) is effective in the degradation of melanin for skin whitening, reducing the number of melanin granules in corneocytes (Shin et al. 2019). Other peroxidases and laccases also have been reported to decolourize human hair (Nagasaki et al. 2008). The melanin is the result of the polymerization of polyphenolic compounds, similar to lignin. Some studies showed that lignin-degrading enzymes and antibiotics can be used against melanin-producing pathogenic microorganisms (Falade et al. 2017).

Flavonoids are polyphenolic compounds already known for their anti-oxidant, anti-inflammatory, anti-viral and anti-allergic activities. These compounds can be synthesized by laccase-catalyzed reactions. Among many examples, the enzymatic oxidation of catechin by a laccase from *Myceliophthora thermophyla* reached a poly-catechin with a superior superoxide scavenging activity and an inhibitory capacity of xanthine oxidase (Kurisawa et al. 2003). For a detailed information regarding the use of laccases in the cosmetic industry, please see Antonopoulou et al. 2016.

Concluding remarks, challenges and opportunities

Lignin-degrading enzymes include a wide number of proteins involved in the degradation of an important feedstock, lignocellulose matter; these enzymes (laccases and heme-peroxidases) are among the most studied over the world. These proteins contribute to the growing global trade market of enzymes because they are commonly used in many industries; however, many of the potential applications are still at a laboratory scale and the investigation for effective mediators is still in progress. In addition, they have potential uses as bioremediation agents. Many organisms are a source of highly efficient catalysts of this kind, including variants with a range of biotechnology applications, from organic synthesis to biofuels, pulping and, beyond.

A comparative study about the degradation ability of laccases and heme-peroxidases using lignin matters as main substrate is a very important issue; unfortunately, there is not a systematic survey comparing the efficiencies of these enzymes. Most works have used technical lignin as a substrate; however, the degradation of lignocellulosic biomass has more challenging problems. Fujii et al. (2020) recently reported the rapid degradation of tropical forest litters by laccases and peroxidases, but the systematic study about the enzymatic degradation of industrial lignocellulosic feedstocks has not been faced yet. Biological treatments are eco-friendly, but the production of enzymes (in this work we do not discuss the potential use of lignin-degrading microbes), mainly recombinant enzymes, represents a big challenge. If these challenges are overcome, the benefits can be enormous, both environmentally and economically, for companies that use lignocellulosic biomass and those producing recombinant enzymes. The production of proteins from their natural sources has important limitations and hence the production of recombinant proteins is a powerful tool; however, the success in the production of recombinant enzymes includes dealing with several steps: the adaptation of the codon use of the gene, the selection of the expression vector and the proper host for heterologous protein expression, the use of the best growth medium and growth conditions, the characteristics of the protein (if it is produced soluble or insoluble), including important postraductional modifications, the protocol of purification, etc. The production of proteins by DNA recombinant technology could be challenging, but

when it is successful, it implies a big success. Currently, most enzymes used industrially are recombinant ones.

A new perspective in the production of proteins is the rational modification or redesign (of proteins) using genetic engineering (protein engineering) or the direct evolution of proteins. Chen et al. (2015a, b) studied the molecular basis of the interaction between the laccase from *T. versicolor* and various lignin model compounds, showing that the hydrophobic interactions between a lignin model compound and the laccase are essential, and this information may be helpful for designing highly efficient laccases. Several investigators have tried the laccase and peroxidase evolution or engineering for improving their activities (Brissos et al. 2017; Rodríguez-Escribano et al. 2017; Stanzione et al. 2020; among others) and showed the potential of manipulating lignin-degrading proteins.

Notwithstanding these considerations, most reported experiences suggest that the best way to degrade lignin matter using different enzymes (laccases and peroxidases), that attack the lignin bonds using different mechanisms (Hofrichter 2002). Thus, we think that the bio-degradation of the lignocellulosic material is still in its infancy, but data supports that the investigators are on the right track.

Compliance with ethical standards

Conflict of interest Authors declare they do not have conflict of interest.

References

Abdel-Hamid AM, Solbiati JO, Cann IKO (2013) Insights into lignin degradation and its potential industrial applications. Adv Appl Microbiol. https://doi.org/10.1016/b978-0-12-407679-2.00001-6

Adav SS et al (2010) Quantitative iTRAQ secretome analysis of cellulolytic *Thermobifida fusca*. J Proteome Res 9(6):3016–3024. https://doi.org/10.1021/pr901174z

Ahmad M et al (2011) Identification of DypB from *Rhodococcus jostii* RHA1 as a lignin peroxidase. Biochemistry 50(23):5096–5107. https://doi.org/10.1021/bi101892z

Alexandre G, Zhulin IB (2000) Laccases are widespread in bacteria [1]. Trends Biotechnol 18(2):41–42. https://doi.org/10.1016/s0167-7799(99)01406-7

Ali, Sreekrishnan (2001) Paper mill eflluent toxicity.pdf. Adv Environ Res 5(2):175–196. https://doi.org/10.1016/S1093-0191(00)00055-1

Ali M, Husain Q, Isqui HM (2019) Fungal peroxidases mediated bioremediation of industrial pollutants. Fungal bioremediation: fundamentals and applications. CRC, Boca Raton, p 22

Alvira P, Ballesteros M, Negro MJ (2010) Bioresource technology pretreatment technologies for an efficient bioethanol production process based on enzymatic hydrolysis: a review. Bioresour Technol 101(13):4851–4861. https://doi.org/10.1016/j.biortech.2009.11.093

Antonopoulou I et al (2016) Enzymatic synthesis of bioactive compounds with high potential for cosmeceutical application. Appl Microbiol Biotechnol 100(15):6519–6543. https://doi.org/10.1007/s00253-016-7647-9

Arakane Y et al (2005) Laccase 2 is the phenoloxidase gene required for beetle cuticle tanning. Proc Natl Acad Sci USA 102(32):11337–11342. https://doi.org/10.1073/pnas.0504982102

Arias ME et al (2003) Kraft pulp biobleaching and mediated oxidation of a nonphenolic substrate by laccase from *Streptomyces cyaneus* CECT 3335. Appl Environ Microbiol 69(4):1953–1958. https://doi.org/10.1128/AEM.69.4.1953-1958.2003

Asgher M, Ahmad Z, Iqbal HMN (2013) Alkali and enzymatic delignification of sugarcane bagasse to expose cellulose polymers for saccharification and bio-ethanol production. Ind Crops Prod 44:488–495. https://doi.org/10.1016/j.indcrop.2012.10.005

Baldrian P (2006) Fungal laccases-occurrence and properties. FEMS Microbiol Rev 30(2):215–242. https://doi.org/10.1111/j.1574-4976.2005.00010.x

Barreca AM et al (2003) Laccase/mediated oxidation of a lignin model for improved delignification procedures. J Mol Catal B Enzym 26(1–2):105–110. https://doi.org/10.1016/j.molcatb.2003.08.001

Basto C, Tzanov T, Cavaco-Paulo A (2007) Combined ultrasound-laccase assisted bleaching of cotton. Ultrason Sonochem 14(3):350–354. https://doi.org/10.1016/j.ultsonch.2006.07.006

Bilal M et al (2017) Immobilized ligninolytic enzymes: an innovative and environmental responsive technology to tackle dye-based industrial pollutants—a review. Sci Total Environ 576:646–659. https://doi.org/10.1016/j.scitotenv.2016.10.137

Bilir K et al (2016) Construction of an oxygen detection-based optic laccase biosensor for polyphenolic compound detection. Turk J Biol 40(6):1303–1310. https://doi.org/10.3906/biy-1602-40

Bollag JM, Leonowicz A (1984) Comparative studies of extracellular fungal laccases. Appl Environ Microbiol 48(4):849–854. https://doi.org/10.1128/aem.48.4.849-854.1984

Bourbonnais R, Paice MG (1990) Oxidation of non-phenolic substrates. An expanded role for laccase in lignin biodegradation. FEBS Lett 267(1):99–102. https://doi.org/10.1016/0014-5793(90)80298-w

Brebu M, Vasile C (2010) Thermal degradation of lignin—a review. Cellul Chem Technol 44(9):353–363

Brissos V et al (2017) Engineering a bacterial DyP-type peroxidase for enhanced oxidation of lignin-related phenolics at alkaline pH. ACS Catal 7(5):3454–3465. https://doi.org/10.1021/acscatal.6b03331

Brown ME et al (2011) Discovery and characterization of heme enzymes from unsequenced bacteria: application to microbial lignin degradation. J Am Chem Soc 133(45):18006–18009. https://doi.org/10.1021/ja203972q

Brown ME, Barros T, Chang MCY (2012) Identification and characterization of a multifunctional dye peroxidase from a lignin-reactive bacterium. ACS Chem Biol 7(12):2074–2081. https://doi.org/10.1021/cb300383y

Bugg TDH et al (2011) Pathways for degradation of lignin in bacteria and fungi. Nat Prod Rep 28(12):1883–1896. https://doi.org/10.1039/c1np00042j

Campos R et al (2001) Indigo degradation with purified laccases from *Trametes hirsuta* and *Sclerotium rolfsii*. J Biotechnol 89(2–3):131–139. https://doi.org/10.1016/s0168-1656(01)00303-0

Castro-Sowinski S, Martinez-Drets G, Okon Y (2002) Laccase activity in melanin-producing strains of *Sinorhizobium meliloti*. FEMS Microbiol Lett 209(1):119–125. https://doi.org/10.1111/j.1574-6968.2002.tb11119.x

Chandra R, Chowdhary P (2015) Properties of bacterial laccases and their application in bioremediation of industrial wastes. Environ Sci Process Impacts 17(2):326–342. https://doi.org/10.1039/c4em00627e

Chandra MRGS, Madakka M (2019) Comparative biochemistry and kinetics of microbial lignocellulolytic enzymes, recent

developments in applied microbiology and biochemistry. Elsevier, Oxford. https://doi.org/10.1016/b978-0-12-816328-3.00011-8
Chauhan PS, Goradia B, Saxena A (2017) Bacterial laccase: recent update on production, properties and industrial applications. 3 Biotech 7(5):1–20. https://doi.org/10.1007/s13205-017-0955-7
Chen C et al (2015a) Characterization of dye-decolorizing peroxidase (DyP) from *Thermomonospora curvata* reveals unique catalytic properties of A-type DyPs. J Biol Chem 290(38):23447–23463. https://doi.org/10.1074/jbc.m115.658807
Chen M et al (2015b) Molecular basis of laccase bound to lignin: insight from comparative studies on the interaction of *Trametes versicolor* laccase with various lignin model compounds. RSC Adv 5(65):52307–52313. https://doi.org/10.1039/c5ra07916k
Chio C, Sain M, Qin W (2019) Lignin utilization: a review of lignin depolymerization from various aspects. Renew Sustain Energy Rev 107(February):232–249. https://doi.org/10.1016/j.rser.2019.03.008
Choinowski T et al (1999) The crystal structure of lignin peroxidase at 1.70 Å resolution reveals a hydroxy group on the C(β) of tryptophan 171: a novel radical site formed during the redox cycle. J Mol Biol 286(3):809–827. https://doi.org/10.1006/jmbi.1998.2507
Chowdhary P et al (2018) Ligninolytic enzymes: an introduction and applications in the food industry, enzymes in food biotechnology: production, applications, and future prospects. Elsevier, Oxford. https://doi.org/10.1016/b978-0-12-813280-7.00012-8
Claus H (2004) Laccases: structure, reactions, distribution. Micron 35(1–2):93–96. https://doi.org/10.1016/j.micron.2003.10.029
Colpa DI, Fraaije MW, Van Bloois E (2014) DyP-type peroxidases: a promising and versatile class of enzymes. J Ind Microbiol Biotechnol 41(1):1–7. https://doi.org/10.1007/s10295-013-1371-6
Coy MR et al (2010) Phenol-oxidizing laccases from the termite gut. Insect Biochem Mol Biol 40(10):723–732. https://doi.org/10.1016/j.ibmb.2010.07.004
Darwesh OM, Matter IA, Eida MF (2019) Development of peroxidase enzyme immobilized magnetic nanoparticles for bioremediation of textile wastewater dye. J Environ Chem Eng. https://doi.org/10.1016/j.jece.2018.11.049
de Gonzalo G et al (2016) Bacterial enzymes involved in lignin degradation. J Biotechnol 236:110–119. https://doi.org/10.1016/j.jbiotec.2016.08.011
de Oliveira PL et al (2009) Purification and partial characterization of manganese peroxidase from *Bacillus pumilus* and *Paenibacillus* sp. Braz J Microbiol 40(4):818–826. https://doi.org/10.1590/s1517-83822009000400012
Dean JFD, Eriksson KEL (1994) Laccase and the deposition of lignin in vascular plants. Holzforschung 48(s1):21–33. https://doi.org/10.1515/hfsg.1994.48.s1.21
Dogaris I, Mamma D, Kekos D (2013) Biotechnological production of ethanol from renewable resources by *Neurospora crassa* : an alternative to conventional yeast fermentations ? Appl Microbiol Biotechnol. https://doi.org/10.1007/s00253-012-4655-2
Falade AO et al (2017) Lignin peroxidase functionalities and prospective applications. MicrobiologyOpen 6(1):1–14. https://doi.org/10.1002/mbo3.394
Fujii K et al (2020) A comparison of lignin-degrading enzyme activities in forest floor layers across a global climatic gradient. Soil Ecol Lett. https://doi.org/10.1007/s42832-020-0042-6
Galliano H et al (1991) Lignin degradation by Rigidoporus lignosus involves synergistic action of two oxidizing enzymes: Mn peroxidase and laccase. Enzyme Microbial Technol 13:478–482
Giardina P et al (2010) Laccases: a never-ending story. Cell Mol Life Sci 67(3):369–385. https://doi.org/10.1007/s00018-009-0169-1
Glenn JK et al (1983) An extracellular H_2O_2-requiring enzyme preparation involved in lignin biodegradation by the white rot basidiomycete *Phanerochaete chrysosporium*. Biochem Biophys Res Commun 114(3):1077–1083. https://doi.org/10.1016/0006-291X(83)90672-1
Glenn JK, Gold MH (1985) Purification and characterization of an extracellular Mn(II)-dependent peroxidase from the lignin-degrading basidiomycete, *Phanerochaete chrysosporium*. Arch Biochem Biophys 242(2):329–341. https://doi.org/10.1016/0003-9861(85)90217-6
Hakulinen N, Rouvinen J (2015) Three-dimensional structures of laccases. Cell Mol Life Sci 72(5):857–868. https://doi.org/10.1007/s00018-014-1827-5
Hatakeyama H, Hatakeyama T (2010) Lignin structure, properties, and applications. Biol Res 5(1):28–37
Heinfling A et al (1998) A study on reducing substrates of manganese-oxidizing peroxidases from *Pleurotus eryngii* and *Bjerkandera adusta*. FEBS Lett 428(3):141–146. https://doi.org/10.1016/S0014-5793(98)00512-2
Hildén K, Hakala TK, Lundell T (2009) Thermotolerant and thermostable laccases. Biotech Lett 31(8):1117–1128. https://doi.org/10.1007/s10529-009-9998-0
Hofrichter M (2002) Review: lignin conversion by manganese peroxidase (MnP). Enzyme Microbial Technol 30(4):454–466. https://doi.org/10.1016/s0141-0229(01)00528-2
Houtman CJ et al (2018) Fungal lignin peroxidase does not produce the veratryl alcohol cation radical as a diffusible ligninolytic oxidant. J Biol Chem 293(13):4702–4712. https://doi.org/10.1074/jbc.ra117.001153
Janusz G et al (2017) Lignin degradation: microorganisms, enzymes involved, genomes analysis and evolution. FEMS Microbiol Rev 41(6):941–962. https://doi.org/10.1093/femsre/fux049
Janusz G et al (2020) Laccase properties, physiological functions, and evolution. Int J Mol Sci. https://doi.org/10.3390/ijms21030966
Johansson T, Welinder KG, Nyman PO (1993) Isozymes of lignin peroxidase and Manganese(II) peroxidase from the white-rot *Basidiomycete Trametes versicolor*. II. Partial Sequences, Peptide Maps, and Amino Acid and Carbohydrate Compositions. Arch Biochem Biophys. https://doi.org/10.1006/abbi.1993.1008
Kim SJUN, Shoda M (1999) Puri cation and characterization of a novel peroxidase. Society 65(3):1029–1035
Kim SJ et al (1995) Characteristics of a newly isolated fungus, *Geotrichum candidum* Dec 1, which decolorizes various dyes. J Ferment Bioeng 79(6):601–607. https://doi.org/10.1016/0922-338X(95)94755-G
Kim Y et al (2011) Soluble inhibitors/deactivators of cellulase enzymes from lignocellulosic biomass. Enzyme Microbial Technol 48(4–5):408–415. https://doi.org/10.1016/j.enzmictec.2011.01.007
Koschorreck K et al (2008) Comparative characterization of four laccases from *Trametes versicolor* concerning phenolic C-C coupling and oxidation of PAHs. Arch Biochem Biophys 474(1):213–219. https://doi.org/10.1016/j.abb.2008.03.009
Kosman DJ (2010) Multicopper oxidases: a workshop on copper coordination chemistry, electron transfer, and metallophysiology. J Biol Inorg Chem 15(1):15–28. https://doi.org/10.1007/s00775-009-0590-9
Koua D et al (2009) PeroxiBase: a database with new tools for peroxidase family classification. Nucleic Acids Res 37(SUPPL. 1):261–266. https://doi.org/10.1093/nar/gkn680
Kuhad RC et al (2004) Developments in microbial methods for the treatment of dye effluents. Adv Appl Microbiol 56:185–213. https://doi.org/10.1016/s0065-2164(04)56006-9
Kunamneni A et al (2008) Engineering and applications of fungal laccases for organic synthesis. Microbial Cell Fact 17:1–17. https://doi.org/10.1186/1475-2859-7-32
Kurisawa M et al (2003) Laccase-catalyzed Synthesis and Antioxidant Property of Poly(catechin). Macromol Biosci 3(12):758–764. https://doi.org/10.1002/mabi.200300038

Lai C et al (2018) Bioresource technology enhanced enzymatic digestibility of mixed wood sawdust by lignin modi fi cation with naphthol derivatives during dilute acid pretreatment. Bioresour Technol 269(June):18–24. https://doi.org/10.1016/j.biortech.2018.08.086

Lambertz C et al (2016) Progress and obstacles in the production and application of recombinant lignin-degrading peroxidases. Bioengineered 7(3):145–154. https://doi.org/10.1080/21655979.2016.1191705

Lantto R et al (2004) Effects of laccase-mediator combinations wool. Text Res J 74(8):713–717

Leonowicz A et al (1999) Biodegradation of lignin by white rot fungi. Fungal Genet Biol 27(2–3):175–185. https://doi.org/10.1006/fgbi.1999.1150

Liers C et al (2010) DyP-like peroxidases of the jelly fungus *Auricularia auricula-judae* oxidize nonphenolic lignin model compounds and high-redox potential dyes. Appl Microbiol Biotechnol 85(6):1869–1879. https://doi.org/10.1007/s00253-009-2173-7

Lundell T et al (1993) Lignin peroxidase L3 from *Phlebia radiata*. Eur J Biochem 402(MARCH):391–402

Lobos S et al (1994) Isoenzymes of manganese-dependent peroxidase and laccase produced by the lignin-degrading basidiomycete *Ceriporiopsis subvermispora*. Microbiology 140(10):2691–2698. https://doi.org/10.1099/00221287-140-10-2691

Machczynski MC et al (2004) Characterization of SLAC: a small laccase from *Streptomyces coelicolor* with unprecedented activity. Protein Sci 13(9):2388–2397. https://doi.org/10.1110/ps.04759104

Margot J et al (2013) Bacterial versus fungal laccase: potential for micropollutant degradation. AMB Expr 3:1–14. https://doi.org/10.1186/2191-0855-3-63

Martins LO et al (2002) Molecular and biochemical characterization of a highly stable bacterial laccase that occurs as a structural component of the *Bacillus subtilis* endospore coat. J Biol Chem 277(21):18849–18859. https://doi.org/10.1074/jbc.M200827200

Mensah CA et al (2012) Reduced tannin content of laccase-treated cocoa (*Theobroma cacao*) pod husk. Int J Biol Chem. https://doi.org/10.3923/ijbc.2012.31.36

Millati R et al (2011) Biological pretreatment: review. BioResources 6(4):5224–5259

Min K et al (2015) A dye-decolorizing peroxidase from *Bacillus subtilis* exhibiting substrate-dependent optimum temperature for dyes and β-ether lignin dimer. Sci Rep 5:1–8. https://doi.org/10.1038/srep08245

Minussi RC, Pastore GM, Durán N (2002) Potential applications of laccase in the food industry. Trends Food Sci Technol 13(6–7):205–216. https://doi.org/10.1016/s0924-2244(02)00155-3

Miyazaki K (2005) A hyperthermophilic laccase from *Thermus thermophilus* HB27. Extremophiles 9(6):415–425. https://doi.org/10.1007/s00792-005-0458-z

Moilanen AM et al (1996) Manganese and malonate are individual regulators for the production of lignin and manganese peroxidase isozymes and in the degradation of lignin by *Phlebia radiata*. Appl Microbiol Biotechnol 45(6):792–799. https://doi.org/10.1007/s002530050764

Morozova OV et al (2007) "Blue" laccases. Biochemistry (Moscow) 72(10):1136–1150

Mostafa KhM, Samarkandy Abdul Rahim (2005) Muatafa 2005.pdf. J Appl Sci 5(7):1206–1213

Munk L et al (2015) Can laccases catalyze bond cleavage in lignin? Biotechnol Adv 33(1):13–24. https://doi.org/10.1016/j.biotechadv.2014.12.008

Muthu SS (2017) Textiles and clothing sustainability. Sustainable technologies. Springer, Singapore

Nagasaki K et al (2008) Purification, characterization, and gene cloning of Ceriporiopsis sp. strain MD-1 peroxidases that decolorize human hair melanin. Appl Environ Microbiol 74(16):5106–5112. https://doi.org/10.1128/aem.00253-08

Ng IS et al (2015) Enzymatic exploration of catalase from a nanoparticle producing and biodecolorizing algae *Shewanella xiamenensis* BC01. Bioresour Technol 184:429–435. https://doi.org/10.1016/j.biortech.2014.09.079

Nowak J, Jarosz-Wilkołazka A, Luterek J (2006) Catalytic activity of versatile peroxidase from *Bjerkandera fumosa* in aqueous solutions of water-miscible organic solvents. Appl Catal A Gen 308:56–61. https://doi.org/10.1016/j.apcata.2006.04.009

Nunes CS, Kunamneni A (2018) Laccases-properties and applications. In: Sug R (ed) Enzymes in human and animal nutrition: principles and perspectives. Elsevier, Oxford

Osma JF, Toca-Herrera JL, Rodríguez-Couto S (2010) Uses of laccases in the food industry. Enzyme Res. https://doi.org/10.4061/2010/918761

Paice MG et al (1993) Manganese peroxidase, produced by *Trametes versicolor* during pulp bleaching, demethylates and delignifies kraft pulp. Appl Environ Microbiol 59(1):260–265. https://doi.org/10.1128/aem.59.1.260-265.1993

Parmar I, Rupasinghe HPV (2013) Bio-conversion of apple pomace into ethanol and acetic acid: enzymatic hydrolysis and fermentation. Biores Technol 130:613–620. https://doi.org/10.1016/j.biortech.2012.12.084

Pazarlioğlu NK, Sariişik M, Telefoncu A (2005) Laccase: production by Trametes versicolor and application to denim washing. Process Biochem 40(5):1673–1678. https://doi.org/10.1016/j.procbio.2004.06.052

Pérez-Boada M et al (2005) Versatile peroxidase oxidation of high redox potential aromatic compounds: site-directed mutagenesis, spectroscopic and crystallographic investigation of three long-range electron transfer pathways. J Mol Biol 354(2):385–402. https://doi.org/10.1016/j.jmb.2005.09.047

Plácido J, Capareda S (2015) Ligninolytic enzymes: a biotechnological alternative for bioethanol production. Bioresour Bioprocess. https://doi.org/10.1186/s40643-015-0049-5

Pokhrel D, Viraraghavan T (2004) Treatment of pulp and paper mill wastewater—a review. Sci Total Environ 333:37–58. https://doi.org/10.1016/j.scitotenv.2004.05.017

Pollegioni L, Tonin F, Rosini E (2015) Lignin-degrading enzymes. FEBS J 282(7):1190–1213. https://doi.org/10.1111/febs.13224

Ponnusamy VK et al (2019) A review on lignin structure, pretreatments, fermentation reactions and biorefinery potential. Bioresour Technol 271:462–472. https://doi.org/10.1016/j.biortech.2018.09.070

Rahmanpour R, Bugg TDH (2015) Characterisation of Dyp-type peroxidases from *Pseudomonas fluorescens* Pf-5: oxidation of Mn(II) and polymeric lignin by Dyp1B. Arch Biochem Biophys 574:93–98. https://doi.org/10.1016/j.abb.2014.12.022

Rahmanpour R, King LDW, Bugg TDH (2016) Identification of an extracellular bacterial flavoenzyme that can prevent re-polymerisation of lignin fragments. Biochem Biophys Res Commun. https://doi.org/10.1016/j.bbrc.2016.10.144

Ravichandran A, Sridhar M (2017) Insights into the mechanism of lignocellulose degradation by versatile peroxidases. Curr Sci 113(1):35–42. https://doi.org/10.18520/cs/v113/i01/35-42

Reiss R et al (2013) Laccase versus laccase-like multi-copper oxidase: a comparative study of similar enzymes with diverse substrate spectra. PLoS One. https://doi.org/10.1371/journal.pone.0065633

Rodriguez-Couto S (2012) Laccases for denim bleaching: an eco-friendly alternative. Open Text J 5(1):1–7. https://doi.org/10.2174/1876520301205010001

Rodriguez-Couto SR, Toca-herrera JL (2006) Lacasses in the textile industry. Biotechnol Mol Biol Rev 1(December):115–120. http://www.academicjournals.org/BMBR%5Cnhttp://academicjournals.org/article/article1381411420_CoutoandToca-Herrera.pdf

Rodríguez-Delgado MM et al (2015) Laccase-based biosensors for detection of phenolic compounds. TrAC 74:21–45. https://doi.org/10.1016/j.trac.2015.05.008

Rodríguez-Escribano D et al (2017) High-throughput screening assay for laccase engineering toward lignosulfonate valorization. Int J Mol Sci 18(8):1–10. https://doi.org/10.3390/ijms18081793

Rosconi F et al (2005) Purification and characterization of a periplasmic laccase produced by *Sinorhizobium meliloti*. Enzyme Microbial Technol 36(5–6):800–807. https://doi.org/10.1016/j.enzmictec.2005.01.003

Ruiz-Dueñas FJ, Martínez ÁT (2009) Microbial degradation of lignin: How a bulky recalcitrant polymer is efficiently recycled in nature and how we can take advantage of this. Microbial Biotechnol 2(2 SPEC. ISS.):164–177. https://doi.org/10.1111/j.1751-7915.2008.00078.x

Saxena A, Chauhan PS (2016) Role of various enzymes for deinking paper : a review. Critical Rev Biotechnol. https://doi.org/10.1080/07388551.2016.1207594

Schneider WDH et al (2019) Lignin degradation and detoxification of eucalyptus wastes by on-site manufacturing fungal enzymes to enhance second-generation ethanol yield. Appl Energy 262:114493. https://doi.org/10.1016/j.apenergy.2020.114493

Sekretaryova AN et al (2016) Total phenol analysis of weakly supported water using a laccase-based microband biosensor. Anal Chim Acta 907:45–53. https://doi.org/10.1016/j.aca.2015.12.006

Selinheimo E et al (2006) Effects of laccase, xylanase and their combination on the rheological properties of wheat doughs. J Cereal Sci 43(2):152–159. https://doi.org/10.1016/j.jcs.2005.08.007

Shiba T et al (2000) Oxidation of isoeugenol and coniferyl alcohol catalyzed by laccases isolated from *Rhus vernicifera* Stokes and *Pycnoporus coccineus*. J Mol Catal B Enzymat 10(6):605–615. https://doi.org/10.1016/s1381-1177(00)00184-3

Shin SK et al (2019) Effective melanin degradation by a synergistic laccase-peroxidase enzyme complex for skin whitening and other practical applications. Int J Biol Macromol. https://doi.org/10.1016/j.ijbiomac.2019.02.027

Sigoillot JC et al (2012) Fungal strategies for lignin degradation. Adv Bot Res. https://doi.org/10.1016/b978-0-12-416023-1.00008-2

Singh G (2017) Enzymes : applications in pulp and paper industry Author' s personal copy. Agro-Ind Wastes Feedstock Enzyme Prod. https://doi.org/10.1016/B978-0-12-802392-1.0007-1

Singh, Singh (2016) White and brown rot fungi as decomposers of lignocellulosic materials and their role in waste and pollution control. Fungal Appl Sustain Eviron Biotechnol. https://doi.org/10.1007/978-3-319-42852-9

Singh R et al (2012) Distal heme pocket residues of B-type dye-decolorizing peroxidase: arginine but not aspartate is essential for peroxidase activity. J Biol Chem 287(13):10623–10630. https://doi.org/10.1074/jbc.m111.332171

Solomon EI, Augustine AJ, Yoon J (2008) O2 Reduction to H_2O by the multicopper oxidases. Dalton Trans 9226(30):3921–3932. https://doi.org/10.1039/b800799c

Stanzione I et al (2020) Beyond natural laccases: extension of their potential applications by protein engineering. Appl Microbiol Biotechnol 104(3):915–924. https://doi.org/10.1007/s00253-019-10147-z

Sugano Y (2009) DyP-type peroxidases comprise a novel heme peroxidase family. Cell Mol Life Sci 66(8):1387–1403. https://doi.org/10.1007/s00018-008-8651-8

Sugiura T et al (2009) Cloning and homologous expression of novel lignin peroxidase genes in the white-rot fungus *Phanerochaete sordida* YK-624. Biosci Biotechnol Biochem 73(8):1793–1798. https://doi.org/10.1271/bbb.90152

Sun Z et al (2018) Bright side of lignin depolymerization: toward new platform chemicals. Chem Rev 118(2):614–678. https://doi.org/10.1021/acs.chemrev.7b00588

Suzuki T et al (2003) A thermostable laccase from *Streptomyces lavendulae* REN-7: purification, characterization, nucleotide sequence, and expression. Biosci Biotechnol Biochem 67(10):2167–2175. https://doi.org/10.1271/bbb.67.2167

Theerachat M et al (2019) Laccases from marine organisms and their applications in the biodegradation of toxic and environmental pollutants: a review. Appl Biochem Biotechnol 187(2):583–611. https://doi.org/10.1007/s12010-018-2829-9

Tkaczyk A, Mitrowska K, Posyniak A (2020) Synthetic organic dyes as contaminants of the aquatic environment and their implications for ecosystems: a review. Sci Total Environ 717:137222. https://doi.org/10.1016/j.scitotenv.2020.137222

Valls C et al (2019) A straightforward bioprocess for a cleaner paper decolorization. J Clean Prod 236:117702. https://doi.org/10.1016/j.jclepro.2019.117702

Virk AP, Sharma P, Capalash N (2012) Use of laccase in pulp and paper industry. Biotechnol Prog 28(1):21–32. https://doi.org/10.1002/btpr.727

Vares T, Niemenmaa O, Hatakka A (1994) Secretion of ligninolytic enzymes and mineralization of ^{14}C-ring- labelled synthetic lignin by three *Phlebia tremellosa* strains. Appl Environm Microbiol 60(2):569–575. https://doi.org/10.1128/aem.60.2.569-575.1994

Welinder KG, Mauro JM, Norskov-Lauritsen L (1992) Structure of plant and fungal peroxidases. Biochem Soc Trans 20(2):337–340. https://doi.org/10.1042/bst0200337

Wong DWS (2009) Structure and action mechanism of ligninolytic enzymes. Appl Biochem Biotechnol. https://doi.org/10.1007/s12010-008-8279-z

Ximenes E et al (2010) Inhibition of cellulases by phenols. Enzyme Microbial Technol 46(3–4):170–176. https://doi.org/10.1016/j.enzmictec.2009.11.001

Xu Q et al (2009) Performance and efficiency of old newspaper deinking by combining cellulase/hemicellulase with laccase-violuric acid system. Waste Manag 29(5):1486–1490. https://doi.org/10.1016/j.wasman.2008.10.007

Yaseen DA, Scholz M (2019) Textile dye wastewater characteristics and constituents of synthetic effluents: a critical review. Int J Environ Sci Technol. https://doi.org/10.1007/s13762-018-2130-z

Yashas SR et al (2018) Laccase biosensor: green technique for quantification of phenols in wastewater (a review). Orient J Chem 34(2):631–637. https://doi.org/10.1300/ojc/340204

Yoshida T et al (2011) The catalytic mechanism of dye-decolorizing peroxidase DyP may require the swinging movement of an aspartic acid residue. FEBS J 278(13):2387–2394. https://doi.org/10.1111/j.1742-4658.2011.08161.x

Zámocký M et al (2015) Independent evolution of four heme peroxidase superfamilies. Arch Biochem Biophys 574:108–119. https://doi.org/10.1016/j.abb.2014.12.025

Zeng J et al (2017) Understanding factors controlling depolymerization and polymerization in catalytic degradation of β-ether linked model lignin compounds by versatile peroxidase. Green Chem 19(9):2145–2154. https://doi.org/10.1039/c6gc03379b

Zhang H et al (2018) Purification and characterization of a novel manganese peroxidase from white-rot fungus Cerrena unicolor BBP6 and its application in dye decolorization and denim bleaching. Process Biochem 66(September):222–229. https://doi.org/10.1016/j.procbio.2017.12.011

HIPÓTESIS

El empleo de preparados multienzimáticos con actividad modificadora de lignina, constituidos por peroxidasas y laccasas recombinantes, permitiría optimizar el blanqueo de pulpas celulósicas. Estas enzimas, al actuar mediante mecanismos catalíticos complementarios, favorecerán una remoción de lignina más eficiente y sustentable en comparación con su aplicación individual. La acción sinérgica de ambas amplía el espectro de sustratos lignocelulósicos susceptibles de modificación, potenciando la eficacia global del proceso deslignificante.

OBJETIVO GENERAL

El objetivo general de esta propuesta es contribuir al desarrollo de métodos biológicos de modificación de material lignocelulósico, para su utilización sustentable en varias industrias de interés nacional, con énfasis en la industria de la pulpa de celulosa

OBJETIVOS ESPECÍFICOS

Los objetivos específicos de la propuesta son:

1 - Producir una DyP peroxidasa, de origen bacteriano, en forma recombinante.

2 - Analizar las propiedades bioquímicas y biotecnológicas de la DyP peroxidasa recombinante.

3 - Realizar un análisis del genoma de *Sinorhizobium meliloti* CE52G e identificar la secuencia codificante para la laccasa.

4 - Producir la laccasa en forma recombinante.

5 - Analizar las propiedades bioquímicas y biotecnológicas de la laccasa recombinante.

6 - Analizar el potencial de estas enzimas en la industria de la pulpa de papel, utilizando lignina kraft como sustrato modelo.

7 - Analizar el potencial de estas enzimas en la degradación de lignina utilizando diferentes sustratos lignocelulósicos, aportados por la industria papelera.

CAPÍTULO I

1. Una peroxidasa del tipo dyp como enzima modificadora de lignina

1.1. Contexto y antecedentes

Este capítulo tiene como objetivo realizar la caracterización estructural, funcional y biotecnológica de una DyP bacteriana proveniente de una cepa antártica, *Pseudomonas* sp. AU10, y corresponde a los Objetivos Específicos 1 y 2.

Las peroxidasas del tipo DyP (*dye-decolorizing peroxidases*, EC 1.11.1.19) constituyen un grupo emergente de enzimas dependientes de hemo que utilizan peróxido de hidrógeno como co-sustrato. Se caracterizan por presentar propiedades estructurales y funcionales únicas, que las diferencian de las peroxidasas clásicas, como la lignina peroxidasa, la manganeso peroxidasa o la tan estudiada peroxidasa vegetal de rábano picante (HRP, *Horseradish peroxidase*). Descubiertas inicialmente por su capacidad de decolorar colorantes industriales [32], las DyPs han despertado un creciente interés en los últimos años debido a su versatilidad catalítica, su estabilidad bajo condiciones extremas y su potencial en la transformación de compuestos recalcitrantes, incluidos sustratos lignocelulósicos [33].

Desde el punto de vista estructural, las DyPs presentan un dominio característico con pliegue α + β y una arquitectura de sitio activo atípica, lo que contribuye a su amplio espectro de sustratos y a una cinética de oxidación eficiente, incluso en condiciones de baja concentración de peróxido de hidrógeno. Filogenéticamente, esta familia se clasificó en diferentes subgrupos (A, B, C y D), mostrando una notable diversidad entre variantes bacterianas y fúngicas [34, 35]. Las DyPs bacterianas, en particular, son de gran interés debido, no solo a sus propiedades únicas, sino también a la facilidad de expresión recombinante y su capacidad de adaptación a ambientes extremos.

En este sentido, los microorganismos antárticos representan una fuente promisoria de nuevos biocatalizadores, ya que han evolucionado bajo condiciones de temperatura extremadamente baja, alta radiación UV y limitada disponibilidad de nutrientes [36]. Estos factores ejercen una fuerte presión selectiva sobre sus enzimas, promoviendo propiedades deseables como la actividad a bajas temperaturas, tolerancia a oxidantes y estabilidad estructural, que resultan de gran interés para aplicaciones industriales sostenibles.

En este contexto, el presente capítulo se centra en el estudio de una peroxidasa bacteriana del tipo DyP, cuyo gen fue identificado en un microorganismo antártico del género *Pseudomonas*. Su caracterización estructural, bioquímica y funcional se abordó en el trabajo titulado "*A bacterial cold-active dye-decolorizing peroxidase from an Antarctic Pseudomonas strain*", publicado en el 2023 en la revista *Applied Microbiology and Biotechnology*.

Durante el desarrollo de este estudio, nos planteamos diversas preguntas que orientaron el diseño experimental y guiaron la interpretación de los resultados. ¿Sería posible producir esta enzima en forma recombinante y obtenerla en un estado soluble y funcional? ¿Qué características estructurales y catalíticas presentaría en comparación con otras peroxidasas previamente descritas? ¿Tendría capacidad para oxidar sustratos complejos como la lignina kraft? Estas inquietudes definieron el enfoque del trabajo y motivaron una caracterización profunda de la enzima, tanto a nivel estructural como funcional.

En base a estas interrogantes, se concretaron dos objetivos: por un lado, producir la peroxidasa del tipo DyP en forma recombinante, optimizando su expresión y purificación a partir de un hospedador bacteriano; y por otro, realizar un análisis de sus propiedades bioquímicas, estructurales y funcionales mediante diversas estrategias experimentales.

En primer lugar, se realizó una caracterización *in silico* de la enzima, incluyendo análisis de motivos conservados y modelado tridimensional mediante herramientas de predicción estructural, que permitió identificar elementos clave del sitio activo y estimar su arquitectura general. Posteriormente, se realizó su producción recombinante en *Escherichia coli* y se optimizó su purificación mediante cromatografía de afinidad a metales inmovilizados (IMAC).

La caracterización bioquímica incluyó la determinación del tamaño molecular, la evaluación de su estado de oligomerización, así como la medición de la actividad peroxidasa en estado estacionario frente a distintos sustratos clásicos. Además, se evaluó la estabilidad de la enzima a distintas temperaturas y se realizaron análisis cinéticos rápidos mediante técnicas de *stopped-flow*. En términos funcionales, se exploró la capacidad de la enzima recombinante (rDyP-AU10) para oxidar lignina kraft, como modelo de sustrato lignocelulósico, así como su eficacia en la decoloración de colorantes industriales.

Estos estudios permitieron demostrar que rDyP-AU10 es una enzima versátil, activa a temperaturas modernamente bajas, con potencial para aplicaciones en biorremediación y valorización de biomasa lignocelulósica. Así, este trabajo no solo aporta al conocimiento funcional de las DyPs bacterianas provenientes de ambientes extremos, sino que también presenta una enzima candidata para futuras aplicaciones en procesos biotecnológicos exigentes.

Applied Microbiology and Biotechnology
https://doi.org/10.1007/s00253-023-12405-7

BIOTECHNOLOGICALLY RELEVANT ENZYMES AND PROTEINS

A bacterial cold-active dye-decolorizing peroxidase from an Antarctic *Pseudomonas* strain

Célica Cagide[1] · Juan José Marizcurrena[1] · Diego Vallés[2] · Beatriz Alvarez[3] · Susana Castro-Sowinski[1,2]

Received: 3 November 2022 / Revised: 13 January 2023 / Accepted: 20 January 2023

Abstract

DyP (dye-decolorizing peroxidase) enzymes are hemeproteins that catalyze the H_2O_2-dependent oxidation of various molecules and also carry out lignin degradation, albeit with low activity. We identified a *dyp* gene in the genome of an Antarctic cold-tolerant microbe (*Pseudomonas* sp. AU10) that codes for a class B DyP. The recombinant protein (rDyP-AU10) was produced using *Escherichia coli* as a host and purified. We found that rDyP-AU10 is mainly produced as a dimer and has characteristics that resemble psychrophilic enzymes, such as high activity at low temperatures (20 °C) when using 2,2′-azino-bis(3-ethylbenzothiazoline-6-sulfonic acid (ABTS) and H_2O_2 as substrates, thermo-instability, low content of arginine, and a catalytic pocket surface larger than the DyPs from some mesophilic and thermophilic microbes. We also report the steady-state kinetic parameters of rDyP-AU10 for ABTS, hydroquinone, and ascorbate. Stopped-flow kinetics revealed that Compound I is formed with a rate constant of $(2.07 \pm 0.09) \times 10^6\ M^{-1}\ s^{-1}$ at pH 5 and that this is the predominant species during turnover. The enzyme decolors dyes and modifies kraft lignin, suggesting that this enzyme may have potential use in bioremediation and in the cellulose and biofuel industries.

Key points

- *An Antarctic Pseudomonas strain produces a dye-decolorizing peroxidase.*
- *The recombinant enzyme (rDyP-AU10) was produced in E. coli and purified.*
- *rDyP-AU10 showed high activity at low temperatures.*
- *rDyP-AU10 is potentially useful for biotechnological applications.*

Keywords Cold-active enzyme · Dye-decolorizing peroxidase · Antarctica · Lignin modification · Bioremediation

Introduction

Peroxidases catalyze the oxidation or polymerization of a wide variety of organic and inorganic substrates using hydrogen peroxide (H_2O_2) or other hydroperoxides as oxidizing agents. Peroxidases are distributed among bacteria, archaea, algae, fungi, plants, and animals. The different superfamilies can be classified as heme and non-heme-containing proteins. Non-heme peroxidases rely on thiol, selenol, or metal ions, while heme-peroxidases accommodate a heme prosthetic group (a protoporphyrin IX derivative) for activity. Comprehensive information regarding peroxidases and other oxido-reductases has been collected in the RedoxiBase (https://peroxibase.toulouse.inra.fr/).

Peroxidases have many biotechnological applications. They catalyze reactions with chromogenic, fluorogenic, or chemiluminescent substrates, which are exploited in the identification of nucleic acids and proteins, including immunoassays (Zhang et al. 2018). They participate in the treatment of wastewater contaminated with phenolic compounds or textile dyes (bioremediation) (Bilal et al. 2017; Li et al. 2019) and in the breakdown of lignin (Cagide and Castro-Sowinski 2020). Among lignin-degrading alternatives, DyP

✉ Susana Castro-Sowinski
s.castro.sow@gmail.com; scs@fcien.edu.uy

[1] Sección Bioquímica, Instituto de Biología, Facultad de Ciencias, Universidad de la República, Iguá 4225, 11400 Montevideo, Uruguay

[2] Laboratorio de Biocatalizadores y sus Aplicaciones, Instituto de Química Biológica, Facultad de Ciencias, Universidad de la República, Iguá 4225, 11400 Montevideo, Uruguay

[3] Laboratorio de Enzimología, Instituto de Química Biológica, Facultad de Ciencias, and Centro de Investigaciones Biomédicas, Universidad de la República, Iguá 4225, 11400 Montevideo, Uruguay

Published online: 11 February 2023

(dye-decolorizing peroxidase) enzymes have emerged as an interesting tool for lignin degradation during pulp cellulose production.

Horseradish peroxidase (HRP) is likely the most studied heme peroxidase. It is a globular monomeric protein with a characteristic α-helical secondary structure and a short β-sheet and contains four disulfide bridges and several N-glycosylation sites. HRP contains metal centers essential for the structural integrity and functionality of the enzyme, an iron (III) protoporphyrin IX (the heme group), and two calcium ions. The heme iron is five-coordinate, attached to the imidazole of a proximal histidine residue. The sixth position, on the distal side, is vacant in the resting ferric enzyme. The HRP mechanism of catalysis can be described by three consecutive reactions: the cycle begins with the two-electron oxidation of the ferric enzyme by a H_2O_2 molecule forming Compound I and water; Compound I contains a ferryl (Fe^{IV}=O) group and a porphyrin π cation radical. In some peroxidases, an amino acid residue is oxidized instead of the porphyrin ring. Compound I is reduced back to the enzyme's resting state in two consecutive one-electron transfer reactions accompanied by the oxidation of two molecules of the substrate. Thus, in the second step of the reaction cycle, the substrate reduces the porphyrin radical forming Compound II, a ferryl species. In the third step, a second substrate molecule reduces Compound II back to the ferric resting state. All heme peroxidases show essentially similar mechanisms of catalysis (Dunford et al. 1982; Poulos 2014).

DyPs show molecular sizes ranging between 40 and 60 kDa and adopt quaternary structures (from monomeric to hexameric). They have highly conserved structures and a non-covalently bound heme group within a C-terminal domain. This domain contains a highly conserved histidine residue and a GXXDG motif important for heme binding. DyPs show a catalytic mechanism similar to other peroxidases; in some cases, Compound II cannot be observed, which has led to the proposal that Compound I is reduced back to the resting enzyme in a single two-electron step (Sugano and Yoshida 2021; Xu et al. 2021), although Compound II formation has indeed been detected in several DyPs including a B-class DyP (Pfanzagl et al. 2018). They may have bifunctional activity (peroxidase and hydrolase), being the DyP from the fungus *Thanatephorus cucumeris* an example of a DyP with hydrolase activity; the H_2O released during the redox reaction is the molecule responsible for promoting the hydrolase activity on an anthraquinone substrate (Sugano 2009). According to their primary structure, DyPs are categorized into classes A, B, C, and D (RedoxiBase); furthermore, classifications based on the tertiary structures allow an assessment of the relationship between structure and function. In this regard, a new classification was proposed as follows: Primitive (P, with DyPs from class B), Intermediate (I, with DyPs from classes A), and Advance (V, with DyPs from classes C and D) (Sugano and Yoshida 2021). Recently, Yoshida and Sugano (2023) informed about unexplored subclasses (I1, I2, P1, P2, and V4) of DyPs. These subclasses conserve the important residues and show novel domains in addition to the characteristic DyP domain and differences in the amino acid sequence length.

In this work, we study biochemical and biotechnological aspects of a DyP from an Antarctic cold-tolerant bacterium. The genetic material from cold-adapted microorganisms is a rich source for identifying novel enzymes. We performed an in silico bio-prospection within the genome of a few Antarctic microorganisms from our collection. We found that the bacterium *Pseudomonas* sp. AU10 (Fullana et al. 2017; Martínez-Rosales and Castro-Sowinski 2011) contains a sequence that codes for a DyP (from now, DyP-AU10). We produced the recombinant enzyme in *Escherichia coli* (rDyP-AU10) and characterized several biochemical properties of the purified enzyme. We also show experiments that suggest the potential use of rDyP-AU10 in the bioremediation of dyes and in the paper pulp industry.

Materials and methods

Bacterial strains, search for a lignin-degrading enzyme, and growth media

Pseudomonas sp. AU10 is a cold-tolerant extracellular protease-producing bacterium (Martínez-Rosales and Castro-Sowinski 2011; García-Laviña et al. 2019), isolated from a water sample collected in the Uruguay Lake (King George Island, maritime Antarctica). The AU10 DNA genome was sequenced (Illumina HiSeq 2000 Sequencer, Macrogen), annotated, and functionally categorized as described in Morel et al. (2016). The coding sequence for a DyP was searched and found working in the automated annotation RAST server (Aziz et al. 2008). The nucleotide sequence was submitted to the GenBank database (Accession number MZ766434).

E. coli DH5α (for plasmid multiplication) and BL21 (DE3) or Arctic Express (DE3) (for recombinant protein expression) strains were used in this work. For the production of rDyP-AU10, *E. coli* strains were grown in the auto-induction medium Zym-5052 (Studier 2005). Strains were maintained in Luria-Bertani broth (LB: 10 g/L tryptone, 5 g/L yeast extract, 10 g/L NaCl) and stored in 15% glycerol at −80 °C.

In silico characterization of the DyP from *Pseudomonas* sp. AU10

The theoretical molecular size and isoelectric point of DyP-AU10 were obtained with the *Compute pI/Mw* tool, from the website ExPASy (https://web.expasy.org/compu

te_pi/; Bjellqvist et al. 1993, 1994; Gasteiger et al. 2005); its potential subcellular localization was determined using the SPL-*Local* (http://sunflower.kuicr.kyoto-u.ac.jp/~smatsuda/slplocal.html; Matsuda et al. 2005) and *pSORTb 3.0* tools (www.psort.org/psortb; Yu et al. 2010); the presence of signal peptides was evaluated using the *SignalP 4.1* tool (https://services.healthtech.dtu.dk/service.php?SignalP-5.0; Almagro Armenteros et al. 2019; Nielsen and Engelbrecht 1997); the presence of possible conserved domains within the amino acid sequence was assessed using the *Prosite* tool from ExPASy and the protein families and domain databases Pfam and InterPros. Finally, the hotspot regions for protein aggregation were predicted using the *Aggrescan* tool (http://bioinf.uab.es/aggrescan/; Conchillo-Solé et al. 2007).

For the phylogenetic affiliation of DyP-AU10, the amino acid sequence was aligned with reference sequences using ClustalW (Larkin et al. 2007), and the phylogenetic trees were inferred using the neighbor-joining (NJ), maximum-likelihood (ML), and unweighted pair group method with arithmetic mean (UPGMA) algorithms, with bootstrap analysis for 1000 replicates, in the MEGA-X software (Kumar et al. 2018). Branches with less than 50% bootstrap replicates were collapsed.

Molecular modeling

The homology modeling of DyP-AU10 was performed with the HHpred server (https://toolkit.tuebingen.mpg.de/tools/hhpred; (Zimmermann et al. 2018); this server uses alignments for the calculation of 3D structural models using the MODELLER software. We used the following bacterial DyP crystal structures as templates (PDB access numbers in parenthesis): *Vibrio cholerae* (5DE0), *Klebsiella pneumoniae* (6FKS), *Enterobacter lignolyticus* (5VJ0), *Streptomyces coelicolor* (4GT2), *Cellulomonas bogoriensis* (6QZO), *Thermobifida fusca* (5FW4), *Thermomonospora curvata* (5JXU), and *Bacillus subtilis* (6KMM). The prediction of the topology of the substrate-binding pocket was carried out using CASTp with a 1.6 Å radius probe (http://sts.bioe.uic.edu/castp/calculation.html; Tian et al. 2018). We also used AlphaFold (free online version) to predict the 3D structure of DyP-AU10. The structures were visualized using *PyMOL 2.3.2* software (https://pymol.org/2/; The PyMOL Molecular Graphics System, Version 2.0 Schrödinger, LLC).

Production of the recombinant DyP-AU10

The *dyP-AU10* gene sequence was synthesized (the codon use was optimized for gene expression in *E. coli*; accession number OP910001) and cloned into the expression vector pET28a (+) (the expression vector encodes for the enzyme with an N-terminal 6-His tag for its purification), through the GenScript service (https://www.genscript.com/, USA). *E. coli* BL21 (DE3) or Arctic Express (DE3) chemocompetent cells were transformed with the recombinant vector. For expression of rDyP-AU10 protein, 5 mL pre-cultures were grown in LB broth in the presence of 50 µg/mL kanamycin, at 37 °C overnight. Pre-cultures were transferred to 2-L flasks containing 200 mL Zym-5052 medium with 50 µg/mL kanamycin and 30 mg/mL hemin (dissolved in DMSO) and incubated for 3 h at 37 °C and 200 rpm, until reaching an absorbance at 600 nm of ~0.3. Then, the flasks were incubated at 14 and 25 (for 60 h) or 37 °C (for 24 h). Cell pellets (*ca.* 8 g) were harvested by centrifugation (5000 *g*, 10 min, at 4 °C) and suspended in 40 mL lysis buffer (50 mM potassium phosphate, 300 mM NaCl, 10 mM imidazole, pH 8.0). Cell lysis was achieved by sonication (three rounds of 40 intermittent pulses with an amplitude of 50) for 10 min on ice; then, the cellular debris and precipitated hemin were removed by centrifugation at 5000 *g* for 10 min. The supernatants were used as starting material for the purification of the rDyP-AU10 protein. The soluble and insoluble (inclusion bodies) fractions were obtained by centrifugation (13000 *g* at 4 °C for 30 min) and were analyzed by SDS-PAGE using 12% and 5% acrylamide for the resolving gel and stacking gel, respectively, as described by Laemmli (1970).

Enzyme purification by immobilized metal affinity chromatography

The purification of rDyP-AU10 was done from the soluble fraction by immobilized metal affinity chromatography (IMAC). The sample (40 mL) was filtered through a 0.45 µm membrane and loaded onto a HisPur™ cobalt resin (#89964, Thermo Fisher Scientific) in lysis buffer and incubated for 1 h at 4 °C. The recombinant protein was eluted using 50 mM potassium phosphate buffer (pH 7.8) containing 300 mM NaCl and 150 mM imidazole; it was then subjected to gel filtration using a PD-10 desalting column (#17-0851-01, Cytiva) in 20 mM Tris containing 130 mM NaCl, at pH 7.4. Protein concentration was determined using the Bradford reagent (#5000006, Bio-Rad) (calibration curve with bovine serum albumin). The purified protein was stored in glycerol 50% at −80 °C. The enzyme identity was verified by mass spectrometry (MALDI-ToF/ToF) in the Analytical Biochemistry and Proteomics Unit of the Institut Pasteur de Montevideo (Uruguay). All fractions were controlled by SDS-PAGE. The activity of fractions was verified using 2,2′-azinobis-(3-ethylbenzthiazoline-6-sulfonate (ABTS) and H_2O_2 as substrates, as described below.

Except for the determination of the oligomeric state (see next item), the characterization of the enzyme was done using the dimeric form of rDyP-AU10. The dimer

was purified by using a HiLoad 16/60 Superdex G-200 column (60 cm × 16 mm, #GE28-9893-35, Cytiva) attached to an AKTA Prime Plus system (Lab-scale protein purification, Cytiva).

Determination of molecular size and oligomer formation

rDyP-AU10 (100 µL, 16 mM) was injected into a size-exclusion chromatography system (Shimadzu UFLC Prominence system), equipped with a Superdex G-75 10/300 column (32 cm × 2.6 cm, GE Healthcare) (at room temperature). The elution buffer was 20 mM Tris with 150 mM NaCl (pH 7.4). The flow rate was 0.5 mL/min, and the elution samples were monitored at 280 and 406 nm. The molecular size was determined using a calibration curve obtained with the Gel Filtration Calibration Kits (#GE28-4038-41, GE Healthcare). The fractions were also analyzed by SDS-PAGE.

The formation of oligomers was also studied by semi-native PAGE and Western blot. For semi-native gels, samples were prepared in a native loading buffer containing 30 mM Tris, 25 % glycerol, and 0.1 mg/mL bromophenol blue, without SDS or reducing agent. We used 10% and 5% acrylamide (containing SDS) for the resolving gel and the stacking gel, respectively. The running buffer consisted of 25 mM Tris, 200 mM glycine, and 3 mM SDS (Arndt 2012). For Western blot, two semi-native SDS-PAGE gels were run in parallel. We loaded 1 µg or 0.1 µg of rDyP-AU10 per well. Proteins from one gel (the one loaded with 1 µg of protein per well) were stained using a Coomassie Brilliant Blue R250 solution. The Western blot technique was performed in the second gel (wells loaded with 0.1 µg of protein) as follows: the proteins were transferred to nitrocellulose membranes (Hybond^{TM}-C extra) using transfer buffer (25 mM Tris at pH 8.3, containing 150 mM glycine and 20% [v/v] ethanol); then, the membrane was incubated with the primary antibody (0.01 µg/mL His-tag antibody, mAb mouse) for 1 h, washed with PBS, blocked with 5% dried skimmed milk in PBS, and finally, treated with the secondary antibody (goat anti-mouse HRP conjugate, 1 mL of 1:5000 dilution). After 1 h incubation, the antibody was removed by washing with PBS, and the His-tag present in rDyP-AU10 was detected by chemiluminescence using the Pierce ECL Western Blotting Substrate kit (#32106, Thermo Fisher).

Steady-state peroxidase activity measurements

The activity of rDyP-AU10 (11 nM) was determined by measuring the initial rate of oxidation of 3 mM ABTS at 420 nm ($\varepsilon = 36\ mM^{-1}\ cm^{-1}$) with 1 mM H_2O_2. Experiments were done at 20 °C and pH 5, in an activity buffer containing a mixture of 0.05 M acetic acid, 0.05 M MES, and 0.1 M Tris (Ellis and Morrison 1981). Control experiments without enzyme and/or H_2O_2 were done. One unit of activity (or enzyme unit, EU) was defined as the amount of enzyme required to oxidize 1 µmol of substrate per minute under these assay conditions. We always used fresh H_2O_2 solutions; the concentration was determined from the absorbance at 240 nm ($\varepsilon = 39.4\ M^{-1}\ cm^{-1}$). We used a stoichiometric coefficient of two $ABTS^+$ formed per H_2O_2 consumed.

The pH dependence of rDyP-AU10 activity was determined at 20 °C, in a pH range from 3.0 to 8.0 using the activity buffer defined above, which has constant ionic strength at the different pHs. The effect of temperature on rDyP-AU10 activity was determined at pH 5, in a temperature range from 10 to 50 °C.

The peroxidase activity of rDyP-AU10 towards a panel of substrates was determined by absorbance measurements as follows: ABTS (0.025–6 mM, $\varepsilon = 36\ mM^{-1}\ cm^{-1}$, 420 nm); 2,4-dichlorophenol (0.010–6 mM, $\varepsilon = 18.5\ mM^{-1}\ cm^{-1}$, 510 nm); guaiacol (0.002–1 mM, $\varepsilon = 26.6\ mM^{-1}\ cm^{-1}$, 465 nm); hydroquinone (0.250–5 mM, $\varepsilon = 21\ mM^{-1}\ cm^{-1}$, 247 nm); pyrogallol (0.025–60 mM, $\varepsilon = 24{,}7\ mM^{-1}\ cm^{-1}$, 430 nm); and ascorbate (0.050–0.3 mM, $\varepsilon = 28\ mM^{-1}\ cm^{-1}$, 290 nm). Assays were performed at 20 °C, in the activity buffer at pH 5, using 11 nM rDyP-AU10 and 1 mM H_2O_2. Control experiments without enzyme and/or H_2O_2 were done. Apparent kinetic parameters (K_M and k_{cat}) were determined by non-linear fittings of the Michaelis–Menten equation using *Origin Pro8* software, considering that $k_{cat} = V_{max}/[E]$. At least two biological replicates (two different rDyP-AU10 productions) and three technical replicates were done for each condition.

The catalase activity of rDyP-AU10 was analyzed following the consumption of H_2O_2 at 240 nm and 20 °C (Murakami et al. 1995). The reaction mixture contained the activity buffer (pH 5), 1 mM H_2O_2, and 11 nM rDyP-AU10.

Stability and storage at different temperatures

The thermo-stability was studied after the incubation of 6.4 µM of the purified enzyme for 1 h at 20, 30, 40, 50, 60, or 70 °C. The activity was then determined at 20 °C using ABTS as substrate, as described above (3 mM ABTS, 1 mM H_2O_2, pH 5). We also determined the time course (5, 10, 20, 30, 40, 45, 50, 55, and 60 min) of inactivation of the enzyme at 60 °C. The activity of rDyP-AU10 after storage at −80 °C in 50% glycerol for 6 months was also determined.

Stopped-flow kinetics

A stopped-flow spectrophotometer equipped with a photodiode array detector was used (Applied Photophysics SX20). To study the reaction between rDyP-AU10 and H_2O_2 to form Compound I, 1 µM enzyme was mixed with

10–40 µM H_2O_2 (final concentrations) in activity buffer at 25 °C and pH 5, and the time-dependent spectral data were recorded. Multiple wavelength data in the 300–700-nm range were analyzed with the *Pro-KIV* Global Analysis software. In parallel, single wavelength data (404 nm) were analyzed. The pseudo-first-order rate constants (k_{obs}) were obtained by fitting single exponential equations to the 404-nm time courses. The second-order rate constants were calculated from plots of k_{obs} as a function of H_2O_2 concentration.

The conversion of Compound I to resting enzyme, possibly via Compound II, was studied determining the turnover of the enzyme in the presence of hydroquinone. The enzyme (1 µM) was premixed with hydroquinone (1 mM) in one syringe and mixed with 10 µM H_2O_2 in the other syringe (final concentrations). Spectra were obtained and analyzed with the *Pro-KIV* software.

Activity of rDyP-AU10 on a lignin model substrate (kraft lignin)

The modification of the model substrate, kraft lignin (#471003, Sigma Aldrich), by rDyP-AU10 was monitored by the decrease in the absorbance at 280 nm (Falkehag and Marton 1966; Bashtan-Kandybovich et al. 2012) and by the increase in absorbance at 465 nm (Ahmad et al. 2010). The assays were carried out at 20 °C and pH 5 in the activity buffer, using kraft lignin (5–25 µM), 4 mM H_2O_2, and 1.3 µM of enzyme (final concentrations). The molar concentration of kraft lignin was calculated using a molecular weight of 10,000 Da (Ahmad et al. 2011).

Dye decolorization assay by rDyP-AU10

The decolorization of several dyes was determined by monitoring the change in absorbance at the maximum absorption (λ max). We used the following dyes: 4-{[4-(dimethylamino)phenyl](phenyl)methylene}cyclohexa-2,5-dien-1-imine or malachite green (λ_{max} = 618 nm), tris(4-(dimethylamino)phenyl) methylium chloride or methyl violet 6B (λ_{max} = 585 nm), and 4-{[4-(dimethylamino)phenyl]diazenyl}benzene-1-sulfonate or methyl orange (λ_{max} = 465 nm). The assays were carried out at 20 °C and pH 5 in the activity buffer, using 30 µM of each dye, 1 mM H_2O_2, and 1.3 µM rDyP-AU10. Control treatments were done without the enzyme and with H_2O_2. The decrease in absorbance for each substrate was monitored at 1-min interval, during 30 min. The decolorization efficiency (DE) was expressed as the percentage of decolorization, following Eq. 1 (Dhankhar et al. 2020).

$$DE(\%) = \frac{InitialAbs - FinalAbs}{InitialAbs} x100 \quad (1)$$

Results

In silico characterization of DyP-AU10

As shown in Fig. 1a, the phylogenetic affiliation of DyP-AU10 supports that this protein is a class B DyP (for the classification of peroxidases, see PeroxiBase) or P (Primitive DyPs) as described by Sugano and Yoshida 2021. DyPs from class B (or class P) are usually short amino acid sequence proteins with a molecular weight that ranges between 30 and 35 kDa (Yoshida and Sugano 2015); in agreement, the in silico analysis of DyP-AU10 shows that the protein contains 287 amino acids, a theoretical molecular weight of 31 kDa, and a theoretical isoelectric point of 4.91. Besides, DyP-AU10 does not contain a signal peptide, suggesting that it would be located in the bacterial cytosol. The prediction of hotspot aggregation showed that DyP-AU10 has 14 sites, a high value, suggesting that this protein is prone to aggregation and would probably be produced as inclusion bodies in *E. coli* hosts.

The sequence alignment of DyP-AU10 with other members of the DyP-type peroxidase family is shown in Fig. 1b. The alignment allowed us to identify two overlapping and similar conserved GXXDG (GLEDG or GIVDG in DyP-AU10) motifs; the presence of a single GXXDG motif is commonly found in DyP-type peroxidases (Colpa et al. 2014).

Structure prediction and amino acid composition

The templates (see Table 1) used for modeling DyP-AU10 showed between 22 and 30% sequence similarity. As the native DyP-AU10 is produced by a cold-tolerant microbe, we compared a few structural features of DyP-AU10 with DyPs produced by mesophilic and thermophilic microbes (Table 1, second column). When comparing DyP-AU10 with DyPs from thermophilic microbes (growth over 45 °C), we found that DyP-AU10 contains a reduced number of arginine residues, a result expected for a psychrophilic enzyme (enzymes produced by psychrophilic or cold-tolerant microbes, with optimal growth temperature under 25 °C). The low number of arginine residues is associated with an increase in protein flexibility (Feller and Gerday 2003). We did not find differences in the percentage of other amino acids, including prolines, glutamic, and aspartic acids. Our analysis also suggests that DyP-AU10 has a catalytic pocket surface larger than DyPs from thermophilic microbes and similar to DyPs from mesophilic microbes (optimal growth temperature in the range of 25 to 40 °C). DyPs from *Rhodococcus josti*, *Pseudomonas putida*, and *Pseudomonas* sp. AU10 have similar size of

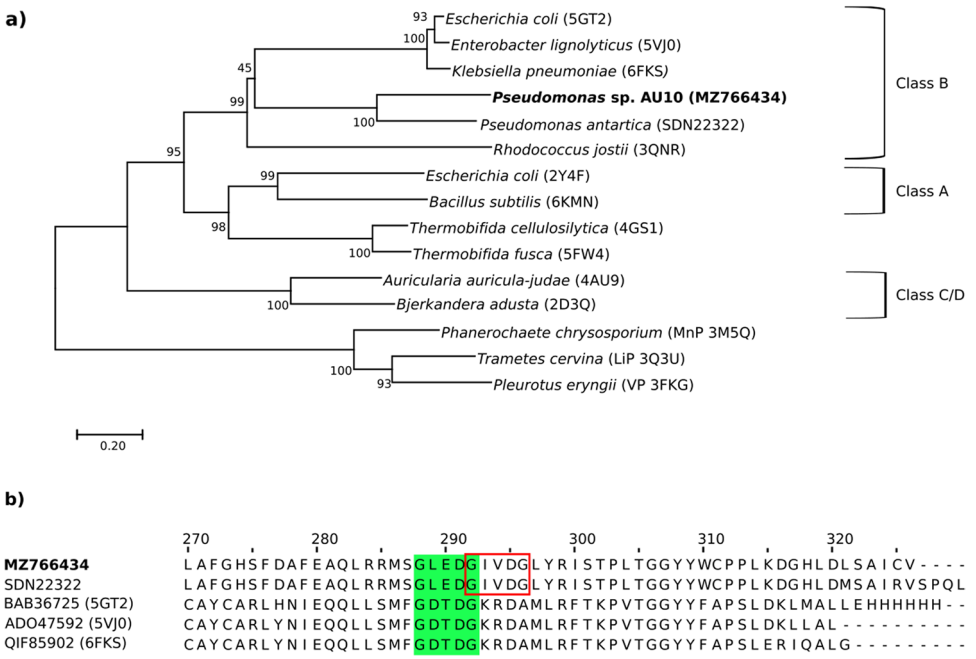

Fig. 1 Phylogenetic tree and alignment of the DyP-type family of peroxidases. **a** The phylogenetic analysis was performed using the MEGA-X software and different algorithms as described in the "Materials and methods" section. We obtained a similar topology in all cases. Thus, we only show the result from the NJ method. The *numbers* settled in branches represent the nodal support values. Accession numbers from the PDB are shown in parentheses. The class and subclass are also shown. The accession numbers of DyPs from *Pseudomonas* sp. AU10 and *P. antarctica* are from the NCBI. The sequences of non-DyP-peroxidases were used as external roots: manganese peroxidase (MnP), lignin peroxidase (LiP), and versatile peroxidase (VP). **b** The alignment of DyPs shows the conserved GXXDG motif and the overlapping motifs found in DyP-AU10 and *Escherichia coli* O157 (5GT2). The accession number from NCBI or PDB (in parenthesis) is indicated

the pocket surface, and interestingly, DyP from *P. putida* has flat temperature-activity dependence from 10 to 30 °C (Santos et al. 2014) (Table 1), supporting that low-temperature active DyPs may have bigger pockets as compared with mesophilic/thermophilic ones.

The inferred 3D structure is shown in Fig. 2. DyP-AU10 contains more polar and aromatic amino acids in the pocket when compared with the other peroxidases we evaluated. We also performed a 3D structure prediction using AlphaFold, and we found that both, AlphaFold and HHpred servers, give structures with no appreciable differences.

Recombinant production and purification of rDyP-AU10

We detected the production of the recombinant DyP-AU10 (rDyP-AU10) protein at all tested conditions. At 37 °C, the recombinant protein was found in the inclusion bodies when using both BL21 (DE3) and Arctic Express (DE3) strains; however, when the recombinant strains were grown at 14 and 25 °C, the protein was obtained in both soluble and insoluble (inclusion bodies) fractions (Fig. 3).

We purified rDyP-AU10 from the soluble fraction obtained after growing the recombinant Arctic Express (DE3) strain at 14 °C. The yield was 0.22 g/L of culture. The enzyme migrated as a single band on SDS-PAGE (Fig. 3, fractions E1 and E2 obtained after the purification by IMAC) with a predicted monomeric mass of 33.5 kDa; it was identified as a "DyP-type enzyme" by MALDI-ToF (MS-MS).

Biochemical characterization of the recombinant DyP-AU10

When analyzed by size exclusion chromatography, rDyP-AU10 resolved in three peaks consistent with the monomeric, dimeric, and trimeric protein, being the dimeric form (~61.5 kDa) the main one (Fig. 4a). The presence of three forms was confirmed by semi-native PAGE and Western blot (Fig. 4b). The UV-Visible spectrum of rDyP-AU10 showed a maximum at 406 nm (Fig. 4c), consistent with the prediction that DyP-AU10 is a hemeprotein.

We produced the protein in the presence of hemin; besides, we also produced rDyP-AU10 using δ-aminolevulinic acid in the bacterial culture medium instead of hemin (data not shown). The *Reinheitszahl* value (*Rz*; the heme/protein ratio as Abs_{406}/Abs_{280}) (Dunford et al. 1982) of the purified enzyme was higher (1.63) when using hemin rather than using δ-aminolevulinic acid (0.62); thus,

Table 1 Amino acid composition and general features of DyPs from the PDB and DyP-AU10

Organism	Optimal growth temperature (°C)	Optimal activity temperature (°C)*	PDB	% Arginine	% Proline	% Glycine	% Glutamic acid	% Aspartic acid	Pocket surface (Å)
Thermobifida fusca	50–55	45–60	5FW4 (430)	10	7	9	6	8	229
Thermomonospora curvata	45–50	30	5JXU (390)	10	8	10	5	8	265
Cellulomonas bogoriensis	30–37	nd	6QZO (383)	10	8	10	6	8	139
Bacillus subtilis	35–37	30	6KMM (363)	4	5	9	5	6	225
Klebsiella pneumoniae	35–37	nd	6FKS (303)	6	4	10	7	7	412
Enterobacter lignolyticus	35–37	30	5VJ0 (311)	6	3	10	8	6	411
Vibrio cholerae	30–37	nd	5DE0 (305)	4	5	8	7	6	382
Streptomyces coelicolor	28–30	nd	4GT2 (455)	9	7	13	5	7	219
Shewanella oneidensis	35**	nd	2HAG (307)	5	5	7	9	7	151
Rhodococcus josti	30	nd	4HOV (308)	5	6	6	5	11	423
Pseudomonas putida	30	10–30***	7QYQ (283)	6	7	9	6	7	387
***Pseudomonas* sp. AU10**	**20**	**20**	**AU10 (287)**	**6**	**6**	**9**	**6**	**7**	**380**

From left to right, the table shows a list of DyP-producing microbes, the optimal growth temperature of these microbes (in °C), the optimal temperature of the DyP (in °C; *nd* means not determined), the PDB accession number of their DyPs, the total number of amino acids (in parenthesis), the content of different amino acids (% of the total number of amino acids), and the size of the surface of the catalytic pocket (in Å). The optimal growth temperature for AU10 was reported in Martínez-Rosales and Castro-Sowinski (2011)

*The optimal activity temperature was included in this table only when it was properly determined

**A mesophilic bacterium with a wide range of growth temperatures, including temperatures near zero (Abboud et al. 2005)

***Presents an optimal temperature from 10 to 30 °C, displaying a flat temperature profile (Santos et al. 2014)

Values in bold highlight the results found for the Antarctic *Pseudomonas* sp. AU10 and DyP-AU10, the subject of the present work

we continued producing the enzyme with hemin. In addition, the *Rz* value of 1.63 was comparable to those reported for other rDyPs (Chen et al. 2015; Mendes et al. 2015b; Pfanzagl et al. 2018; Rahmanpour and Bugg 2015).

The purified protein oxidized ABTS using H_2O_2 as cosubstrate, showing maximum activity at 20 °C and pH 5 (Fig. 4d and e), and maintained 100% activity after 6 months of storage at −80 °C in 50% glycerol. A thermo-stability study (percentage of residual activity after exposure of the enzyme for 1 h at different temperatures) showed that the enzyme is fully active after 1 h at 20 °C; but it has reduced activity at higher temperatures (70% residual activity at 30 to 50 °C and 20% residual activity at 60 °C) (Fig. 4f). Then, we analyzed the time course of inactivation at 60 °C and observed that the thermal inactivation of the enzyme occurred 5 min after the onset of the incubation (20% residual activity; Fig. 4f, inset graph) as expected for a psychrophilic enzyme (Kobori et al. 1984).

The enzyme also oxidized hydroquinone and ascorbate using H_2O_2 as cosubstrates. The values of the apparent kinetic parameters (K_M, k_{cat}, and k_{cat}/K_M) for these substrates, as well as ABTS, are shown in Table 2. We did not detect oxidizing activity when using guaiacol, pyrogallol, or 2,4-dichlorophenol as substrates, in the tested conditions. The enzyme did not show activity using H_2O_2 as a single substrate, suggesting that rDyP-AU10 does not have catalase activity.

Stopped-flow kinetics

We studied the fast kinetics of formation of Compound I (rDyP-AU10-I) by stopped-flow spectrophotometry. Figure 5a shows the spectral changes observed when we mixed rDyP-AU10 (1 µM) and H_2O_2 (20 µM). We observed a slight shift to shorter wavelengths in the maximum of the *Soret* band (404 to 398 nm), as well as a marked decrease in the absorptivity of the species formed. This result is compatible with the formation of rDyP-AU10-I (Lučić et al. 2020; Mendes et al. 2015b; Pfanzagl et al. 2018; Rahmanpour and Bugg 2015; Roberts et al. 2011; Shrestha et al. 2017).

Multiple wavelength time courses were analyzed globally with *Pro-KIV*. A model consisting of the transformation of rDyP-AU10 (with its heme in the ferric state) to rDyP-AU10-I in a single irreversible step with a second-order constant (k_{H2O2}) (Ec. 2) was fitted to kinetic data obtained between 300 and 700 nm for 10 half-lives.

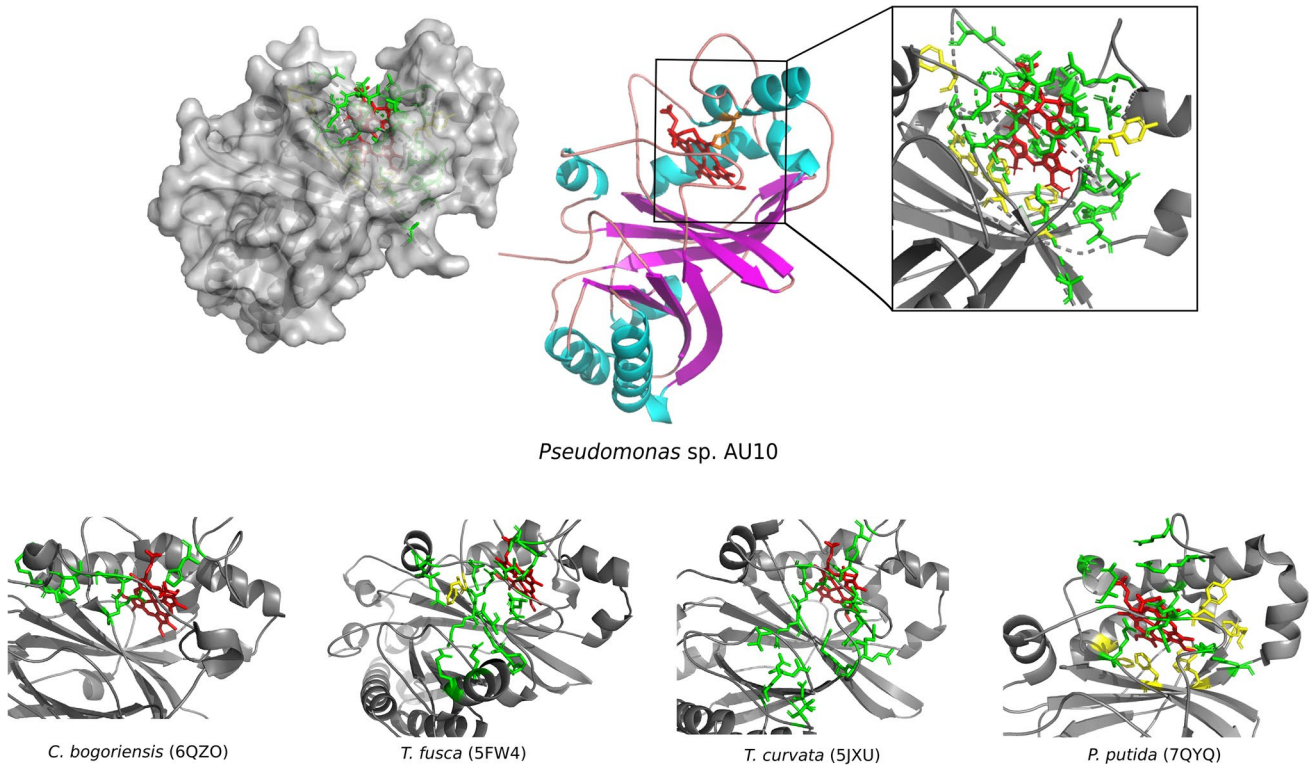

Fig. 2 Structure prediction of DyP-AU10. **a** Proposed 3D structure of DyP-AU10, including a surface and ribbon protein representation. **b** Amplification of the catalytic pocket. **c** Proposed 3D structure of the catalytic pocket of DyPs from the mesophilic microbes *Cellulomonas bogoriensis* and *Pseudomonas putida*, and the thermophilic microbes *Thermobifida fusca* and *Thermomonospora curvata.* PDB accession numbers are in parentheses. Some amino acids from the catalytic pocket are highlighted. The heme group is depicted in red, the proximal histidine residue in orange, polar residues in green, and aromatic residues in yellow

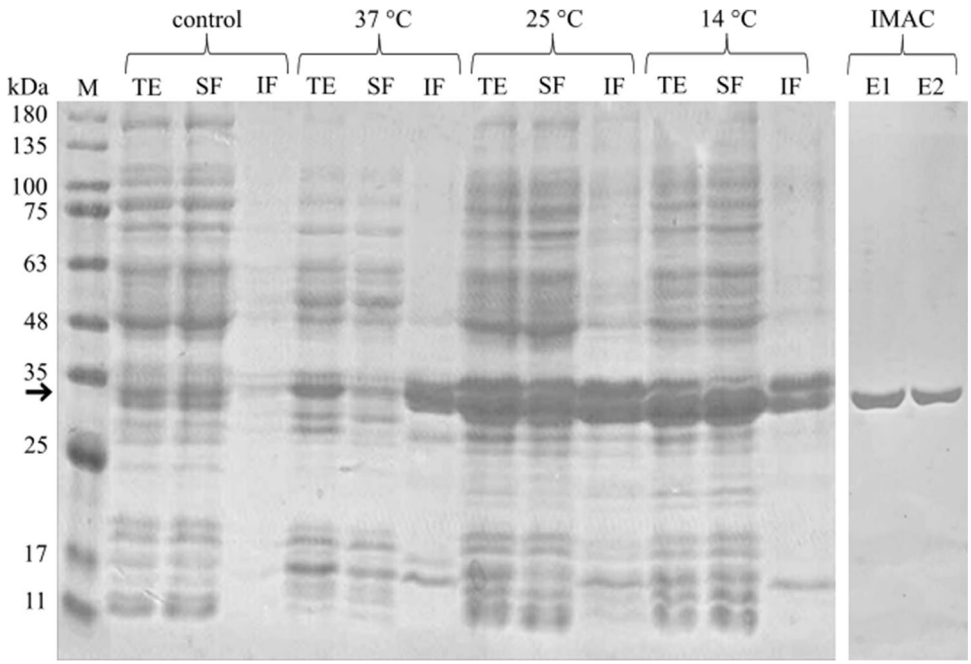

Fig. 3 Analysis by SDS-PAGE of the production and purification of rDyP-AU10. The temperature used for protein expression (14, 25, and 37 °C) is indicated at the top. The different fractions are named as follows: TE, total extract; SF, soluble fraction; IF, insoluble fraction; eluates obtained after the purification procedures by IMAC are as follows: E1, first eluate; E2, second eluate. M indicates the molecular weight marker (#02101-250, Mastrogen). The arrow shows the overexpressed protein. The rows named "control" show the protein fractions obtained from *E. coli* ARCTIC cells transformed with the pET28a(+) vector, without the *dyp* gene, growing at 14 °C

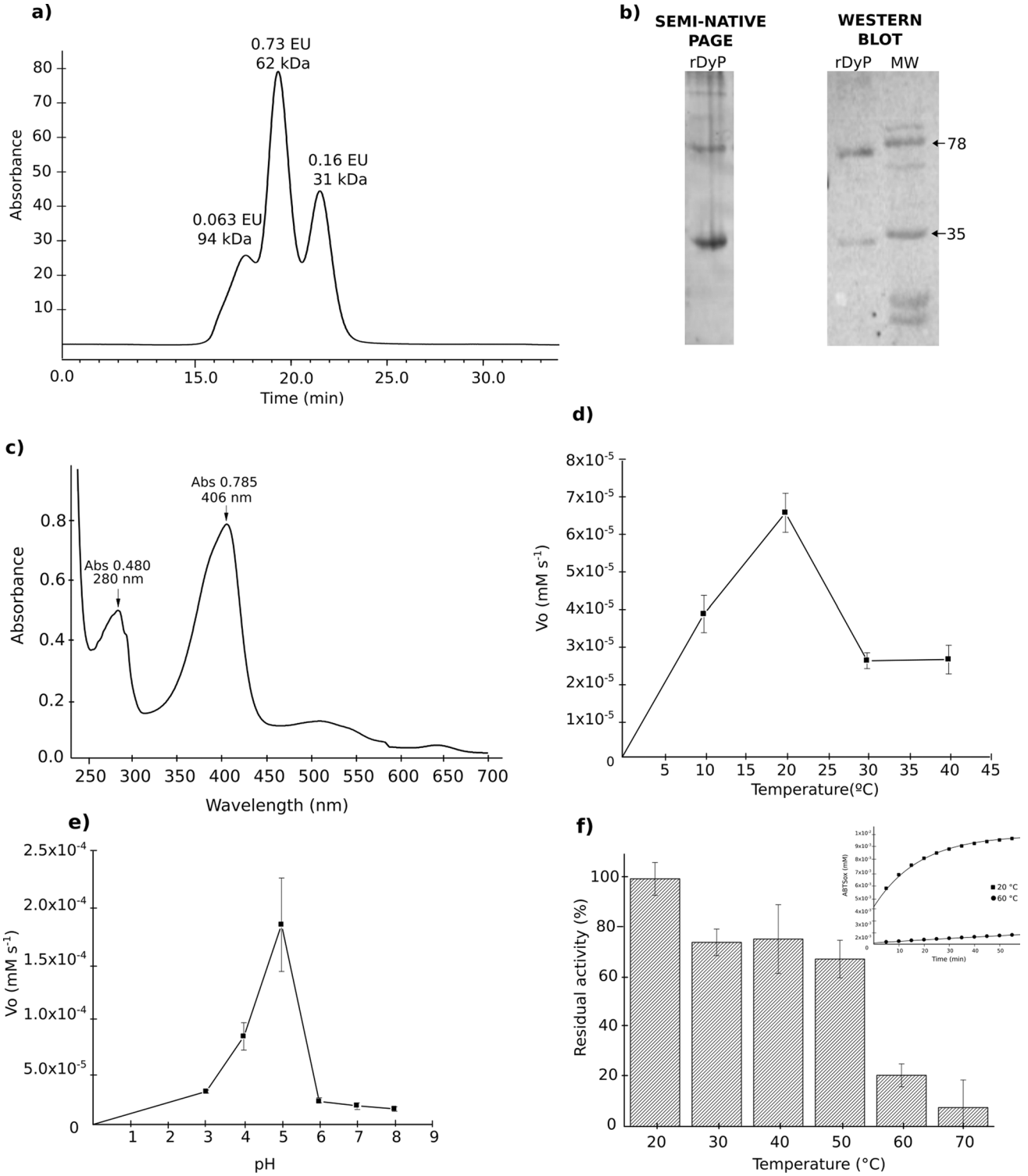

Fig. 4 Partial characterization of rDyP-AU10. **a** Size exclusion chromatography of rDyP-AU10. The oligomers (monomer, dimer, and trimer) size and activity (EU) are shown on each peak. **b** Semi-native PAGE (left) and immunoblotting (right); MW represents the molecular weight marker. **c** UV-Vis spectrum of the dimeric form of rDyP-AU10 (6.4 µM). **d** Temperature-dependence of enzyme activity; ABTS oxidizing activity at pH 7 at a temperature range from 10 to 40 °C. **e** pH-dependence of enzyme activity; ABTS oxidizing activity at 20 °C at a pH range from 3 to 8. **f** Thermal stability of rDyP-AU10 at different temperatures; residual activity (%) after 1 h of incubation at different temperatures; activities were determined using 3 mM ABTS and 1 mM H_2O_2 at pH 5 and 20 °C. The inset graph in Fig. 4f shows the time course of inactivation of DyP-AU10 at 60 °C and 20 °C

Table 2 Apparent steady-state kinetic parameters for rDyP-AU10

Substrate	K_M (mM)	k_{cat} (s^{-1})	k_{cat}/K_M (M^{-1} s^{-1})
ABTS*	0.86 ± 0.18	20 ± 2	(2.4 ± 0.4) × 10^4
Hydroquinone*	0.15 ± 0.01	41 ± 3	(2.7 ± 0.1) × 10^4
Ascorbate*	0.33 ± 0.07	20 ± 6	(5.8 ± 0.6) × 10^4
H_2O_2**	0.48 ± 0.27	61± 13	(15 ± 5) × 10^4

Assays were performed in buffer mix at 20 °C and pH 5

*The kinetic constants were determined using 1 mM H_2O_2

**The kinetic constants were determined using 3 mM ABTS as cosubstrate

$$\mathrm{rDyP-AU10} + \mathrm{H_2O_2} \rightarrow \mathrm{rDyP-AU10-I} + \mathrm{H_2O} \quad (2)$$

The fits were excellent. We did not find evidence for the existence of additional steps in the transformation of rDyP-AU10 into rDyp-AU10-I. From a total of 14 measurements, the second-order rate constant was determined to be (2.07 ± 0.09) × 10^6 M^{-1} s^{-1} (average value with its corresponding standard deviation). In parallel, we analyzed single wavelength data. To monitor the formation of rDyp-AU10-I, the wavelength of 404 nm was selected, where a clear decrease in absorbance was observed (Fig. 5b). Single exponential equations were fitted to the data. The pseudo-first-order rate constants (k_{obs}) increased linearly with the concentration of H_2O_2 (Fig. 5c). In addition, the *y*-axis intercept was close to zero, as expected for the transformation of rDyP-AU10 to rDyp-AU10-I in a single irreversible step. The second-order rate constant was calculated from the linear fit of the plot of k_{obs} versus H_2O_2 concentration. The value obtained was (2.09 ± 0.03) × 10^6 M^{-1} s^{-1}, which is consistent with the value obtained from the global analysis.

To study the stability of rDyP-AU10-I, we registered the spectra resulting from mixing rDyP-AU10 (1 µM) with 20 µM H_2O_2 at 0.005 s (freshly mixed enzyme), at 0.170 s (10 half-lives of the reaction with H_2O_2) and at 10 s (maximum time analyzed, ~600 half-lives) (Fig. 5d). Except for a slight increase in the absorbance at all wavelengths at 10 s, possibly due to minor turbidity, the spectra of the products at 0.170 and 10 s were similar and presented maxima at 398 nm, suggesting that rDyP-AU10-I remained stable.

The regeneration of resting enzyme from rDyP-AU10-I and the possible formation of Compound II (rDyP-AU10-II) were analyzed under turnover conditions in the presence of hydroquinone as substrate. Hydroquinone was chosen because its absorbance does not interfere with the absorbance of the heme (Morales et al. 2012). As observed in Fig. 5e, the enzymatic form that predominated during turnover was rDyP-AU10-I. Although isosbestic points were not clearly resolved, no evidence was obtained for the formation of rDyP-AU10-II, which, in the case of the Compound II of the DyP class B from *Klebsiella pneumoniae*, has absorbance peaks at 418, 527, and 553 nm (Pfanzagl et al. 2018). Accordingly, the absorbance at 404 nm remained at a relatively low value during most of the time course of the reaction (Fig. 5f). The failure to detect rDyP-AU10-II could suggest that rDyP-AU10-I reacted with hydroquinone to regenerate the ferric species in only one step (Eq. 3, where *S* represents, in this case, hydroquinone, and Sox represents the two-electron oxidized quinone).

$$\mathrm{rDyP-AU10-I} + S \rightarrow \mathrm{rDyP-AU10} + \mathrm{Sox} \quad (3)$$

Alternatively, the failure to clearly detect rDyP-AU10-II could suggest, in the context of a two-step regeneration of ferric enzyme (Eqs. 4–5, where $S^{\bullet}$ represents the one-electron oxidation product), that rDyP-AU10-II does not accumulate to a significant extent. This would be the case if the rate constant for the conversion of rDyP-AU10-I to rDyP-AU10-II (Eq. 4) was slower than that for conversion of rDyP-AU10-II to resting enzyme (Eq. 5) ($k_{II/Fe3+} > k_{I/II}$).

$$\mathrm{rDyP-AU10-I} + S \rightarrow \mathrm{rDyP-AU10-II} + S \quad (4)$$

$$\mathrm{rDyP-AU10-II} + S \rightarrow \mathrm{rDyP-AU10} + S \quad (5)$$

Through global analysis with *Pro-KIV*, the fit of these two models to the spectra kinetic data was assessed. The one-step model consisting of the regeneration of the enzyme directly from rDyP-AU10-I (Eq. 3) was able to converge well, with a rate constant value of (654 ± 1) M^{-1} s^{-1} (n= 9). The model that also included rDyP-AU10-II (Eqs. 4–5) either did not converge or converged with a rate constant several orders of magnitude lower for the transformation of rDyP-AU10-I to rDyP-AU10-II than for the transformation of rDyP-AU10-II to resting enzyme, depending on the particular run analyzed.

Last, the possibility that rDyP-AU10-II had a spectrum very similar to that of resting enzyme was discarded because it would not be consistent with the finding that the Compound II of the DyP class B from *Klebsiella pneumoniae* has an absorption maximum at 418 nm, with a similar absorptivity as resting enzyme (Pfanzagl et al. 2018).

The biotechnological potential of rDyP-AU10: kraft lignin modification and decolorization of dyes

We analyzed the ability of rDyP-AU10 to modify lignin using kraft lignin as a model substrate. We observed a time-dependent decrease in the absorbance at 280 nm (6% decolorization after 100 s), as well as an increase in the absorbance at 465 nm when kraft lignin was treated with rDyP-AU10 (Fig. 6a). The change at 465 nm fitted to a straight line (Fig. 6b).

Among potential biotechnological properties of rDyP-AU10, we analyzed if it decolors dyes. The results

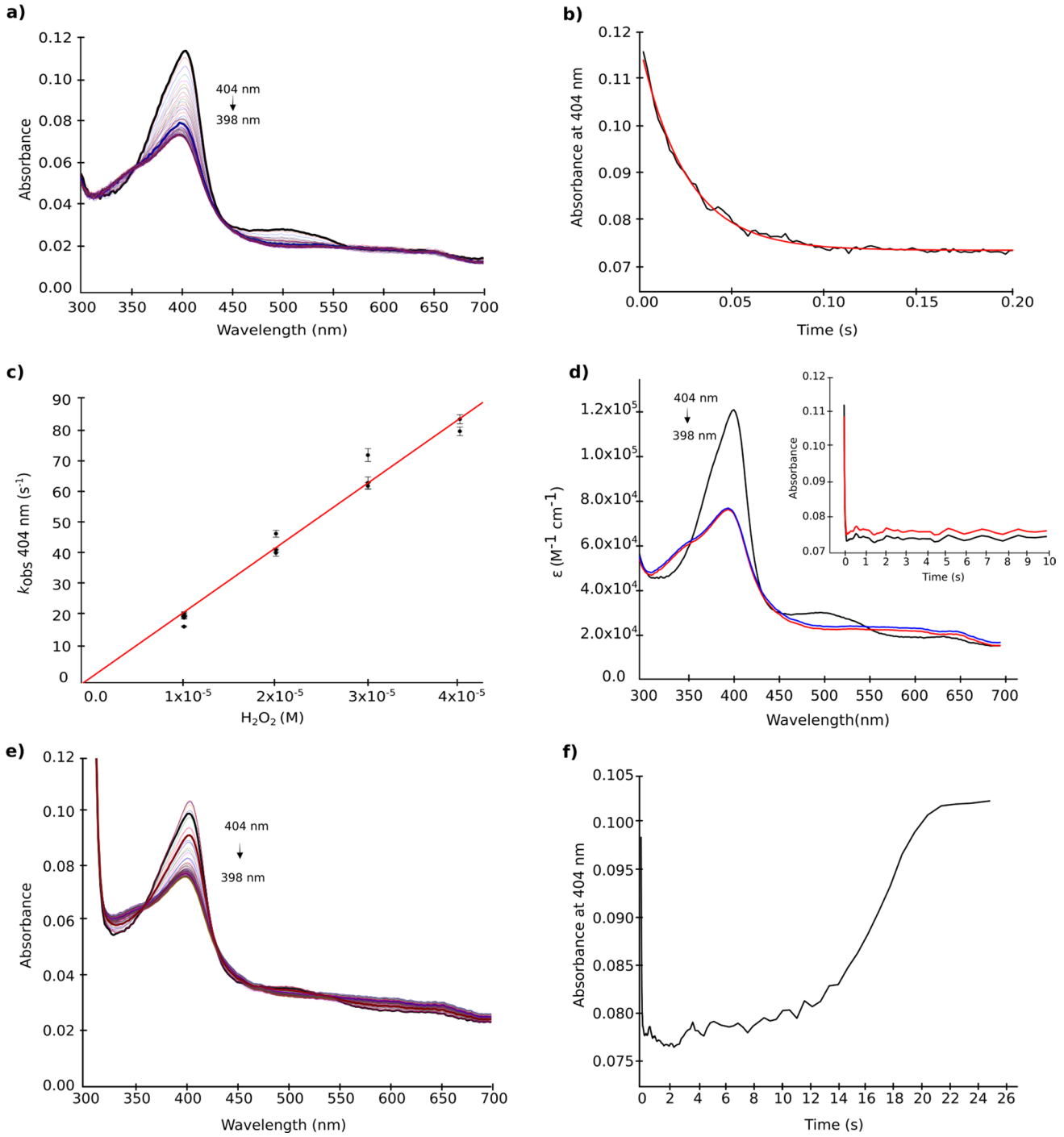

Fig. 5 Stopped-flow kinetics of rDyP-AU10 reaction with H_2O_2 and hydroquinone. **a** Time-dependent UV-Vis spectra of the reaction with H_2O_2. The enzyme (1 μM) was mixed with H_2O_2 (20 μM, concentrations after mixing) at 25 °C in the activity buffer at pH 5. Spectra were registered in logarithmic mode between 0 and 0.2 s. The arrow indicates the direction of the absorbance change. **b** Time course of the absorbance at 404 nm for the experiment shown in panel **a**. The red trace represents the fitted single exponential equation. **c** Dependence of the exponential rate constant k_{obs} at 404 nm on H_2O_2 concentration. The data points represent the fitted value of k_{obs} with the corresponding error of the fit. **d** Spectra at 0.005 (black), 0.170 (red), and 10 (blue) s; inset: absorbance at 404 nm (black) and 398 nm (red) during a 10 s run. **e** Time-dependent UV-Vis spectra of rDyP-AU10 in turnover. The enzyme (1 μM) and hydroquinone (1 mM) were mixed with H_2O_2 (10 μM). Spectra were registered in logarithmic mode between 0.012 and 25 s. The thick traces represent the spectra at 0.012 s (black), 2.030 s (dark yellow), and 17.046 s (wine). **f** Absorbance at 404 nm vs time for the experiment is shown in **e**

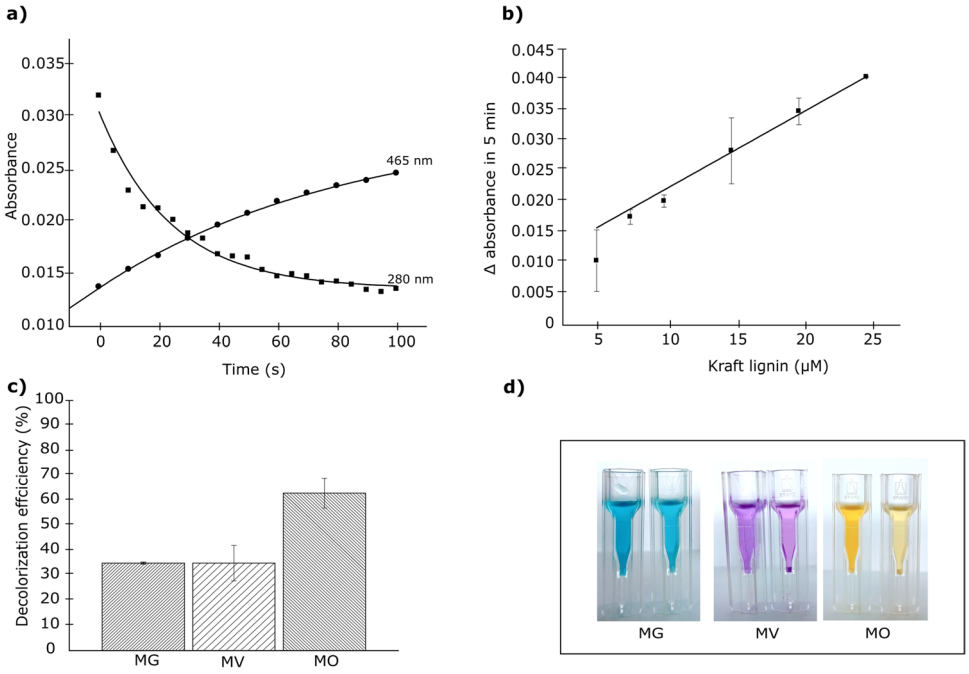

Fig. 6 The biotechnological potential of rDyP-AU10. **a** Time-dependent change in absorbance at 280 nm (black square) and 465 nm (black circle) of kraft lignin (5 μM) mixed with rDyP-AU10 (1.3 μM) and H_2O_2 (4 mM), in activity buffer at 20 °C and pH 5. **b** Change in absorbance at 465 nm after 5 min of reaction of kraft lignin (5 to 25 μM), 1.3 μM rDyP-AU10, and 4 mM H_2O_2; values are the mean and standard deviation, $n = 3$. The rate fitted to a straight line with an *R*-squared 0.996. **c** Percentage (%) of decolorization of malachite green (MG), methyl violet (MV), and methyl orange (MO). The bars represent the mean and standard deviation, $n = 3$, obtained after 30 min of reaction (30 μM of each dye, 1.3 μM rDyP-AU10, and 1 mM H_2O_2 at pH 5 and 20 °C). **d** Change in the color of dyes observed in the cuvettes after 30 min of reaction

(Fig. 6c and d) show that rDyP-AU10 decolorizes malachite green, methyl violet 6B, and methyl orange up to 35%, 35%, and 63%, respectively, within 30 min. No decoloring was observed with H_2O_2 alone. Thus, this enzyme can likely be used in the bioremediation of textile effluents.

Discussion

Hydrolases are the most significant contributors to the worldwide market of enzymes with industrial applications, followed by oxido-reductases. The demand for oxido-reductases is segmented mainly into catalase, glucose oxidase, and laccase, with applications in the food, beverage, detergent, textile, and pharmaceutical industries. Peroxidases also have an important place in the market of oxido-reductases, mainly horseradish peroxidase. According to BioSpace (https://www.biospace.com/), the global HRP market is expanding at a compound annual growth rate of 7% from 2020 (USD 49 million) to 2030. HRP is commonly used in immunohistochemistry, Western blotting, and ELISA. The demand for HRP in the healthcare industry is increasing and is expected to drive the market. In addition, other peroxidases have shown important uses in the paper industry. They can modify the lignin that remains in the cellulose pulp after the physical-chemical treatment of wood chips (delignification in the kraft pulping process); the lignin that remains after the process produces a brownish pulp and can be treated with peroxidases, thus increasing the whiteness and brightness of the paper (bio-bleaching activity) (Abdel-Hamid et al. 2013; Cagide and Castro-Sowinski 2020). The typical decoloring process uses enzymes with lignocellulosic activity such as laccase and lignin peroxidase. Fungal enzymes have more potential for decoloring applications than bacterial ones. However, the bacterial enzymes present some advantages because bacteria are easily grown and, due to that, the processes of scaling up, protein engineering, and expression are also easier to set up. In this scenario, we searched for peroxidases with novel properties, such as psychrophilic properties. Searching in the genome of the cold-tolerant microbe *Pseudomonas* sp. AU10 (Martínez-Rosales and Castro-Sowinski 2011; García-Laviña et al. 2019), we found a coding sequence for a DyP-like enzyme; DyPs have been described as lignin-degrading ones, with potential uses in the pulp industry and in bioremediation (Cagide and Castro-Sowinski 2020; Yang et al. 2018).

The phylogenetic analysis of the protein suggested that DyP-AU10 belongs to the class B (or class P) of DyPs

(Fig. 1a). As such, it shows the characteristic motif of this group of enzymes, which consists of GXXDG (Fig. 1b). Furthermore, it shows a non-previously reported feature, such as the presence of two overlapping and similar GXXDG (GLEDG or GIVDG) motifs. The partial in silico characterization of this protein also suggests that it belongs to the group of psychrophilic enzymes. In particular, DyP-AU10 shows a larger catalytic pocket, a decrease in arginine residues (involved in the formation of salt bridges and H-bonds) when compared with the homologous enzymes produced by mesophilic or thermophilic organisms (Table 1). These characteristics have previously been described for psychrophilic enzymes by Struvay and Feller (2012). Interestingly, we found a high number of aromatic and polar amino acids in the catalytic pocket (Fig. 2) as compared with DyPs from mesophilic and thermophilic microbes. We think that DyP-AU10 could accommodate more water molecules and promote stacking stabilization interactions between aromatic residues, affecting the activity at low temperatures.

For full activity, during the recombinant production of rDyP-AU10, the growth medium was supplemented with hemin. If we did not add hemin, the enzyme produced was inactive. The biochemical characterization showed that the enzyme has maximum activity at pH 5 and 20 °C (using ABTS or hydroquinone as a substrate) (Fig. 4d and e). The maximum activity at acidic pH was previously reported for DyPs (Rahmanpour and Bugg 2015); thus, this is not an unusual characteristic. The best temperature of activity of DyPs ranges from 50 (DyP from *Thermobifida fusca*; Rahmanpour et al. 2016b) to 30 °C (DyP from *Streptomyces avermitilis*; Sugawara et al. 2017). As an interesting feature, rDyP-AU10 was cold-active, showing an optimum temperature of activity at 20 °C. In addition, we found that rDyP-AU10 did lose activity after 5 min at 60 °C (thermo-instability), another characteristic of psychrophilic enzymes (Cavicchioli et al. 2011; Feller and Gerday 2003).

rDyP-AU10 has a molecular mass of 31 kDa (33 kDa, including the His-tag) and is mainly produced as a homodimer (Fig. 4a and b). These properties are similar to those found in other class B DyPs, such as DyPT1 from *Rhodococcus* sp. T1 (Roberts et al. 2011), DyP class B from *Rhodococcus jostii* RHA1 (Ahmad et al. 2011), and DyP1 class B from *Pseudomonas fluorescens* Pf-5 (Sahinkaya et al. 2019), including the quaternary structure (many bacterial DyPs are produced in oligomeric states ranging from monomers to hexamers; Colpa et al. 2014; Chen et al. 2015).

We determined the kinetic parameters for rDyP-AU10 using ABTS and H_2O_2 as substrates, and we compared the apparent specificity constant value, k_{cat}/K_M, $(2.4 \pm 0.4) \times 10^4$ M^{-1} s^{-1}, with those reported for a few microbial DyPs (wild-type and mutants). We found that rDyP-AU10 has a similar value as compared with the wild-type enzyme from *Pseudomonas* sp. strain Q8 (7 mM^{-1} s^{-1}) (Yang et al. 2018), *Pseudomonas putida* strain MET94 (9 mM^{-1} s^{-1}; 250 mM^{-1} s^{-1} for a variant obtained by directed evolution) (Brissos et al. 2017), and *Pseudomonas fluorescens* Pf-5 strain (25.2 mM^{-1} s^{-1}; 293 mM^{-1} s^{-1} for a Mn-binding site mutant H127R) (Rahmanpour and Bugg 2015; Rahmanpour et al. 2016a). Much higher specificity constants were reported for the DyPs produced by the Gram-positive bacterium *Thermomonospora curvata* (1.7×10^4 mM^{-1} s^{-1}) (Chen et al. 2015), *Bacillus* sp. strain BL25 (372 mM^{-1} s^{-1}) (Khan et al. 2021), and *Rhodococcus jostii* RHA1 (495 mM^{-1} s^{-1}) (Shrestha et al. 2021). In general, these results suggest that the rDyP-AU10 enzyme has a specificity constant value as reported for DyPs produced by *Pseudomonas* strains and that this value could be improved by directed evolution or site-directed mutagenesis, reaching values similar to those found for DyPs from *Bacillus* and *Rhodococcus* strains.

The linear plots obtained from the stopped-flow experiments for the reaction between rDyP-AU10 and H_2O_2 (Fig. 5) show that rDyP-AU10-I is formed in one apparent single step that is dependent on H_2O_2. This implies that the initial formation of a ferric hydroperoxide complex is rate-limiting and that the cleavage of the peroxide bond is fast, a behavior typically observed in class B DyP enzymes as well as in other peroxidases (Lučić et al. 2020; Mendes et al. 2015b; Pfanzagl et al. 2018; Rahmanpour and Bugg 2015; Roberts et al. 2011; Shrestha et al. 2017). In contrast, the A-type DyP from *Bacillus subtilis* exhibits saturation behavior indicative of a two-step mechanism (Mendes et al. 2015a). The rate constant obtained for the reaction between rDyP-AU10 and H_2O_2 to form rDyP-AU10-I was $(2.07 \pm 0.09) \times 10^6$ M^{-1} s^{-1} at pH 5. This value is lower than that reported for HRP (1.8×10^7 M^{-1} s^{-1}) (Dolman et al. 1975), but similar to those reported for other class B DyPs: $(1.4 \pm 0.3) \times 10^6$ M^{-1} s^{-1} for that of *Pseudomonas putida* MET94 (Mendes et al. 2015b), $(2.35 \pm 0.02) \times 10^6$ M^{-1} s^{-1} for that of *Enterobacter lignolyticus* (Shrestha et al. 2017), $(6.2 \pm 0.2) \times 10^6$ M^{-1} s^{-1} for that of *Klebsiella pneumoniae* (Pfanzagl et al. 2018). Nevertheless, class B DyPs of *Rhodococcus jostii* and *Streptomyces lividans* presented significantly lower values of $(1.79 \pm 0.06) \times 10^5$ M^{-1} s^{-1} (Roberts et al. 2011) and of $(2.9 \pm 0.1) \times 10^5$ M^{-1} s^{-1} (Lučić et al. 2020), respectively, suggesting that subtle differences in the enzymes impact in the rate of Compound I formation and begging for further structural and mechanistic studies. Variations are also found in class A enzymes (Chen et al. 2015; Lučić et al. 2020; Mendes et al. 2015a).

DyP-AU10-I showed relatively high stability. In some peroxidases, Compound I spontaneously decomposes by electron transfer from nearby amino acids at the enzyme's catalytic site, but this did not appear to be the case in DyP-AU10-I. Compound I can also react with H_2O_2 present in excess, as in the enzyme catalase (Dunford 1995), but this did not occur in DyP-AU10-I either. The stability of

Compound I appears to be a hallmark of class B DyPs and has been reported for those of *Klebsiella pneumoniae* (Pfanzagl et al. 2018), *Rhodococcus jostii* (Singh et al. 2012), *Pseudomonas putida* MET94 (Mendes et al. 2015b), *Streptomyces lividans* (Lučić et al. 2020b), *Enterobacter lignolyticus* (Shrestha et al. 2017), and *Pseudomonas fluorescens* (Rahmanpour and Bugg 2015). In contrast, in several class A DyPs, Compound I decays spontaneously to Compound II (Chen et al. 2015; Lučić et al. 2020).

Under turnover conditions with the substrate hydroquinone, DyP-AU10-I was the predominant species, and DyP-AU10-II could not be detected, either because the substrate was oxidized directly by two-electrons or because the rate constant for DyP-AU10-II was higher than for DyP-AU10-I. This behavior has been observed before for class B DyPs, albeit with other substrates (Pfanzagl et al. 2018; Shrestha et al. 2017, 2021). In contrast, in class A enzymes, the conversion of Compound II to resting enzyme appears to be slower than the conversion of Compound I to Compound II, as in typical peroxidases (Chaplin et al. 2017; Chen et al. 2015; Mendes et al. 2015a).

Based on crystallographic structures and multiple alignments, four conserved residues have been proposed to make up the peroxide binding pocket, key residues for the catalytic cycle of DyP (Yoshida et al. 2011). An aspartate (Asp171 in DyP-AU10) could act as a proton acceptor, facilitating the heterolytic cleavage of the O-O bond to form Compound I. An arginine (Arg329 in DyP-AU10) could transiently stabilize and polarize the negative charge during Compound I formation (Lučić et al. 2021; Pfanzagl et al. 2018; Singh et al. 2012). Of note, for the class B DyP of *Streptomyces lividans* (DtpB), in which the active site shows the absence of water molecules, it has been proposed that the arginine acts as proton acceptor (Lučić et al. 2020). The structure of Compound I was obtained and shows the formation of hydrogen bonds between the oxo species and critical arginine and asparagine residues. The lack of water molecules has been related to Compound I stability and to the oxidation of substrates by apparent two-electron processes, without the intermediacy of Compound II (Lučić et al. 2020, 2021). The possible molecular mechanisms operative in DyP-AU10 remain to be established.

We found that rDyP-AU10 modified kraft lignin, an interesting activity from a biotechnological point of view (Fig. 6a and b). The recordings of absorbance at 465 nm and 280 nm report on the release of chromophores and on the loss of polymer aromaticity (ring cleavage reactions), respectively (Olajuyigbe et al. 2022); Crawford and Crawford (1980). rDyP-AU10 presented catalyst behavior (Fig. 6a) such as found for *R. jostii* DyP class B (Ahmad et al. 2010), *P. fluorescens* DyP1 class B (Rahmanpour and Bugg 2015), and *Pseudomonas* sp. Q18 (Yang et al. 2018), suggesting that some part of the kraft lignin substrate undergoes oxidation by rDyP-AU10 at low temperature.

At this point, we wonder why would a *Pseudomonas* strain, isolated from a water sample collected in a lake in Antarctica, produce a cold-active DyP-type enzyme that also modifies lignin. Furthermore, consider that only two species of vascular plants have colonized Antarctica (*Deschampsia antarctica* and *Colobanthus quitensis*), 33 moss species, and 68 lichen species (Parnikoza et al. 2011). What function could this enzyme have in the metabolism of *Pseudomonas* sp. AU10 in the natural Antarctic environment? We do not have an answer to these questions. However, the presence of a coding sequence for a DyP in the genome of the Antarctic *Pseudomonas* sp. strain PAMC 29040 (Kim and Lee 2019), suggests that this enzyme could constitute a common feature of this genus in this cold environment. The metagenome analysis of a soil sample collected at the Barton Peninsula, located in the King George Island (Antarctica) (Oh et al. 2019), confirmed the presence of lignin-degrading enzymes, including DyPs. However, the authors did not report *Pseudomonas* in their phylogenetic analysis of samples. We think this peroxidase has a different function in the natural habitat rather than lignin degradation.

There is a wide range of industrial dyes that are attacked by DyPs, mainly anthraquinone-derived dyes. Our results showed that rDyP-AU10 decolorizes malachite green, methyl violet, and methyl orange. These dyes are commonly used in the textile industry and are pH indicators in titrations. In addition, malachite green is used as an antibacterial, antifungal, and antiparasitic agent. In aquaculture, its main metabolite, leuco-malachite green is commonly found in fishes treated with malachite green, and this is a controversial matter because leuco-malachite green shows cytotoxicity towards mammalian cells and is an irritant to the gastrointestinal tract, skin, and eyes. Methyl violet is used as a disinfectant and is an ingredient in Gram's staining and produces genotoxic interactions with calf thymus DNA (Chen and Ting 2017). Both are triphenylmethane (TPM) dyes, persistent in the environment as they are resistant to degradation. Their remediation can be performed by conventional physical-chemical (coagulation-flocculation, ozonization, adsorption, and membrane filtration) and biological approaches (removal using microbes or enzymes). Methyl orange belongs to the group of azo dyes. It is used as pH indicator, and it has applications in histological microscopy and in the textile industry. Our results suggest that rDyP-AU10 can be used in the bioremediation of TPM and azo dyes. TPM could be degraded by the laccase from *Bacillus vallismortis* (Zhang et al. 2012), a heme-peroxidase from the fungus *Caldariomyces fumago* (Liu et al. 2014), or a manganese peroxidase from the white-rot fungus *Irpex lacteus* (Yang et al. 2016), among others.

We also wonder, what could be the function of DyP-AU10 as dye-decolorizing agent in its natural environment? Antarctica is highly exposed to UV radiation. Among the biological mechanisms involved in UV resistance, organisms produce pigments, and Antarctica is a source of pigment-producing and UV-resistant microbes (Marizcurrena et al. 2017). The microbial pigments have biological roles beyond UV resistance, such as antioxidant and antibiotic agents (Marizcurrena et al. 2019). Our research group also informed about an Antarctic purple bacterium, *Janthinobacterium* sp. UV13, which produces a pigment identified as violacein, which shows antiproliferative activity in a cancer cell line (Alem et al. 2020, 2022). Thus, we think that *Pseudomonas* sp. AU10 may produce this DyP as a part of a repertoire of molecules involved in the defense against the pigments produced by other microbes. In future work, we will examine the ability of rDyP-AU10 to degrade a wider set of dyes and TPM-derived pesticides. Overall, the biotechnological potential of this cold-active DyP deserves further study, particularly regarding bioremediation and lignin degradation.

To the best of our knowledge, this is the first report regarding the identification, recombinant production; purification and partial biochemical characterization of a bacterial cold-active DyP enzyme from an Antarctic isolate (*Pseudomonas* sp. AU10). The recombinant protein presented interesting biochemical features, including the potential for modifying lignin (surface oxidation and/or depolymerization) and degrading dyes. We also report kinetic parameters of this enzyme, including the rate constant for the formation of Compound I. We think that this enzyme has potential biotechnological applications. Future work will deal with the improvement of the lignin- and dye-degrading activity of this enzyme by directed evolution, for the bioremediation, and the cellulose pulp bleaching and/or the biofuel industries.

Acknowledgements The authors thank the Uruguayan Antarctic Institute for partial financial and for the logistic support during the stay in the Antarctic Base Artigas. We thank Gerardo Ferrer-Sueta (Universidad de la República) for helping with the stopped-flow experiments. S. Castro-Sowinski, B. Alvarez; D. Vallés, and J.J. Marizcurrena are members of the National Research System (SNI, Sistema Nacional de Investigadores).

Author contribution CC produced and purified the recombinant DyP and performed the biochemical and biotechnological characterization of the enzyme (including the stopped-flow experiments), the structure prediction, and the pocket description. JJM assisted during the recombinant production and purification of DyP and during the structure prediction. DV conducted the HPLC experiments. BA assisted during stopped-flow experiments and was actively involved in writing. SCS guided most experiments and wrote the manuscript.

Funding This work was partially supported by the Basic Sciences Development Program (PEDECIBA, Programa de Desarrollo de las Ciencias Básicas) and the Superior Council of Scientific Investigations (CSIC, Comisión Sectorial de Investigación Científica, Universidad de la República) (Projects C916-347 and Grupos 2018_47). The work of CC was supported by the National Research and Innovation Agency (ANII, Agencia Nacional de Investigación e Innovación).

Declarations

Compliance with ethical standards This article does not contain any studies with human participants or animals performed by any of the authors.

Conflict of interest The authors declare no competing interests.

References

Abboud R, Popa R, Souza-Egipsy V, Giometti CS, Tollaksen S, Mosher JJ, Findlay RH, Nealson KH (2005) Low-temperature growth of Shewanella oneidensis MR-1. Appl Environ Microbiol 71(2):811–16. https://doi.org/10.1128/AEM.71.2.811-816.2005

Abdel-Hamid AM, Solbiati JO, Cann IKO (2013) Insights into lignin degradation and its potential industrial applications, vol 82. Elsevier

Ahmad M, Taylor CR, Pink D, Burton K, Eastwood D, Bending GD, Bugg TDH (2010) Development of novel assays for lignin degradation: comparative analysis of bacterial and fungal lignin degraders. Mol BioSyst 6(5):815–21. https://doi.org/10.1039/b908966g

Ahmad M, Roberts JN, Hardiman EM, Singh R, Eltis LD, Bugg TDH (2011) Identification of DypB from *Rhodococcus jostii* RHA1 as a lignin peroxidase. Biochemistry 50(23):5096–5107. https://doi.org/10.1021/bi101892z

Alem D, Marizcurrena JJ, Saravia V, Davyt D, Martinez-Lopez W, Castro-Sowinski S (2020) Production and antiproliferative effect of violacein, a purple pigment produced by an antarctic bacterial isolate. World J Microbiol Biotechnol 36(8):1–11. https://doi.org/10.1007/s11274-020-02893-4

Alem D, Canclini L, Castro-Sowinski S, Martínez-López W (2022) Chemosensitizer effect of violacein on cisplatin-treated bladder cancer cells. CCMP 2(2):100036. https://doi.org/10.1016/j.ccmp.2022.100036

Armenteros A, Juan J, Tsirigos KD, Sønderby CK, Petersen TN, Winther O, Brunak S, von Heijne G, Nielsen H (2019) SignalP 5.0 improves signal peptide predictions using deep neural networks. Nat Biotechnol 37(4):420–23. https://doi.org/10.1038/s41587-019-0036-z

Arndt (2012) Native polyacrylamide gels Claudia, pp 49–53 in Vol. 869

Aziz RK, Bartels D, Best A, DeJongh M, Disz T, Edwards RA, Formsma K, Gerdes S, Glass EM, Kubal M, Meyer F, Olsen GJ, Olson R, Osterman AL, Overbeek RA, McNeil LK, Paarmann D, Paczian T, Parrello B, Pusch GD, Reich C, Stevens R, Vassieva O, Vonstein V, Wilke A, Zagnitko O (2008) The RAST server: rapid annotations using subsystems technology. BMC Genom 9:1–15. https://doi.org/10.1186/1471-2164-9-75

Bashtan-Kandybovich I, Venkatesagowda B, Barbosa AM, Malek L, Dekker RFH (2012) Modification of kraft lignin by biological demethylation. J-For 2(4):16–27. https://doi.org/10.13140/2.1.1440.3528

Bilal M, Rasheed T, Iqbal HMN, Hongbo H, Wang W, Zhang X (2017) Novel characteristics of horseradish peroxidase immobilized onto the polyvinyl alcohol-alginate beads and its methyl orange degradation potential. Int J Biol Macromol 105:328–35. https://doi.org/10.1016/j.ijbiomac.2017.07.042

Bjellqvist B, Hughes GJ, Pasquali C, Paquet N, Ravier F, Sanchez J-C-C, Frutiger S, Hochstrasser D (1993) The focusing positions of polypeptides in immobilized pH gradients can be predicted from their amino acid sequences. Electrophor 14(1):1023–31. https://doi.org/10.1002/elps.11501401163

Bjellqvist B, Basse B, Olsen E, Celis JE (1994) Reference points for comparisons of two-dimensional maps of proteins from different

human cell types defined in a pH scale where isoelectric points correlate with polypeptide compositions. Electrophor 15(1):529–39. https://doi.org/10.1002/elps.1150150171

Brissos V, Tavares D, Sousa AC, Robalo MP, Martins LO (2017) Engineering a bacterial dyp-type peroxidase for enhanced oxidation of lignin-related phenolics at alkaline pH. ACS Catal 7(5):3454–65. https://doi.org/10.1021/acscatal.6b03331

Cagide C, Castro-Sowinski S (2020) Technological and biochemical features of lignin-degrading enzymes: a brief review. Environ Sustain 3(4):371–89. https://doi.org/10.1007/s42398-020-00140-y

Cavicchioli R, Charlton T, Ertan H, Mohd Omar S, Siddiqui KS, Williams TJ (2011) Biotechnological uses of enzymes from psychrophiles. Microb Biotechnol 4(4):449–60. https://doi.org/10.1111/j.1751-7915.2011.00258.x

Chaplin AK, Wilson MT, Worrall JAR (2017) Kinetic characterisation of a dye decolourising peroxidase from *Streptomyces lividans*: new insight into the mechanism of anthraquinone dye decolourisation. Dalton Trans 46(29):9420–29. https://doi.org/10.1039/c7dt01144j

Chen, Ting (2017) Microfungi for the removal of toxic triphenylmethane dyes. Min Microbial Wealth MetaGenomics 1–461. https://doi.org/10.1007/978-981-10-5708-3

Chen C, Shrestha R, Jia K, Gao PF, Geisbrecht BV, Bossmann SH, Shi J, Li P (2015) Characterization of dye-decolorizing peroxidase (Dyp) from *Thermomonospora curvata* reveals unique catalytic properties of A-type DyPs. J Bio Chem 290(38):23447–63. https://doi.org/10.1074/jbc.M115.658807

Colpa DI, Fraaije MW, Van Bloois E (2014) DyP-type peroxidases: a promising and versatile class of enzymes. J Indust Microbiol Biotechnol 41(1):1–7. https://doi.org/10.1007/s10295-013-1371-6

Conchillo-Solé O, de Groot NS, Avilés FX, Vendrell J, Daura X, Ventura S (2007) AGGRESCAN: a server for the prediction and evaluation of 'hot spots' of aggregation in polypeptides. BMC Bioinform 8. https://doi.org/10.1186/1471-2105-8-65

Crawford DL, Crawford RL (1980) Microbial degradation of lignin. Enzyme Microb Technol 2(1):11–22. https://doi.org/10.1016/0141-0229(80)90003-4

Dhankhar P, Dalal V, Mahto JK, Gurjar BR, Tomar S, Sharma AK, Kumar P (2020) Characterization of dye-decolorizing peroxidase from *Bacillus subtilis*. ABB 693(July):108590. https://doi.org/10.1016/j.abb.2020.108590

Dolman D, Newell GA, Thurlow MD (1975) A kinetic study of the reaction of horseradish peroxidase with hydrogen peroxide. Can J Biochem 53(5):495–501. https://doi.org/10.1139/o75-069

Dunford HB (1995) One-electron oxidations by peroxidases. Xenobiotica 25(7):725–33. https://doi.org/10.3109/00498259509061888

Dunford HB, Araiso T, Job D, Ricard J, Rutter R, Hager LP, Wever R, Kast WM, Boelens R, Ellfolk N, Ronnberg M (1982) "1982 Dunford." 2:337–55

Ellis, Morrison (1981) [23] Buffers for studying pH-dependent processes 405 [23] Buffers of constant ionic strength for studying pH-dependent processes. Biochemistry 20:1805

Feller G, Gerday C (2003) Psychrophilic enzymes: hot topics in cold adaptation. Nat Rev Microbiol 1(3):200–208. https://doi.org/10.1038/nrmicro773

Fullana N, Braña V, Marizcurrena JJ, Morales D, Betton J-M, Marín M, Castro-Sowinski S (2017) Identification, recombinant production and partial biochemical characterization of an extracellular cold-active serine-metalloprotease from an antarctic *Pseudomonas* isolate. AIMS Bioengin 4(3):386–401. https://doi.org/10.3934/bioeng.2017.3.386

García-Laviña CX, Castro-Sowinski S, Ramón A (2019) Reference genes for real-time RT-PCR expression studies in an antarctic *Pseudomonas* exposed to different temperature conditions. Extremoph 23(5):625–33. https://doi.org/10.1007/s00792-019-01109-4

Gasteiger E, Hoogland C, Gattiker A, Duvaud S, Wilkins MR, Appel RD, Bairoch A (2005) The proteomics protocols handbook. The Proteomics Protocols Handbook, p 571–608. https://doi.org/10.1385/1592598900

Ingemar Falkehag S, Marton J (1966) Chromophores in kraft lignin. Am Chem Soc 59:1–21

Khan SI, Zada NS, Sahinkaya M, Colak DN, Ahmed S, Hasan F, Belduz AO, Çanakçi S, Khan S, Badshah M, Shah AA (2021) Cloning, expression and biochemical characterization of lignin-degrading Dyp-type peroxidase from Bacillus sp strain BL5. Enzyme Microb Technol 151(September). https://doi.org/10.1016/j.enzmictec.2021.109917

Kim D, Lee H (2019) Draft genome sequence of humic substance-degrading *Pseudomonas* sp. PAMC 29040 from Antarctic tundra soil. Korean J Microbiol 55(1):83–85. https://doi.org/10.7845/kjm.2019.9008

Kobori H, Sullivan CW, Shizuya H (1984) Heat-labile alkaline phosphatase from Antarctic bacteria: rapid 5' end-labeling of nucleic acids. PNAS 81(21 I):6691–95. https://doi.org/10.1073/pnas.81.21.6691

Kumar S, Stecher G, Li M, Knyaz C, Tamura K (2018) MEGA X: Molecular evolutionary genetics analysis across computing platforms. Mol Biol Evol 35(6):1547–49. https://doi.org/10.1093/molbev/msy096

Laemmli (1970) © 1970 Nature Publishing Group. NPG 228:1979

Larkin MA, Blackshields G, Brown NP, Chenna R, Mcgettigan PA, McWilliam H, Valentin F, Wallace IM, Wilm A, Lopez R, Thompson JD, Gibson TJ, Higgins DG (2007) Clustal W and Clustal X version 2.0. Bioinformatics 23(21):2947–48. https://doi.org/10.1093/bioinformatics/btm404

Li J, Chen X, Dongfeng X, Pan K (2019) Immobilization of horseradish peroxidase on electrospun magnetic nanofibers for phenol removal. Ecotoxicol Environ Saf 170(November 2018):716–21. https://doi.org/10.1016/j.ecoenv.2018.12.043

Liu L, Zhang J, Tan Y, Jiang Y, Mancheng H, Li S, Zhai Q (2014) Rapid decolorization of anthraquinone and triphenylmethane dye using chloroperoxidase: catalytic mechanism, analysis of products and degradation route. Chem Eng J 244:9–18. https://doi.org/10.1016/j.cej.2014.01.063

Lučić M, Svistunenko DA, Wilson MT, Chaplin AK, Davy B, Ebrahim A, Axford D, Tosha T, Sugimoto H, Owada S, Dworkowski FSN, Tews I, Owen RL, Hough MA, Worrall JAR (2020) Serial femtosecond zero dose crystallography captures a water-free distal heme site in a dye-decolorising peroxidase to reveal a catalytic role for an arginine in Fe IV =O formation. Angew Chem 132(48):21840–46. https://doi.org/10.1002/ange.202008622

Lučić M, Wilson MT, Svistunenko DA, Owen RL, Hough MA, Worrall JAR (2021) Aspartate or arginine? Validated redox state X-ray structures elucidate mechanistic subtleties of FeIV = O formation in bacterial dye-decolorizing peroxidases. J Biol Inorg Chem 26(7):743–61. https://doi.org/10.1007/s00775-021-01896-2

Marizcurrena JJ, Morel MA, Braña V, Morales D, Martinez-López W, Castro-Sowinski S (2017) Searching for novel photolyases in UVC-resistant Antarctic bacteria. Extremoph 21(2):409–18. https://doi.org/10.1007/s00792-016-0914-y

Marizcurrena JJ, Herrera LM, Costábile A, Morales D, Villadóniga C, Eizmendi A, Davyt D, Castro-Sowinski S (2019) Validating biochemical features at the genome level in the Antarctic bacterium *Hymenobacter* sp. strain UV11. FEMS Microbiol Lett 366(14):1–10. https://doi.org/10.1093/femsle/fnz177

Martínez-Rosales C, Castro-Sowinski S (2011) Antarctic bacterial isolates that produce cold-active extracellular proteases at low temperature but are active and stable at high temperature. Polar Res 30(SUPPL.1). https://doi.org/10.3402/polar.v30i0.7123

Matsuda S, Vert J-P, Saigo H, Ueda N, Toh H, Akutsu T (2005) A novel representation of protein sequences for prediction of subcellular

location using support vector machines. Prot Sci 14(11):2804–13. https://doi.org/10.1110/ps.051597405

Mendes S, Catarino T, Silveira C, Todorovic S, Martins LO (2015a) The catalytic mechanism of a-type dye-decolourising peroxidase BsDyP: neither aspartate nor arginine is individually essential for peroxidase activity. Catal Sci Technol 5(12):5196–5207. https://doi.org/10.1039/c5cy00478k

Mendes S, Brissos V, Gabriel A, Catarino T, Turner DL, Todorovic S, Martins LO (2015b) An integrated view of redox and catalytic properties of B-type PpDyP from *Pseudomonas putida* MET94 and its distal variants. ABB 574:99–107. https://doi.org/10.1016/j.abb.2015.03.009

Morales M, Mate MJ, Romero A, Martínez MJ, Martínez ÁT, Ruiz-Dueñas FJ (2012) Two oxidation sites for low redox potential substrates: a directed mutagenesis, kinetic, and crystallographic study on *Pleurotus eryngii* versatile peroxidase. JBC 287(49):41053–67. https://doi.org/10.1074/jbc.M112.405548

Morel M, Iriarte A, Jara E, Musto H, Castro-Sowinski S (2016) Revealing the biotechnological potential of *Delftia* sp. JD2 by a genomic approach. AIMS Bioengin 3(2):156–75. https://doi.org/10.3934/bioeng.2016.2.156

Murakami K, Okajima K, Okabe H (1995) Catalase. Nippon Rinsho Jpn J Clin Med 53(1):358–60. https://doi.org/10.1086/330448

Nielsen H, Engelbrecht J (1997) Identification of prokaryotic and eukaryotic signal peptides and prediction of their cleavage sites artificial neural networks have been used for many biological. Prot Eng 10(1):1–6. https://doi.org/10.1142/S0129065797000537

Oh HN, Park D, Seong HJ, Kim D, Sul WJ (2019) Antarctic tundra soil metagenome as useful natural resources of cold-active lignocelluolytic enzymes. J Microbiol 57(10):865–73. https://doi.org/10.1007/s12275-019-9217-1

Olajuyigbe FM, Afere FP, Adetuyi OY, Fatokun CO (2022) Decolorization of lignin-mimicking dyes by *Stenotrophomonas* sp. CFB-09: enzyme activity, transformation dynamics and process optimization. Biocat Biotransf 40(5):351–64. https://doi.org/10.1080/10242422.2021.1935898

Parnikoza I, Kozeretska I, Kunakh V (2011) Vascular plants of the maritime antarctic: origin and adaptation. AJPS 02(03):381–95. https://doi.org/10.4236/ajps.2011.23044

Pfanzagl V, Nys K, Bellei M, Michlits H, Mlynek G, Battistuzzi G, Djinovic-Carugo K, Van Doorslaer S, Furtmüller PG, Hofbauer S, Obinger C (2018) Roles of distal aspartate and arginine of B-class dye-decolorizing peroxidase in heterolytic hydrogen peroxide cleavage. JBC 293(38):14823–38. https://doi.org/10.1074/jbc.RA118.004773

Poulos TL (2014) Heme enzyme structure and function. Cheml Rev 114(7):3919–62

Rahmanpour R, Bugg TDH (2015) Characterisation of Dyp-type peroxidases from *Pseudomonas fluorescens* PF-5: oxidation of Mn(II) and polymeric lignin by Dyp1B. ABB 574:93–98. https://doi.org/10.1016/j.abb.2014.12.022

Rahmanpour R, King LDW, Bugg TDH (2016a) Biochemical and biophysical research communications identification of an extracellular bacterial Fl avoenzyme that can prevent re-polymerisation of lignin fragments, p 1–5. https://doi.org/10.1016/j.bbrc.2016.10.144

Rahmanpour R, Rea D, Jamshidi S, Fülöp V, Bugg TDH (2016b) Structure of *Thermobifida fusca* DyP-type peroxidase and activity towards kraft lignin and lignin model compounds. ABB 594:54–60. https://doi.org/10.1016/j.abb.2016.02.019

Roberts JN, Singh R, Grigg JC, Murphy ME, Bugg TD, Eltis LD (2011) Characterization of dye-decolorizing peroxidases from *Rhodococcus jostii* RHA1. Biochemistry 50(23):5108–5119

Sahinkaya C, Nigar D, Ozer A, Canakci S, Deniz I, Belduz AO (2019) Cloning, characterization and paper pulp applications of a newly isolated Dyp type peroxidase from *Rhodococcus* sp. T1. Mol Biol Rep 46(1):569–80. https://doi.org/10.1007/s11033-018-4509-9

Santos A, Mendes S, Brissos V, Martins LO (2014) New dye-decolorizing peroxidases from *Bacillus subtilis* and *Pseudomonas putida* MET94: towards biotechnological applications. AMB 98(5):2053–65. https://doi.org/10.1007/s00253-013-5041-4

Shrestha R, Huang G, Meekins DA, Geisbrecht BV, Li P (2017) Mechanistic insights into dye-decolorizing peroxidase revealed by solvent isotope and viscosity effects. ACS Catal 7(9):6352–64. https://doi.org/10.1021/acscatal.7b01861

Shrestha R, Jia K, Khadka S, Eltis LD, Li P (2021) Mechanistic insights into DyPB from *Rhodococcus jostii* RHA1 via kinetic characterization. ACS Catal 11(9):5486–95. https://doi.org/10.1021/acscatal.1c00703

Singh R, Grigg JC, Armstrong Z, Murphy MEP, Eltis LD (2012) Distal heme pocket residues of B-type dye-decolorizing peroxidase: arginine but not aspartate is essential for peroxidase activity. JBC 287(13):10623–30. https://doi.org/10.1074/jbc.M111.332171

Struvay C, Feller G (2012) Optimization to low temperature activity in psychrophilic enzymes. Int J Mol Sci 13(9):11643–65. https://doi.org/10.3390/ijms130911643

Studier FW (2005) Protein production by auto-induction in high density shaking cultures. Protein Express Purif 41(1):207–34. https://doi.org/10.1016/j.pep.2005.01.016

Sugano Y (2009) DyP-Type peroxidases comprise a novel heme peroxidase family. CMLS 66(8):1387–1403. https://doi.org/10.1007/s00018-008-8651-8

Sugano Y, Yoshida T (2021) Dyp-type peroxidases: recent advances and perspectives. Int J Mol Sci 22(11). https://doi.org/10.3390/ijms22115556

Sugawara K, Nishihashi Y, Narioka T, Yoshida T, Morita M, Sugano Y (2017) Characterization of a novel Dyp-type peroxidase from *Streptomyces avermitilis*. J Biosci Bioeng 123(4):425–30. https://doi.org/10.1016/j.jbiosc.2016.12.001

Tian W, Chen C, Lei X, Zhao J, Liang J (2018) CASTp 3.0: computed atlas of surface topography of proteins. Nucleic Acids Res 46(W1):W363-67. https://doi.org/10.1093/nar/gky473

Xu L, Sun J, Qaria MA, Gao L, Zhu D (2021) Dye decoloring peroxidase structure, catalytic properties and applications: current advancement and futurity. Catalyst 11(8):1. https://doi.org/10.3390/catal11080955

Yang X, Zheng J, Yongming L, Jia R (2016) Degradation and detoxification of the triphenylmethane dye malachite green catalyzed by crude manganese peroxidase from *Irpex lacteus* F17. ESPR 23(10):9585–97. https://doi.org/10.1007/s11356-016-6164-9

Yang C, Yue F, Cui Y, Yuanmei X, Shan Y, Liu B, Zhou Y, Lü X (2018) Biodegradation of lignin by *Pseudomonas* sp. Q18 and the characterization of a novel bacterial dyp-type peroxidase. J Ind Microbiol Biotech 45(10):913–27. https://doi.org/10.1007/s10295-018-2064-y

Yoshida T, Sugano Y (2015) A structural and functional perspective of Dyp-type peroxidase family. ABB 574(February):49–55. https://doi.org/10.1016/j.abb.2015.01.022

Yoshida T, Sugano Y (2023) Unexpected diversity of dye-decolorizing peroxidases. BB Reports 33(October 2022):101401. https://doi.org/10.1016/j.bbrep.2022.101401

Yoshida T, Tsuge H, Konno H, Hisabori T, Sugano Y (2011) The catalytic mechanism of dye-decolorizing peroxidase Dyp may require the swinging movement of an aspartic acid residue. FEBS J 278(13):2387–94. https://doi.org/10.1111/j.1742-4658.2011.08161.x

Zhang C, Diao H, Fengxia L, Bie X, Wang Y, Zhaoxin L (2012) Degradation of triphenylmethane dyes using a temperature and pH stable spore laccase from a novel strain of *Bacillus vallismortis*. Bioresour Technol 126:80–86. https://doi.org/10.1016/j.biortech.2012.09.055

Zhang Z, Lai J, Kesen W, Huang X, Guo S, Zhang L, Liu J (2018) Peroxidase-catalyzed chemiluminescence system and its application in immunoassay. Talanta 180:260–70. https://doi.org/10.1016/j.talanta.2017.12.024

Zimmermann L, Stephens A, Nam SZ, Rau D, Kübler J, Lozajic M, Gabler F, Söding J, Lupas AN, Alva V (2018) A completely reimplemented MPI bioinformatics toolkit with a new HHpred server at its core. J Mol Biol 430(15):2237–43. https://doi.org/10.1016/j.jmb.2017.12.007

CAPÍTULO II

2. Estudio genómico de *Sinorhizobium meliloti* CE52G, búsqueda y producción recombinante de una laccasa

2.1. Contexto y antecedentes

El objetivo de este capítulo fue identificar el gen que codifica para una laccasa bacteriana, producirla en forma recombinante y caracterizarla en forma bioquímica, así como estudiar su potencial biotecnológico. El capítulo aborda los Objetivos Específicos 3, 4 y 5.

Las laccasas (EC 1.10.3.2) son cobre-oxidasas ampliamente distribuidas en hongos, plantas y bacterias. Catalizan la oxidación de una gran variedad de sustratos fenólicos y no fenólicos con la concomitante reducción de oxígeno molecular a agua [37, 38]. Esta notable versatilidad catalítica, junto a su capacidad para actuar sobre compuestos recalcitrantes en ausencia de cofactores adicionales, ha impulsado su valorización como herramientas clave en diversos procesos biotecnológicos, incluyendo la biorremediación de contaminantes ambientales, la modificación de lignina, la biosíntesis de pigmentos, y la elaboración de productos de valor agregado en las industrias alimenticia, textil, papelera y cosmética [39, 40]

Desde el punto de vista estructural, las laccasas pertenecen a la superfamilia de las multicobre oxidasas, y su mecanismo catalítico involucra centros metálicos altamente conservados: un sitio tipo I (cobre azul) responsable de la oxidación del sustrato, y un centro trinuclear (T2/T3) donde ocurre la reducción del oxígeno [38]. Si bien las laccasas de origen fúngico han sido estudiadas en mayor profundidad respecto a las de origen bacteriano, estas últimas han mostrado poseer ventajas particulares para su producción y aplicación industrial, como mayor estabilidad en condiciones extremas (pH, temperatura), posibilidad de producción recombinante en sistemas bacterianos, y en algunos casos, actividad específica sobre sustratos no transformables por las versiones fúngicas [41, 42].

En este contexto, la búsqueda y caracterización molecular de nuevas laccasas bacterianas funcionales representa un campo de investigación activo y cada vez más relevante. En particular, la cepa bacteriana *Sinorhizobium meliloti* CE52G fue reportada por nuestro grupo como un microorganismo capaz de sintetizar melanina y producir una laccasa activa bajo condiciones específicas de cultivo. Esta cepa, que se aisló a partir del ambiente, particularmente de nódulos de plantas de alfalfa, y fue estudiada en profundidad por nuestro equipo, dando lugar a varias publicaciones científicas y tesis académicas, centradas en su fisiología, metabolismo y producción de pigmentos [43–46]. No obstante, pese a los avances generados, aún persistían interrogantes clave que no habíamos logrado responder. ¿Cuál era

el gen que codifica para la enzima con actividad laccasa detectada en la cepa? ¿Existía más de un gen que codificara para enzimas con actividad oxidasa en esta cepa? Si existía un gen codificante de laccasa en su genoma, ¿cómo se relaciona con otras laccasas bacterianas conocidas en términos de secuencia, estructura y dominios conservados? ¿Qué elementos genómicos o funcionales podrían estar vinculados a la capacidad para producir pigmentos y/o al metabolismo del cobre en esta cepa?

Hasta ese momento, no contábamos con la secuenciación completa del genoma de CE52G, ni con información concluyente sobre la base genética de su capacidad oxidativa. Esta falta de datos limitaba su aprovechamiento biotecnológico y dificultaba el desarrollo de estrategias para su expresión recombinante y caracterización funcional.

Con el fin de abordar estas preguntas, este capítulo se estructuró en torno a tres objetivos: secuenciar, ensamblar y anotar el genoma completo de CE52G, con especial énfasis en la identificación de secuencias codificantes de posibles laccasas; producir la enzima laccasa en forma recombinante, y analizar sus propiedades bioquímicas, aportando información clave sobre su funcionalidad y potencial aplicación.

Presentamos por primera vez, el estudio genómico completo de CE52G con énfasis en la búsqueda e identificación de genes codificantes para enzimas con potencial actividad laccasa. Mediante estos estudios contribuimos a posicionar a CE52G como un modelo interesante para el estudio de laccasas bacterianas periplásmicas, particularmente en contextos asociados a la respuesta al estrés oxidativo, interacción planta-microorganismo y producción de compuestos bioactivos.

El presente capítulo se compone de dos secciones: 1) Inicialmente se presenta el abordaje genómico mediante el artículo científico publicado, aportando el marco molecular sobre el cual se estructuran las siguientes etapas del desarrollo experimental, titulado *Descriptive analysis of the draft genome from the melanin-producing bacterium Sinorhizobium (Ensifer) meliloti CE52G*; y 2) En la segunda sección, se describen las estrategias experimentales orientadas a la expresión y caracterización funcional de la enzima.

Respecto al punto 2), se abordó brevemente el trabajo experimental, tanto de los intentos de producción recombinante de la laccasa de CE52G en un sistema heterólogo, usando *E. coli*, como los ensayos de producción nativa bajo condiciones inductoras. También se incluye un análisis comparativo con enzimas candidatas de otras cepas bacterianas de origen ambiental de nuestra colección.

Environmental Sustainability
https://doi.org/10.1007/s42398-023-00273-w

ORIGINAL ARTICLE

Descriptive analysis of the draft genome from the melanin-producing bacterium *Sinorhizobium* (*Ensifer*) *meliloti* CE52G

Célica Cagide[1] · César X. García-Laviña[1] · María A. Morel[2,3] · Susana Castro-Sowinski[1,3]

Received: 31 October 2022 / Revised: 20 April 2023 / Accepted: 23 April 2023

Abstract

Herein we present the draft genome (7.32 Mb and 62% GC content) of melanin- and laccase-producing *Sinorhizobium* (*Ensifer*) *meliloti* strain CE52G isolated from alfalfa nodules. We analyzed the genome and, performed a few in-bench experiments to corroborate some information. We found the gene for the laccase, probably involved in the production of the pigment melanin. CE52G shows genes for: (i) Embden-Meyerhof (EMP) and Entner-Doudoroff (ED) pathways; (ii) dissimilation and assimilation of nitrate, assimilation to ammonia, and conversion of nitrous oxide to nitrogen; (iii) Nodulation Factor and Mo-nitrogenase synthesis; (iv) synthesis and degradation of polyhydroxybutyrate and glycogen; (v) succinoglycan (EPS I) and galactoglucan (EPS II); and (vi) acidic and oxidative stress endurance. This bacterium does not produce siderophores but has the genomic machinery for the acquisition of siderophores (produced by other organisms) and hemophores for the uptake of heme from the environment. Among others, we found genes for two-component systems involved in the uptake of dicarboxylic acids and, the response to acidic conditions. The general information is discussed in terms of their relevance during CE52G association with plants and environmental adaptation.

Keywords *Ensifer meliloti* · Draft genome · Nitrogen metabolism · Stress endurance

Introduction

Leguminous plants are economically and culturally important crops. Their yield improves after inoculation with plant growth-promoting rhizobial strains. *Rhizobium* is a genus of Gram-negative soil bacteria that fix nitrogen, thus contributing to the total nitrogen pool of the plant (Morel et al. 2012). These bacteria induce the expression of specific genes from the root and shoot of legumes, a process that concludes with the formation of root nodules and the establishment of the nitrogen fixing-rhizobia into the nodules (bacteroids); for more information about the microbe-plant interaction, events see Morel and Castro-Sowinski (2013) and Fields and Friman (2022).

Among leguminous plants, the worldwide production of soybean has grown significantly in Latin America, since 2003 (Schorr 2019). However, the establishment of pastures (*Medicago* and *Trifolium*, commonly known as alfalfa and clover, respectively) is still of the utmost importance due to their use in cattle rising; e.g. the livestock activity in Uruguay is among the most important export sector, with an income of USD 3614 million in 2021. This income is of great economical relevance for a small country like Uruguay (176.215 km^2, population of 3.426.260, gross domestic product growth of 4.4% in 2021).

Sinorhizobium (*Ensifer*) *meliloti* strains are rhizobial guests that induce the formation of root nodules that fix atmospheric nitrogen in plants such as *Medicago*, *Melilotus*, and *Trigonella* (Hirsch et al. 2001). These strains are

✉ Susana Castro-Sowinski
scs@fcien.edu.uy

Célica Cagide
ccagide@fcien.edu.uy

César X. García-Laviña
cgarcia@fcien.edu.uy

María A. Morel
mmorel@fcien.edu.uy

[1] Sección Bioquímica, Facultad de Ciencias, Universidad de la República, Igua 4225, 11400 Montevideo, Uruguay

[2] Laboratorio de Microbiología de Suelos, Facultad de Ciencias, Universidad de la República, Igua 4225, 11400 Montevideo, Uruguay

[3] Microbiología Molecular, Instituto de Investigaciones Biológicas Clemente Estable, Av. Italia 3318, Montevideo, Uruguay

Published online: 23 May 2023

used worldwide for the production of bio-formulations for sustainable agriculture. The use of bio-formulations based on *E. meliloti* strains has a long history in Latin America; unfortunately, most countries from this area have acidic soils that impact the interaction between these microbes and their plant hosts (Botero et al. 2019; Tabares-da Rosa et al. 2019). In this scenario, some works reported the isolation and characterization of native acid-tolerant alfalfa-nodulating strains (Del Papa et al. 1999; Castro-Sowinski et al. 2002a, among others) that may help to overcome the stress imposed by acidic soils during the rhizobia-leguminous interaction.

Ensifer meliloti CE52G strain is a melanin- and laccase-producing bacterium isolated from alfalfa nodules (Castro-Sowinski et al. 2002b, 2007; Rosconi et al. 2005). It was isolated from alfalfa nodules collected in acidic soil from Uruguay. Some members of this collection were previously reported and, their symbiotic properties were described (Del Papa et al. 1999; Castro-Sowinski et al. 2002a). CE52G was the first laccase-producing rhizobial strain reported (Castro-Sowinski et al. 2002b). Laccases belong to the superfamily of multicopper oxidases and, are enzymes with wide substrate specificities and diverse biological functions, including melanin production (Janusz et al. 2020).

CE52G is an alfalfa (*Medicago sativa*) and rice (*Oryza sativa*) growth-promoting bacterium. It increased by 50% the shoot dry matter of alfalfa plants as compared with control plants (without rhizobial inoculation, nor nitrogen) (Castro-Sowinski et al. 2007) and also promotes the growth of shoot (250%) and root dry matter of rice plants (150%), as compared with non-inoculated plants (Castro-Sowinski et al. 2002a, b). Among other features of CE52G, a mutant obtained by the inactivation of a thioredoxin gene does not produce melanin and shows an impaired response to oxidative stress and reduced nitrogen-fixation (Castro-Sowinski et al. 2007). In this work we present the draft genome of *E. meliloti* strain CE52G, analyzing a few biochemical and genomic features.

Materials and methods

Description of *E. meliloti* strain CE52G

As described above, CE52G is a melanin-producing and alfalfa-nodulating strain isolated from acidic soil in Uruguay (Castro-Sowinski et al. 2002a, b); it promotes plant growth in alfalfa and rice, and a mutant in a thioredoxin gene (obtained by random mutagenesis using a Mini-Tn5 transposon) showed impaired melanin-production, nitrogen-fixation ability, and oxidative stress endurance (Castro-Sowinski et al. 2007).

Genomic DNA preparation, sequencing and, reconstruction of metabolic pathways

A fresh culture of CE52G (grown in Luria–Bertani—LB—medium for 24 h at 30 °C) was used for the isolation of total DNA. We used the conventional phenol–chloroform extraction method according to Sambrook (1989). The concentration and purity of the extracted DNA were measured using a NanoDrop Lite (Thermo Scientific) and its quality was assessed by agarose-electrophoresis.

The genomic library preparation and its further sequencing were outsourced to Macrogen (Seoul, South Korea). The library was prepared using a TruSeq DNA PCR-free kit (Illumina) and sequencing was performed with an Illumina HiSeq 2500 system, obtaining paired-ended reads of 151 bp. All reads were quality-checked with FastQC (v.0.11.6) and then quality-trimmed with Trimmomatic (v.0.38) for a Phred quality threshold of Q_{30} (Bolger et al. 2014). Illumina adapters were also removed with Trimmomatic. De novo genome assembly was performed with Velvet (v. 1.2.10) in conjunction with the VelvetOptimiser (k-mer 131) (Zerbino and Birney 2008). The genome was annotated and the functions of genes were predicted and compared using the Rapid Annotations using Subsystems Technology (RAST) (Aziz et al. 2008) and, NCBI Prokaryotic Genome Annotation Pipeline (PGAP) servers, under the accession number JAMKQB000000000.1. The predicted genes were functionally categorized using the SEED subsystems (Overbeek et al. 2005) at the RAST server. The reconstruction of KEGG metabolic pathways was assessed at the KAAS (KEGG Automatic Annotation Server) webserver (https://www.genome.jp/kegg/kaas/). The genomic relatedness analysis was performed using the average nucleotide identity determined with the BLASTn algorithm (ANIb) available at the JSpecies server (http://jspecies.ribohost.com/jspeciesws). The digital DNA-DNA hybridization (dDDH) was achieved using the genome-to-genome distance calculator (GGDC v.3.0) available at Leibniz Institute web server (https://ggdc.dsmz.de/).

Partial phenotypic characterization

Partial characterization of *E. meliloti* CE52G was done as described by de Araujo et al. (2017). Briefly, the growth was determined in: (i) a temperature range from 15 to 37 °C in YMA (0.2 g/L K_2HPO_4, 0.2 g/L $MgSO_4$, 10.0 g/L mannitol, 0.3 g/L Yeast extract, 0.05 g/L NaCl) and modified TY (5 g/L tryptone, 3 g/L yeast extract 3 g/L, 0.175 g/L $CaCl_2$) media; (ii) pH between 5 and 8, in both media; (iii) in the presence of 0.1% (w/v) NaCl in YMA and TY media; (iv) on modified-YMA with bromothymol

and; (v) the growth in minimal medium (MM) (Del Papa et al. 1999) supplemented with 10 mM sucrose as sole carbon source. We also analyzed the catalase activity by adding 200 µL of 30% of hydrogen peroxide to 3 mL of cell culture and observing the production of bubbles.

The resistance to antibiotics was evaluated using the disc diffusion method on YMA plates with the following antibiotics (concentration per disc): ampicillin (7.3 µg), chloramphenicol (8.8 µg), neomycin (8.15 µg), streptomycin (7.75 µg), spectinomycin (5.85 µg), kanamycin (5.8 µg), tetracycline (4 µg), and vancomycin (6.65 µg). The production of siderophores was analyzed in Petri dishes containing CAS medium (Shin et al. 2001).

Results

General features of the genome

We obtained a draft genome of 7,318,600 bp with a 460-fold coverage, assembled in 132 scaffolds of above 260 bp, with an *N*50 of 300,884 bp, L50 of 1,006,532 bp, and a GC content of 62%. The annotated genome using RAST and NCBI showed similar results. With RAST we identified 7789 protein-coding sequences (CDS) (2718 hypotheticals and, 3528 classified into subsystems; functional categorization of 45% of the proteome), 51 tRNAs, one copy of each rRNA gene (23S, 16S, 5S), ten prophages and 86 pseudogenes. The 16S rRNA gene showed 100% identity and coverage with the non-melanin-producing type strain *E. meliloti* USDA 1002 (accession number D14509) and the model strain *E. meliloti* 1021 (accession number AL591688). Also, the genomic relatedness of both strains (CE52G and 1002) was 98.7% for ANIb and 91.6% for dDDH, indicating that CE52G belongs to the *E. meliloti* species.

General features of the metabolic pathways

Bench experiments showed that CE52G grows in MM supplemented with sucrose and, searching into the genome we found a CDS for a α-glucosidase (EC 3.2.1.20), an enzyme involved in the hydrolysis of sucrose to glucose and fructose, being both major carbon and energy sources. The identification of pathways using KEGG showed that CE52G presents both the Embden-Meyerhof-Parnas and Entner-Doudoroff pathways with pyruvate as the end product, and also catabolizes glucose by the Pentose Phosphate pathway producing D-ribose 5-phosphate (presenting both the oxidative and the non-oxidative branches). CE52G oxidizes pyruvate to acetyl-CoA using the classical Pyruvate Dehydrogenase complex. This bacterium has the enzymes for both the Tricarboxylic Cycle (TCA cycle, Krebs cycle) and Glyoxylate Cycle for the metabolism of acetyl-CoA and, the propanoyl-CoA metabolism (transformation of propionyl-CoA to succinyl-CoA for supplying carbon source to the TCA). It also may produce glucose from oxalacetate (gluconeogenesis).

This bacterium produces the nitrogen-fixing enzyme nitrogenase (described below), performs the dissimilatory (genes *napAB*; we did not find the dissimilatory process by the *nar* genes) and assimilatory (genes *nasAB* or *narB*) reduction of nitrate to nitrite, and the assimilatory metabolism of nitrite to ammonia (genes *nirBD*); also performs the transformation of nitrous oxide (N_2O) to nitrogen (gene *nosZ*) (Fig. 1). We also found a cluster of genes for a nitrate reductase cytochrome c550-type subunit, periplasmic nitrate reductase (*napD*), ferredoxin-type periplasmic nitrate reductase (*napF*), and periplasmic nitrate reductase component (*napE*).

We also found that CE52G may synthesize and degrade canonical amino acids. Regarding sulfur metabolism, CE52G produces L-cysteine from L-serine, using the sulfur from sulfides, through the enzymes coded by *cysE*, *cysK,* and *cysO*. It may degrade other amino compounds such as taurine (an amino sulfonic acid) and selenocysteine. These compounds are metabolized to 5-glutamyl taurine using a gamma-glutamyl transpeptidase and, to methyl-selenol (genes *metBCH*) and/or alanine plus hydrogen selenide using a selenocysteine lyase (*sulS*), respectively.

We found several ABC transporters for mineral and organic ions (sulfate, nitrate, nitrite, taurine, molybdate, iron (III), thiamine, spermidine/putrescine, glycine betaine/proline, and other osmoprotectants), oligosaccharides (raffinose/melibiose, lactose, L-arabinose, sorbitol, mannitol, α-glucoside, trehalose/maltose, phospholipids, and nucleosides), monosaccharides (glucose/mannose, ribose, L-arabinose, glucofuranose, D-xylose, fructose, rhamnose, erythritol, myo-inositol, glycerol, sn-glycerol 3-phosphate), phosphate and amino acids (phosphate, phosphonate, glutamate/aspartate, cysteine, hydroxyproline, branched-chain amino acids, D-methionine, and urea), peptides (oligopeptides, heme, and δ-aminolevulinic acid and microcin C), metallic cations (Fe-siderophore, zinc, iron (II), manganese), vitamins (biotin) and others (capsular polysaccharide, lipooligosaccharide, lipoprotein, lipopolysaccharides). Among the molecules mentioned above, we only analyzed if CE52G can grow in mannitol; we found that CE52G shows an acidic reaction on modified-YMA with bromothymol, turning the medium yellow, indicative of mannitol fermentation.

We found Fe-siderophore sensor and receptor systems. We did not find the genomic information for the production of any kind of siderophore and this result was supported by bench experiments (no siderophore production in the CAS assay). These findings suggest that CE52G does not produce siderophores, but incorporates iron using siderophores produced for other organisms. Interestingly, we found the information for the production of a hemophore, and outer

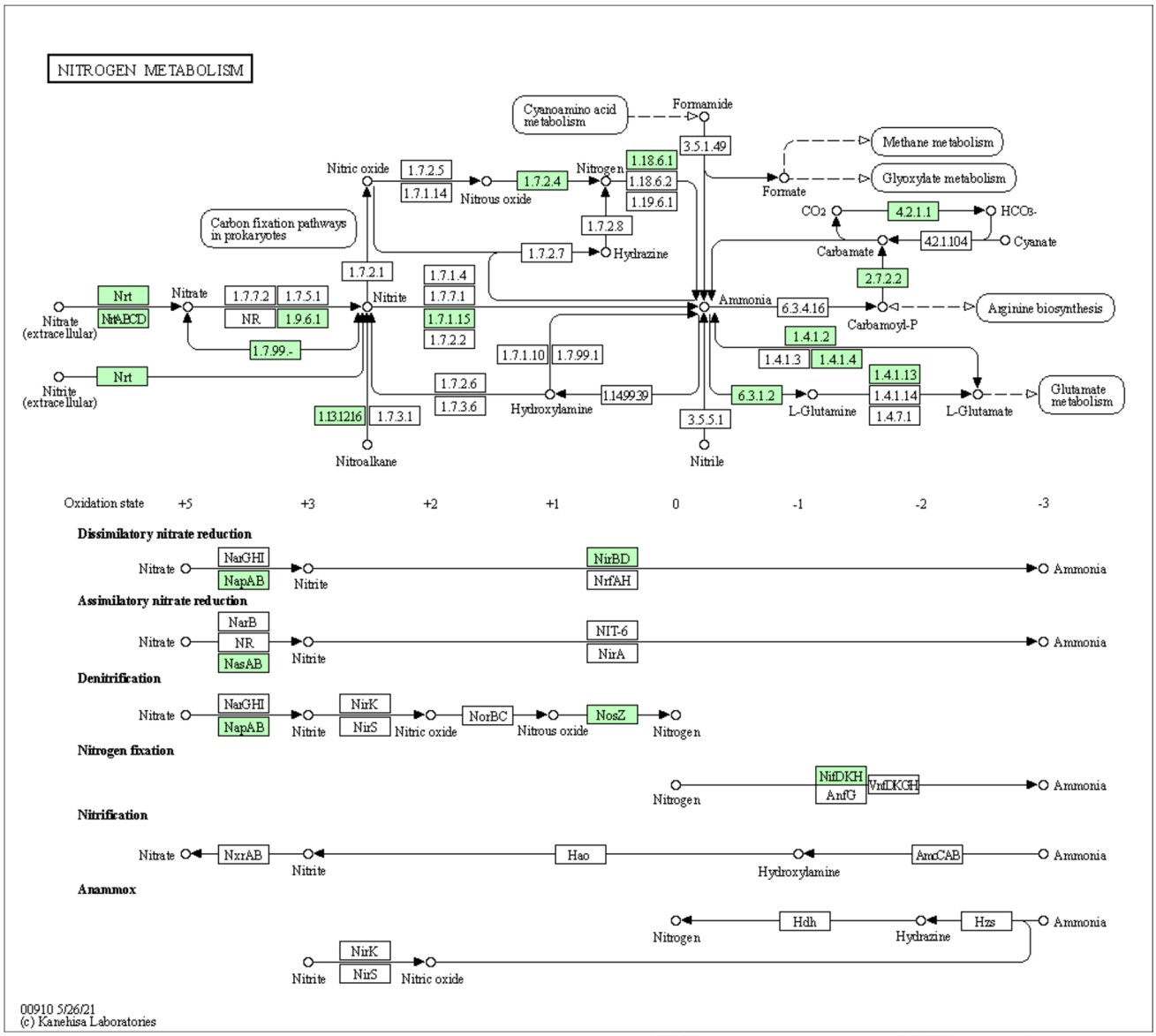

Fig. 1 KEGG pathway diagram for nitrogen metabolism in *E. meliloti* CE52G. The total proteome, as obtained from the RAST annotation, was uploaded to the KAAS-KEGG Automatic Annotation Server for orthologous assignment and pathway mapping

membrane receptor and acquisition (HasRA) system, for the incorporation of heme as an iron source (Has for heme assimilation system). This hemophore could be important for the synthesis of heme-containing proteins, such as heme-peroxidases among others.

Regarding secretion systems, we found that CE52G has the genomic information for TolC (the outer membrane protein found in the Type I secretion system), the Type III and Type IV, and, the Sec-SRP and Twin arginine targeting (Tat) systems; CE52G does not have the genomic information for Type II, V, and VI secretion systems.

We found several two-component systems for phosphate limitation, osmotic upshift (K^+), K^+ limitation, catabolite repression, dicarboxylate transport (*dctBC*), tricarboxylates transport (*tctW*, *tctD*), and the *ampC* gene for β-lactam resistance. We found the two-component system ChvG/ChvI that triggers a cellular response to acid conditions in *Rhizobium* (Vanderlinde and Yost 2012); thus, we analyzed if CE52G can grow at a low pH, and we found that it grows at a pH from 6 to 8 in YMA and, from 5 to 8 in TY. We found the CDS for Des, the membrane phospholipid desaturase involved in fluidizing membranes during a down-shift in temperature. However, we did not find the DesK/DesR two-component system involved in sensing a decrease in temperature (de Mendoza and Pilon 2019). Thus, we analyzed the growth of CE52G at different

temperatures; it grows between 15 to 37 °C in both YMA and TY media. We found that CE52G has optimal growth at 28 °C, at pH 7 and, it does not grow at 15 °C.

We also found the two-component system for the uptake of C4-dicarboxylates (*dctB*, *dctD,* and *dctA*), for low nitrogen availability (Gln and Ntr systems) and nitrogen fixation (*fixL* and *fixJ*), and redox signal (*regB* and *regA*) linked to electron transfer systems, aerobic respiration and nitrogen fixation (*nifA*).

It has the genomic information for flagella assembly, chemotaxis (the Che, Fli, and Mot systems), and a quorum-sensing system (such as the Lsr system of *E. coli* for AI-2), the Tra system (TraI and TraR) for AI-1.

Based on the genome analysis, CE52G can repair DNA using the most known systems (base-excision, nucleotide excision, mismatch repair systems, homologous recombination, and non-homologous end-joining) and does not have a CDS for a photolyase. The absence of a photolyase was expected since this enzyme repairs the DNA damage induced by UV light (Marizcurrena et al. 2017) and CE52G is a soil bacterium that probably does not face solar light, at least when immersed in soil or nodules.

We found a CDS coding for a laccase with 99–100% identity to multicopper oxidases from *Sinorhizobium* strains. The amino acid sequence for the laccase was analyzed using the SignalP 5.0 server (http://www.cbs.dtu.dk/services/SignalP/) and the results suggest that this protein contains an SPI signal peptide with a cleavage site between position 26 and 27 (Sec/SPI). The Sec pathway secretes proteins from the bacterial cytoplasm to the periplasm; thus, the result suggests that the CE52G laccase is a periplasmic protein, as reported by Rosconi et al. (2005). The authors observed the laccase activity of CE52G in the periplasmic fraction of protein extracts. The identification of a CDS for a laccase was elusive until the sequencing of CE52G genome; thus, now we are checking the recombinant production of these enzymes for further analysis of its biotechnological potential.

Analysis of genes involved in the plant–microbe interaction

This bacterium has the genomic information for synthesizing the Nodulation Factor (NF), a lipo-chitooligosaccharide involved in the legume-microbe communication (Buhian and Bensmihen 2018) (Fig. 2a). We found a transcriptional unit containing the genes *nodABCIJ* and; the *nodD* gene for the production of the transcriptional regulator. NodD recognizes the presence of a plant-produced flavonoid and triggers the synthesis of the NF. We found three copies of *nodD* genes (*nodD1*, *nodD2,* and *nodD3*), located in distant regions of the genome, with 100% identity to *nodD* genes found in the reference strain *S. meliloti* 1021. The gene *nodD1* is located close to the transcriptional unit that contains the constitute genes for the NF formation and, *nodD2* and *nod3* are located in the vicinity of several ABC-transporters and *nifHDKEX*, respectively.

We also found the genes *nodI* and *nodJ* that encode the ATPase and permease of an ABC-type transport system, and the *nodN* gene, being NodN a protein probably involved in the synthesis of sufficient amounts of NF and its excretion as reported by Baev et al. (1992). We did not find the *nodH*, *nodP,* and *nodQ* genes; NodH, NodP, and NodQ incorporate phosphate groups in the NF from *E. meliloti* strain (Roumiantseva et al. 2022); thus, we wonder if CE52G produces a phosphate-free NF. We found the *nolO* gene that encodes a secreted protein containing repeated calcium-binding domains in the N-terminal region, a protein with a non-recognized function during the formation of the nodule as reported by Kirienko et al. (2019).

CE52G has genes for synthesizing the nitrogen-fixing enzyme, nitrogenase (Fig. 2b). The genome has a transcriptional unit containing the CDSs for the reductase nitrogenase (*nifH*), for both chains (alpha and beta chains; *nifDK*) for the reduced ferredoxin, and the dinitrogen oxidoreductase (place for the hydrolysis of ATP) proteins. It also shows the genes for synthesizing the FeMo-cofactor (*nifE*) and the nitrogenase FeMo-cofactor carrier protein (*nifX*). We

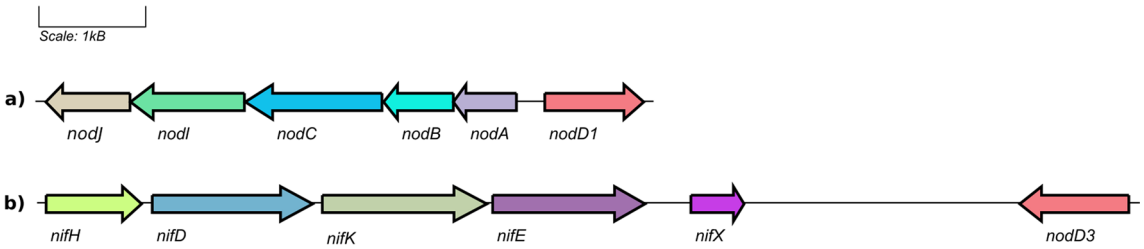

Fig. 2 The genomic organization of genes involved in the production of the nodulation factor and nitrogenase**.** The figure shows the organization of the *nod* (**a**) and the *nif* operons (**b**). The DNA sequence between the *nifE* and *nifX* genes was analyzed using different bioinformatics tools and, even they are in the same contig, we did not find a putative promoter between these two genes. Created by genegraphics.net/app from RAST server data

also found genomic information for the uptake of Mo (*modABCE*). It has a transcriptional unit containing the genes *fixA* and *fixB* (beta and alpha subunits for the electron transfer flavoprotein), *fixC* (electron transfer flavoprotein-quinone oxidoreductase), *fixX* (ferredoxin-like protein), *nifA* (a transcriptional regulator), *nifB* (nitrogenase FeMo-cofactor synthesis), a 4Fe-4S ferredoxin and *nifT*. The CE52G genome also contains individual *nif* genes such as *nifN* (nitrogenase FeMo-cofactor scaffold and assembly protein) and *nifU*.

This bacterium also has the information for sulfur metabolism using taurine, L-cysteine, and L-serine as donors, taurine being an alternative sulfur source (see above). Sulfur is an essential element for living organisms. Also, molybdenum is essential for bacterial growth and it is found in the FeMo-cofactor of the nitrogenase. Both sulfur and molybdenum metabolisms are linked because these chemical elements have to be in balance for efficient nitrogen fixation (Cheng et al. 2016).

E, meliloti requires bacterial exopolysaccharides (EPS) to facilitate a successful root invasion (Reinhold et al. 1994); thus, we searched for genes involved in EPS production. *E. meliloti* strains produce two different EPSs (EPS I or succinoglycan and, EPS II or galactoglucan), with different functions in the symbiotic process (Acosta-jurado et al. 2021). The CE52G genome has information for the synthesis of both EPSs. We found at least 64 genes located in a larger unit; this unit contains information for the transportation of sugars, polymerization sugars, surface polysaccharides/antigens, succinoglycan biosynthesis protein and its transport (*exoT* and *exoM*), phosphate glycophosphotransferase, EPS polymerization, and transport (*exoF*, *exoQ*), an acetyl transferase (*exoZ*), and glycosyltransferase (*epsF*), among others. We did not find the *mucR* gene; MucR is responsible for the differential regulation of EPS I and EPS II production (Acosta-Jurado et al. 2021). The production of EPS II is currently induced at low phosphate concentration, through the regulation of a two-component system PhoR-PhoB; we found the transcriptional regulatory protein PhoB and we did not find the response regulator PhoR.

We previously reported that a thioredoxin mutant from CE52G does not produce melanin (Fig. 3a) and is impaired in nitrogen fixation (Castro-Sowinski et al. 2007); thus, we searched for the occurrence of thioredoxin genes in the CE52G genome. We found four CDSs annotated as thioredoxins (called *trx*1, *trx*2, *trx*3, and *trx*4). They are ubiquitous proteins with major cellular functions such as redox regulation of protein function and signaling via thiol redox control (Arnér and Holmgren 2000). The thioredoxin system is formed by a thioredoxin, a thioredoxin reductase, and NADPH, nonetheless, thioredoxins can also serve as an electron donor for other reductases. This electron donor has a dithiol/disulfide active site with a characteristic CGPC motif. Among the four thioredoxins, we found that Trx1 and Trx2 present the CGPC motif and, Trx3 and Trx4 present a CQPC and CLPC motif, respectively (Fig. 3b). The thioredoxin involved in melanin production and nitrogen fixation is Trx3 and presents the CQPC motif; the G (glycine, small amino acid involved in the formation of alpha-helices) to Q (glutamine; polar charged amino acid, involves in salt bridge formation) change may imply an important change in the protein structure and function. Thus, we decided to go forward in the characterization of the thioredoxins, mainly Trx3. Thioredoxin isoforms are found in most organisms and cellular compartments (Arnér and Holmgren 2000). We analyzed the presence of signal peptides using the SignalP 5.0 tool (http://www.cbs.dtu.dk/services/SignalP/) and found that the four Trx proteins do not have a signal peptide, suggesting that they have a function in the cytoplasm of CE52G, which were confirmed with the PROSITE tool (https://prosite.expasy.org/). Searching in the genome, we did find four thioredoxin reductase CDSs that are not closely located to the four thioredoxins CDSs. Thus, we analyzed the genes around *trx*3 and found that downstream *trx*3 there is a gene that codes for a NPP1 family protein. NPP1s are commonly found in plant pathogens and, are involved in plant cell death, acting as positive virulence factors (Gijzen and Nürnberger 2006). We wonder if Trx3 is involved in the redox regulation of this NPP1-like protein and successful non-pathogenic infection of CE52G in alfalfa plants. We also performed modeling of the Trx proteins using AlphaFold (Jumper et al. 2021) and align the structures using PyMol (The PyMOL Molecular Graphics System, Version 2.0 Schrödinger, LLC). We found that the four thioredoxins show a good structural alignment and display a characteristic tertiary structure consisting of a core of four-stranded antiparallel beta sheets and, four exposed alpha helices (Fig. 3c; see the CXPC motif).

Genomic features and mechanisms for environmental adaptation

We found many genes related to oxidative, osmotic, and nitrosative stress alleviation, including a redox-sensitive transcriptional activator SoxR. We highpoint the presence of CDSs that codes for Cu–Zn and Mn superoxide dismutases, NnrS involved in response to NO, several thioredoxin-disulfide reductases, organic hydroperoxide resistance protein, catalase-peroxidase KatG and KatE, glutathione reductase, among others. In this regard, we observed bubbling with the addition of hydrogen peroxide to CE52G cells, thus confirming the catalase activity.

CE52G also has the genomic information for synthesizing proteins involved in osmotic stress endurance as the uptake and synthesis of choline and betaine. CE52G genome contains a transcriptional unit for the ABC transport of choline (*choVWX*) and betaine (*betT*); it also has the information

a)

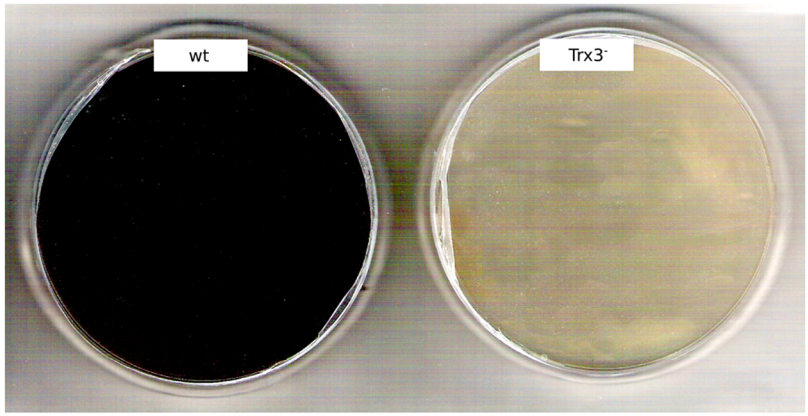

b)

```
Trx 1  -MPTL---------KVDTSNFQKEVLNSAEPVVVDFWAPWCGPCKMIAPS 40
Trx 2  -MATV---------KVDTANFQKEVLNSAEPVVVDFWAEWCGPCKMIAPS 40
Trx 3  MNTTTPNEHPSAIVKVDTSNFSEEVLQSAEPVIVDFWKNGCQPCDMIVPF 50
Trx 4  -MPTAPNEHPTDG-KVDTCTFPEEVLNSPLPVVAAFSGEHCLPCDAIAFS 48

Trx 1  LEEISTELAGKVKLVKLNIDENPELTAEYGVRSIPMLAMFKAGEVADTKV 90
Trx 2  LEEIATELAGKVKVVKLNIDENPELAAQYGVRSIPTLAMFKGGEVADIKV 90
Trx 3  LEQIATELAGKVKVVKINKAENPELVARYGVRGYPTLALFKDGEVADIDY 100
Trx 4  LKEIATELAGKLKVVKIDVDENLDLAARYGVRGVPTLLMFKGGEVADIYV 98

Trx 1  GAAPKTALISWILNAIG---- 107
Trx 2  GAAPKTALSSWISSAVA---- 107
Trx 3  DYE-PGSLRSSISEALASLRT 120
Trx 4  G---TGSLRSWISKALA---- 112
```

c)

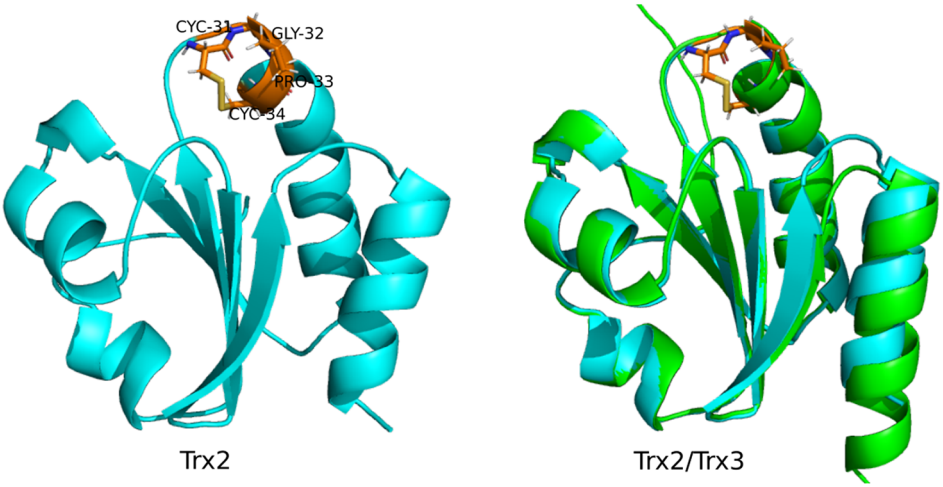

Fig. 3 Thioredoxins from *E. meliloti* CE52G**.** The figure shows: **a** the production of melanin by the wide type *S. meliloti* CE52G strain (wt) and the thioredoxin (*trx3*) mutant ($Trx3^{-}$); cells were grown in TY medium supplemented with tyrosine (0.6 mg/mL) and $CuSO_4$ (0.16 mM). **b** The alignment of Trx1, Trx2, Trx3, and Trx4; the consensus amino acid are shown in green and, the characteristic CXPC motif is shown framed in orange. **c** structural prediction of thioredoxins as predicted by AlphaFold (Jumper et al. 2021) and visualization using PyMol (The PyMOL Molecular Graphics System, Version 2.0 Schrödinger, LLC); on the left, the predicted 3D structure of Trx2 (the CXPC motif is shown in orange) and, on the right, the superimposed 3D structures of Trx2 and Trx3

for synthesizing choline from betaine. Located in the same transcriptional unit, we found the genes *betC* (choline-*O*-sulfatase), *betA* (choline dehydrogenase), and *betB* (betaine aldehyde dehydrogenase). The experiments done on the bench showed that CE52G does not grow in the presence of 0.1% (w/v) NaCl. The results suggest that beyond the presence of CDSs involved in osmotic stress endurance, free-living CE52G cells have a low tolerance to ionic osmolarity, in the tested condition.

CE52G also has genomic information involved in the production and degradation of carbon-storage compounds such as polyhydroxyalkanoates and glycogen. We found genes coding for the synthesis and degradation of polyhydroxy butyrate (PHB) as follows: PHB synthase, 3-hydroxybutyrate-CoA dehydratase, acetoacetyl-CoA synthetase, acetyl-CoA acetyltransferase, acetoacetyl-CoA reductase, enoyl-CoA hydratase, 3-oxoadipyl-CoA thiolase, 3-hydroxybutyrate-CoA dehydrogenase, 3-hydroxybutyrate-CoA epimerase, 3-ketoacyl-CoA thiolase. CE52G presents two CDSs for the degradation of PHB (PHB depolymerase genes *phaZ-1* and *phaZ-2* that codes for 364 and 424 amino acid proteins, respectively). PhaZ-1 and PhaZ-2 show 100% identity (100% coverage) with PHB depolymerase family esterase and polyhydroxyalkanoate (PHA) depolymerase from *E. meliloti* 1021, respectively.

Regarding the synthesis and degradation of glycogen, we found CDSs for the production of bacterial glycogenin (the primer that initiates the synthesis of glycogen) and the enzymes involved in the growth and branching of the sugar chain, the enzymes glycogen phosphorylase, GH-13 type 1,4-alpha-glycogen branching enzyme, glycogen synthase, and, phosphoglucomutase; all CDSs in the same transcriptional unit with a limit dextrin alpha-1,6-maltotetraose-hydrolase. We also found a CDS for the glycogen debranching enzyme.

Searching in KEGG, we found that CE52G has the RND efflux pump (genes *oprM*, *acrB,* and *acrA*) for pumping β-lactams and the ability for transforming penicillin to penicilloic acid (*penP*). Thus, we evaluated the antibiotic resistance of CE52G by performing the disc-diffusion method and we found that CE52G is resistant to streptomycin, spectinomycin, and vancomycin; and it is sensitive to tetracycline, chloramphenicol, neomycin, ampicillin, and kanamycin, at the tested concentrations (see "Materials and methods").

Discussion

CE52G has a genome size and GC content comparable with *E. meliloti* strains such as GR4 (7.14 Mb; Martínez-Abarca et al. 2013), CCNWSX0020 (7.00 Mb; 60%; Li et al. 2012) and, the reference strain *E. meliloti* 1021 (7.15 Mb; 62.1%; Guo et al. 2003). In addition, its 16S rRNA shows 100% identity and coverage with other *E. meliloti* strains, including *E. meliloti* 1002 and 1021. This result and, the data obtained from ANIb and dDDH, confirm that CE52G belongs to the *E. meliloti* species.

Ensifer strains contain a large genome, with a chromosome and two symbiotic megaplasmids. In this work, we did not search for the megaplasmids; however, we found genes that suggest that the CE52G genome concludes at least a plasmid. We found several copies of the plasmid replication protein RepCAB, IncQ plasmid conjugative transfer protein TraG, and the chromosome (plasmid) partitioning protein ParAB. We found a contig containing a CDS for a plasmid replication protein RepC just 1250 pb from the *nod* operon. Thus, the data suggests that CE52G has different replicons as demonstrated in other *Ensifer* strains (Nelson et al. 2018).

The genomic information suggests that CE52G uses both Embden-Meyerhof (EMP) and Entner-Doudoroff (ED) pathways. In *E. coli*, the hexose catabolic ED pathway is an alternative pathway of glycolysis to the EMP pathway. Probably, like *E. meliloti* 1021, CE52G uses the EMP pathway in a gluconeogenic role rather than a glycolytic one (Geddes and Oresnik 2014) and uses ED as an aerobic glycolytic pathway for obtaining energy (ATP) and reducing power.

We found that CE52G performs the dissimilation (*napAB*) and assimilation (*nasAB*) of nitrate to nitrite, assimilation to ammonia (*nirBD*), and the transformation of nitrous oxide to nitrogen (*nosZ*). Nitrate may follow the following pathways: (i) denitrification at the periplasmic space or (ii) nitrification at the cytoplasmic space (Ruiz et al. 2019). During denitrification, NapAB reduces nitrate to nitrite, and then NirK reduced nitrite to nitric oxide, with a further transformation to N_2O and N_2 by NorC and NosZ, respectively. During nitrification, NarB reduces nitrate to nitrite, and NirBD reduces nitrite to ammonia. We did not find all the genes, but our results suggest that CE52G performs the assimilation of nitrate into the periplasm and, the nitrification in the cytoplasm. Ruiz et al. (2019) also reported that in aerobic conditions and the absence of ammonium, the expression of *narB* (nitrate assimilatory pathway) does not play a role in the symbiosis and; that NirB (assimilatory pathway) participates indirectly in the synthesis of nitric oxide (NO) cooperating with the denitrification pathway. Thus, results suggest that CE52G may produce NO from nitrate. Interestingly, we found a CDS coding for the flavohaemoglobin nitric oxide dioxygenase (NOD) located close to *nnrS*, being NnrS a protein involved in the response to NO (detected at various steps of the rhizobium-legume symbiosis). The NOD oxygenates leghemoglobin (LegHb) and NO, forming ferric LegHb and nitrate.

Among many two-component systems, we found the DctBC. This system is involved in the uptake of dicarboxylic acids, an energy and carbon source for the bacteroid (Wheatley et al. 2020). This two-component system is

under the control of RpoN and plays a role in nitrogen-fixing symbiosis (Yurgel and Kahn 2004; Wongdee et al. 2023). We found that the CE52G genome presents a *rpoN* gene upstream to ribosome hibernation-promoting factor Hpf, a PTS IIA-like nitrogen regulatory protein PtsN, a heat shock protein GrpE and a Heat-inducible transcription repressor HrcA. We think that this two-component system may have an important role during symbiosis as was demonstrated in *E. meliloti* L5-30 (Batista et al. 1992) and reviewed by Ledermann et al. (2021). Let's remember that the plant supplies C4-dicarboxylates to the bacteroids, instead of sucrose, and they enter the Krebs cycle generating large amounts of reduced electron carriers essential for ATP synthesis and nitrogen fixation (Ledermann et al. 2021).

Free-living soil rhizobia are exposed to nutrient starvation, desiccation, and pH stress, and during the transition to an endosymbiotic bacteroid lifestyle they have to cope with the stress imposed by the plant host. Thus, rhizobia have mechanisms to alleviate the stress that induces cellular damage, including chaperones, DNA repair systems, and reactive oxygen species. Regarding two-component systems involved in sensing some physical environmental conditions (temperature and acidity), we did find ChvG/ChvI and did not find DesK/DesR, for triggering the cellular response to acidic conditions and a decrease in temperature, respectively. ChvG/ChvI is involved in the regulation of acid-inducible genes in *Rhizobium* as demonstrated by Vanderlinde and Yost (2012). The authors showed that the sensor kinase ChvG negatively impacts cellular metabolism, outer membrane stability, and symbiosis in *Rhizobium leguminosarum*. The gene *chvG* from *Agrobacterium tumefaciens* (Li et al. 2002) and *S. meliloti* (Wang et al. 2010) is required for growth at acidic pH, and the mutants have an impaired growth at pH 5. Also, ChvG from *A. tumefaciens* is involved in resistance to antibiotics targeting cell wall synthesis (Williams et al. 2022). We wonder if ChvG/ChvI from CE52G is involved in its adaptation to acid soils since this bacterium was isolated from an acidic soil in Uruguay (Castro-Sowinski et al. 2002a, b) and/or to antibiotics produced by other microbes.

We found the gene *des* for the desaturation of fatty acids, a characteristic of psychrophilic microbes, but we did not find DesK/DesR. DesK is a membrane sensor histidine kinase that activates when the temperature decreases and, in turn, DesK activates the response regulator DesR that triggers *des*. The protein Des is involved in the unsaturation of membrane lipids when the temperature is shifted down, adapting the membranes of a microbe to function at low temperatures (Saita and De Mendoza 2015). We found that CE52G does not grow at low temperatures and does not have the DesK/DesR system. Thus, we think that CE525G *des* is not involved in cold-adaptation and, is involved in introducing unsaturation in fatty acids that are needed for other metabolic requirements.

Like other *Ensifer* strains, CE52G nodulates alfalfa roots and fixes atmospheric nitrogen (Castro-Sowinski et al 2002a, b, 2007). As expected, we found the *nod* and *nif/fix* genes to perform these activities. We found three *nodD* genes, responsible for the production of NodD, the protein that senses compounds produced by alfalfa plants, mainly luteolin, and triggers the formation of the NF (Morel and Castro-Sowinski 2013). As previously reported, NodD1 and NodD2 are constitutively expressed and detect flavonoids and betaines, respectively, and; NodD3 does not need an external compound for *nod* genes induction (Barnett et al. 2015). CE52G, contains the genomic information for the production of the NF; however, we did not find the genes involved in the decoration of the NF with a phosphate group as found in *E. meliloti* strains (Roumiantseva et al. 2022). As rhizobial strains evolved several distinct strategies to enter into symbiosis with legumes, we think that CE52G may produce an effective and phosphate-free NF as part of the chemical communication with alfalfa plants. This NF will be purified and the chemical structure will be elucidated by NMR spectroscopy.

Diazotrophs contain one out of three nitrogenase: Nif (Mo-dependent), Vnf (vanadium-dependent), and Anf (iron-dependent, devoid of Mo and V). The number of proteins involved in the formation and regulation of nitrogenases is coded from many genes (Mus et al. 2018) and, we found a set of genes that show that CE52G produces the classical Mo-dependent nitrogenase.

In addition to NF, *E. meliloti* strains produce a succinoglycan known as EPS I, involved in a successful bacterial invasion of roots, and a galactoglucan known as EPS II, involved in biofilm formation and root colonization (Acosta-Jurado et al. 2021). We found that CE52G has the genomic information for the production of both EPS. We did not find the regulators MucR (differential regulation of EPS I and EPS II production) and PhoR (response regulator induced at low phosphate concentration and involved in EPS II production). We think that the potential lack of the MucR and PhoR regulators could be involved in the constitutive production of EPS II and, the production of EPS II could be responsible for a mucous phenotype, as we observed in CE52G.

Both EPS I and EPS II are also involved in oxidative-stress, water deficiency, and salinity-stress protection in *E. meliloti* (Lehman and Long 2013) and their over-production could affect nodulation; EPS forms a physical barrier (viscosity, acidity, hydrophilicity) for accessing the root and, could mask the exchange of molecules between the microbe and the plant (Ozga et al. 1994). We think that the over-production of EPS (I or II) by CE52G could be linked to survival in different stress conditions as suggested by Lehman and Long (2013) and Primo et al. (2020).

We previously reported that a thioredoxin mutant from CE52G has impaired nitrogen fixation and is sensitive to oxidative stress (Castro-Sowinski et al. 2007) and, we found that at least one out of four thioredoxins in the CE52G genome is involved in the plant growth promoting ability of this microbe. This thioredoxin was called Trx3 and show structural similarity with Trx2. Thus, we think EPS production and thioredoxin activity could be involved in oxidative stress endurance and the establishment of effective nodulation. As previously reported thioredoxin is involved in bacterial differentiation and the formation of the alfalfa nodule (Alloing et al. 2018). The presence of genes for the uptake of choline and betaine and, the transformation of choline to betaine, suggests that CE52G is prepared to face an osmotic stress situation, at least in the nodule (Fougere and Le Rudulier 1990; Roumiantseva et al. 2022). In summary, CE52G has the genomic information to endure low pH, oxidative and osmotic environments. What about biotic stress? Recently, Contreras-Moreno et al. (2020) showed that multicopper oxidases and melanin production play a role in *Myxococcus xanthus* predation on *E meliloti*; thus, we think that CE52G may have a genomic background to survive bacterial predation. This is an interesting issue that we will face shortly while performing bench experiments.

The production of PHA is also linked to stress endurance (adaptability to stressful conditions), UV radiation, salinity, thermal and oxidative stress, desiccation, and osmotic shock among others, improving microbial survival (Kadouri et al. 2005). We found the genomic information for synthesizing and degrading PHB and glycogen. Both carbon storage compounds are involved in the development of bacteroids, competitiveness, and symbiotic efficiency (Wang et al. 2007; Ledermann et al. 2021), and probably PHB is degraded to fuel during bacteroid differentiation (Lodwig et al. 2005).

Conclusions

E. meliloti CE52G is an alfalfa-nodulating and nitrogen-fixing bacterium that presents a large genome as expected for a rhizobial strain. The genomic information and the data obtained from a few bench experiments show that this strain has the canonical machinery for the production of a Nodulation Factor (probably a phosphate-free NF) and symbiotic nitrogen fixation. CE52G does not produce siderophores but incorporates iron using siderophores produced for other organisms and uptaking heme through an outer membrane receptor and acquisition system, a hemophore. It has the genomic information for survival at acidic pH and oxidizing conditions and, for the production of PHB and glycogen; all these properties are probably involved in stress endurance in the soil and the bacteroid phase. CE52G produces gummy or mucous colonies probably due to the production of both EPS I and II, and these EPSs are probably involved in nodulation and oxidative stress.

Acknowledgements We thank Dr. Juan José Marizcurrena for his support during AlphaFold working.

Funding This work was financially supported by the Basic Sciences Development Program (PEDECIBA; Programa de Desarrollo de las Ciencias Básicas). S. Castro-Sowinski, C. García and María A. Morel are members of the National Research System (SNI, Sistema Nacional de Investigadores). The work of C. Cagide was supported by the National Agency for Research and Innovation (ANII; Agencia Nacional de Investigación e Innovación). We thank the Uruguayan Antarctic Institute (IAU, Instituto Antártico Uruguayo) for partial financial support and logistics during the stay in the Artigas Scientific Antarctic Base.

Data availability The genome data associated with this paper is available in the NCBI Prokaryotic Genome Annotation Pipeline (PGAP) servers, under the accession number JAMKQB000000000.1.

Declarations

Conflict of interest The authors declare that the research was conducted without any commercial or financial relationships that could be construed as a potential conflict of interest.

References

Acosta-jurado S, Fuentes-romero F, Ruiz-sainz JE et al (2021) Rhizobial exopolysaccharides: genetic regulation of their synthesis and relevance in symbiosis with legumes. Int J Mol Sci. https://doi.org/10.3390/ijms22126233

Alloing G, Mandon K, Boncompagni E et al (2018) Involvement of glutaredoxin and thioredoxin systems in the nitrogen-fixing symbiosis between Legumes and Rhizobia. Antioxidants. https://doi.org/10.3390/antiox7120182

Arnér ESJ, Holmgren A (2000) Physiological functions of thioredoxin and thioredoxin reductase. Eur J Biochem 267:6102–6109. https://doi.org/10.1046/j.1432-1327.2000.01701.x

Aziz RK, Bartels D, Best A et al (2008) The RAST Server: rapid annotations using subsystems technology. BMC Genom 9:1–15. https://doi.org/10.1186/1471-2164-9-75

Baev N, Schultze M, Barlier I et al (1992) Rhizobium *nod*M and *nod*N genes are common nod genes: *nod*M encodes functions for efficiency of nod signal production and bacteroid maturation. J Bacteriol 174:7555–7565. https://doi.org/10.1128/jb.174.23.7555-7565.1992

Barnett MJ, Long SR (2015) The *Sinorhizobium meliloti* SyrM Regulon: effects on global gene expression are mediated by *syr*A and *nod*D3. J Bacteriol 197:1792–1806. https://doi.org/10.1128/JB.02626-14

Batista S, Castro S, Aguilar OM, Martinez-Drets G (1992) Induction of C4-dicarboxylate transport genes by external stimuli in *Rhizobium meliloti*. Can J Microbiol 38:51–55. https://doi.org/10.1139/m92-008

Bolger AM, Lohse M, Usadel B (2014) Trimmomatic: a flexible trimmer for Illumina sequence data. Bioinformatics 30:2114–2120. https://doi.org/10.1093/bioinformatics/btu170

Botero A, García C, Gossen BD et al (2019) Clubroot disease in Latin America: distribution and management strategies. Plant Pathol 68:827–833. https://doi.org/10.1111/ppa.13013

Buhian WP, Bensmihen S (2018) Mini-review: nod factor regulation of phytohormone signaling and homeostasis during rhizobia-legume symbiosis. Front Plant Sci. https://doi.org/10.3389/fpls.2018.01247

Castro-Sowinski S, Carrera I, Catalán AI et al (2002a) Occurrence, diversity and effectiveness of mid-acid tolerant alfalfa nodulating rhizobia in Uruguay. Symbiosis 32:105–118

Castro-Sowinski S, Martinez-Drets G, Okon Y (2002b) Laccase activity in melanin-producing strains of *Sinorhizobium meliloti*. FEMS Microbiol Lett 209:119–125. https://doi.org/10.1111/j.1574-6968.2002.tb11119.x

Castro-Sowinski S, Matan O, Bonafede P, Okon Y (2007) A thioredoxin of *Sinorhizobium meliloti* CE52G is required for melanin production and symbiotic nitrogen fixation. Mol Plant-Microbe Interact 20:986–993. https://doi.org/10.1094/MPMI-20-8-0986

Cheng G, Karunakaran R, East AK, Poole PS (2016) Multiplicity of sulfate and molybdate transporters and their role in nitrogen fixation in *Rhizobium leguminosarum bv. viciae* rlv3841. Mol Plant-Microbe Interact 29:143–152. https://doi.org/10.1094/MPMI-09-15-0215-R

Contreras-Moreno FJ, Muñoz-Dorado J, García-Tomsig NI et al (2020) Copper and melanin play a role in *Myxococcus xanthus* predation on *Sinorhizobium meliloti*. Front Microbiol 11:1–13. https://doi.org/10.3389/fmicb.2020.00094

de Mendoza D, Pilon M (2019) Control of membrane lipid homeostasis by lipid-bilayer associated sensors: a mechanism conserved from bacteria to humans. Prog Lipid Res 76:100996. https://doi.org/10.1016/j.plipres.2019.100996

de Araujo ASF, de Almeida Lopes AC, Teran JCBM et al (2017) Nodulation ability in different genotypes of *Phaseolus lunatus* by rhizobia from California agricultural soils. Symbiosis 73:7–14. https://doi.org/10.1007/s13199-016-0465-0

Del Papa MF, Balagué LJ, Sowinski SC et al (1999) Isolation and characterization of alfalfa-nodulating rhizobia present in acidic soils of Central Argentina and Uruguay. Appl Environ Microbiol 65:1420–1427. https://doi.org/10.1128/aem.65.4.1420-1427.1999

Fields B, Friman VP (2022) Microbial eco-evolutionary dynamics in the plant rhizosphere. Curr Opin Microbiol 68:102153. https://doi.org/10.1016/j.mib.2022.102153

Fougere F, Le Rudulier D (1990) Uptake of glycine betaine and its analogues by bacteroids of *Rhizobium meliloti*. J Gen Microbiol 136:157–163. https://doi.org/10.1099/00221287-136-1-157

Geddes BA, Oresnik IJ (2014) Physiology, genetics, and biochemistry of carbon metabolism in the alphaproteobacterium *Sinorhizobium meliloti*. Can J Microbiol 60:491–507. https://doi.org/10.1139/cjm-2014-0306

Gijzen M, Nürnberger T (2006) Nep1-like proteins from plant pathogens: recruitment and diversification of the NPP1 domain across taxa. Phytochemistry 67:1800–1807. https://doi.org/10.1016/j.phytochem.2005.12.008

Guo X, Flores M, Mavingui P et al (2003) Natural genomic design in *Sinorhizobium meliloti*: novel genomic architectures. Genome Res 13:1810–1817. https://doi.org/10.1101/gr.1260903

Hirsch AM, Lum MR, Downie JA (2001) What makes the Rhizobia-legume symbiosis so special? Plant Physiol 127:1484–1492. https://doi.org/10.1104/pp.010866

Janusz G, Pawlik A, Świderska-Burek U et al (2020) Laccase properties, physiological functions, and evolution. Int J Mol Sci. https://doi.org/10.3390/ijms21030966

Jumper J, Evans R, Pritzel A et al (2021) Highly accurate protein structure prediction with AlphaFold. Nature 596:583–589. https://doi.org/10.1038/s41586-021-03819-2

Kadouri D, Jurkevitch E, Okon Y, Castro-Sowinski S (2005) Ecological and agricultural significance of bacterial polyhydroxyalkanoates. Crit Rev Microbiol 31:55–67. https://doi.org/10.1080/10408410590899228

Kirienko AN, Vishnevskaya NA, Kitaeva AB et al (2019) Structural variations in LysM domains of LysM-RLK psK1 may result in a different effect on Pea-Rhizobial symbiosis development. Int J Mol Sci 20:1–20. https://doi.org/10.3390/ijms20071624

Ledermann R, Schulte CCM, Poole PS (2021) How rhizobia adapt to the nodule environment. J Bacteriol. https://doi.org/10.1128/JB.00539-20

Lehman AP, Long SR (2013) Exopolysaccharides from *Sinorhizobium meliloti* can protect against H2O2-dependent damage. J Bacteriol 195:5362–5369. https://doi.org/10.1128/JB.00681-13

Li L, Jia Y, Hou Q et al (2002) A global pH sensor: agrobacterium sensor protein ChvG regulates acid-inducible genes on its two chromosomes and Ti plasmid. Proc Natl Acad Sci U S A 99:12369–12374. https://doi.org/10.1073/pnas.192439499

Li Z, Ma Z, Hao X, Wei G (2012) Draft genome sequence of *Sinorhizobium meliloti* CCNWSX0020, a nitrogen-fixing symbiont with copper tolerance capability isolated from lead-zinc mine tailings. J Bacteriol 194:1267–1268. https://doi.org/10.1128/JB.06682-11

Lodwig EM, Leonard M, Marroqui S et al (2005) Role of polyhydroxybutyrate and glycogen as carbon storage compounds in pea and bean bacteroids. Mol Plant-Microbe Interact 18:67–74. https://doi.org/10.1094/MPMI-18-0067

Marizcurrena JJ, Morel MA, Braña V et al (2017) Searching for novel photolyases in UVC-resistant Antarctic bacteria. Extremophiles 21:409–418. https://doi.org/10.1007/s00792-016-0914-y

Martínez-Abarca F, Martínez-Rodríguez L, López-Contreras JA et al (2013) Complete genome sequence of the alfalfa symbiont *Sinorhizobium/Ensifer meliloti* strain GR4. Genome Announc 1:486–487. https://doi.org/10.1128/genomeA.00174-12

Morel MA, Braa V, Castro-Sowinski S (2012) Legume crops, importance and use of bacterial inoculation to increase production. Crop Plant. https://doi.org/10.5772/37413

Morel M, Castro-Sowinski S (2013) The complex molecular signalling network in microbe-plant interaction. In Plant microbe symbiosis: Fundamentals and Advances (Ed Arora NK). Springer New Delhi, pp 69–199

Mus F, Alleman AB, Pence N et al (2018) Exploring the alternatives of biological nitrogen fixation. Metallomics 10:523–538. https://doi.org/10.1039/c8mt00038g

Nelson M, Guhlin J, Epstein B et al (2018) The complete replicons of 16 *Ensifer meliloti* strains offer insights into intra- and inter-replicon gene transfer, transposon-associated loci, and repeat elements. Microb Genom. https://doi.org/10.1099/mgen.0.000174

Overbeek R, Begley T, Butler RM et al (2005) The subsystems approach to genome annotation and its use in the project to annotate 1000 genomes. Nucleic Acids Res 33:5691–5702. https://doi.org/10.1093/nar/gki866

Ozga DA, Lara JC, Leig JA (1994) The regulation of exopolysaccharide production is important at two levels of nodule development in *Rhizobium meliloti*. Mol Plant-Microbe Interact 7:758–765. https://doi.org/10.1094/MPMI-7-0758

Primo E, Bogino P, Cossovich S et al (2020) Exopolysaccharide II is relevant for the survival of *Sinorhizobium meliloti* under water deficiency and salinity stress. Molecules. https://doi.org/10.3390/molecules25214876

Reinhold BB, Chan SY, Reuber TL et al (1994) Detailed structural characterization of succinoglycan, the major exopolysaccharide of *Rhizobium meliloti* Rm1021. J Bacteriol 176:1997–2002. https://doi.org/10.1128/jb.176.7.1997-2002.1994

Rosconi F, Fraguas LF, Martínez-Drets G, Castro-Sowinski S (2005) Purification and characterization of a periplasmic laccase produced by *Sinorhizobium meliloti*. Enzyme Microb Technol 36:800–807. https://doi.org/10.1016/j.enzmictec.2005.01.003

Roumiantseva ML, Vladimirova ME, Saksaganskaia AS et al (2022) *Ensifer meliloti* L6-AK89, an effective inoculant of *Medicago*

lupulina varieties: phenotypic and deep-genome screening. Agronomy. https://doi.org/10.3390/agronomy12040766

Ruiz B, Le Scornet A, Sauviac L et al (2019) The nitrate assimilatory pathway in *Sinorhizobium meliloti*: contribution to NO production. Front Microbiol 10:1–12. https://doi.org/10.3389/fmicb.2019.01526

Saita EA, De Mendoza D (2015) Thermosensing via transmembrane protein–lipid interactions. Biochim Biophys Acta Biomembr 1848:1757–1764. https://doi.org/10.1016/j.bbamem.2015.04.005

Sambrook (1989) Cloning techniques molecular cloning: a laboratory manual T. Maniatis E R Pritsch J Sambrook. Bioscience 33:721–722. https://doi.org/10.2307/1309366

Schorr B (2019) Extractivism in Latin America: the global-national-local link. Lat Am Res Rev 54:509–516. https://doi.org/10.25222/larr.392

Shin SH, Lim Y, Lee SE et al (2001) CAS agar diffusion assay for the measurement of siderophores in biological fluids. J Microbiol Methods 44:89–95. https://doi.org/10.1016/S0167-7012(00)00229-3

Tabares-da Rosa S, Signorelli S, Del Papa MF et al (2019) Rhizobium inoculants for alfalfa in acid soils: a proposal for Uruguay. Agrociencia 23:1–13. https://doi.org/10.31285/agro.23.120

Vanderlinde EM, Yost CK (2012) Mutation of the sensor kinase chvG in *Rhizobium leguminosarum* negatively impacts cellular metabolism, outer membrane stability, and symbiosis. J Bacteriol 194:768–777. https://doi.org/10.1128/JB.06357-11

Wang C, Saldanha M, Sheng X et al (2007) Roles of poly-3-hydroxybutyrate (PHB) and glycogen in symbiosis of *Sinorhizobium meliloti* with Medicago sp. Microbiology 153:388–398. https://doi.org/10.1099/mic.0.29214-0

Wang C, Kemp J, Da Fonseca IO et al (2010) *Sinorhizobium meliloti* 1021 loss-of-function deletion mutation in chvl and its *phenotypic* characteristics. Mol Plant-Microbe Interact 23:153–160. https://doi.org/10.1094/MPMI-23-2-0153

Wheatley RM, Ford BL, Li L et al (2020) Lifestyle adaptations of *Rhizobium* from rhizosphere to symbiosis. Proc Natl Acad Sci U S A 117:23823–23834. https://doi.org/10.1073/pnas.2009094117

Williams MA, Bouchier JM, Mason AK, Brown PJB (2022) Activation of ChvG-ChvI regulon by cell wall stress confers resistance to β-lactam antibiotics and initiates surface spreading in *Agrobacterium tumefaciens*. PLoS Genet 18:1–27. https://doi.org/10.1371/journal.pgen.1010274

Wongdee J, Piromyou P, Songwattana P et al (2023) Role of two RpoN in *Bradyrhizobium* sp. strain DOA9 in symbiosis and free-living growth. Front Microbiol. https://doi.org/10.3389/fmicb.2023.1131860

Yurgel SN, Kahn ML (2004) Dicarboxylate transport by rhizobia. FEMS Microbiol Rev 28:489–501. https://doi.org/10.1016/j.femsre.2004.04.002

Zerbino DR, Birney E (2008) Velvet: algorithms for de novo short read assembly using de Bruijn graphs. Genome Res 18:821–829. https://doi.org/10.1101/gr.074492.107

2.3. Expresión y producción recombinante de laccasas bacterianas

2.3.1. Materiales y Métodos

2.3.1.1. Identificación preliminar de las cepas bacterianas con potencial actividad laccasa

Para la detección preliminar de microorganismos con actividad laccasa, se cultivaron cinco cepas de nuestra colección: *Pseudomonas* sp. AU10, *Pseudomonas* sp. UV5, UV4 y AU13, y *Sinorhizobium meliloti* CE52G, a partir de stocks conservados en glicerol almacenados en freezer a -80 °C. La siembra se realizó por estrías sobre placas de medio TSA suplementado con 0,01 % de 2,6-dimetoxifenol (DMP; Sigma-Aldrich #D135550) y 30 µg ml^{-1} de $CuSO_4$. Las placas sembradas se incubaron a 30 °C durante un período de entre 24 y 72 horas dependiendo de cada cepa evaluada. Una vez que se constató crecimiento, se monitoreó visualmente a diario el crecimiento hasta observar algún cambio de coloración en las colonias. Este ensayo permite visualizar cualitativamente la actividad laccasa mediante la oxidación del DMP. Esta oxidación en el medio de cultivo genera un producto coloreado de tonalidad naranja o marrón ladrillo alrededor de las colonias bacterianas. La aparición de coloración se interpreta como un indicador indirecto de la presencia de enzimas oxidativas del tipo laccasa, capaces de transformar dicho sustrato fenólico [47].

2.3.1.2. Análisis in silico de los genes codificantes de laccasas en CE52G y AU10

Como se describió en la sección anterior, se identificó en el genoma de *Sinorhizobium meliloti* CE52G una secuencia génica (de ahora en más denominada *lacc-ce52g*) anotada en el servidor RAST, con una función probablemente asociada a una enzima laccasa. Del mismo modo, se identificó una secuencia génica (de ahora en más denominada *lacc-au10)* en el genoma de *Pseudomonas* sp. AU10 (con el que ya contábamos). A partir de las secuencias de aminoácidos codificadas por estas potenciales laccasas (en adelante denominada LACC-CE52G y LACC-AU10, respectivamente), se realizó una caracterización *in silico* con el objetivo de acercarnos a su identidad funcional, y obtener información relevante para el diseño de una estrategia destinada a su producción recombinante.

Para este análisis se utilizaron distintas herramientas bioinformáticas disponibles en línea. El tamaño molecular teórico y el punto isoeléctrico de las enzimas se calcularon utilizando la herramienta Compute pI/Mw y ProtParam, disponibles en el sitio web ExPASy: https://web.expasy.org/compute_pi/ y https://web.expasy.org/protparam/ [48–50]. Su posible localización subcelular se determinó con la herramientas pSORTb 3.0 (www.psort.org/psortb [51]. La presencia de péptidos señal se evaluó utilizando SignalP 4.1 (https://services.healthtech.dtu.dk/service.php?SignalP-5.0 [52, 53]. La búsqueda de posibles dominios conservados en la secuencia de aminoácidos se llevó a cabo mediante la herramienta ScanProsite (https://prosite.expasy.org/scanprosite/) de ExPASy [54], utilizada para detectar motivos funcionales y patrones conservados en proteínas; así como mediante las bases de datos de familias y dominios proteicos de la base de datos Pfam (https://www.ebi.ac.uk/jdispatcher/pfa/pfamscan), empleada para identificar dominios y familias proteicas mediante modelos ocultos de Markov (HMM) [55], e InterPro (https://www.ebi.ac.uk/interpro/search/sequence/), que integra múltiples bases de datos para ofrecer una visión global de los dominios funcionales, familias proteicas y sitios activos presentes en las secuencias analizadas [56]. El estado de oxidación de los residuos de cisteína se evaluó utilizando la herramienta bioinformática DISULFIND (http://disulfind.dsi.unifi.it/). La secuencia aminoacídica se analizó con el objetivo de identificar cisteínas potencialmente oxidadas, con el fin de predecir la formación de enlaces disulfuro en la proteína [57]. Finalmente, las regiones potencialmente propensas a agregación proteica (*hotspots*) se predijeron utilizando la herramienta Aggrescan (http://bioinf.uab.es/agrescan/; [58].

2.3.1.3. Diseño de vectores de expresión para la producción recombinante de LACC-CE52G

Con base en el análisis *in silico* de la secuencia aminoacídica de LACC-CE52G, se diseñaron tres estrategias de clonación en diferentes vectores de expresión para su producción recombinante. En la primera estrategia se utilizó el vector de expresión pET32a(+), que incluye una etiqueta de histidinas (His-tag) para la purificación de la proteína, una fusión con tiorredoxina (TrxA) para favorecer el correcto plegado, y un sitio de corte para la proteasa TEV. En la segunda estrategia se empleó el vector pMAL-C5E, que fusiona la enzima con la proteína de unión a maltosa (MBP), con el propósito de mejorar la solubilidad y el plegado de la proteína, y un sitio de corte para la enzima enteroquinasa. En la tercera estrategia se utilizó el vector pET28a(+), que incorpora únicamente una etiqueta His-tag y un sitio de corte para trombina. En todos los casos, se eliminó el péptido señal previamente identificado,

conservándose únicamente la secuencia codificante de la enzima. La secuencia génica *lacc-ce52g* fue sintetizada para su expresión en *Escherichia coli* (optimizándose el uso de codones), y clonada en los vectores de expresión mencionados anteriormente. Tanto la síntesis como la clonación del gen fueron realizadas mediante el servicio de GenScript (https://www.genscript.com/, USA).

2.3.1.4. Expresión recombinante de la enzima rLACC-CE52G

Con los vectores de expresión mencionados, se transformaron células de *E. coli* DH5α (para la multiplicación de los plásmidos, [59]) y BL21(DE3), Arctic Express (DE3) y BL21(pLys) para la expresión de la proteína recombinante. Se prepararon células quimicompetentes [59] para cada cepa, y se transformaron mediante shock térmico con cada vector de expresión por separado. Para la obtención de clones transformantes se cultivaron las células transformadas en caldo Luria-Bertani (LB) suplementado con 50 µg mL^{-1} kanamicina o 100 µg mL^{-1} de ampicilina, según correspondía, para mantener la selección del plásmido. A partir de los clones obtenidos, se realizaron pre-cultivos en caldo LB de 5 ml también suplementado con el antibiótico correspondiente, y se incubaron a 37 °C y 200 rpm por 24 h. Se realizó un control de pureza del cultivo en medio LB sólido sin antibióticos previo al ensayo de expresión. Para la expresión recombinante de las enzimas, se inocularon tres matraces de 2 L conteniendo 200 ml de medio autoinductor Zym-5052 (Triptona 10 g, extracto de levadura 5 g, glucosa 0,5 g, lactosa 0,2 g, $MgCl_2$ 2 mM, Na_2HPO_4 0,45 g, NaH_2PO_4 0,34 g, NH_4CL 0,27 g, Na_2SO_4 0,07, $CaCl_2$ 20 µM, $MnCl_2$ 10 µM, $ZnSO_4$ 10 µM, $CoCl_2$ 2 µM, $CuCl_2$ 2 µM, $NiCl_2$ 2 µM, Na_2MoO_4 2 µM, H_3BO_3 2 µM, y agua csp 1 L) [60], con 2 mL de pre-cultivo y suplementado con el antibiótico que corresponda según el vector. El medio autoinductor Zym-5052, es un medio de cultivo líquido, que regula la expresión génica mediante el promotor *lac*, sin necesidad de añadir IPTG, optimizando la producción de proteínas en cultivos de alta densidad. Los matraces inoculados se incubaron durante 3 h a 37 °C y 200 rpm, hasta alcanzar una DO a 600 nm de aproximadamente 0,3 UA. Posteriormente, los matraces se incubaron a 200 rpm y 14 °C (durante 60 h) o a 37 °C (durante 24 h).

2.3.1.5. Cosecha celular y clarificación

La cosecha celular se realizó por centrifugación de los cultivos durante 10 minutos a 6000 × g y 4 °C. Posteriormente, se llevó a cabo la suspensión de las células en tampón fosfato de sodio 50 mM suplementado con 50 mM de NaCl (pH 7,4), y lisis celular mediante sonicación para liberar el contenido

intracelular. El programa de sonicación empleado consistió en ciclos de 10 minutos a una amplitud de 40 %, con tres repeticiones y descansos de 2 minutos entre cada ciclo. Para verificar el grado de lisis, se midió el cambio en la DO a 600 nm, continuando el proceso hasta alcanzar al menos un 70 % de células lisadas. Se guardó una alícuota del extracto obtenido denominado extracto total (ET).

Tras la lisis, se realizó la clarificación del ET para eliminar restos celulares y células no lisadas, mediante centrifugación a 6000 × g durante 10 minutos a 4 °C. El sobrenadante obtenido se sometió posteriormente a una centrifugación a 20.000 × g durante 30 minutos a 4 °C, con el fin de separar las fracciones soluble (FS) e insoluble (FI, correspondiente a los cuerpos de inclusión). Todas las fracciones se analizaron mediante electroforesis desnaturalizante (SDS-PAGE), empleando un gel discontinuo de poliacrilamida (gel separador al 12 % y gel concentrador al 5 %). Las muestras se mezclaron con tampón de carga [61] y se desnaturalizaron a 95 °C durante 5 min antes de la carga. La electroforesis se realizó a 120 V durante aproximadamente 90 min. Los geles se tiñeron con Azul de Coomassie Brilliant Blue R-250 (CBB R-250) durante 1 h y se destiñeron en una solución de etanol:agua:ácido acético (50:40:10).

2.3.1.6. Solubilización de los cuerpos de inclusión y replegamiento de rLACC-CE52G

El pellet de cuerpos de inclusión se suspendió en tampón fosfato de sodio 50 mM, NaCl 50 mM, a pH 8, suplementado con urea en concentraciones de 2, 4, 6 y 8 M, en una relación de 10 mL de tampón por gramo de pellet. Las suspensiones se incubaron durante 1 h a 4 °C, bajo agitación suave. Tras la incubación, se centrifugaron a 12.000 × g durante 15 min a 4 °C para separar las fracciones solubles e insolubles [59, 62].

La eficacia de solubilización de los cuerpos de inclusión se evaluó mediante SDS-PAGE, empleando un gel discontinuo. Las muestras se prepararon y sembraron en el gel de la misma forma que se describió anteriormente [61].

Para el replegamiento, las fracciones solubilizadas se sometieron a un procedimiento de disminución progresiva de la concentración de urea mediante dilución paso a paso, utilizando un tampón MES 50 mM, NaCl 50 mM, a pH 7, suplementado con 0,16 mM de $CuSO_4$, manteniéndose la mezcla en hielo [62]. La eficiencia del replegamiento se evaluó a través del porcentaje de solubilización (Ecuación 1) y

el porcentaje de replegamiento (Ecuación 2), calculados luego del tratamiento con urea y su posterior dilución. Para ello, se determinó la concentración proteica en las fracciones solubles (FS) e insolubles (CI) mediante el método de Bradford.

$$\%\ de\ proteína\ soluble = (\frac{proteína\ en\ fracción\ soluble}{proteína\ total\ en\ CI\ inicial})x100 \quad \text{(Ec. 1)}$$

$$\%\ de\ replegamiento = \left(\frac{U\ totales\ de\ enzima\ replegada}{Cantidad\ total\ de\ proteína\ soluble\ antes\ del\ replegamiento\ x\ actividad\ específica\ teórica}\right) x\ 100 \quad \text{(Ec. 2)}$$

La actividad enzimática de la rLACC-CE52G se determinó empleando dos sustratos habituales de las laccasas, tales como ABTS y siringaldazina, según se describe a continuación.

Para el ensayo de actividad laccasa con ABTS como sustrato, se utilizó una solución de ABTS 1 mM preparada en tampón MES 0,1 M, pH 5. La reacción se inició añadiendo 50 µL de la enzima replegada a 950 µL de sustrato, obteniendo un volumen final de 1 mL. La reacción se incubó a 25 °C y se monitoreó el aumento de absorbancia a 420 nm durante 3 min en un espectrofotómetro UV-Vis. Se utilizó un coeficiente de extinción molar de 36.000 $M^{-1}{\cdot}cm^{-1}$ para el cálculo de la actividad enzimática. Una unidad de actividad se definió como la cantidad de enzima que oxida 1 µmol de ABTS por minuto bajo las condiciones del ensayo [37].

Para el ensayo con siringaldazina como sustrato, se empleó una solución de siringaldazina 70 µM preparada en etanol absoluto y posteriormente diluida en tampón MES 0,1 M, pH 5, para obtener una concentración final de etanol en la mezcla de reacción menor al 5 % (v/v). Se mezclaron 50 µL de enzima con 950 µL de sustrato, y se monitoreó el producto de oxidación de la siringaldazina como el incremento de la absorbancia a 525 nm durante 3 min. Se utilizó un coeficiente de extinción molar de 65.000 $M^{-1}{\cdot}cm^{-1}$. Una unidad de actividad se definió como la cantidad de enzima que oxida 1 µmol de siringaldazina por minuto [45].

Los ensayos se realizaron por triplicado y se incluyeron blancos sin enzima, para descartar la oxidación no enzimática de los sustratos.

2.3.1.7. Expresión recombinante de LACC-CE52G bajo condiciones microaeróbicas y suplementación con cobre

Se prepararon pre-cultivos de 5 mL utilizando clones de *E. coli* BL21(DE3) y Arctic Express transformados con el vector de expresión pET28(a)+, portador del gen lacc-CE52G. Estos pre-cultivos se inocularon en 200 mL de medio autoinductor Zym-5052, suplementado con ampicilina (100 µg ml^{-1}) y $CuSO_4$ (2 mM), en matraces de 2 L. La incubación inicial se realizó a 18 °C y 200 rpm durante 4 h. A continuación, se continuó la incubación a 18 °C y 80 rpm durante 60 h, con el objetivo de generar condiciones microaeróbicas [63] las cuales han demostrado favorecer la acumulación intracelular de cobre en *E. coli*.

Las células se recolectaron mediante centrifugación a 6.000 × g durante 10 min a 4 °C y se suspendieron en tampón de unión (Tris-HCl 20 mM, NaCl 300 mM, imidazol 40 mM, pH 7,4). La lisis celular se efectuó por sonicación. El extracto total (ET) obtenido se clarificó por centrifugación a 20.000 × g durante 30 min a 4 °C, con el fin de separar las fracciones soluble e insoluble. La expresión de la proteína recombinante rLACC-CE52G se verificó mediante análisis por SDS-PAGE.

La purificación de rLACC-AU10 se realizó por IMAC a partir de la fracción soluble utilizando una matriz Ni-NTA, dado que la proteína posee una cola de histidinas (Hisx6). Para ello, se mezclaron 10 mL de la fracción soluble (FS) con 1 mL de resina (Thermo Scientific™ Resina de Ni-NTA HisPur™, Cat. No. 88221), previamente equilibrada en tampón de unión, y se incubó la mezcla durante 1 h a 4 °C bajo agitación suave para asegurar un contacto adecuado entre la proteína y la matriz. Tras dejar decantar la resina en una columna de purificación y escurrir el tampón de unión, la matriz se lavó con cinco volúmenes de tampón de unión para eliminar proteínas no específicas. Finalmente, la proteína de interés se eluyó utilizando tampón de elución (Tris-HCl 20 mM, NaCl 0,3 M, imidazol 150 mM, pH 7,4). La purificación de la proteína de interés se control mediante SDS-PAGE. La actividad enzimática de la enzima purificada se determinó empleando los sustratos y metodología anteriormente mencionada.

2.3.1.8. Expresión recombinante de la enzima rLACC-AU10

La expresión de rLACC-AU10 se realizó siguiendo una estrategia similar a la utilizada para la producción de rLACC-CE52G. Se emplearon las cepas *E. coli* BL21(DE3) y Arctic Express(DE3), transformadas con el

vector pMAL-CE5e que porta el gen codificante para la laccasa de *Pseudomonas* sp. AU10 (lacc-AU10). Las células se pre-cultivaron en medio LB suplementado con ampicilina (100 µg mL^{-1}), a 37 °C, 200 rpm por 24 h. Se transfirieron 2 mL de pre-cultivo a 200 mL de medio autoinductor Zym-5052 suplementado con ampicilina 100 µg mL^{-1} en matraces de 2 L y se incubaron a 37 °C y 200 rpm hasta alcanzar una DO_{600} de aproximadamente 0,3 UA. Posteriormente, se suplementó con $CuSO_4$ 2 mM y se continuó la incubación a 200 rpm bajo dos condiciones: a 37 °C durante 24 h, o a 14 °C durante 60 h, con el objetivo de optimizar la expresión soluble de la proteína.

Las células se cosecharon por centrifugación a 6.000 × g durante 10 min a 4 °C, y suspendieron en tampón de unión (Tris-HCl 20 mM, NaCl 300 mM y EDTA 1 mM, pH 7,4), para luego proceder a la lisis celular por sonicación. El extracto total (ET) obtenido se clarificó por centrifugación a 20.000 × g durante 30 min a 4 °C, para separar las fracciones soluble e insoluble. La expresión de rLACC-AU10 se verificó mediante análisis por SDS-PAGE.

2.3.1.9. Purificación de rLACC-AU10 mediante cromatografía de afinidad

La purificación de rLACC-AU10 se realizó a partir de la fracción soluble utilizando cromatografía de afinidad en matriz de amilosa, dado que la proteína de interés se fusiona a la proteína de unión a maltosa (MBP, maltose-binding protein). Para ello, se mezclaron 10 mL de la fracción soluble (FS) con 1 mL de resina de amilosa (NEB, Cat. No. E8021S) y se incubó la mezcla durante 1 h a 4 °C bajo agitación suave para asegurar un contacto adecuado entre la proteína y la matriz. Tras dejar decantar la resina en una columna de purificación y escurrir el tampón de unión, la matriz se lavó con cinco volúmenes de tampón de unión para eliminar proteínas unidas de forma no específicas. Finalmente, la proteína de interés se eluyó utilizando un tampón de elución que contiene maltosa (Tris-HCl 20 mM, NaCl 0,2 M, EDTA 1 mM, maltosa 10 mM, a pH 7,4). La expresión de la proteína de interés se control mediante SDS-PAGE.

La actividad enzimática de la rLACC-AU10 se determinó empleando dos sustratos habituales de las laccasas, ABTS y siringaldazina, como se describió para rLACC-CE52G.

2.3.2. Resultados

2.3.2.1. Identificación preliminar de las cepas bacterianas con potencial actividad laccasa

Tres de las cepas bacterianas analizadas mostraron capacidad para oxidar DMP, lo que sugiere la producción de enzimas con actividad laccasa. Esta actividad se evidenció por la aparición de una coloración naranja a marrón ladrillo en el medio de cultivo alrededor de las colonias, resultado de la oxidación del sustrato fenólico. La intensidad y extensión de la coloración variaron ligeramente entre las cepas, pero en todos los casos fue claramente visible, confirmando su potencial actividad oxidativa. Estos resultados se muestran en la Figura 2. A partir de estos resultados se decidió avanzar en la identificación y producción recombinante de las posibles laccasas de las cepas CE52G y AU10. Para ello, se emplearon las secuencias genómicas disponibles: en el caso de CE52G, el genoma se secuenció en el marco de esta tesis, identificándose un gen candidato a laccasa; mientras que para AU10 se utilizó el genoma previamente secuenciado y anotado por otro integrante del equipo, del cual se seleccionó una secuencia codificante identificada como una cobre-oxidasa, considerada un gen potencial para una laccasa.

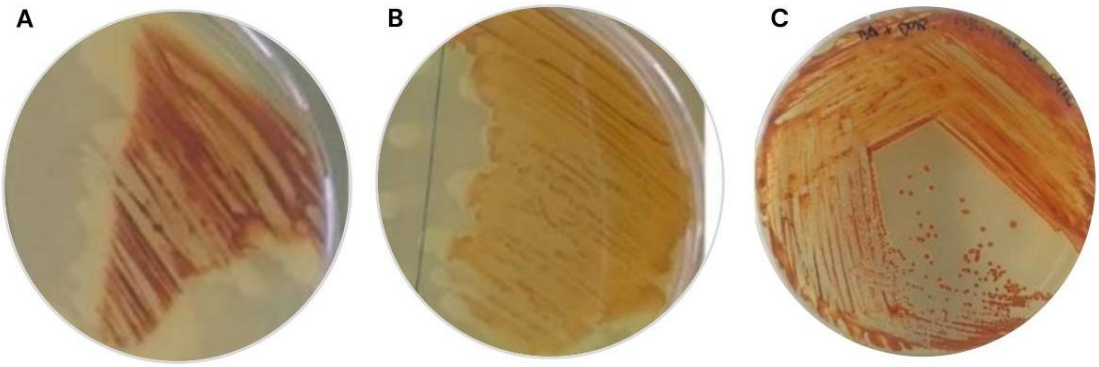

Figura 2. Ensayo preliminar de detección de actividad laccasa en cepas bacterianas cultivadas en medio TSA sólido suplementado con DMP. Se observa la coloración naranja ladrillo característica de la oxidación de DMP en **(A)** *Pseudomonas* sp. UV5, **(B)** *Pseudomonas* sp. AU10 y **(C)** *Sinorhizobium meliloti* CE52G, indicando actividad oxidativa asociada a laccasas.

2.3.2.2. Caracterización y producción de la laccasa producida *por Sinorhizobium meliloti* CE52G

2.3.2.2.1. Caracterización in silico de LACC-CE52G

Se realizó una caracterización *in silico* de la secuencia codificante para la laccasa de interés, con el objetivo de predecir propiedades relevantes de esta familia enzimática y orientar estrategias para su expresión recombinante.

En el genoma de *S. meliloti* CE52G se identificó una secuencia codificante para una laccasa, con un 99–100 % de identidad respecto a oxidasas multicúpricas de otras cepas del género *Sinorhizobium*. La secuencia aminoacídica correspondiente, compuesta por 649 residuos, fue analizada con la herramienta ProtParam (ExPASy), obteniéndose un tamaño molecular teórico de 70.409,20 Da y un punto isoeléctrico (pI) de 5,64.

El análisis mediante SignalP-5.0 predijo la presencia de una señal peptídica del tipo Sec/SPI (Secretory pathway/Signal Peptidase I) con alta probabilidad (0.9705), localizando un sitio potencial de corte entre los aminoácidos 26 y 27 (secuencia AVA-QE), con una probabilidad de 0.7839. Las probabilidades para otros tipos de señales peptídicas fueron considerablemente menores, lo que indica una clara preferencia por la vía Sec (secreción de proteínas vía retículo endoplasmático). De manera complementaria, PSORTb predijo su localización subcelular como periplásmica, con una puntuación de 9.76, valor considerado de alta confianza. Las puntuaciones obtenidas para otras localizaciones fueron notablemente inferiores (0.00 para citoplasmática, 0.06 para membranas citoplasmática y externa, y 0.11 para extracelular), sustentando la hipótesis de una localización periplásmica en su organismo nativo, según había informado anteriormente nuestro equipo [44].

El análisis de motivos conservados mediante Prosite reveló la presencia de dos secuencias características de sitios de unión a cobre: el motivo PS00079 (Copper-binding site signature 1) localizado entre los aminoácidos 613 y 633, y el motivo PS00080 (Copper-binding site signature 2) entre las posiciones 618 y 629, ambos fundamentales para la actividad catalítica de las multicobre oxidasas.

El análisis con la base de datos Pfam, identificó tres dominios conservados propios de enzimas multicúpricas: dos dominios Cu-oxidase_3 (PF07732.21), ubicados entre los residuos 106–136 y 149–221, y un dominio Cu-oxidase_2 (PF07731.20) entre los aminoácidos 494–634. Todos estos dominios pertenecen al clan CL0026, característico de proteínas multicobre oxidasas, lo cual coincide plenamente con los resultados de InterPro.

Por su parte, InterPro clasificó a la proteína dentro de la familia Multicopper oxidase (IPR045087), confirmando su identidad funcional y destacando la presencia de dominios específicos y residuos conservados relacionados con sitios de unión a iones cobre, esenciales para la función enzimática de las laccasas.

Se analizaron los residuos de cisteína presentes en la secuencia de la proteína con el objetivo de predecir la probabilidad de formación de puentes disulfuro, mediante la estimación de su estado de oxidación. En total se identificó siete cisteínas, de las cuales cinco fueron clasificadas como potencialmente oxidadas y, por tanto, candidatas a participar en enlaces disulfuro. Entre ellas, los residuos CYS 135, CYS 147 y CYS 356 mostraron una alta confiabilidad (≥8), lo que respalda de manera sólida su posible implicancia estructural en la formación de dichos enlaces. En contraste, las predicciones correspondientes a CYS 269 y CYS 403 presentaron una confiabilidad nula, por lo que sus resultados deben interpretarse con precaución. Por otra parte, las cisteínas CYS 258 y CYS 619 fueron clasificadas como no oxidadas, con niveles de confiabilidad moderada y alta, respectivamente, lo que sugiere que podrían permanecer en estado reducido en la conformación nativa de la proteína.

Finalmente, el análisis con Aggrescan indicó que la laccasa CE52G presenta una baja tendencia global a la agregación (a3vSA = -0.069; Na4vSS = -7.1). No obstante, se identificaron 20 regiones específicas (*hot spots*) potencialmente susceptibles de agregación, lo que sugiere que, aunque la proteína es en general soluble, podrían existir zonas localizadas que afecten su solubilidad o correcto plegado durante su producción recombinante.

2.3.2.2.2. Producción recombinante de la laccasa (rLACC-CE52G) de S. meliloti CE52G, en condiciones de aerobiosis

A partir del análisis *in silico* de la secuencia aminoacídica de LACC-CE52G, se diseñaron tres estrategias de clonación en distintos vectores de expresión, con el objetivo de optimizar su producción recombinante en *Escherichia coli*. Para ello, se tuvieron en cuenta: distintas estrategias de purificación, la posibilidad de formación de puentes disulfuro, así como la propensión local a la agregación proteica, aspectos clave para garantizar la correcta solubilidad, plegado y funcionalidad de la enzima. En la Figura 3 se muestran los esquemas de los vectores de expresión diseñados.

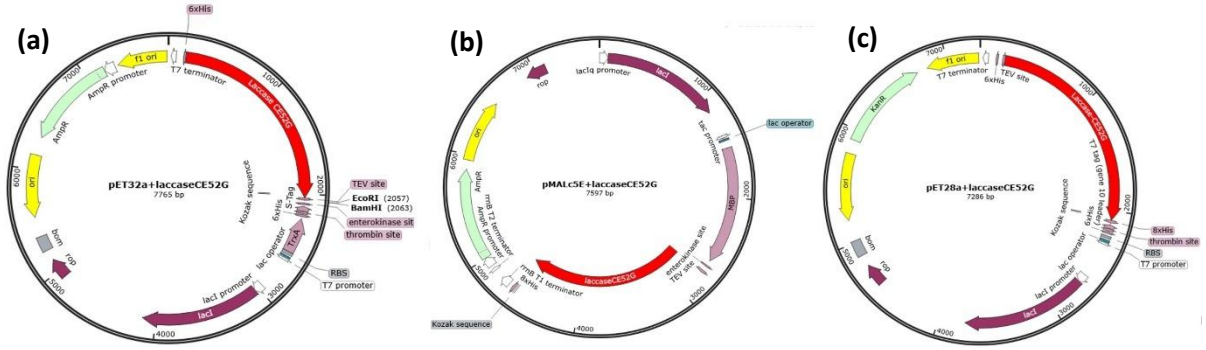

Figura 3. Mapas esquemáticos de los vectores de expresión diseñados para la producción recombinante de LACC-CE52G en *Escherichia coli*. (a) Vector pET32a(+), que incluye una fusión a TrxA y una etiqueta His-tag para la purificación de la proteína, junto con sitios de corte para TEV y trombina. (b) Vector pMAL-C5E, que fusiona LACC-CE52G a la proteína MBP para mejorar su solubilidad, y contiene sitios de corte para enteroquinasa y TEV. (c) Vector pET28a(+), que incorpora únicamente una etiqueta His-tag y sitios de corte para trombina y TEV. En todos los casos, la secuencia codificante de la laccasa se insertó sin el péptido señal, y se optimizó para su expresión en *E. coli*. Diseños elaborados con el software SnapGene 8.1.1 (Insightful Science).

La secuencia génica *lacc-CE52G* fue sintetizada y optimizada mediante el servicio GenSmart de GenScript, considerando el uso preferencial de codones en *Escherichia coli*, la reducción del contenido de GC del 60,3 % al 56,44 %, y la eliminación de sitios de restricción indeseados. Esta optimización buscó maximizar la eficiencia de expresión, reducir la formación de estructuras secundarias en el ARNm y evitar motivos desestabilizantes, contribuyendo así a la correcta producción recombinante de la enzima en las cepas seleccionadas.

Tras la transformación de células quimicompetentes de las cepas de expresión seleccionadas, se llevó a cabo el protocolo de expresión descripto en la sección Materiales y Métodos, obteniéndose cultivos correspondientes a las tres estrategias de expresión planteadas.

La expresión de rLACC-CE52G se analizó mediante SDS-PAGE de las fracciones obtenidas tras la producción recombinante con cada uno de los tres vectores de expresión utilizados, cultivados a 37 ^{o}C y realizando la expresión a dos temperaturas (14 y 37 ^{o}C), según se describe en Materiales y Métodos. En todos los ensayos, se observó una banda proteica intensa en la fracción insoluble (FI), con pesos moleculares aproximados de ~67 kDa, ~87 kDa y ~112 kDa, correspondientes a la proteína recombinante sin fusión y a las versiones fusionadas con TrxA y MBP, respectivamente. Estos resultados indican que la enzima se expresó principalmente en forma de cuerpos de inclusión (Figura

4).

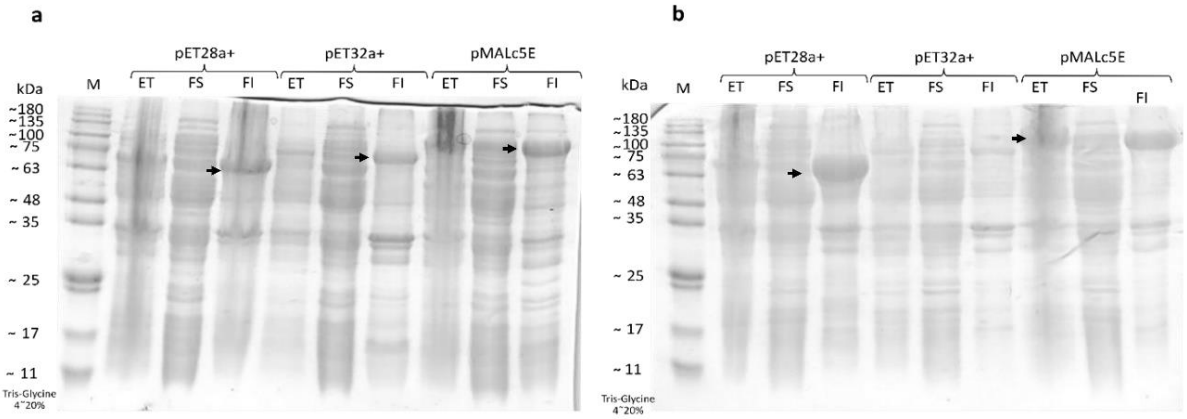

Figura 4. Análisis por SDS-PAGE de la expresión recombinante de rLACC-CE52G en *Escherichia coli* BL21(DE3) utilizando distintos vectores de expresión. (a) Cultivos incubados a 14 °C durante 60 h. **(b)** Cultivos incubados a 37 °C durante 24 h. Se muestran las fracciones de extracto total **(ET),** fracción soluble **(FS)** y fracción insoluble **(FI)** para cada constructo: pET28a(+), pET32a(+) y pMAL-c5E. Las flechas indican las bandas correspondientes a la proteína recombinante, con pesos moleculares aproximados de ∼67 kDa para la enzima sin fusión (pET28a(+)), ∼87 kDa para la fusión con TrxA (pET32a(+)) y ∼112 kDa para la fusión con MBP (pMAL-c5E). Como marcador de tamaño molecular **(M)** se utilizó PageRuler™ Prestained Protein Ladder (Thermo Scientific™, Cat. No. 26616).

Para solubilizar los cuerpos de inclusión, el pellet insoluble se trató con soluciones de urea en concentraciones crecientes (2, 4, 6 y 8 M). El análisis por SDS-PAGE mostró que la rLACC-CE52G comenzó a solubilizarse a partir de 2 M de urea, aunque en baja cantidad, observándose bandas de menor intensidad en comparación con las fracciones insolubles. A concentraciones mayores de urea se observó un incremento de la cantidad de proteína solubilizada, si bien parte de la proteína permaneció en la fracción insoluble, evidenciando una solubilización incompleta (Figura 5).

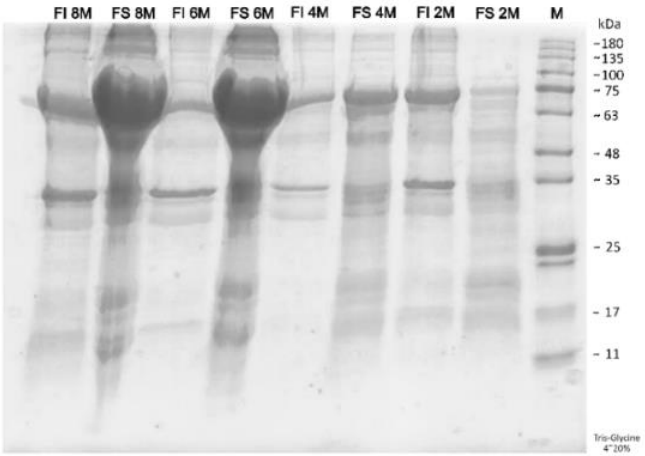

Figura 5. Solubilización de los cuerpos de inclusión de la expresión a 37 °C; cuerpos de inclusión obtenidos a partir del uso del vector pET28a+. SDS-PAGE de las fracciones insoluble (**FI**) o soluble (**FS**) obtenidas tras la solubilización de los cuerpos de inclusión en tampón fosfato de sodio 50 mM, NaCl 50 mM, a pH 8 y concentraciones decrecientes de urea (8, 6, 4 y 2 M), a temperatura ambiente con agitación a 150 rpm. Como marcador de tamaño molecular (**M**) se utilizó PageRuler™ Prestained Protein Ladder (Thermo Scientific™, Cat. No. 26616).

Las fracciones solubles obtenidas se replegaron mediante una dilución gradual de urea en presencia de 0,16 mM de $CuSO_4$. El porcentaje de solubilización se estimó a partir de la cuantificación proteica de las fracciones tratadas, obteniéndose valores de aproximadamente 1 % para 2 M, 8 % para 4 M, 60 % para 6 M y 65 % para 8 M de urea. Sin embargo, a pesar de haber obtenido buenos porcentajes de solubilización para las muestras tratadas con 6 y 8 M de urea, ninguna de las fracciones mostró actividad enzimática detectable frente a los sustratos modelo ABTS ni siringaldazina, lo que indicaría un replegamiento incorrecto o nulo. Estos resultados sugieren que, si bien la proteína fue solubilizada, la rLACC-CE52G no adquirió una conformación catalíticamente activa tras el proceso de replegamiento. Cabe destacar que la intensidad de las bandas correspondientes a las fracciones insolubles (FI) puede no ser proporcional a la concentración proteica real, debido a dificultades en la suspensión y carga homogénea de los pellets (CI).

2.3.2.2.3. Expresión recombinante de la laccasa (rLACC-CE52G) de S. meliloti CE52G, bajo condiciones microaeróbicas

La expresión recombinante de la enzima rLACC-CE52G se evaluó también en condiciones microaeróbicas y suplementación con cobre. El análisis por SDS-PAGE luego de la cosecha, lisis celular y clarificación, reveló una banda intensa en la fracción soluble (FS), con una migración cercana a ~67 kDa (indicada con una flecha), correspondiente al tamaño molecular teórico de la proteína recombinante fusionada a la etiqueta Hisx6 (Figura 6). Tras la purificación mediante cromatografía de

afinidad a partir de la fracción soluble, se observó una disminución progresiva de proteínas contaminantes en las fracciones de elución (E1–E6). Las fracciones E2 y E3 presentaron una banda dominante en torno a ~67 kDa, correspondiente a rLACC-CE52G, mientras que su intensidad disminuyó notablemente en E4–E6, lo que indica que la mayor parte de la proteína fue recuperada en las primeras eluciones. No obstante, tanto el percolado (flow through; FT), como la fracción de lavado (W) mostraron la presencia de la banda de interés, lo que sugiere una retención parcial en la matriz y posibles pérdidas de proteína durante la etapa de lavado (Figura 6).

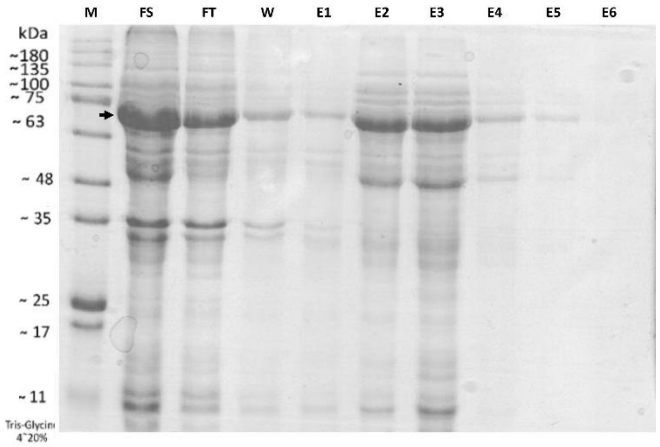

Figura 6. Análisis por SDS-PAGE de la expresión recombinante de rLACC-CE52G (vector pET28(a)+) en *Escherichia coli* BL21(DE3) bajo condiciones microaeróbicas. Se muestran las siguientes fracciones: fracción soluble (**FS**), percolado (**FT**), lavado (**W**) y fracciones de elución **E1–E6**. La flecha indica la banda correspondiente a la proteína recombinante rLACC-CE52G, con un peso molecular estimado de ~67 kDa. Como marcador de tamaño molecular (**M**) se utilizó PageRuler™ Prestained Protein Ladder (Thermo Scientific™, Cat. No. 26616).

La fracción purificada no mostró actividad enzimática detectable frente a los sustratos modelo ABTS ni siringaldazina.

2.3.2.3. Caracterización y producción de la potencial laccasa producida por *Pseudomonas* sp. AU10

Con el objetivo de producir una laccasa recombinante alternativa, se seleccionó del genoma de *Pseudomonas* sp. AU10 (ya secuenciado), un gen que identificamos y clasificamos como una cobre-oxidasa.

2.3.2.3.1. Caracterización in silico de la laccasa de Pseudomonas sp. AU10

El análisis *in silico* de la secuencia aminoacídica de LACC-AU10 (número de acceso: JAIUXL000000000) reveló que la proteína tiene una longitud de 458 aminoácidos e indicó la presencia de un péptido señal de tipo Sec/SPI de 38 residuos, con un sitio de corte predicho entre las posiciones 38 y 39. Al igual que en el caso de la expresión de LACC-CE52G, se eliminó el péptido señal para probar la expresión recombinante de la proteína en forma citoplasmática. La proteína madura, sin péptido señal, presenta un tamaño molecular teórico de 47 kDa.

2.3.2.3.2. Expresión recombinante de la potencial laccasa (rLACC-AU10) producida por Pseudomonas sp. AU10

Dado que en experiencias anteriores la laccasa de CE52G se expresó principalmente en forma de cuerpos de inclusión, en este caso se optó por emplear exclusivamente la estrategia de fusión a MBP (Maltose Binding Protein), con el fin de favorecer la solubilidad y el correcto plegado de la proteína recombinante.

La síntesis del gen optimizado y clonación en el vector pMAL-c5E se realizó en el servicio de GenScrip como se describió en Materiales y Métodos. Se transformaron células de *E. coli* BL21(DE3) y Arctic Express(DE3) con el vector recombinante, obteniéndose clones viables en medio LB suplementado con ampicilina. Para identificar las condiciones óptimas de expresión, se ensayaron dos temperaturas: 14 °C y 37 °C.

El análisis mediante SDS-PAGE permitió confirmar la expresión de rLACC-AU10 fusionada a MBP, observándose una banda de aproximadamente 91 kDa, correspondiente a la suma de los tamaños moleculares de LACC-AU10 y MBP. Para las cepas cultivadas a 14 °C, la proteína recombinante se detectó principalmente en la fracción soluble (FS) de las células BL21(DE3), mientras que en Arctic Express(DE3), la proteína se acumuló mayoritariamente en la fracción insoluble (FI). A 37 °C, en ambas cepas, la expresión fue menor y predominó la presencia de proteína en la fracción insoluble, indicando una menor solubilidad a temperaturas más elevadas de expresión (Figura 7).

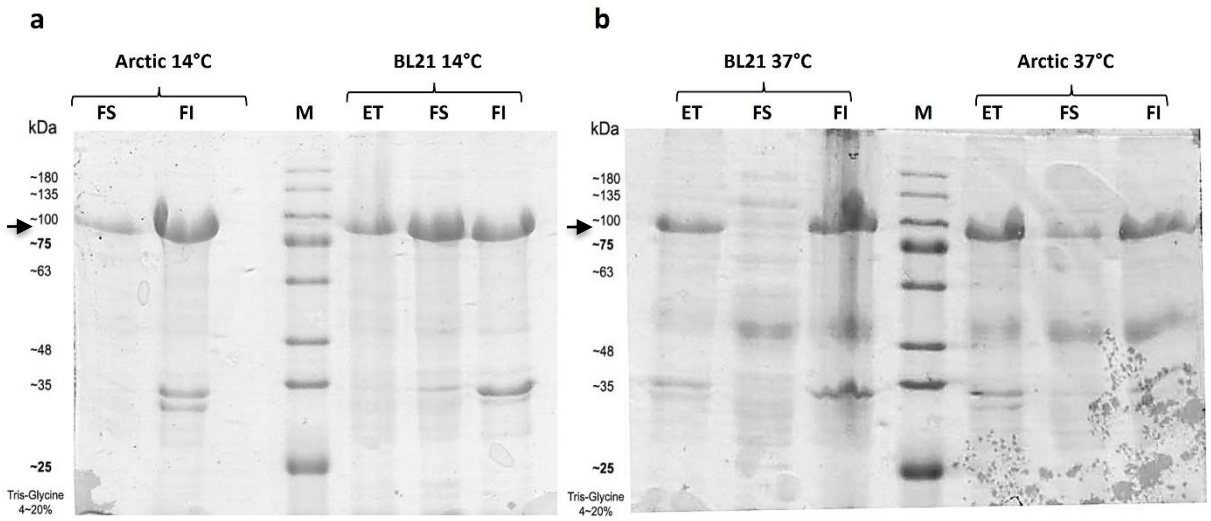

Figura 7. Análisis por SDS-PAGE de la expresión recombinante de rLACC-AU10 fusionada a MBP en *E. coli* BL21(DE3) y Arctic Express(DE3) cultivadas a (a) 14 °C y (b) 37 °C. Se observan las fracciones soluble **(FS)** e insoluble **(FI)**. Las flechas indican la banda correspondiente a la proteína recombinante, con un peso molecular aproximado de 91 kDa. Como marcador de tamaño molecular (**M**) se utilizó PageRuler™ Prestained Protein Ladder (Thermo Scientific™, Cat. No. 26616).

En el proceso de purificación mediante IMAC, la proteína recombinante correspondiente a la fusión rLACC-AU10+MBP se detectó en los eluídos E1-E5 (Figura 8), mostrando una alta concentración en las fracciones E3 y E4. Se observa pérdida de proteína de interés en el percolado (FT) y en las fracciones de lavado (W), lo que indica una retención en la resina, pero no completa. Quedaría pendiente optimizar las condiciones de unión de la proteína a la matriz.

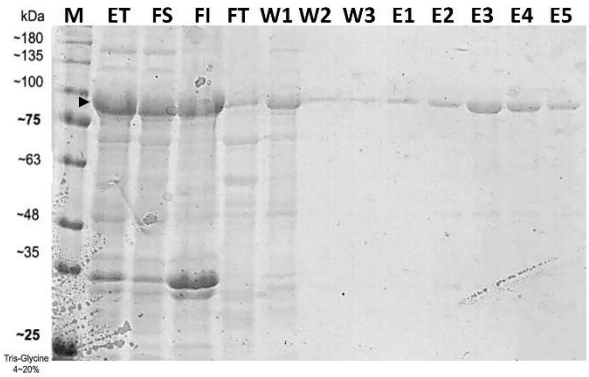

Figura 8. Expresión de laccasa-AU10 a 14 °C. SDS-PAGE de las fracciones obtenidas de la expresión de laccasa-MBP en *E. coli* y purificación de la fracción soluble mediante IMAC. **ET**: extracto total. **FS**: fracción soluble. **FI**: fracción insoluble. **FT:** (percolado o flow-through). **W1,2,3**: lavados de la columna. E1,2,3,4: eluídos. Se indica con una flecha la sobreexpresión de cada fusión recombinante. Como marcador de tamaño molecular (**M**) se utilizó PageRuler™ Prestained Protein Ladder (Thermo Scientific™, Cat. No. 26616).

El estudio de la enzima purificada, por espectroscopía UV-vis, mostró que la enzima carecía de cobre en su sitio activo, como evidenció la ausencia de un espectro característico. La falta de cobre catalítico explica también la falta de actividad, sobre siringaldazina y ABTS como sustratos.

2.3.3. Discusión

Las proteínas multicobre azules conforman una familia ampliamente distribuida en todos los dominios de la vida, caracterizada por la presencia de cuatro dominios conservados ricos en histidina que coordinan centros de cobre. Estos centros metálicos, denominados Cu tipo 1 (azul), 2 (normal) y 3 (acoplado), confieren propiedades redox y espectroscópicas particulares a estas proteínas [64]. Entre ellas, las multicobre oxidasas catalíticamente activas, como las laccasas, ascorbato oxidasa, bilirrubina oxidasa y ceruloplasmina, han sido ampliamente estudiadas, especialmente en hongos. Sin embargo, también se han identificado proteínas multicobre oxidasas en múltiples géneros bacterianos [41, 65] con funciones tan variadas tales como la participación en la biosíntesis de pigmentos, degradación de compuestos xenobióticos, homeostasis a metales y tolerancia al cobre, entre otras [45, 66].

En el contexto bacteriano, las laccasas han sido menos exploradas respecto a las fúngicas, pero con múltiples reportes hasta la fecha, y estudios recientes destacan su diversidad funcional y su potencial biotecnológico. Su capacidad para oxidar compuestos aromáticos fenólicos las posiciona como herramientas promisorias en procesos industriales y ambientales. Sin embargo, la identificación funcional de estas enzimas en bacterias sigue siendo un desafío, especialmente en ausencia de secuencias canónicas o dominios bien definidos [66, 67].

Una estrategia para la detección preliminar de la actividad laccasa consiste en el uso de sustratos cromogénicos. Si bien los compuestos como ABTS y siringaldazina han sido ampliamente utilizados en ensayos enzimáticos, su aplicabilidad en cultivos bacterianos es limitada debido a problemas de estabilidad, requerimientos de pH estrictos o interferencias por oxidación espontánea [47, 68, 69], además de su alto costo. En este sentido, el 2,6-dimetoxifenol (DMP) se ha propuesto como una alternativa ventajosa: no sólo es estable en condiciones moderadamente ácidas (pH ~5), sino que su producto oxidado, el 3,3’,5,5’-tetrametoxidifenilquinona, presenta una coloración intensa y un elevado coeficiente de absorción molar (14.800 $M^{-1} \cdot cm^{-1}$), superior al de otros sustratos comunes como el guaiacol [47].

En este trabajo, la utilización de DMP permitió realizar un cribado rápido, económico y sensible de cepas bacterianas de nuestra colección con potencial actividad laccasa. La coloración anaranjada-marrón (presencia de 3,3',5,5'-tetrametoxidifenilquinona) en el medio de cultivo indicó una actividad oxidativa compatible con actividad laccasa u oxidasa. Cabe señalar que si bien esta técnica no es específica y puede detectar otras fenol oxidasas, su alta sensibilidad la convierte en una primera aproximación válida para estudios exploratorios. De hecho, resultados similares han sido utilizados como criterio funcional preliminar para seleccionar cepas fúngicas o bacterianas productoras de enzimas oxidativas [70]. En nuestro caso, la detección positiva en dos cepas bacterianas antárticas del género *Pseudomonas* refuerza la idea de que las laccasas bacterianas pueden estar más difundidas de lo que se pensaba, aunque con variabilidad en su expresión, secreción y especificidad de sustrato. Para la cepa *Sinorhizobium meliloti* CE52G, los resultados fueron consistentes con estudios previos de nuestro grupo, que realizaron la caracterización parcial, bioquímica y molecular, de una laccasa activa en esta cepa [44, 45].

Finalmente, es relevante considerar que la actividad oxidativa detectada mediante DMP puede no corresponder a laccasas clásicas, sino a proteínas multicobre con actividad oxidasa inducida por cobre, como las laccasas descritas en *Escherichia coli* (CueO) o *Bacillus subtilis* (CotA), que presentan actividad dependiente de Cu^{2+} y patrones cinéticos variables [71, 72].

En consecuencia, la confirmación de la identidad enzimática requiere de ensayos adicionales con sustratos múltiples, caracterización molecular y bioquímica bajo distintas condiciones, y por ello se decidió producir las enzimas laccasas de forma recombinante en un hospedero bacteriano.

La producción recombinante de estas enzimas bacterianas presenta desafíos considerables, especialmente cuando se expresan en sistemas heterólogos como *Escherichia coli*. Si bien los análisis *in silico* de LACC-CE52G sugirieron que se trata de una multicobre oxidasa típicamente estructurada, incluyendo los dominios conservados de unión a cobre y una señal de localización periplásmica, los resultados experimentales muestran que su expresión ocurre mayoritariamente en forma de cuerpos de inclusión y que, incluso tras protocolos de solubilización y replegamiento, no se recupera la actividad enzimática esperable.

Este fenómeno no es inusual. Estudios previos han demostrado que muchas laccasas bacterianas, especialmente aquellas con estructura compleja o requerimientos de cofactores metálicos específicos, tienden a formar agregados insolubles cuando se expresan en *E. coli* [73]. En particular, la correcta incorporación de iones cobre en los centros activos tipo T1, T2 y T3 es crítica para la funcionalidad catalítica, y este proceso puede verse comprometido durante la expresión heteróloga o el replegamiento *in vitro* [64].

La expresión de laccasas recombinantes en *Escherichia coli* enfrenta el desafío de lograr la incorporación eficiente de los iones cobre requeridos en los centros catalíticos tipo T1, T2 y T3, necesarios para obtener una holoenzima funcional. Durão et al., 2007 [63] han demostrado que *E. coli* cultivada en condiciones microaeróbicas acumula una cantidad significativamente mayor de cobre intracelular, hasta 80 veces más, en comparación con cultivos aeróbicos, debido a cambios en la homeostasis del metal y en los sistemas de transporte y almacenamiento intracelular. Esta acumulación favorece la incorporación secuencial de los átomos de cobre durante la biosíntesis de la enzima, facilitando la correcta formación del sitio trinuclear y del centro T1, lo cual no ocurre eficientemente bajo condiciones altamente oxigenadas. En condiciones aeróbicas, por el contrario, la limitación de cobre disponible y la alteración del estado redox celular suelen conducir a la síntesis de apoenzimas o formas parcialmente metaladas, estructuralmente incompletas y carentes de actividad catalítica. Por tanto, el cultivo de *E. coli* bajo condiciones microaeróbicas con suplementación de cobre constituye una estrategia crítica para favorecer la correcta incorporación del metal y el plegamiento activo de laccasas bacterianas recombinantes [63]. En este trabajo, se replicó esta estrategia con el objetivo de favorecer la correcta incorporación de cobre en rLACC-CE52G durante su biosíntesis. Si bien los resultados obtenidos permiten confirmar la producción de una fracción soluble de la proteína recombinante, los análisis espectrales no evidenciaron los picos característicos asociados a los centros de cobre tipo T1 (máximo de absorción ~ 600 nm) ni a los centros trinucleares T2/T3 (máximo de absorción ~ 330 nm) [74], lo que indica una probable ausencia, o incorporación incompleta del cobre. Esta hipótesis se ve reforzada por la falta de actividad catalítica detectada frente a los sustratos ABTS y siringaldazina. Asimismo, la baja retención observada en parte de la proteína durante la purificación podría estar relacionada con una estructura incompleta del sitio activo o con alteraciones conformacionales que impiden la adecuada exposición de la etiqueta de afinidad, y que fue evidenciado durante la purificación donde la proteína fue detectada en todas las fracciones del proceso. En conjunto, estos hallazgos sugieren que, a pesar de los intentos por mejorar las condiciones intracelulares para la incorporación de cobre mediante la estrategia microaeróbica, esta no fue suficiente para obtener una holoenzima catalíticamente funcional en este caso particular. Por tanto, aunque las condiciones microaeróbicas con suplemento de cobre representan una vía promisoria para la expresión de multicobre oxidasas en *E. coli*, los resultados aquí presentados destacan la necesidad de seguir optimizando tanto la estrategia de expresión como las etapas posteriores, incluyendo el replegamiento asistido, la incorporación dirigida de cofactores y la exploración de sistemas alternativos de expresión que posean una maquinaria de ensamblaje metálico más eficiente.

La presencia de motivos conservados de unión a cobre y la predicción de una localización periplásmica de LACC-CE52G sugieren que, en su organismo nativo, esta enzima podría plegarse de forma asistida

en un entorno oxidante, posiblemente con la ayuda de chaperonas o sistemas específicos de inserción de cobre, como se ha descripto para las laccasas CueO en *E. coli* o Copt en *Bacillus subtilis* [71, 75]. En ausencia de estos sistemas en el citoplasma de *E. coli*, la proteína tiende a formar agregados. En caso de rLACC-CE52G, aunque se logró su solubilización por agentes desnaturalizantes como la urea, el replegamiento no garantizó la restauración de su conformación funcional o la toma del cobre. Además, el hecho de que la enzima no haya recuperado actividad frente a ABTS ni siringaldazina, incluso con suplemento de $CuSO_4$ durante el replegamiento, podría deberse a una incorrecta formación del entorno tridimensional del sitio activo o a la falta de incorporación ordenada de los cuatro átomos de cobre [76]. La literatura también reporta que algunos cofactores metálicos pueden actuar como inhibidores si no se coordinan adecuadamente, promoviendo la inactivación o el mal plegamiento de la enzima [64]. Además, el patrón de cisteínas de LACC-CE52G, analizado de forma *in silico*, sugiere una alta probabilidad de formación de puentes disulfuro con posible relevancia estructural. Sin embargo, cuando estas proteínas se expresan en *E. coli*, especialmente en el citoplasma, la formación adecuada de dichos enlaces covalentes constituye un desafío crítico para la adquisición de una conformación funcional. Si bien *E. coli* posee la capacidad de formar puentes disulfuro, esta actividad está restringida al compartimento periplásmico, donde actúan sistemas oxidativos como DsbA/DsbC [77]. Por tanto, sería interesante evaluar la expresión recombinante de LACC-CE52G conservando su péptido señal nativo de localización periplásmica, o bien diseñar una construcción que incluya un péptido señal compatible con *E. coli* que dirija la proteína hacia el periplasma, donde las condiciones redox favorecerían un plegamiento más adecuado y una correcta formación de los centros metálicos. En el citoplasma, las condiciones reductoras naturales impiden la formación espontánea de enlaces disulfuro, lo que favorece el mal plegamiento y la acumulación en cuerpos de inclusión. Este fenómeno ha sido reportado en múltiples estudios sobre proteínas recombinantes con alto contenido de cisteínas [78]. Durante el replegamiento de rLACC-CE52G, pudo haber ocurrido una formación no controlada o errónea de los puentes disulfuro generando estados parcialmente plegados o inactivos y afectando la correcta organización del sitio activo o la estabilidad de los dominios estructurales [79]. Un ejemplo es la estructura cristalográfica de CotA de *Bacillus subtilis,* que reveló un puente disulfuro entre Cys229 y Cys322, ubicado cerca del centro catalítico. Fernandes et al. (2011) analizaron mutantes de los aminoácidos de este enlace y observaron que, si bien no se afectó la estabilidad termodinámica, sí alteró la dinámica de incorporación de cobre, evidenciando su relevancia estructural y funcional [80].

Por otro lado, las cisteínas de LACC-CE52G, predichas como no oxidadas (CYS258 y CYS619), podrían permanecer reducidas en la conformación nativa, pero también están expuestas a oxidación inespecífica bajo las condiciones artificiales del replegamiento, lo que representa un riesgo adicional para el plegamiento correcto de la proteína. En este contexto, resulta relevante considerar que la

presencia de cobre libre (Cu^{2+}) en la solución de replegamiento puede actuar como un agente redox no específico, promoviendo reacciones de oxidación no controladas que afecten tanto a las cisteínas como a otros residuos sensibles [62].

Para mitigar estos efectos, podrían evaluarse condiciones alternativas de replegamiento que incluyan el uso de aditivos estabilizantes como glicerol, sorbitol o imidazol, conocidos por favorecer la correcta conformación nativa y disminuir la agregación proteica. Además, el control estricto de la concentración de proteína en el replegamiento resulta clave, recomendándose trabajar en un rango bajo (0,02–0,15 mg/mL), ya que las concentraciones elevadas favorecen las reacciones de agregación y el plegado incorrecto. Por otra parte, el uso de sistemas redox suaves, o la incorporación secuencial del cobre una vez finalizado el replegamiento primario, podrían favorecer la incorporación ordenada de los cofactores metálicos y la formación controlada de los enlaces disulfuro estructurales, mejorando así la probabilidad de obtener una enzima funcional [62, 78].

Por otro lado, el análisis con Aggrescan mostró regiones locales con alta tendencia a la agregación. Esto sugiere que, aunque la proteína presenta una propensión global baja al autoagregación, ciertas zonas pueden favorecer la formación de agregados incluso en condiciones optimizadas. Este hallazgo respalda la necesidad de explorar variantes fusionadas con proteínas solubilizantes como MBP o TrxA. En este estudio, solo la co-expresión con MBP permitió recuperar expresión soluble de rLACC-CE52G, mientras que con la fusión con TrxA no se logró este resultado. Estos hallazgos abren la posibilidad de explorar otras estrategias de co-expresión con chaperonas, o incluso el uso de hospedadores alternativos como *Pichia pastoris* o *Bacillus subtilis*, que han demostrado ser más eficaces para la producción de multicobre oxidasas funcionales [81–83]. Actualmente, y fuera de esta tesis de Doctorado, se está probando la expresión de esta laccasa en otros hospederos, como *Aspergillus*.

Frente a estos desafíos, diversas estrategias han sido propuestas para mejorar la correcta formación de puentes disulfuro en *E. coli*. Entre ellas, el uso de cepas genéticamente modificadas como Origami™ o SHuffle™, que poseen un entorno citoplasmático oxidante favorable para la formación de enlaces disulfuros [78], o la expresión dirigida al periplasma mediante la conservación del péptido señal, aprovechando el ambiente más oxidante de esa localización, donde el plegamiento proteico puede ser más eficiente.

CAPÍTULO III

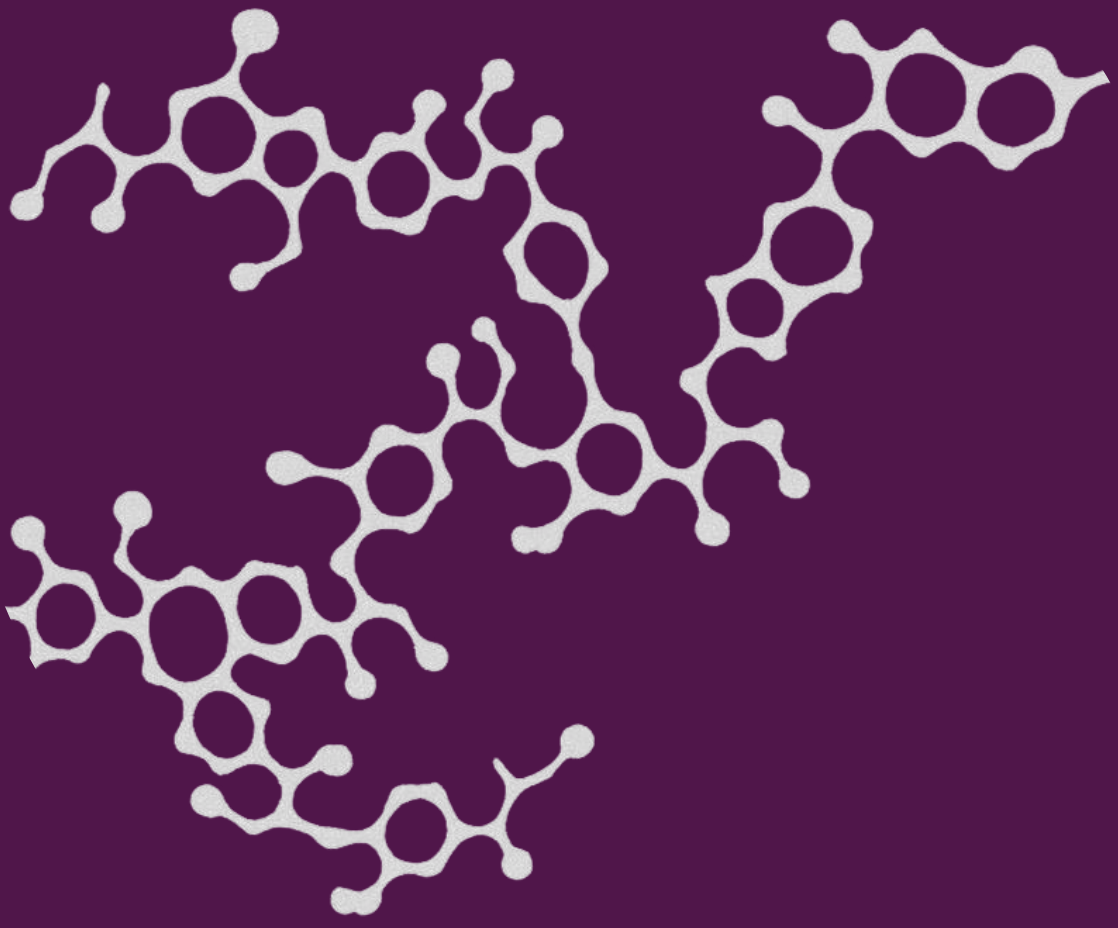

3. Un preparado multienzimático para la modificación de lignina

3.1. Contexto y antecedentes

El último capítulo de esta tesis aborda el uso de un preparado multienzimático orientado a la modificación de la lignina, empleando tanto un sustrato modelo como materiales lignocelulósicos provistos por una industria papelera radicada en Uruguay. Tal como se describió en el capítulo anterior, no fue posible obtener nuestra propia laccasa en forma recombinante y activa, por lo que se optó por utilizar una laccasa comercial. No obstante, el grupo de trabajo continuará con el desarrollo y la optimización de la producción recombinante de la laccasa de *S. meliloti* CE52G.

Con este escenario, el objetivo de este capítulo fue evaluar el uso combinado de rDyP-AU10 y una laccasa comercial en la modificación de la lignina presente en sustratos lignocelulósicos de origen industrial. Aquí se abordan los Objetivos específicos 6 y 7.

La creciente demanda de procesos más sostenibles en la industria de pulpa y papel ha impulsado el desarrollo de estrategias enzimáticas que permitan reemplazar, total o parcialmente, los tratamientos químicos tradicionales utilizados para la remoción de lignina residual. En este contexto, el uso de enzimas oxidativas como las peroxidasas y las laccasas han ganado relevancia, dado su potencial para catalizar transformaciones selectivas sobre lignina técnica, como la kraft, bajo condiciones operativas más suaves y con menor impacto ambiental.

En el Capítulo I se describió la caracterización de una peroxidasa tipo DyP (rDyP-AU10) producida en forma recombinante, a partir de un gen identificado en *Pseudomonas* sp. AU10, un microorganismo psicrotolerante aislado de la Antártida. Esta enzima mostró capacidad para modificar lignina kraft en condiciones moderadas de temperatura y pH, y fue seleccionada como candidata para aplicaciones de bioblanqueo y biomodificación de sustratos lignocelulósicos.

Dado que uno de los enfoques más prometedores en la biotransformación de lignina consiste en el uso combinado de enzimas con mecanismos complementarios de acción, se propuso evaluar la actividad conjunta de la peroxidasa rDyP-AU10 con una laccasa. En principio, se intentó la producción recombinante de varias laccasas de nuestra colección bacteriana, proceso documentado en el Capítulo II; sin embargo, no se logró obtener una preparación activa. Por esta razón, se optó por utilizar una laccasa comercial de *Trametes versicolor*, como referencia funcional para el tratamiento combinado.

A partir de los hallazgos presentados en los capítulos anteriores, surgieron nuevas preguntas orientadas a evaluar la aplicabilidad de estas enzimas en contextos industriales reales: ¿Podría rDyP-AU10 actuar de manera eficiente sobre lignina técnica, como la kraft, en condiciones operativas compatibles con procesos industriales? ¿Existe sinergia funcional entre esta peroxidasa y una laccasa, que potencie su acción sobre distintos tipos de sustratos lignocelulósicos? ¿Qué impacto químico y estructural podría lograrse mediante el uso de sistemas enzimáticos combinados sobre pulpas de celulosa, provenientes de etapas reales del proceso de producción de papel? Para responder a estos interrogantes, en este capítulo se propuso dos objetivos principales: analizar el potencial de la peroxidasa rDyP-AU10, sola o en combinación con una laccasa, para modificar lignina kraft y pulpas celulósicas industriales, y evaluar su eficacia sobre diferentes sustratos lignocelulósicos, con el fin de explorar su potencial en la industria papelera.

Los resultados de este capítulo se presentan en el artículo titulado *"Kraft lignin biobleaching by a dye-decolorizing peroxidase from the Antarctic Pseudomonas sp. AU10 strain"*, publicado en 2024 en la revista *Brazilian Journal of Microbiology*. En este artículo se analizan los efectos de rDyP-AU10, tanto de forma individual como en combinación con la laccasa comercial, sobre lignina kraft y pulpas celulósicas de dos etapas del proceso industrial de producción de papel. El capítulo aborda desde la determinación de las condiciones óptimas de actividad enzimática sobre lignina kraft, hasta la evaluación del impacto químico y estructural de los tratamientos, determinado mediante métodos espectrofotométricos y cromatográficos. Así mismo, se presenta información sobre el biotratamiento de un sustrato industrial, aplicando las condiciones óptimas determinadas para lignina kraft. Los resultados permiten discutir el potencial sinérgico entre ambas enzimas y proponer escenarios de aplicación para este tipo de sistemas enzimáticos mixtos.

Brazilian Journal of Microbiology
https://doi.org/10.1007/s42770-024-01595-5

BIOTECHNOLOGY AND INDUSTRY - RESEARCH PAPER

Kraft lignin biobleaching by a dye-decolorizing peroxidase from the Antarctic *Pseudomonas* sp. AU10 strain

Célica Cagide[1] · Diego Vallés[2] · Susana Castro-Sowinski[1,2]

Received: 14 October 2024 / Accepted: 12 December 2024

Abstract

Pseudomonas sp. AU10 is an Antarctic psychrotolerant bacterium that produces a dye-decolorizing peroxidase (DyP-AU10). The recombinant enzyme (rDyP-AU10) is a heme-peroxidase that decolors dyes and modifies kraft lignin. In this work, we report the best activity parameters for lignin modification (at 45 °C and pH 4) and show that the enzyme increases the number of aldehydes, ketones, and phenolic compounds. The analyses of the HPLC profile of samples also support that rDyP-AU10 induces the chemical change of kraft lignin. The enzyme also acts as a biobleaching agent on cellulose pulps, as shown by the reduction in kappa number. We also included experiments with a commercial laccase from *Trametes versicolor* and performed experiments using single enzymes and, in combination. The results show that rDyP-AU10 and the commercial laccase do not have a synergic activity as a modifying system, on cellulose pulp as substrates. However, results suggest that rDyP-AU10 holds potential as a member of the portfolio of lignin-modifying enzymes.

Keywords Cold-active peroxidase · Kraft lignin modification · Kappa number · Cellulose pulp

Introduction

The pulp and paper industry uses wood and other fibrous materials to produce paper and thick paper-based (paperboard) goods, including everyday life products such as facial tissue and paper towels. This is a growing industry that is projected to grow from USD 351.53 to USD 372.70 billion in the period 2021–2029, at a CAGR of 0.72% during the forecast period 2022–2029 (https://finance.yahoo.com/news/pulp-paper-market-size-worth-053000191.html?guccounter=1&guce_referrer=aHR0cHM6Ly93d3cuZ29vZ2xlLmNvbS8&guce_referrer_sig=AQAAACs0cF_KPNntrwsHvS7tvyIp6Tl_aSQ6u8VwgMGcS56w04hHGjVG9yHO43O3fCOxcqe_IVQft-0qH3px_Q-9YDxbYDWUF1gepakxb9ESJWilAyeqByZsn9v86QbZ5mHtj_-ZeaSTN_4UNwGWKafzEtiIoq_VLq450fb9EN-QH4VQ). Among different potential uses of paper, the toilet paper market showed an impressive revenue of USD 113.80 billion, in 2024 (https://www.statista.com/outlook/cmo/tissue-hygiene-paper/toilet-paper/worldwide). This kind of paper is made from bleached pulp, due to a process that uses chemicals that could be toxic to humans and affect different natural environments [1]. Thus, researchers always seek to contribute to sustainable and environmentally friendly papermaking, searching for less polluting biological processes.

The process of papermaking includes different steps: wood chipping, wood-pulp production by the chemical and/or mechanical treatment of the lignocellulosic fibrous materials (the kraft process), and paper production by pressing-drying the pulp and cutting sheets [2, 3]. A shortcoming of the kraft process (removal of the recalcitrant lignin from cellulose) is that the pulp contains a residual dark brown lignin that should be bleached. Usually, bleaching is a multistep procedure involving delignification followed by brightening, which uses many chemicals. Delignification is carried out by oxidation using a chlorine solution, followed by treatment with NaOH (replacement of chlorine substitutions with OH groups, ionization of phenolic groups, and dissolution of degraded lignin). Brightness is reached using ClO_2 (chlorine-dioxide; oxidation of lignin, destruction of

Communicated by Luiz Henrique Rosa

✉ Susana Castro-Sowinski
scs@fcien.edu.uy; s.castro.sow@gmail.com

[1] Sección Bioquímica, Instituto de Biología, Facultad de Ciencias, Universidad de la República, Iguá 4225, Montevideo 11400, Uruguay

[2] Laboratorio de Biocatalizadores y sus Aplicaciones, Instituto de Química Biológica, Facultad de Ciencias, Universidad de La República, Igua 4225, Montevideo 11400, Uruguay

Published online: 24 December 2024

chromophores) [4, 5]. Public concern is currently about the discharge of chlorinated organic and other potentially toxic (H_2SO_4, Cl_2, and H_2O_2) compounds that may have environmental impacts. An alternative is to use biobleaching instead of chemical bleaching.

Biobleaching is an eco-friendly alternative to reduce the use of potentially toxic chemicals. This process uses xylanases, pectinases, laccases, manganese peroxidases (MnP), and/or lignin-peroxidases, which either individually or in combination reduce the kappa number (the residual lignin content), increase ISO brightness (measured as the percentage of blue light reflected from the surface at 457 nm), improve physical strength properties and viscosity, and reduce both the consumption of chemicals and production of pollutants, among others benefits [6, 7]. The use of enzymes with different mechanisms of action appears to be a promising approach to improving the final product quality; however, enzymes active in carbohydrates produce a significant amount of degradation products, mainly released from the cellulose fiber network, negatively impacting pulp value. For this reason, the use of enzymes in pulp bleaching has a poor reputation in the paper industry. Recently, Immerzeel and Fiskari (2023) [8] reviewed the advantages of incorporating different enzymatic preparations in pulp bleaching, concluding that xylanase/laccase is the most effective enzymatic mixture for pulp bleaching.

An additional issue is that most commercial enzymatic formulations do not meet the demanding requirements during the industrial process; they must remain active and stable under extreme conditions, such as alkalinity and high temperatures. However, there is a list of bacterial enzymes for pulp biobleaching active in the range of 50 to 100 °C and pH 6–10 [8]. For example, Almeida et al. (2022) [9] reported the production, purification, and effect on kraft pulp of a thermal and alkaline-tolerant xylanase from *Pseudothermotoga thermarum*, active at 90 °C and pH 10.5. The authors validated their results at a pilot scale, reducing the use of ClO_2 by 25% and the production of organochlorinated compounds by 18%, retaining pulp quality and papermaking properties. Successful enzymatic formulations could reduce the chemicals used during bleaching, thus reducing the level of organochlorine compounds in effluents. However, resistance to biobleaching persists because chemical bleaching of pulp remains more effective and cost-efficient.

Enzymes used during biopulping and biobleaching are obtained from mesophilic or thermophilic microbes, and the use of cold-active enzymes (or psychrophilic enzymes) has been poorly addressed. Cold-active enzymes are produced by cold-adapted microbes (psychrotolerant or psychrophilic), usually found in cold environments. Most of Earth's surface has cold environments (Polar, deep-sea waters, mountain regions, freezers, etc.) and the organisms that inhabit them thrive under the imposed extreme conditions (cold, oligotrophic, low water availability, among others). During cold adaptation, organisms change the structure and composition of membranes, produce molecules that protect cells against crystal formation, reorganize their metabolic pathways, and produce cold-adapted proteins [10]. Among others, cold adaptation of enzymes includes changes in a few amino acids which explains why they have major flexibility, less substrate specificity, lower activation enthalpy, and reduced thermal stability compared to mesophilic enzymes (produced by mesophilic microbes) [11]. These cold-active enzymes show biochemical features suitable for some biotechnological processes, *e.g.*, they allow energy saving and are easily inactivated by increasing temperature [12]. As a research team that works analyzing the biotechnological potential of enzymes produced by Antarctic microbes, we wonder if we could contribute to a growing industry, such as the papermaking one, searching for decolorizing bacterial-cold-active enzymes that may modify lignin.

Previously, we reported the recombinant production, purification, biochemical characterization, and potential use in the cellulose pulp industry of a DyP (dye-decolorizing peroxidase), produced by an Antarctic *Pseudomonas* strain named AU10. The recombinant enzyme chemically modifies kraft lignin, a lignin model substrate, inducing a loss of polymer aromaticity, and the release of chromophores; it also produced a 6% decolorization of dyes after 100 s [13]. *Pseudomonas* sp. AU10 is a psychrotolerant extracellular-producing microbe isolated from the Uruguay Lake in King George Island, Antarctica [14, 15]. AU10 growth profile, including the validation of reference genes for gene expression analysis, at different temperatures, was carefully described by Garcia-Laviña et al. (2019) [16]. This bacterium also resists many antibiotics and heavy metals and produces an exopolysaccharide with high Cr(VI)-biosorption capacity [17].

We hypothesize that using a mix of enzymes, with different mechanisms of action, we can augment lignin modification and biobleaching. Peroxidases and laccases belong to the family of lignin-degrading enzymes that act on lignin, using different mechanisms of action [18]. Among other differences, laccases and peroxidases use oxygen and hydrogen peroxide (H_2O_2) as co-substrates, respectively; and laccases use mediator molecules involved in the regeneration of the oxidized nicotinamide co-factors that expand the oxidative capacity of laccases [18].

In the current work, we studied the best conditions (pH and temperature) for efficiently modifying kraft lignin using the purified recombinant DyP produced by AU10 (rDyP-AU10), and we analyzed the effect in a pulp substrate (industrial cellulose pulp) provided by a papermaking industry (UPM; a Finnish forest industry company, with branches in Finland, Germany, Great Britain, France, Austria, United States, and Uruguay). We aimed to evaluate the potential of rDyP-AU10 to improve the delignification of chemically

bleached cellulose pulp that still contains some brown lignin. We also included a commercial laccase as a control and analyzed the potential of using a mix of rDyP-AU10 and the laccase (enzymatic combo).

Materials and methods

Production and purification of rDyP-AU10

rDyP-AU10 was produced using recombinant DNA technology and purified by immobilized metal affinity chromatography (IMAC). Briefly, the expression vector pET28a (+), containing the *dyp*-AU10 gene was transformed to *Escherichia coli* BL21 (DE3) chemocompetent cells. The recombinant protein was produced in Zym-5052 medium, in the presence of 50 µg/mL kanamycin, at 37 °C (overnight) and then incubated at 14 °C for 60 h. The cell pellet was harvested by centrifugation and the cell lysis was achieved by sonication. We recovered rDyp-AU10 from the soluble fraction, and the recombinant protein was purified by IMAC using a HisPur™ cobalt resin (#89964, Thermo Fisher Scientific), followed by gel filtration using a PD-10 desalting column (#17–0851-01, Cytiva). The activity was determined using 2,2′-azinobis(3-ethylbenzothiazoline-6-sulfonic acid) (ABTS) and 1 mM H_2O_2 as substrates. One unit of activity (or enzyme unit, EU) was defined as the amount of enzyme required to oxidize 1 µmol of substrate per minute under these assay conditions. Procedures were previously described by Cagide et al. (2023) [13]. The activity of the commercial laccase from *Trametes versicolor* (#38429 Sigma-Aldrich) was also determined using ABTS as a substrate but without H_2O_2.

The activity of rDyP-AU10 on kraft lignin, at different pHs and temperatures

The activity of rDyP-AU10 on kraft lignin (#471003, Sigma-Aldrich) was monitored by the increase in absorbance at 465 nm [19], showing the release of chromophores. The assays were carried out within a temperature range of 25 to 45 °C (we did not analyze higher temperatures since the enzyme is inactive at 50 °C as previously reported by Cagide et al. (2023) [13]), and at two pH values (4 and 5), using the activity buffer described by Ellis and Morrison (1982) [20] (0.05 M acetic acid, 0.05 M MES, and 0.1 M Tris). The reaction mix contained 10 µM kraft lignin and, 0.76 EU of rDyP-AU10 (with 4 mM H_2O_2) and/or 2.5 EU of commercial laccase. We also performed control experiments without enzymes and/or H_2O_2. The modification of kraft lignin was reported as absorbance units per second (AU/sec).

Physicochemical and enzymatic modification of kraft lignin

We analyzed: 1) the contribution of temperature and H_2O_2, and 2) the effect of rDyP-AU10, commercial laccase, and the enzymatic combo (peroxidase and laccase), in the chemical modification of kraft lignin. We determined the production of phenolic compounds, aldehydes, and ketones, as well as the HPLC profile, as described below.

The physicochemical effect of pH and temperature was analyzed on 100 µM kraft lignin at pH 4 and 45 °C (determined as the best conditions for enzymatic modification by rDyP-AU10; see Results). The enzymatic modification of kraft lignin was studied treating samples at pH 4 and 45 °C, for 1, 6, 24, or 48 h, with 0.76 EU of rDyP-AU10 (with 4 mM H_2O_2) and/or 2.5 EU of commercial laccase. After treatments, the samples were centrifuged (8864 g, 5 min, room temperature) and filtered through a 0.22 µm membrane filter. The filtered solutions were used for further experiments. When indicated, we included mediator molecules to enhance the laccase enzymatic activity. We used the mediators veratryl alcohol (5 mM VA) and manganese chloride ($MnCl_2$) [21]

Determination of phenolic compounds by Folin–Ciocalteu assay

We used the protocol described by Rashid and Bugg (2021) [22]. Briefly, 20 µL of the sample was mixed with 100 µL of distilled water and 10 µL of Folin-Ciocalteu reagent (#47641, from Fluka); after 4 min we added 100 µL of 4% $NaCO_3$. The mixture was incubated in darkness at room temperature for 30 min, and the production of phenolic compounds was determined at 750 nm, using a microplate reader (TECAN Infinite M200pro).

Determination of aldehyde and ketone products

We also used the protocol outlined by Rashid and Bugg (2021) [22]. Briefly, we mixed 20 µL of samples, 30 µL of 0.1 M HCl, and 50 µL of 1 mM 2,4-dinitrophenylhydrazine (DNP, prepared in 100 mM HCl); after 5 min, we added 100 µL of 0.1 M NaOH and recorded the absorbance at 450 nm using a microplate reader (TECAN Infinite M200pro).

HPLC analysis

HPLC analysis was conducted using a Viva C 18 (250 × 4,6 mm, 5 µm particle size, 300 A pore size, Restek U.S.) reverse phase column on a Shimadzu UFLC Prominence System (with a photodiode array detector SPD-M20A) at a flow rate of 0.5 mL/min, monitoring at 270, 310, and 465 nm. The gradient for HPLC was as follows: water/0.1%

formic acid as solvent A, and methanol/0.1% formic acid as solvent B. The method started with 10% solvent B from 0–5 min; then 10–30% B from 5–10 min; 30–70% B from 10–25 min; 70–100% B from 25–30 min; 100% B from 30–35 min; 100–10% B from 35–40 min and 100% A from 40–55 min [22].

We performed additional control experiments: 10 µM kraft lignin without or with 4 mM H_2O_2 (effect of the oxidant on kraft lignin), and 10 µM kraft lignin at room temperature (without H_2O_2; effect of temperature on kraft lignin). We also analyzed the effect of H_2O_2 on 10 µM kraft lignin doing treatments as follows: a) 4 mM H_2O_2 for 1 h, then rDyP-AU10 plus 4 mM H_2O_2; b) 4 mM H_2O_2 for 1 h, then rDyP-AU10; c) 4 mM H_2O_2 for 1 h, then 4 mM H_2O_2; d) 10 mM H_2O_2 for 1 h, then rDyP-AU10 plus 4 mM H_2O_2; e) 10 mM H_2O_2 for 1 h, then rDyP-AU10.

Enzymatic modification of cellulose pulp

Once we determined the best conditions for kraft lignin modification, we analyzed the change in the kappa number using cellulose pulp from Eucalyptus as substrate. The samples were: Pulp A (washed raw pulp of brownish color, obtained after wood cooking with NaOH and H_2S, under high pressure and temperature) and Pulp B (unbleached pulp of light beige color, obtained by delignification with O_2 and washing with O_2 from Pulp A).

Assays were carried out on 40 mg of pulp, in activity buffer at pH 4. We added 84 EU rDyP-AU10 (supplemented with 4 mM H_2O_2) and/or 2.5 EU commercial laccase; when indicated we added 20 mM veratryl alcohol. Samples were incubated at 45 °C with shaking (200 rpm) for 24 h. Afterward, the treated pulp was filtered through Whatman No. 1 paper, washed with distilled water, and dried at 60 °C until constant weight. The kappa number was determined following the protocol for titration of residual lignin established in Tappi Standards (T 236 cm-85).

Statistical analysis

At least two biological replicates (two different rDyPAU10 productions) and three technical replicates were done for each experiment. The data were subjected to one-way analysis of variance (ANOVA) using GraphPad Prism version 10.0.0 with post-pair-wise comparison based on Tukey´s HSD (honestly significant difference) test when the ANOVA showed significant inequality of means. Statistical significance was determined at $p < 0.05$. For pairwise comparisons, a paired *t*-test was used with statistical significance set at $p < 0.05$.

Results

Effect of pH and temperature on the lignin modification rate

Table 1 shows the lignin modification rate of kraft lignin using rDyP-AU10, a commercial laccase, or the enzymatic combo at different pHs and temperatures. Results suggest that rDyP-AU10 or laccase shows higher values of modification rate at pH 4, rather than at pH 5, and at a temperature

Table 1 Kraft lignin modification rate at different pH and temperature

(AU/sec) × 10^{-03}						
	pH 4			pH 5		
Temperature (°C)	Enzymatic combo	rDyP-AU10	Laccase	Enzymatic combo	rDyP-AU10	Laccase
25	0.30 ± 0.05 *	0.80 ± 0.08 *	0.09 ± 0.02	0.30 ± 0.05 *	0.400 ± 0.004 *	0.09 ± 0.05
30	0.02 ± 0.01 *	0.040 ± 0.004 *	0.010 ± 0.001	0.40 ± 0.03 *	0.60 ± 0.05 *	0.200 ± 0.002
35	5.0 ± 0.4 *	5.0 ± 0.6 *	0.10 ± 0.07	0.90 ± 0.03 *	0.80 ± 0.05 *	0.10 ± 0.02
40	5.00 ± 0.04 *	5.00 ± 0.03 *	0.20 ± 0.04	0.80 ± 0.06 *	0.80 ± 0.04 *	0.06 ± 0.09
45	8.0 ± 0.3 *(**)	5.0 ± 0.5 *	0.40 ± 0.03	0.4 ± 0.2 *	1.00 ± 0.08 *	0.050 ± 0.006

Values are absorbance units at 465 nm per second (AU/sec), averaged from three independent replicates ± standard deviation. The reactions were conducted in the activity buffer (as described in Materials and Methods), with 10 µM kraft lignin and 0.76 EU of rDyP-AU10 (with 4 mM H_2O_2) and/or 2.5 EU of commercial laccase. Experiments without enzyme and/or H_2O_2 were performed as controls. * the asterisk means significant differences ($p < 0.05$) compared to the laccase treatment, determined by one-way ANOVA. (*) the asterisk in parenthesis means significant differences ($p < 0.05$) when comparing the enzymatic combo with rDyP-AU10 as determined by a Paired *t*-test, at 45 °C and pH 4

range from 35 to 45 °C. Under all tested conditions, rDyP-AU10 exhibited higher values for lignin modification, when compared with laccase. We obtained the best lignin modification rate using the combo at pH 4 and 45 °C, showing significant values higher than those obtained when treating the kraft lignin with rDyP-AU10 or the commercial laccase in individual experiments, at least at the tested conditions.

Chemical compounds detected during kraft lignin modification

Then, we faced the analysis of potential chemical modifications that could occur during the enzymatic process. We determined total phenolic compounds, ketones, aldehydes, and the profile of released compounds by HPLC at different treatment times (at pH 4 and 45 °C) (Fig. 1, 2, and 3).

Beyond certain fluctuations of values over time (discussed in the following section), we found that the enzymatic combo produces a significant increase in the formation of phenolic compounds as compared with the treatment with rDyP-AU10 and commercial laccase (Fig. 1a), suggesting that the combined use of both enzymes has a synergistic effect on the production of phenolic compounds.

Then, we decided to analyze the effect of potential mediator compounds, commonly used to increase the activity of laccases; we used veratryl alcohol (VA) and $MnCl_2$. We

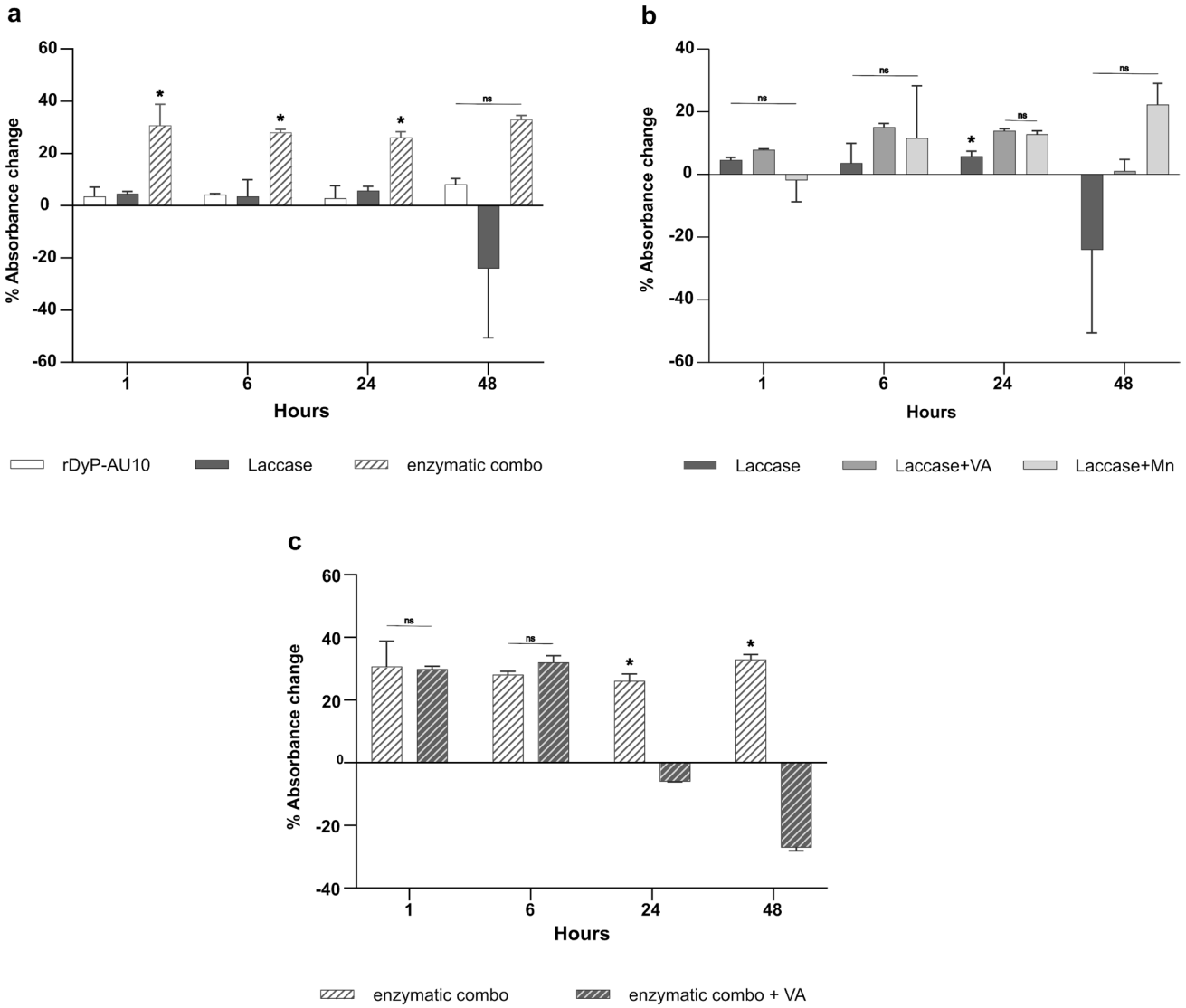

Fig. 1 The effect of enzymes in the formation of phenolic compounds, over time, using kraft lignin as a substrate. **1a)** The effect of rDyP-AU10, commercial laccase, and enzymatic combo; **1b)** the effect of the commercial laccase in the presence of mediator compounds, veratryl alcohol (VA) and $MnCl_2$ (Mn); **1c)** the effect of the enzymatic combo in the presence of VA. Data were plotted using GraphPad Prism 10.2.3 (403) software. Statistics compared values among treatments at the same time. ns means $p \geq 0.05$, and * means $p < 0.05$

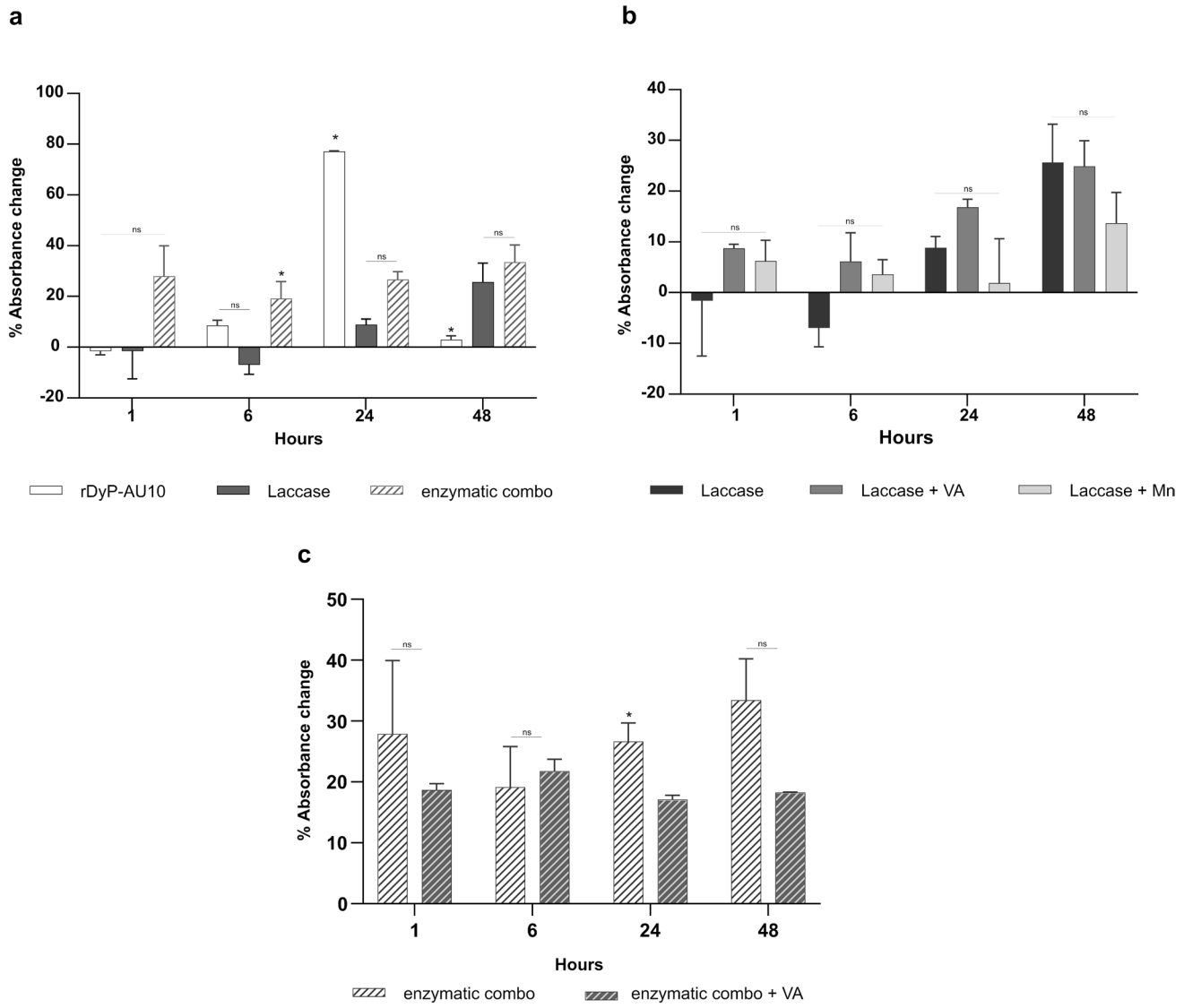

Fig. 2 The effect of enzymes in the formation of aldehydes and ketones, over time, using kraft lignin as a substrate. **1a)** The effect of rDyP-AU10, commercial laccase, and enzymatic combo; **1b)** the effect of the commercial laccase in the presence of mediator compounds, veratryl alcohol (VA) and $MnCl_2$ (Mn); **1c)** the effect of the enzymatic combo in the presence of VA. Data were plotted using GraphPad Prism 10.2.3 (403) software. Statistics compared values among treatments at the same time. ns means $p \geq 0.05$, and * means $p < 0.05$

found that these compounds significantly increased the number of phenolic compounds, at least 24 h after treatment, and these mediators may control the repolymerization activity (see Discussion), if any (Fig. 1b).

We also tested the effect of VA in the enzymatic combo activity, on kraft lignin; Fig. 1a shows that, in the absence of mediators, the combo significantly increased the formation of phenolic compounds yet observed at the first hour of incubation (*ca*. four times greater compared to the single enzymes), at the tested conditions. However, VA did not increase the formation of phenolic compounds; instead, they reduced their formation, at 24 and 48 h treatment.

The formation of ketones and aldehydes is shown in Fig. 2. Results suggest that rDyP-AU10 affects the formation of these compounds, showing an unexpected significant increase at 24 h treatment followed by a decrease at 48 h treatment (Fig. 2a). This effect was consistently observed using the different biological replicates. The commercial laccase catalyzed the formation of these compounds, which significantly increased the level of compounds at 48 h (Fig. 2a). In general, the enzymatic combo showed a better performance compared with rDyP-AU10, at least after 6 and 48 h treatment. We also found that the

molecular mediators did not increase the production of ketones and aldehydes (Fig. 2b).

We attempted to increase the activity of the enzymatic combo by using VA as a mediator. However, the results (Fig. 2c) show that VA is not an effective mediator of the enzymatic combo, as it may reduce the production of ketones and aldehydes. We wonder if VA has a detrimental effect on rDyP-AU10 activity; thus, we measured the peroxidase activity in the presence of VA using ABTS as a substrate, and we found that the peroxidase did not use VA as substrate and did not affect activity.

In summary, results suggest that single enzymes modified kraft lignin. However, values of phenolic compounds were significantly higher when we used the enzymatic combo, at least during the first 24 h of treatment; and aldehydes and ketones increased at 6 and 48 h, mainly when comparing the enzymatic combo with rDyP-AU10.

Analysis of the HPLC profile

The profile of produced compounds determined by HPLC analysis is shown in Fig. 3. We worked with samples collected at 24 h treatments (rDyP-AU10, commercial laccase, and enzymatic combo), with and without VA. We chose 24 h because results showed positive production of phenolic compounds, or aldehyde, and ketone, with no evidence of product repolymerization, as previously reported by other authors (see Discussion).

We first considered whether H_2O_2 and temperature (45 °C) might have a physicochemical effect on kraft lignin, independent of the enzymatic treatment. Therefore, we performed control experiments to determine the effect of the oxidant and temperature on the profile of produced compounds, as described in Material and Methods. We analyzed the HPLC profile of kraft lignin after 24 h of incubation with H_2O_2 at 45 °C and, at room temperature in a free-enzyme experiment (Fig. 3a). Although the HPLC profiles were similar under all tested conditions, we observed differences in peaks within the range of the shortest retention times (5.5 to 7.5 min; see inset in Fig. 3a). We also detected differences in the ranges 30–32, 35–37, and 38–42 min, mainly due to the temperature effect. Results suggest that the increase in temperature and the addition of H_2O_2 affect the profile of chemical compounds detected in kraft lignin. Thus, for further experiments including enzymes, we attributed the differences in these picks to a physicochemical effect on kraft lignin (by the increase in temperature and chemical oxidation by H_2O_2).

As H_2O_2 is required for rDyP-AU10 activity, we compared the chromatographic profiles obtained after treatment of kraft lignin with H_2O_2 and with the enzyme, at 45 °C. We observed changes in the profile of compounds, mainly at retention time from 32 to 48 min, suggesting that rDyP-AU10 impacted the chemical structure of kraft lignin.

Then, we implemented a sequential treatment: 1 h with H_2O_2 followed by 24 h treatment with rDyP-AU10 and additional H_2O_2 (Fig. 3b), as described in Materials and Methods. We detected changes by comparing the chromatogram obtained by treatment with the enzyme and the sequential one, such as the differences in the retention time range from 13 to 18 min. These differences could not be attributed to the addition of H_2O_2. However, we detected many differences in the range from 33 to 48 min, indicating the impact of the enzymatic treatment on the HPLC profile.

The next step was to analyze the HPLC profile of kraft lignin using the enzymatic combo and the single enzymes as the lignin-modifying systems (Fig. 3c). We zoomed on the two differential parts of the chromatograms (Fig. 3c1 and 3c2). We detected different profiles when kraft lignin was treated with rDyP-AU10 or the commercial laccase, and important differences in peaks when kraft lignin was treated with the enzymatic combo. In summary, these results show that rDyP-AU10 and the control commercial laccase, used alone or in combination (enzymatic combo), affect the chemical structure of kraft lignin.

Then, we faced the enzymatic modification of paper pulp as substrate, using the physicochemical conditions found to be optimal for kraft lignin modification (pH 4 and 45 °C).

Modification of cellulose pulp

The enzymatic effect of rDyP-AU10, commercial laccase, and the enzymatic combo was assessed on cellulose pulp from two stages of the production process. The samples were courtesy of the UPM company. As described above, we determined the kappa number of samples after each enzymatic treatment and performed the controls.

We found (Table 2) a decrease in the kappa number of both pulps, partly due to the oxidant activity of H_2O_2. We detected similar values of kappa number when samples were treated with the commercial laccase or rDyP-AU10, even without adding H_2O_2 during the treatment with the commercial laccase; the addition of the mediator VA did not improve pulp modification. We did not observe that the enzymatic combo improved pulp modification compared to the results obtained using the single enzymes, with or without the mediator VA. Moreover, the results suggest that VA had a negative effect when the enzymatic combo was used as a lignin-modifying system (see Fig. 1 and 2, as well as Table 2). We think the conditions for optimal use of the enzyme combo must still be set up.

Our key finding is that the cold-active enzyme, rDyP-AU10, modifies the lignin content of two commercial cellulose pulps; reducing the kappa number by 4 and 3 units for Pulp A and Pulp B, respectively.

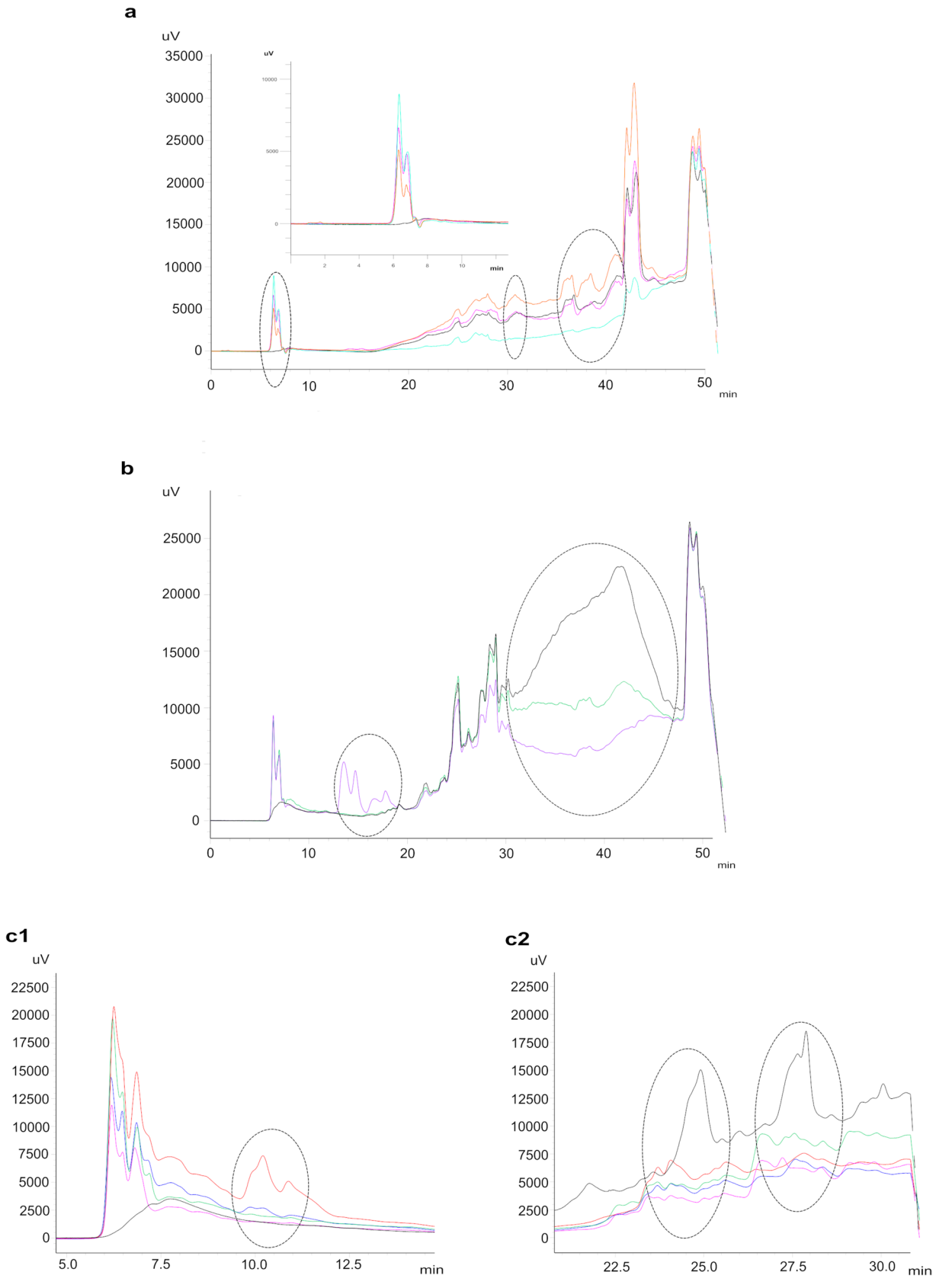
a
uV
35000
30000
25000
20000
15000
10000
5000
0
0
10
20
30
40
50
min
b
uV
25000
20000
15000
10000
5000
0
0
10
20
30
40
50
min
c1
uV
22500
20000
17500
15000
12500
10000
7500
5000
2500
0
5.0
7.5
10.0
12.5
min
c2
uV
22500
20000
17500
15000
12500
10000
7500
5000
2500
0
22.5
25.0
27.5
30.0
min

◂**Fig. 3** The HPLC profile of kraft lignin. The chromatogram shows new or enhanced product peaks produced by physicochemical (temperature, and hydrogen peroxide) and enzymatic treatments. **3a)** The effect of temperature (45 °C and 25 °C) and H_2O_2, in a free-enzyme experiment; colors are as follows: black is kraft lignin without any treatment, pink is kraft lignin with H_2O_2 at 45 °C; sky blue is kraft lignin with H_2O_2 at 25 °C; orange is kraft lignin without H_2O_2 at 45 °C; the inset zoom in of the shortest retention times (5.5 to 7.5 min). **3b)** The effect of H_2O_2 in different steps of kraft lignin treatment; colors are as follows: green is kraft lignin with H_2O_2 and rDyP-AU10 at 45 °C for 24 h; violet is a sequential treatment with H_2O_2 for 1 h, and then rDyP-AU10 with H_2O_2 for 1 h. **3c)** The effect of the enzymatic combo at 45 °C for 24 h; samples are as follows: blue is kraft lignin with laccase, green is kraft lignin with H_2O_2, and with rDyP-AU10, red is kraft lignin with H_2O_2 and the enzymatic combo, and pink is kraft lignin H_2O_2; the figure was split in **3c1)** and **3c2)** showing different range of retention times. All experiments were done using 10 µM kraft lignin and 4 mM H_2O_2. Chromatograms were analyzed using LCSolution—Shimadzu software. The images were designed in Inkscape 0.92/1.0. We marked the differences in the peaks with ellipses, which helps to distinguish differences between treatments. These differences in peak shapes and areas mean the presence of different chemical moieties

Discussion

Based on our previous results [13], rDyP-AU10 from *Pseudomonas* sp. AU10 showed the best activity conditions at 20 °C and pH 5 when using ABTS as a substrate; we also showed that it modifies kraft lignin. Now, we aimed to determine if rDyP-AU10 modifies cellulose pulp. Following this objective, we searched for the best pH and temperature conditions for lignin modification, using kraft lignin as a substrate, and analyzed some possible chemical modifications that could have occurred. Then, we analyzed the activity of rDyP-AU10 on cellulose pulp, using the previously determined conditions. We also used a commercial laccase, alone or in combination (enzymatic combo) with the recombinant peroxidase.

We demonstrated that rDyP-AU10 shows the best conditions for kraft lignin modification at pH 4 and in the range of 35–45 °C. Differences in the optimal activity conditions of rDyP-AU10 using either ABTS or lignin kraft were expected because substrates differentially interact with the amino acids in the catalytic site of enzymes. These interactions change with pH and temperature, affecting both amino acids and substrates, either favoring or disfavoring the binding and catalytic rate. Whatever substrate is used, ABTS or kraft lignin, rDyP-AU10 is a psychrophilic or cold-active enzyme, by definition [10, 11].

We wonder if the ability of rDyP-AU10 to modify kraft lignin has a meaning in the Antarctic context. *Pseudomonas* sp. AU10 is a psychrotolerant bacterium isolated from a water sample collected in Uruguay Lake, King George Island, Antarctica [14]. This continent never faces temperatures comparable to the range of optimal activity for kraft lignin modification. For instance, Esperanza station, near the northern tip of the Antarctic Peninsula (63.4°S, 57.0°E) reported 17.5 °C, the highest temperature detected in Antarctica [23]. Furthermore, Antarctica has a limited number of plants containing lignin; it only has two species of vascular plants (*Deschampsia antarctica* and *Colobanthus quitensis*), 33 moss species, and 68 lichen species [24]. We think that the ability of rDyP-AU10 for lignin's modification lacks biological meaning in the Antarctic environment. It might be a moonlighting activity (a secondary activity outside the normal one) or may have an alternative unknown natural substrate. Moonlighting proteins are ubiquitous and offer a plus because they allow microbes to perform different functions using the same protein, as was shown for glutathione peroxidase from different organisms [25, 26].

To the best of our knowledge, this is the first biochemical characterization of a DyP enzyme produced by a psychrotolerant bacterium, on kraft lignin as a substrate. Previously, Rahmanpour and Bugg (2015) [27] showed that the mesophilic and biological control bacterium *Pseudomonas fluorescens* Pf-5 produces a DyP that also modifies kraft lignin; they performed the experiments at 25 °C and pH 5.5 and did not search for the best conditions of activity. There is a thermo-relationship between psychrophilic/psychrotolerant and mesophilic organisms and the activity of their enzymes, which show a maximal catalytic efficiency at 40 °C and 60 °C, respectively [10, 11]. Thus, we think DyP from Pf-5 may have optimal activity above 25 °C.

Also, *Thermobifida fusca*, a thermophilic bacterium, produces a DyP with activity toward kraft lignin [28]; again, the authors analyzed the activity at pH 5.5 at 25 °C and did not determine the best conditions of activity. We believe that, among others, our contribution is to report the optimal conditions of activity where rDyP-AU10 (a cold-active enzyme; [13]) works best on kraft lignin, and to show the chemical modification of the substrate, opening up the potential application of rDyP-AU10 in the modification of cellulose pulp.

The combined use of enzymes, such as laccase and xylanase, in sequential and/or simultaneous systems to carry out delignification has been frequently described, even though xylanases are usually inactivated by laccase-generated oxidants [29]. Thus, we faced the analysis of mixing rDyP-AU10 and a commercial laccase (enzymatic combo) in the kraft lignin modification process. Instead of a laccase and a hydrolytic enzyme as a xylanase, we mixed two oxidative enzymes with a different mechanism of action [18]. The combined use of laccase and peroxidases (lignin- and Mn-peroxidase) was successfully reported during the enzymatic treatment of corn stover lignin [30]; this report encourages us to work with our peroxidase in combination with a laccase. Our results (Table 1) show that the enzymatic combo has an improved activity compared with the single enzymes, mainly at 45 °C and pH 4. Thus, we think DyPs from psychrophilic/psychrotolerant microbes could be included in the

Table 2 Effect of enzymes, the oxidant H_2O_2, and a mediator compound (veratryl alcohol) in the kappa number of cellulose pulps

Treatment	Kappa number	
	Pulp A	Pulp B
Control	40 ± 1	23 ± 2
H_2O_2	33 ± 3	21 ± 3
rDyP-AU10	29 ± 3 ***	18 ± 3
Laccase	29 ± 3 ***	17 ± 1 *
Laccase + VA	28 ± 2 ***	17 ± 4 *
Enzymatic combo	30 ± 3 **	17 ± 1 *
Enzymatic combo + VA	29 ± 1 ***	20 ± 1

Values are mean ± standard deviation of the kappa number, calculated from three independent replicates. VA is 5 mM veratryl alcohol. Pulp A and Pulp B were described in Materials and Methods. Control experiments correspond to untreated pulp. * Means significant differences ($p < 0.05$), as compared with the control treatment, as determined by one-way ANOVA

portfolio of enzymes that modify lignin, alone or in combination with laccases.

The chemical analyses of potential products produced during kraft lignin modification showed that rDyP-AU10, the commercial laccase, and the enzymatic combo may produce an increase in the content of phenolic compounds, aldehydes, and ketones. We found fluctuations in the values of chemical compounds, over time, suggesting potential depolymerization/repolymerization events guided by the enzymes. This phenomenon was previously observed during lignin modification with peroxidases [28] and laccases [31], and may imply the depolymerization and repolymerization via phenoxy radical formation and phenoxy radical coupling, respectively. More recently, Rashid and Bugg (2021) [22] showed that the recombinant DyP from the mesophilic *P. fluorescens* Pf-5 increases the content of phenolic compounds, aldehydes, and ketones; the authors also report that values of compounds varied over time, indicating that some repolymerization of compounds took place.

The results from the HPLC experiment support the modification of kraft lignin by the enzymatic treatment (single enzymes, or in combination) (Fig. 3). Results also show that H_2O_2 has an effect modifying kraft lignin, in the tested conditions. We detected new or enhanced product peaks as other authors reported [22, 29]. We cannot assign differences to specific chemical groups; we just detected the formation of new or enhanced product peaks. We found differences due to the temperature, oxidizing agent, and enzymes. We determined that moderate temperatures and low concentrations of H_2O_2 such as 45 °C and 4 mM, respectively, affect the kraft lignin chemical composition. For instance, the papermaking industry uses much higher temperatures and oxidizing agent concentrations during bleaching, such as 50 °C to 90 °C and 3 (0.88 M) to 5% (1.47 M) H_2O_2. The results support that the differences observed during the enzymatic treatment are due to physicochemical and biological factors. We did not identify the peaks, but the results show that rDyP-AU10 modifies kraft lignin.

Performing an elegant experimental procedure, Rashid and Bugg (2021) [22] showed that the combinations of different oxidases (DyP and multicopper oxidases) and accessory enzymes (arylsulfotransferase, β-etherase, dihydrolipoamide dehydrogenase, among others) enhance the release of phenolic compounds, ketones, and aldehydes from technical lignins. However, they did not include laccases in the experiments. They also found fluctuations in the values of chemical compounds produced over time and, suggested that the activity of DyP peroxidases is assisted by reductive accessory enzymes that may prevent repolymerization via trapping phenoxy radicals. We found that the enzymatic combo produces a 30% increase in absorbance for both phenolic compounds and ketones/aldehydes after 1 h and 24 h (even 48 h) of incubation, suggesting that there is a chemical modification observed as fast as at the first hour of incubation.

We analyzed if two mediator molecules of laccases increase the values of chemicals (phenols, ketones, and aldehydes) during the treatment of kraft lignin. Mediator systems are commonly used to improve laccase activity and showed increased depolymerization activity of industrial lignins (organosolv lignin, kraft lignin, and sodium lignosulfonate) [32, 33]. Herein, we showed that VA is not a good mediator assisting kraft lignin modification, at least in the tested conditions. We think a broader panel of mediators must be analyzed to find a suitable combination of laccase and mediator; however, the peroxidase rDyP-AU10, used alone or in combination with the commercial laccase, is our focus of work.

The best pH and temperature conditions for kraft lignin modification by rDyP-AU10 (45 °C and pH 4) are unfit for the delignification of cellulose pulp (see Introduction) in the cellulose paper-making industry. Still, the enzymatic system may improve the quality of cellulose pulp obtained after some stage of the paper-making process. According to UPM, the dried pulp (the final product, not paper) is obtained following these steps: cooking (wood is cooked with NaOH and H_2S at high pressure and temperature), washing (referred as Pulp A in this article), delignification (with O_2 in an alkaline medium), sieving (to separate knots and uncooked remains) and washing again; then, feeding of the tower with an acidified "unbleached pulp" (referred as Pulp B in this article), and a final bleaching (acid reactor and ClO_2/washing/alkaline reactor with H_2O_2

and O_2/washing/ClO_2/washing/H_2O_2 in alkaline medium/washing) and drying. We wonder if rDyP-AU10 (alone or in combination with the laccase) could be used as a biobleaching agent in some of these stages. We found that rDyP-AU10 reduces the kappa number of cellulose pulp, but this reduction is due, in part, to the bleaching effect of H_2O_2. The decrease in the kappa number was similar for both the peroxidase and the laccase, suggesting that both enzymes can be used for cellulose pulp modification. The enzymatic combo (with or without a mediator) did not show a synergic activity on cellulose pulp bleaching; we wonder if one enzyme produces oxidants that inactivate the other enzyme; as it was previously suggested by Woolridge (2014) [29].

Sahinkaya et al. (2019) [34] analyzed the DyP-type peroxidase from *Rhodococcus* sp. T1 such as a bleaching agent, and they found a decrease of 5.2 units for kappa number in eucalyptus kraft pulp. However, this number (5.2 units) includes the contribution of H_2O_2. rDyP-AU10 reduced 11 and 5 units of the kappa number for Pulp A and B, respectively; and 4 and 3 units if we remove the contribution of H_2O_2. These values sound so promising, mainly compared with the results reported by Arias et al. (2003) [21]. The authors analyzed the laccase from *Streptomyces cyaneus* CECT 3335 as a bleaching agent, and they found a decrease of 2.3 units for kappa number in eucalyptus kraft pulp, using ABTS as a mediator. In summary, our results suggest that rDyP-AU10 may be considered a candidate as a bleaching agent, at least for Pulp A.

In summary, the Antarctic bacterium *Pseudomonas* sp. AU10 produces a DyP that modifies kraft lignin and cellulose pulp. The recombinant enzyme has the best conditions of activity at 45 °C and pH 4 using kraft lignin as a substrate; in these conditions, the enzyme modifies kraft lignin. The enzyme also has activity as a biobleaching agent on cellulose pulps, as shown by the determination of the kappa number of treated samples.

Further works will face the in-depth study of conditions for the bleaching of different lignins using rDyP-AU10 as the modifying enzyme.

Acknowledgements The authors thank the Uruguayan Antarctic Institute for the logistic support during the stay in the Antarctic Base Artigas. S. Castro-Sowinski is member of the National Research System (SNI, Sistema Nacional de Investigadores).

Authors contributions CC performed most experiments, and data processing, and also contributed to writing the manuscript; DV performed the HPLC analyses and revised the manuscript; SCS had the main idea, achieved funding, guided the experiments, and wrote the manuscript. All authors read and approved the submitted version.

Funding This work was partially supported by the Program for the Development of Basic Sciences (PEDECIBA, Programa de Desarrollo de las Ciencias Básicas) and the Superior Council of Scientific Investigations (CSIC, Comisión Sectorial de Investigación Científica, Universidad de la República) (Projects ID 244). The work of CC was supported by the National Research and Innovation Agency (ANII, Agencia Nacional de Investigación e Innovación).

Data availability *Pseudomonas* sp. AU10 is part of the bacterial Antarctic collection deposited in the Sección Bioquímica, Facultad de Ciencias, Universidad de la República, Iguá 4225, Montevideo, Uruguay.

Declarations

Ethical approval No ethical approval is required for this study.

Consent to participate Not applicable.

Consent to publish Not applicable.

Competing interests The authors declare that they have no conflict of interest.

References

1. Adjei JK, Essumang DK, Twumasi E, Nyame E, Muah I (2019) Levels and risk assessment of residual phthalates, polycyclic aromatic hydrocarbons and semi-volatile chlorinated organic compounds in toilet tissue papers. Toxicol Reports 6:1263–1272. https://doi.org/10.1016/J.TOXREP.2019.11.013
2. Bajpai P (2018) Brief description of the pulp and papermaking process. Biotechnol Pulp Pap Process 9–26. https://doi.org/10.1007/978-981-10-7853-8_2
3. Rullifank KF, Roefinal ME, Kostanti M, Sartika L, Evelyn (2020) Pulp and paper industry: An overview on pulping technologies, factors, and challenges. IOP Conf Ser Mater Sci Eng 845:012005. https://doi.org/10.1088/1757-899X/845/1/012005
4. Bajpai P (2004) Biological bleaching of chemical pulps. Crit Rev Biotechnol 24:1–58. https://doi.org/10.1080/07388550490465817
5. Nagar S, Kumari K, Goyal S, Kharor N (2022) Chemical science review and letters different type of paper pulping and process of green bleaching. Chem Sci Rev Lett 11:410–416. https://doi.org/10.37273/chesci.cs205309534
6. Kumar A (2021) Biobleaching: An eco-friendly approach to reduce chemical consumption and pollutants generation. Phys Sci Rev 6:. https://doi.org/10.1515/PSR-2019-0044/XML
7. Chaurasia SK, Bhardwaj NK (2019) Biobleaching - An ecofriendly and environmental benign pulp bleaching technique: A review. J Carbohydr Chem 38:87–108. https://doi.org/10.1080/07328303.2019.1581888
8. Immerzeel P, Fiskari J (2023) Synergism of enzymes in chemical pulp bleaching from an industrial point of view: A critical review. Can J Chem Eng 101:312–321
9. Almeida N, Meyer V, Burnet A, Boucher J, Talens-Perales D, Pereira S, Ihalainen P, Levée T, Polaina J, Petit-Conil M, Camarero S, Pinto P (2022) Use of a novel extremophilic xylanase for an environmentally friendly industrial bleaching of kraft pulps. Int J Mol Sci 23:13423. https://doi.org/10.3390/IJMS232113423/S1
10. Ramón A, Esteves A, Villadóniga C, Chalar C, Castro-Sowinski S (2023) A general overview of the multifactorial adaptation to cold: biochemical mechanisms and strategies. Braz J Microbiol 54:2259–2287. https://doi.org/10.1007/S42770-023-01057-4
11. Feller G, Gerday C (2003) Psychrophilic enzymes: Hot topics in cold adaptation. Nat Rev Microbiol 1:200–208. https://doi.org/10.1038/nrmicro773

12. Bhatia RK, Ullah S, Hoque MZ, Ahmad I, Yang YH, Bhatt AK, Bhatia SK (2021) Psychrophiles: A source of cold-adapted enzymes for energy efficient biotechnological industrial processes. J Environ Chem Eng 9:104607. https://doi.org/10.1016/J.JECE.2020.104607
13. Cagide C, Marizcurrena JJ, Vallés D, Alvarez B, Castro-Sowinski S (2023) A bacterial cold-active dye-decolorizing peroxidase from an Antarctic *Pseudomonas* strain. Appl Microbiol Biotechnol 107:1707–1724. https://doi.org/10.1007/S00253-023-12405-7
14. Martínez-Rosales C, Castro-Sowinski S (2011) Antarctic bacterial isolates that produce cold-active extracellular proteases at low temperature but are active and stable at high temperature. Polar Res 30:. https://doi.org/10.3402/POLAR.V30I0.7123
15. Fullana N, Braña V, Marizcurrena JJ, Morales D, Betton J-M, Marín M, Castro-Sowinski S, Fullana N, Braña V, Marizcurrena JJ, Morales D, Betton J-M, Marín M, Castro-Sowinski S (2017) Identification, recombinant production and partial biochemical characterization of an extracellular cold-active serine-metalloprotease from an Antarctic *Pseudomonas* isolate. AIMS Bioeng 4:386–401. https://doi.org/10.3934/BIOENG.2017.3.386
16. García-Laviña CX, Castro-Sowinski S, Ramón A (2019) Reference genes for real-time RT-PCR expression studies in an Antarctic *Pseudomonas* exposed to different temperature conditions. Extremophiles 23:625–633. https://doi.org/10.1007/S00792-019-01109-4
17. García-Laviña CX, Morel MA, García-Gabarrot G, Castro-Sowinski S (2023) Phenotypic and resistome analysis of antibiotic and heavy metal resistance in the Antarctic bacterium *Pseudomonas* sp. AU10. Braz J Microbiol 54:2903–2913. https://doi.org/10.1007/S42770-023-01135-7
18. Cagide C, Castro-Sowinski S (2020) Technological and biochemical features of lignin-degrading enzymes: a brief review. Environ Sustain 3:371–389. https://doi.org/10.1007/S42398-020-00140-Y
19. Ahmad M, Taylor CR, Pink D, Burton K, Eastwood D, Bending GD, Bugg TDH (2010) Development of novel assays for lignin degradation: comparative analysis of bacterial and fungal lignin degraders. Mol Biosyst 6:815–821. https://doi.org/10.1039/B908966G
20. Ellis KJ, Morrison JF (1982) Buffers of constant ionic strength for studying pH-dependent processes. Methods Enzymol 87:405–426. https://doi.org/10.1016/S0076-6879(82)87025-0
21. Arias ME, Arenas M, Rodríguez J, Soliveri J, Ball AS, Hernández M (2003) Kraft pulp biobleaching and mediated oxidation of a nonphenolic substrate by laccase from *Streptomyces cyaneus* CECT 3335. Appl Environ Microbiol 69:1953–1958. https://doi.org/10.1128/AEM.69.4.1953-1958.2003
22. Rashid GMM, Bugg TDH (2021) Enhanced biocatalytic degradation of lignin using combinations of lignin-degrading enzymes and accessory enzymes. Catal Sci Technol 11:3568–3577. https://doi.org/10.1039/d1cy00431j
23. Turner J, Lu H, King JC, Carpentier S, Lazzara M, Phillips T, Wille J (2022) An extreme high temperature event in coastal east Antarctica associated with an atmospheric river and record summer downslope winds. Geophys Res Lett 49:1–11. https://doi.org/10.1029/2021GL097108
24. Parnikoza I, Kozeretska I, Kunakh V, Parnikoza I, Kozeretska I, Kunakh V (2011) Vascular plants of the maritime Antarctic: origin and adaptation. Am J Plant Sci 2:381–395. https://doi.org/10.4236/AJPS.2011.23044
25. Yadav P, Singh R, Sur S, Bansal S, Chaudhry U, Tandon V (2023) Moonlighting proteins: beacon of hope in era of drug resistance in bacteria. Crit Rev Microbiol 49:57–81. https://doi.org/10.1080/1040841X.2022.2036695
26. Foyer CH, Kunert K (2024) The ascorbate-glutathione cycle coming of age. J Exp Bot 75:2682–2699. https://doi.org/10.1093/JXB/ERAE023
27. Rahmanpour R, Bugg TDH (2015) Characterisation of Dyp-type peroxidases from *Pseudomonas fluorescens* Pf-5: Oxidation of Mn(II) and polymeric lignin by Dyp1B. Arch Biochem Biophys 574:93–98. https://doi.org/10.1016/J.ABB.2014.12.022
28. Rahmanpour R, Rea D, Jamshidi S, Fülöp V, Bugg TDH (2016) Structure of *Thermobifida fusca* DyP-type peroxidase and activity towards Kraft lignin and lignin model compounds. Arch Biochem Biophys 594:54–60. https://doi.org/10.1016/J.ABB.2016.02.019
29. Woolridge EM (2014) Mixed enzyme systems for delignification of lignocellulosic biomass. Catalysts 4:1–35. https://doi.org/10.3390/CATAL4010001
30. Zhang S, Dong Z, Shi J, Yang C, Fang Y, Chen G, Chen H, Tian C (2022) Enzymatic hydrolysis of corn stover lignin by laccase, lignin peroxidase, and manganese peroxidase. Bioresour Technol 361:. https://doi.org/10.1016/J.BIORTECH.2022.127699
31. Majumdar S, Lukk T, Solbiati JO, Bauer S, Nair SK, Cronan JE, Gerlt JA (2014) Roles of small laccases from *Streptomyces* in lignin degradation. Biochemistry 53:4047–4058. https://doi.org/10.1021/BI500285T
32. Euring M, Ostendorf K, Rühl M, Kües U (2022) Enzymatic oxidation of Ca-lignosulfonate and kraft lignin in different lignin-laccase-mediator-systems and MDF production. Front Bioeng Biotechnol 9:788622. https://doi.org/10.3389/FBIOE.2021.788622/BIBTEX
33. Dillies J, Vivien C, Chevalier M, Rulence A, Châtaigné G, Flahaut C, Senez V, Froidevaux R (2020) Enzymatic depolymerization of industrial lignins by laccase-mediator systems in 1,4-dioxane/water. Biotechnol Appl Biochem 67:774–782. https://doi.org/10.1002/BAB.1887
34. Sahinkaya M, Colak DN, Ozer A, Canakci S, Deniz I, Belduz AO (2019) Cloning, characterization and paper pulp applications of a newly isolated DyP type peroxidase from *Rhodococcus* sp. T1. Mol Biol Rep 46:569–580. https://doi.org/10.1007/S11033-018-4509-9

DISCUSIÓN GLOBALIZADORA

Desde el punto de vista económico, el proceso tradicional de blanqueo de pulpa de celulosa con productos químicos como el cloro o el dióxido de cloro suele presentar un costo inicial bajo por tonelada de pulpa tratada, debido a la disponibilidad y eficiencia inmediata de estos agentes (Tabla 2). Sin embargo, este modelo implica costos ambientales y operativos asociados al tratamiento de efluentes, la generación de compuestos tóxicos como los organoclorados, y posibles penalizaciones o inversiones requeridas para cumplir con normativas ambientales cada vez más estrictas.

En contraste, las estrategias enzimáticas, por ejemplo, basadas en xilanasas o EML pueden tener un costo inicial mayor en cuanto a adquisición o producción de las enzimas. No obstante, este costo puede compensarse por varios factores: la reducción en el uso de químicos agresivos y sus costos asociados, una menor carga contaminante en los efluentes que disminuye los requerimientos de tratamiento, y la posible conservación de la integridad de las fibras, lo que puede mejorar el rendimiento del producto final. Además, las condiciones operativas más suaves, propias del tratamiento enzimático, pueden reducir el desgaste de los equipos y el consumo energético. Estudios piloto y reportes de implementación parcial, como el caso de UPM en su planta de Alemania, han demostrado que la integración de enzimas como etapa previa o complementaria al blanqueo químico puede reducir el consumo de dióxido de cloro entre un 15 % y un 30 %, lo que representa un ahorro económico neto en procesos bien optimizados [84, 85]. Por ejemplo, el uso industrial de la hemicelulasa comercial Albazyme-10, en Canadá, permitió reducir el consumo de dióxido de cloro en un 15–20 %, con un ahorro estimado de aproximadamente 5 dólares por tonelada de pulpa procesada [86]. Asimismo, se ha reportado una reducción significativa en los niveles de compuestos orgánicos clorados (AOX) en los efluentes, con disminuciones de hasta un 28 % [84], así como un ahorro energético de hasta 468 MJ por tonelada de pulpa tratada [87].

Si bien la implementación de tecnologías enzimáticas aún enfrenta desafíos técnicos y económicos, su adopción progresiva puede ofrecer ventajas significativas tanto desde el punto de vista ambiental como financiero, especialmente en un contexto de regulación ambiental creciente y presión por la sostenibilidad industrial. En los últimos años, los avances en biotecnología y en ingeniería de proteínas han contribuido a reducir la brecha entre el desarrollo científico y las exigencias operativas del entorno industrial. En particular, la integración de herramientas como la inteligencia artificial y la biología sintética en el descubrimiento y diseño racional de enzimas está generando biocatalizadores con

propiedades mejoradas, como mayor estabilidad, eficiencia y especificidad, lo que fortalece su potencial como alternativas tecnológicas de alto rendimiento y refuerza su viabilidad para aplicaciones a escala industrial [88–90].

Tabla 2. Comparación técnica y económica entre el blanqueo químico tradicional y el pre-blanqueo enzimático

Indicador	**Blanqueo químico***	**Pre-blanqueo enzimático**
ClO_2 usado	100%	-15-20%
AOX en efluentes	Alta	-25-28%
Ahorro químico	-	+≈ 5 USD/t de pulpa
Consumo energético	-	250–468 MJ/t

Los valores indicados representan rangos típicos reportados en estudios piloto e industriales [84, 85, 87]. Los resultados pueden variar según el tipo de pulpa, las condiciones del proceso y la formulación enzimática empleada.

*Blanqueo químico tradicional

El trabajo desarrollado en el marco de esta tesis doctoral se inserta en este escenario, con el objetivo de identificar, producir en forma recombinante y caracterizar enzimas bacterianas con potencial para la modificación de lignina, un área de gran interés por sus aplicaciones en la industria papelera, biorrefinerías y procesos de biorremediación. Los resultados obtenidos permitieron avanzar desde una visión general del potencial biotecnológico de las enzimas modificadoras de lignina hacia la descripción detallada de casos concretos, aportando evidencia experimental inédita y publicaciones arbitradas que consolidan una línea de investigación en expansión.

En primer lugar, la revisión publicada en 2020 sistematizó el conocimiento sobre las principales enzimas modificadoras de lignina, destacando su versatilidad catalítica y la variedad de sustratos que pueden transformar. En ese trabajo se discutieron los mecanismos de acción de las laccasas y las peroxidasas, así como los desafíos técnicos que limitan su uso industrial, como la necesidad de mediadores, la baja estabilidad en condiciones extremas y el problema de la repolimerización de los productos derivados de lignina. Esta síntesis constituyó el punto de partida conceptual para el desarrollo experimental posterior, orientado a la exploración de nuevas fuentes microbianas y al análisis de enzimas con características singulares, como las adaptadas al frío. En este contexto, la

caracterización de la peroxidasa DyP-AU10 constituye uno de los principales aportes de la tesis, ya que demostró tener rasgos psicrófilos, incluyendo la actividad a bajas temperaturas, además de modificar lignina kraft y decolorar tintas. Estos hallazgos coinciden con reportes de otras DyPs bacterianas activas a temperaturas moderadas, como las de *Pseudomonas putida* o *Rhodococcus jostii*, donde se describieron bolsillos catalíticos amplios y cierta flexibilidad estructural [29, 91, 92]. En comparación, rDyP-AU10 mostró una marcada sensibilidad térmica, con inactivación rápida a 60 °C. Este comportamiento puede interpretarse de distintas maneras: por un lado, representa una limitación frente a procesos industriales que habitualmente se realizan a temperaturas elevadas; por otro, podría constituir una ventaja en aplicaciones que se benefician de condiciones suaves de operación, donde la fácil inactivación enzimática simplifica el control del proceso. Esto plantea un desafío interesante: ¿es más valioso apostar a enzimas psicrófilas, fáciles de inactivar por aumento de temperatura, que podrían adaptarse a esquemas de bajo consumo energético o procesos secuenciales controlados, o priorizar enzimas termotolerantes, como algunas xilasas o peroxidasas fúngicas, que ya fueron probadas en escalas piloto con buenos resultados?

En relación con la acción de las enzimas sobre lignina kraft, los resultados obtenidos con rDyP-AU10 mostraron la generación de fenoles, aldehídos y cetonas. Aunque la magnitud de este efecto fue más moderada que la reportada para otras enzimas termotolerantes validadas en condiciones industriales [93], los datos obtenidos en esta tesis confirman la capacidad de la enzima para actuar sobre un sustrato complejo y real, como es la lignina kraft. Esto sugiere la posibilidad de evaluar si rDyP-AU10 podría desempeñar un papel más complementario dentro de consorcios enzimáticos, en lugar de ser un sustituto directo de los químicos de blanqueo, aportando beneficios particulares en ciertas condiciones de proceso.

El análisis de la combinación de rDyP-AU10 con una laccasa comercial mostró interacciones interesantes en la generación de compuestos fenólicos, aunque no se evidenció sinergia clara en la reducción del número kappa. Este hallazgo contrasta con algunos reportes que describen sinergia entre laccasas y peroxidasas, especialmente en presencia de mediadores, logrando mayor decoloración o degradación de lignina [94]. El hecho de, en nuestras condiciones, no se observara este efecto abre otras interrogantes: ¿podría deberse a la naturaleza bacteriana de la DyP, distinta de las peroxidasas fúngicas habitualmente estudiadas? ¿o a las limitaciones de estabilidad y cinética observadas bajo las condiciones ensayadas? Estos resultados sugieren que la complementariedad entre laccasas y DyPs no es un fenómeno universal, sino dependiente de la especificidad de cada enzima y del diseño experimental, lo que a su vez resalta la necesidad de seguir explorando combinaciones y condiciones de reacción más amplias.

Por otro lado, la identificación de una laccasa periplásmica en *S. meliloti* CE52G constituye un hallazgo novedoso que amplía el espectro de bacterias con potencial oxidativo sobre lignina. Sin embargo, hasta ahora la mayoría de los estudios exitosos a escala piloto o industrial se han basado en laccasas fúngicas de alto potencial redox, capaces de oxidar incluso compuestos no fenólicos. Comparada con estas, la laccasa de CE52G aún debe ser evaluada en cuanto a actividad, estabilidad y necesidad de mediadores para estimar su verdadero potencial. Además, la dificultad encontrada para expresar en forma activa laccasas bacterianas en *E. coli* refuerza la percepción de que, si bien existen nuevas fuentes genéticas, todavía resta superar importantes barreras biotecnológicas antes de lograr un uso real en la industria.

CONCLUSIONES

En conjunto, la tesis demuestra que la investigación de enzimas degradadoras de lignina bacterianas provenientes de ambientes extremos, como la Antártida, constituye una vía prometedora para diversificar el portafolio de biocatalizadores aplicables a la industria papelera y posibilidades en procesos de biorremediación. Los resultados publicados y los experimentos inéditos aquí presentados permiten concluir que: i) Es posible producir y caracterizar enzimas bacterianas con actividad modificadora de lignina, como DyP-AU10, que presentan propiedades diferenciales frente a las enzimas fúngicas clásicas. ii) Estas enzimas muestran capacidad para actuar sobre sustratos industriales reales, aunque sus efectos deben entenderse en clave de complementariedad más que de reemplazo de productos actualmente utilizados a nivel industrial. iii) El hallazgo de nuevas laccasas bacterianas amplía el horizonte de biocatalizadores disponibles y abre oportunidades para el diseño de consorcios enzimáticos adaptados a condiciones específicas. iv) Las limitaciones técnicas encontradas en la expresión recombinante y estabilidad constituyen desafíos que deberán ser abordados mediante ingeniería de proteínas, coexpresión de chaperonas y optimización de sistemas de producción. v) Desde la perspectiva económica e industrial, los resultados se insertan en un escenario de creciente presión regulatoria y demanda de procesos sostenibles, donde la aplicación de enzimas modificadoras de lignina puede generar ahorros en químicos, energía y tratamiento de efluentes, además de mejorar la calidad del producto final, implementando un sistema de producción más amigable con el ambiente.

Finalmente, esta tesis contribuye al aporte de conocimiento original sobre enzimas bacterianas modificadoras de lignina, destacando la relevancia de fuentes no tradicionales como los ambientes

antárticos. Los resultados obtenidos, tanto publicados como inéditos, sientan bases sólidas para el desarrollo futuro de bioprocesos que reduzcan la dependencia de tratamientos químicos agresivos y promuevan la adopción de alternativas más limpias y sostenibles en la transformación de biomasa lignocelulósica.

PERSPECTIVAS

Los resultados alcanzados en esta tesis doctoral abren múltiples aristas de investigación y desarrollo que pueden potenciar el uso de enzimas bacterianas modificadoras de lignina en bioprocesos sostenibles. En primer lugar, el caso de la peroxidasa DyP-AU10 demuestra que los ambientes extremos, como la Antártida, constituyen reservorios valiosos de biocatalizadores con propiedades singulares. Un desafío inmediato consiste en profundizar en la ingeniería de proteínas. La inestabilidad térmica observada en DyP-AU10 sugiere la necesidad de explorar estrategias de ingeniería orientadas a mejorar su robustez, por ejemplo, mediante el diseño racional de sitios activos y regiones de flexibilidad que puedan conferir mayor estabilidad, sin comprometer la actividad catalítica. En este sentido, el uso de metodologías basadas en inteligencia artificial y predicciones estructurales (como AlphaFold para identificar regiones desordenadas o sensibles, o Rosetta para modelar y evaluar mutaciones estabilizantes) puede acelerar la generación de variantes más resistentes a la temperatura y con mejor desempeño en condiciones industriales.

Desde el punto de vista funcional, será relevante profundizar en los estudios de consorcios enzimáticos, evaluando combinaciones de DyPs, laccasas, xilasas y/o enzimas auxiliares bajo un rango más amplio de condiciones, en presencia de mediadores adecuados o en matrices lignocelulósicas diferentes.

Otro camino promisorio para profundizar la línea de investigación, una vez sorteados los obstáculos de estabilidad de las enzimas, radica en el estudio de la acción enzimática sobre matrices complejas a escala piloto, lo que permitirá evaluar, en condiciones cercanas a las industriales, aspectos como estabilidad operacional, reusabilidad y compatibilidad con procesos de blanqueo existentes. En este sentido, la colaboración con la industria papelera y de biorrefinerías será clave para validar la aplicabilidad real y cuantificar beneficios económicos y ambientales.

Además de su potencial en la industria papelera, la capacidad de rDyP-AU10 para decolorar tintes textiles posiciona a esta enzima como una candidata atractiva para aplicaciones en biorremediación de efluentes industriales, particularmente aquellos provenientes del sector textil, que constituyen una fuente relevante de contaminantes aromáticos recalcitrantes. El uso de DyPs bacterianas adaptadas a bajas temperaturas podría facilitar la implementación de tratamientos enzimáticos en condiciones ambientales, reduciendo los costos energéticos del proceso. No obstante, un aspecto crítico a abordar en futuros estudios será la caracterización de los compuestos derivados de la oxidación enzimática. La decoloración no garantiza necesariamente una disminución de la toxicidad, ya que algunos subproductos pueden conservar actividad biológica o incluso resultar más tóxicos que los colorantes parentales. Por ello, será necesario evaluar no solo la eficacia de rDyP-AU10 frente a mezclas complejas de tintes y compuestos fenólicos en efluentes reales, sino también el perfil de toxicidad de los productos generados, mediante bioensayos ecotoxicológicos y análisis químicos complementarios, a fin de validar su verdadera contribución a procesos de remediación ambiental.

En paralelo, el descubrimiento de una laccasa periplásmica en *Sinorhizobium meliloti* CE52G invita a profundizar en la caracterización de laccasas bacterianas. Su rol en la pigmentación, tolerancia al estrés y producción de compuestos bioactivos sugiere que estas enzimas podrían tener aplicaciones más allá del ámbito papelero, incluyendo biorremediación de contaminantes y síntesis de materiales funcionales.

A futuro, será necesario explorar estrategias más específicas de optimización de la expresión recombinante, incluyendo el uso de cepas de *E. coli* diseñadas para una traducción más eficiente de genes con codones poco frecuentes, como Rosetta™, o bien la coexpresión con chaperonas que favorezcan el correcto plegamiento y la incorporación de cobre en el sitio activo. De igual manera, la incorporación de péptidos señal alternativos que dirijan a las laccasas hacia el periplasma podría mejorar su maduración oxidativa, un aspecto crítico en este tipo de enzimas. En paralelo, resulta promisorio evaluar sistemas heterólogos distintos, como levaduras (*Pichia pastoris*), bacterias Gram positivas como *Bacillus subtilis* o incluso plataformas fúngicas, que ofrecen entornos más compatibles para enzimas multicobre y aumentan las posibilidades de obtener variantes activas y estables a escala. En este sentido, cabe destacar que otro integrante de la Sección Bioquímica ha logrado recientemente producir esta laccasa en *Aspergillus* como microorganismo recombinante, lo cual refuerza la viabilidad de explorar alternativas fúngicas para la obtención de enzimas funcionales.

En conjunto, las perspectivas a futuro señalan un camino claro: pasar de la caracterización básica hacia la maduración tecnológica de las enzimas bacterianas oxidativas, combinando bioprospección,

ingeniería de proteínas, validación a escala piloto y análisis de impacto económico y ambiental. Este camino será esencial para consolidar a estas herramientas biotecnológicas como verdaderas alternativas dentro de la bioeconomía y la transición hacia procesos industriales más sostenibles.

BIBLIOGRAFÍA

1. UNECE/FAO (2024) Forest products annual market review 2023–2024. ECE/TIM/SP/58. United Nations, Geneva. ISBN 978-92-1-003184-4
2. FAO. 2024. Pulp and paper capacities, survey 2023–2025/Capacités de la pâte et du papier, enquête 2023-2025/Capacidades de pulpa y papel, estudio 2023-2025. Rome/Roma.
3. Bajpai P, Anand A, Bajpai PK (2006) Bleaching with lignin-oxidizing enzymes. Biotechnol Annu Rev 12:349–378. https://doi.org/10.1016/S1387-2656(06)12010-4
4. Bajpai, P. (2004). Biological bleaching of chemical pulps. *Critical reviews in biotechnology*, *24*(1), 1-58
5. Virk AP, Sharma P, Capalash N (2012) Use of laccase in pulp and paper industry. Biotechnol Prog 28:21–32. https://doi.org/10.1002/btpr.727
6. Walia A, Guleria S, Mehta P, Chauhan A, Parkash J (2017) Microbial xylanases and their industrial application in pulp and paper biobleaching: a review. 3 Biotech 7:1–12. https://doi.org/10.1007/s13205-016-0584-6
7. ONYSKO KA (1993) Biological bleaching of chemical pulps. Biotech Adv 11:179–198. https://doi.org/10.1016/0734-9750(93)90040-t
8. Kumar A, Chandra R (2020) Ligninolytic enzymes and its mechanisms for degradation of lignocellulosic waste in environment. Heliyon 6:1–4. https://doi.org/10.1016/j.heliyon.2020.e03170
9. Haile A, Gelebo GG, Tesfaye T, Mengie W, Mebrate MA, Abuhay A, Limeneh DY (2021) Pulp and paper mill wastes: utilizations and prospects for high value-added biomaterials. Bioresour Bioprocess 8:. https://doi.org/10.1186/s40643-021-00385-3
10. Ding K, Liu D, Chen X, Zhang H, Shi S, Guo X, Zhou L, Han L, Xiao W (2024) Scalable lignocellulosic biorefineries: Technoeconomic review for efficient fermentable sugars production. Renew Sustain Energy Rev 202:114692. https://doi.org/10.1016/j.rser.2024.114692
11. Sheng Y, Lam SS, Wu Y, Ge S, Wu J, Cai L, Huang Z, Le Q Van, Sonne C, Xia C (2021) Enzymatic conversion of pretreated lignocellulosic biomass: A review on influence of structural changes of lignin. Bioresour Technol 324:124631. https://doi.org/10.1016/j.biortech.2020.124631
12. Hasunuma T, Okazaki F, Okai N, Hara KY, Ishii J, Kondo A (2013) A review of enzymes and microbes for lignocellulosic biorefinery and the possibility of their application to consolidated bioprocessing technology. Bioresour Technol 135:513–522. https://doi.org/10.1016/j.biortech.2012.10.047

13. Krasznai DJ, Champagne Hartley R, Roy HM, Champagne P, Cunningham MF (2018) Compositional analysis of lignocellulosic biomass: conventional methodologies and future outlook. Crit Rev Biotechnol 38:199–217. https://doi.org/10.1080/07388551.2017.1331336
14. Zoghlami A, Paës G (2019) Lignocellulosic Biomass: Understanding Recalcitrance and Predicting Hydrolysis. Front Chem 7:. https://doi.org/10.3389/fchem.2019.00874
15. Singh AK, Bilal M, Iqbal HMN, Meyer AS, Raj A (2021) Bioremediation of lignin derivatives and phenolics in wastewater with lignin modifying enzymes: Status, opportunities and challenges. Sci Total Environ 777:. https://doi.org/10.1016/j.scitotenv.2021.145988
16. Kumar A, Chandra R (2020) Ligninolytic enzymes and its mechanisms for degradation of lignocellulosic waste in environment. Heliyon 6:e03170. https://doi.org/10.1016/j.heliyon.2020.e03170
17. Sharma N, Bhardwaj NK, Singh RBP (2020) Environmental issues of pulp bleaching and prospects of peracetic acid pulp bleaching: A review. J Clean Prod 256:120338. https://doi.org/10.1016/j.jclepro.2020.120338
18. Martínez ÁT, Speranza M, Ruiz-Dueñas FJ, Ferreira P, Camarero S, Guillén F, Martínez MJ, Gutiérrez A, Del Río JC (2005) Biodegradation of lignocellulosics: Microbial, chemical, and enzymatic aspects of the fungal attack of lignin. Int Microbiol 8:195–204. https://doi.org/10.2436/im.v8i3.9526
19. Janusz G, Pawlik A, Sulej J, Świderska-Burek U, Jarosz-Wilkolazka A, Paszczyński A (2017) Lignin degradation: Microorganisms, enzymes involved, genomes analysis and evolution. FEMS Microbiol Rev 41:941–962. https://doi.org/10.1093/femsre/fux049
20. Sharma A, Thakur VV, Shrivastava A, Jain RK, Mathur RM, Gupta R, Kuhad RC (2014) Xylanase and laccase based enzymatic kraft pulp bleaching reduces adsorbable organic halogen (AOX) in bleach effluents: A pilot scale study. Bioresour Technol 169:96–102. https://doi.org/10.1016/j.biortech.2014.06.066
21. De Araújo JHB, De Moraes FF, Zanin GM (1999) Bleaching of kraft pulp with commercial xylanases. Appl Biochem Biotechnol - Part A Enzym Eng Biotechnol 77–79:713–722. https://doi.org/10.1385/abab:79:1-3:713
22. Sridevi A, Ramanjaneyulu G, Suvarnalatha Devi P (2017) Biobleaching of paper pulp with xylanase produced by Trichoderma asperellum. 3 Biotech 7:1–9. https://doi.org/10.1007/s13205-017-0898-z
23. Bajpai PK (2010) Solving the problems of recycled fiber processing with enzymes. BioResources 5:1311–1325. https://doi.org/10.15376/biores.5.2.1311-1325
24. Kmiotek M, Dybka-Stępień K, Karmazyn A (2021) Mild Enzymatic Treatment of Bleached Pulp

for Tissue Production. BioResources 16:4221–4236. https://doi.org/10.15376/biores.16.2.4221-4236

25. Žnidaršič-Plazl P, Rutar V, Ravnjak D (2009) The effect of enzymatic treatments of pulps on fiber and paper properties. Chem Biochem Eng Q 23:497–506
26. Ali and Sreekrishnan (2001) Paper mill eflluent toxicity.pdf. Adv Environ Res 5:175–196. https://doi.org/https://doi.org/10.1016/S1093-0191(00)00055-1
27. Pokhrel D, Viraraghavan T (2004) Treatment of pulp and paper mill wastewater — a review. 333:37–58. https://doi.org/10.1016/j.scitotenv.2004.05.017
28. Cagide C, Castro-Sowinski S (2020) Technological and biochemical features of lignin-degrading enzymes: a brief review. Environ Sustain 3:371–389. https://doi.org/10.1007/s42398-020-00140-y
29. Cagide C, Marizcurrena JJ, Vallés D, Alvarez B, Castro-Sowinski S (2023) A bacterial cold-active dye-decolorizing peroxidase from an Antarctic Pseudomonas strain. Appl Microbiol Biotechnol 107:1707–1724. https://doi.org/10.1007/s00253-023-12405-7
30. Cagide C, García-Laviña CX, Morel MA, Castro-Sowinski S (2023) Descriptive analysis of the draft genome from the melanin-producing bacterium Sinorhizobium (Ensifer) meliloti CE52G. Environ Sustain 6:259–270. https://doi.org/10.1007/s42398-023-00273-w
31. Cagide C, Vallés D, Castro-Sowinski S (2024) Kraft lignin biobleaching by a dye-decolorizing peroxidase from the Antarctic Pseudomonas sp. AU10 strain. Brazilian J Microbiol 2:. https://doi.org/10.1007/s42770-024-01595-5
32. Kim SJ, Shoda M (1999) Purification and characterization of a novel peroxidase from Geotrichum candidum Dec 1 involved in decolorization of dyes. Appl Environ Microbiol 65:1029–1035. https://doi.org/10.1128/aem.65.3.1029-1035.1999
33. Sugano Y, Yoshida T (2021) Dyp-type peroxidases: Recent advances and perspectives. Int J Mol Sci 22:. https://doi.org/10.3390/ijms22115556
34. Zámocký M, Hofbauer S, Schaffner I, Gasselhuber B, Nicolussi A, Soudi M, Pirker KF, Furtmüller PG, Obinger C (2015) Independent evolution of four heme peroxidase superfamilies. Arch Biochem Biophys 574:108–119. https://doi.org/10.1016/j.abb.2014.12.025
35. Sugano Y (2009) DyP-type peroxidases comprise a novel heme peroxidase family. Cell Mol Life Sci 66:1387–1403. https://doi.org/10.1007/s00018-008-8651-8
36. Ramón A, Esteves A, Villadóniga C, Chalar C, Castro-Sowinski S (2023) A general overview of the multifactorial adaptation to cold: biochemical mechanisms and strategies. Brazilian J Microbiol 54:2259–2287. https://doi.org/10.1007/s42770-023-01057-4

37. Reiss R, Ihssen J, Richter M, Eichhorn E, Schilling B, Thöny-Meyer L (2013) Laccase versus Laccase-Like Multi-Copper Oxidase: A Comparative Study of Similar Enzymes with Diverse Substrate Spectra. PLoS One 8:. https://doi.org/10.1371/journal.pone.0065633
38. Janusz G, Pawlik A, Świderska-Burek U, Polak J, Sulej J, Jarosz-Wilkołazka A, Paszczyński A (2020) Laccase properties, physiological functions, and evolution. Int J Mol Sci 21:. https://doi.org/10.3390/ijms21030966
39. Upadhyay P, Shrivastava R, Agrawal PK (2016) Bioprospecting and biotechnological applications of fungal laccase. 3 Biotech 6:1–12. https://doi.org/10.1007/s13205-015-0316-3
40. Nunes CS, Kunamneni A (2018) Laccases-properties and applications. Elsevier Inc.
41. Guan ZB, Luo Q, Wang HR, Chen Y, Liao XR (2018) Bacterial laccases: promising biological green tools for industrial applications. Cell Mol Life Sci 75:3569–3592. https://doi.org/10.1007/s00018-018-2883-z
42. Arregui L, Ayala M, Gómez-Gil X, Gutiérrez-Soto G, Hernández-Luna CE, Herrera De Los Santos M, Levin L, Rojo-Domínguez A, Romero-Martínez D, Saparrat MCN, Trujillo-Roldán MA, Valdez-Cruz NA (2019) Laccases: structure, function, and potential application in water bioremediation. Microb Cell Fact 18:1–33. https://doi.org/10.1186/s12934-019-1248-0
43. Castro-Sowinski S, Matan O, Bonafede P, Okon Y (2007) A thioredoxin of Sinorhizobium meliloti CE52G is required for melanin production and symbiotic nitrogen fixation. Mol Plant-Microbe Interact 20:986–993. https://doi.org/10.1094/MPMI-20-8-0986
44. Rosconi F, Fraguas LF, Martínez-Drets G, Castro-Sowinski S (2005) Purification and characterization of a periplasmic laccase produced by Sinorhizobium meliloti. Enzyme Microb Technol 36:800–807. https://doi.org/10.1016/j.enzmictec.2005.01.003
45. Castro-Sowinski S, Martinez-Drets G, Okon Y (2002) Laccase activity in melanin-producing strains of Sinorhizobium meliloti. FEMS Microbiol Lett 209:119–125. https://doi.org/10.1111/j.1574-6968.2002.tb11119.x
46. Castro S (2000) Methods to evaluate nodulation competitiveness between Sinorhizobium meliloti strains using melanin production as a marker. 41:173–177
47. Solano F, Lucas-Elío P, López-Serrano D, Fernández E, Sanchez-Amat A (2001) Dimethoxyphenol oxidase activity of different microbial blue multicopper proteins. FEMS Microbiol Lett 204:175–181. https://doi.org/10.1016/S0378-1097(01)00400-1
48. Gasteiger E, Hoogland C, Gattiker A, Duvaud S, Wilkins MR, Appel RD, Bairoch A (2005) The Proteomics Protocols Handbook. Proteomics Protoc Handb 571–608. https://doi.org/10.1385/1592598900
49. Bjellqvist B, Basse B, Olsen E, Celis JE (1994) Reference points for comparisons of two-

dimensional maps of proteins from different human cell types defined in a pH scale where isoelectric points correlate with polypeptide compositions. Electrophoresis 15:529–539. https://doi.org/10.1002/elps.1150150171

50. Bjellqvist B, Hughes GJ, Pasquali C, Paquet N, Ravier F, Sanchez J -C, Frutiger S, Hochstrasser D (1993) The focusing positions of polypeptides in immobilized pH gradients can be predicted from their amino acid sequences. Electrophoresis 14:1023–1031. https://doi.org/10.1002/elps.11501401163
51. Yu NY, Wagner JR, Laird MR, Melli G, Rey S, Lo R, Dao P, Cenk Sahinalp S, Ester M, Foster LJ, Brinkman FSL (2010) PSORTb 3.0: Improved protein subcellular localization prediction with refined localization subcategories and predictive capabilities for all prokaryotes. Bioinformatics 26:1608–1615. https://doi.org/10.1093/bioinformatics/btq249
52. Almagro Armenteros JJ, Tsirigos KD, Sønderby CK, Petersen TN, Winther O, Brunak S, von Heijne G, Nielsen H (2019) SignalP 5.0 improves signal peptide predictions using deep neural networks. Nat Biotechnol 37:420–423. https://doi.org/10.1038/s41587-019-0036-z
53. Nielsen H, Engelbrecht J (1997) Identification of prokaryotic and eukaryotic signal peptides and prediction of their cleavage sites Artificial neural networks have been used for many biological. Protein Eng 10:1–6. https://doi.org/10.1142/S0129065797000537
54. Sigrist CJA, De Castro E, Cerutti L, Cuche BA, Hulo N, Bridge A, Bougueleret L, Xenarios I (2013) New and continuing developments at PROSITE. Nucleic Acids Res 41:344–347. https://doi.org/10.1093/nar/gks1067
55. Madeira F, Madhusoodanan N, Lee J, Eusebi A, Niewielska A, Tivey ARN, Lopez R, Butcher S (2024) The EMBL-EBI Job Dispatcher sequence analysis tools framework in 2024. Nucleic Acids Res 52:W521–W525. https://doi.org/10.1093/nar/gkae241
56. Blum M, Chang HY, Chuguransky S, Grego T, Kandasaamy S, Mitchell A, Nuka G, Paysan-Lafosse T, Qureshi M, Raj S, Richardson L, Salazar GA, Williams L, Bork P, Bridge A, Gough J, Haft DH, Letunic I, Marchler-Bauer A, Mi H, Natale DA, Necci M, Orengo CA, Pandurangan AP, Rivoire C, Sigrist CJA, Sillitoe I, Thanki N, Thomas PD, Tosatto SCE, Wu CH, Bateman A, Finn RD (2021) The InterPro protein families and domains database: 20 years on. Nucleic Acids Res 49:D344–D354. https://doi.org/10.1093/nar/gkaa977
57. Ceroni A, Passerini A, Vullo A, Frasconi P (2006) Disulfind: A disulfide bonding state and cysteine connectivity prediction server. Nucleic Acids Res 34:177–181. https://doi.org/10.1093/nar/gkl266
58. Conchillo-Solé O, de Groot NS, Avilés FX, Vendrell J, Daura X, Ventura S (2007) AGGRESCAN: A server for the prediction and evaluation of “hot spots” of aggregation in polypeptides. BMC

Bioinformatics 8:. https://doi.org/10.1186/1471-2105-8-65

59. Sambrook (1989) Cloning Techniques Molecular Cloning: A Laboratory Manual T. Maniatis E. R. Pritsch J. Sambrook. Bioscience 33:721–722. https://doi.org/10.2307/1309366
60. Studier FW (2005) Protein production by auto-induction in high density shaking cultures. Protein Expr Purif 41:207–234. https://doi.org/10.1016/j.pep.2005.01.016
61. Laemmli (1970) © 1970 Nature Publishing Group. Nat Publ Gr 228:1979
62. Mollania N, Khajeh K, Ranjbar B, Rashno F, Akbari N, Fathi-Roudsari M (2013) An efficient in vitro refolding of recombinant bacterial laccase in Escherichia coli. Enzyme Microb Technol 52:325–330. https://doi.org/10.1016/j.enzmictec.2013.03.006
63. Durão P, Chen Z, Fernandes AT, Hildebrandt P, Murgida DH, Todorovic S, Pereira MM, Melo EP, Martins LO (2008) Copper incorporation into recombinant CotA laccase from Bacillus subtilis: Characterization of fully copper loaded enzymes. J Biol Inorg Chem 13:183–193. https://doi.org/10.1007/s00775-007-0312-0
64. Giardina P, Faraco V, Pezzella C, Piscitelli A, Vanhulle S, Sannia G (2010) Laccases: A never-ending story. Cell Mol Life Sci 67:369–385. https://doi.org/10.1007/s00018-009-0169-1
65. Martins LO, Durão P, Brissos V, Lindley PF (2015) Laccases of prokaryotic origin: Enzymes at the interface of protein science and protein technology. Cell Mol Life Sci 72:911–922. https://doi.org/10.1007/s00018-014-1822-x
66. Martin E, Dubessay P, Record E, Audonnet F, Michaud P (2024) Recent advances in laccase activity assays: A crucial challenge for applications on complex substrates. Enzyme Microb Technol 173:. https://doi.org/10.1016/j.enzmictec.2023.110373
67. Gogotya A, Nnolim NE, Nwodo UU (2025) Bacillus sp. GLN Laccase Characterization: Industry and Biotechnology Implications. Appl Sci 15:. https://doi.org/10.3390/app15095144
68. Abd El Aty AA, El-Shamy AR, Atalla SMM, El-Diwany AI, Hamed ER (2015) Screening of fungal isolates for laccase enzyme production from marine sources. Res J Pharm Biol Chem Sci 6:221–228
69. Kiiskinen LL, Rättö M, Kruus K (2004) Screening for novel laccase-producing microbes. J Appl Microbiol 97:640–646. https://doi.org/10.1111/j.1365-2672.2004.02348.x
70. Nishida T (1989) Lignin Biodegradation by Fungi. 紙パ技協誌 43:1071-
71. Gunne M, Al-Sultani D, Urlacher VB (2013) Enhancement of copper content and specific activity of CotA laccase from Bacillus licheniformis by coexpression with CopZ copper chaperone in E. coli. J Biotechnol 168:252–255. https://doi.org/10.1016/j.jbiotec.2013.06.011
72. Outten FW, Outten CE, Hale J, O'Halloran T V. (2000) Transcriptional activation of an Escherichia coli copper efflux regulon by the chromosomal MerR homologue, CueR. J Biol

Chem 275:31024–31029. https://doi.org/10.1074/jbc.M006508200

73. Mital S, Christie G, Dikicioglu D (2021) Recombinant expression of insoluble enzymes in Escherichia coli: a systematic review of experimental design and its manufacturing implications. Microb Cell Fact 20:1–20. https://doi.org/10.1186/s12934-021-01698-w
74. Conigliaro P, Portaccio M, Lepore M, Delfino I (2023) Optical Properties of Laccases and Their Use for Phenolic Compound Detection and Quantification: A Brief Review. Appl Sci 13:. https://doi.org/10.3390/app132312929
75. Argüello JM, Raimunda D, Padilla-Benavides T (2013) Mechanisms of copper homeostasis in bacteria. Front Cell Infect Microbiol 4:1–14. https://doi.org/10.3389/fcimb.2013.00073
76. Mot AC, Silaghi-Dumitrescu R (2012) Laccases: Complex architectures for one-electron oxidations. Biochem 77:1395–1407. https://doi.org/10.1134/S0006297912120085
77. Kadokura H, Katzen F, Beckwith J (2003) Protein disulfide bond formation in prokaryotes. Annu Rev Biochem 72:111–135. https://doi.org/10.1146/annurev.biochem.72.121801.161459
78. de Marco A (2009) Strategies for successful recombinant expression of disulfide bond-dependent proteins in Escherichia coli. Microb Cell Fact 8:. https://doi.org/10.1186/1475-2859-8-26
79. Ventura S, Villaverde A (2006) Protein quality in bacterial inclusion bodies. Trends Biotechnol 24:179–185. https://doi.org/10.1016/j.tibtech.2006.02.007
80. Fernandes AT, Pereira MM, Silva CS, Lindley PF, Bento I, Melo EP, Martins LO (2011) The removal of a disulfide bridge in CotA-laccase changes the slower motion dynamics involved in copper binding but has no effect on the thermodynamic stability. J Biol Inorg Chem 16:641–651. https://doi.org/10.1007/s00775-011-0768-9
81. Yadav D, Ranjan B, Mchunu N, Le Roes-Hill M, Kudanga T (2021) Enhancing the expression of recombinant small laccase in Pichia pastoris by a double promoter system and application in antibiotics degradation. Folia Microbiol (Praha) 66:917–930. https://doi.org/10.1007/s12223-021-00894-w
82. Xia J, Wang Q, Luo Q, Chen Y, Liao XR, Guan ZB (2019) Secretory expression and optimization of Bacillus pumilus CotA-laccase mutant GWLF in Pichia pastoris and its mechanism on Evans blue degradation. Process Biochem 78:33–41. https://doi.org/10.1016/j.procbio.2018.12.034
83. Välimets S, Pedetti P, Virginia LJ, Hoang MN, Sauer M, Peterbauer C (2023) Secretory expression of recombinant small laccase genes in Gram-positive bacteria. Microb Cell Fact 22:1–14. https://doi.org/10.1186/s12934-023-02075-5
84. Thakur V V., Jain RK, Mathur RM (2012) Studies on xylanase and laccase enzymatic

prebleaching to reduce chlorine-based chemicals during CEH and ECF bleaching. BioResources 7:2220–2235. https://doi.org/10.15376/biores.7.2.2220-2235

85. Bajpai P (2018) Brief Description of the Pulp and Papermaking Process. Biotechnol Pulp Pap Process 9–26. https://doi.org/10.1007/978-981-10-7853-8_2
86. Mathur S, Kumar S, Rao NJ (2001) Application of commercial xylanases in bleaching - A review. IPPTA Q J Indian Pulp Pap Tech Assoc 13:13–24
87. Kumar S, Satish K, Chhaya S, Parveen K (2011) Reduction in chlorine dioxide consumption by xyianase during ecf bleaching of mixed hardwood kraft pulp. IPPTA Q J Indian Pulp Pap Tech Assoc 23:117–119
88. Ming Y, Wang W, Yin R, Zeng M, Tang L, Tang S, Li M (2023) A review of enzyme design in catalytic stability by artificial intelligence. Brief Bioinform 24:1–19. https://doi.org/10.1093/bib/bbad065
89. Victorino da Silva Amatto I, Gonsales da Rosa-Garzon N, Antônio de Oliveira Simões F, Santiago F, Pereira da Silva Leite N, Raspante Martins J, Cabral H (2022) Enzyme engineering and its industrial applications. Biotechnol Appl Biochem 69:389–409. https://doi.org/10.1002/bab.2117
90. Buller R, Lutz S, Kazlauskas RJ, Snajdrova R, Moore JC, Bornscheuer UT (2023) From nature to industry: Harnessing enzymes for biocatalysis. Science (80-) 382:. https://doi.org/10.1126/SCIENCE.ADH8615
91. Santos A, Mendes S, Brissos V, Martins LO (2014) New dye-decolorizing peroxidases from Bacillus subtilis and Pseudomonas putida MET94: Towards biotechnological applications. Appl Microbiol Biotechnol 98:2053–2065. https://doi.org/10.1007/s00253-013-5041-4
92. Chen C, Shrestha R, Jia K, Gao PF, Geisbrecht B V., Bossmann SH, Shi J, Li P (2015) Characterization of dye-decolorizing peroxidase (DyP) from Thermomonospora curvata reveals unique catalytic properties of A-type DyPs. J Biol Chem 290:23447–23463. https://doi.org/10.1074/jbc.M115.658807
93. Saldarriaga-Hernández S, Velasco-Ayala C, Leal-Isla Flores P, de Jesús Rostro-Alanis M, Parra-Saldivar R, Iqbal HMN, Carrillo-Nieves D (2020) Biotransformation of lignocellulosic biomass into industrially relevant products with the aid of fungi-derived lignocellulolytic enzymes. Int J Biol Macromol 161:1099–1116. https://doi.org/10.1016/j.ijbiomac.2020.06.047
94. Rashid GMM, Bugg TDH (2021) Enhanced biocatalytic degradation of lignin using combinations of lignin-degrading enzymes and accessory enzymes. Catal Sci Technol 11:3568–3577. https://doi.org/10.1039/d1cy00431j